ANL-5841

ARGONNE NATIONAL LABORATORY
P. O. Box 299
Lemont, Illinois

BIOLOGICAL AND MEDICAL RESEARCH DIVISION SEMIANNUAL REPORT

July through December, 1957

March 1958

Preceding Report:
ANL-5732 - January through June, 1957

Operated by The University of Chicago
under
Contract W-31-109-eng-38
with the
United States Atomic Energy Commission

DISCLAIMER

This report was prepared as an account of work sponsored by an agency of the United States Government. Neither the United States Government nor any agency Thereof, nor any of their employees, makes any warranty, express or implied, or assumes any legal liability or responsibility for the accuracy, completeness, or usefulness of any information, apparatus, product, or process disclosed, or represents that its use would not infringe privately owned rights. Reference herein to any specific commercial product, process, or service by trade name, trademark, manufacturer, or otherwise does not necessarily constitute or imply its endorsement, recommendation, or favoring by the United States Government or any agency thereof. The views and opinions of authors expressed herein do not necessarily state or reflect those of the United States Government or any agency thereof.

DISCLAIMER

Portions of this document may be illegible in electronic image products. Images are produced from the best available original document.

TABLE OF CONTENTS

Page

Hemolysin production in irradiated rabbits. Part VII.
William H. Taliaferro and Bernard N. Jaroslow. 7

The role of structural degradation in the loss of serological activity of gamma-irradiated ovalbumin
Hugo Fricke, Charles A. Leone, and Wendell Landmann . . . 9

Ultracentrifuge studies of gamma-irradiated ovalbumin
Arthur L. Koch, Wendell Landmann, and
Charles A. Leone 12

Paper electrophoretic analyses of sera from irradiated, tuberculin-positive and tuberculin-negative Rhesus monkeys
Charles A. Leone, Anne R. Hartnett, Robert Christ, and
Carolee McBeth 16

Some observations on Krebs-2 mouse ascites carcinoma in rats
Agnes N. Stroud, Austin M. Brues, and
Beverly M. Richard 25

Progress report: New strains and species
The mongolian gerbil
Robert J. Flynn 31

Progress report: Diseases of laboratory animals
Studies on the etiology of ringtail
Robert J. Flynn 33

Progress report: The use of IBM equipment to analyze biological data
Joan M. Gurian 37

The induction of phase shift in cellular rhythmicity by far ultraviolet and its restoration by visible radiant energy
Charles F. Ehret 41

Progress report: Colony-formation inhibition of a T5-resistant variant of *Escherichia coli* by the bacteriophage T5
Harold E. Bendigkeit and Herbert E. Kubitschek 49

Toxicity of Sr^{90} and Ca^{45} in mice. III. Effect of Sr^{90} upon life span and neoplasms of bone and the blood-forming tissues
Miriam P. Finkel, Birute O. Biskis, and
Gertrude M. Scribner 51

TABLE OF CONTENTS

Page

Xanthine concentration and xanthine oxidase activity in chicken liver homogenates in the initial postirradiation period
S. Phyllis Stearner, Margaret H. Sanderson, and Emily J. Christian 60

Progress report: The homocysteine transmethylase system
Stanley K. Shapiro and David A. Yphantis 62

The metabolic relation between adenine and sulfur amino acids
The stability and hydrolysis of S-adenosylmethionine
Leo W. Parks and F. Schlenk 64

The biosynthesis of S-adenosylmethionine by yeast mutants
I. The adenine requirement for synthesis
Irving Yall 71

S-Adenosylmethionine as a growth factor substitute for an adenine-requiring yeast mutant
Irving Yall 75

Electronic counting and sizing of bacteria
Herbert E. Kubitschek. 78

3-Amino-1,2,4-triazole
VII. Effect on liver catalase of repeated injections of amino-triazole, and of aminotriazole in the drinking water
Robert N. Feinstein 79

VIII. Differential effect on the catalase of erythrocytes and of liver
Robert N. Feinstein 82

Progress report: Density gradient centrifugation
Polyvinylpyrrolidone-sucrose gradients
John F. Thomson and Florence J. Klipfel 85

New electron microscopic observations on fibrillogenesis in the regenerating achilles tendon of normal, scorbutic, and recovering guinea pigs
F. Wassermann 87

Progress report: Gamma ray toxicity program
Response of mice to conditioning doses of whole-body irradiation
George A. Sacher and Douglas Grahn 95

TABLE OF CONTENTS

Page

Thymic lymphomas in mice exposed to low-dose daily Co^{60} gamma irradiation
Samuel Lesher, George A. Sacher, Douglas Grahn, and Joan M. Gurian 98

A preliminary report on a histopathological study of the mouse duodenum after starvation
Samuel Lesher and Anthony Sallese 99

A comparative histological study of duodenal damage produced by fission neutrons and Co^{60} gamma rays
Samuel Lesher and Howard H. Vogel, Jr. 101

Variability in the expression of tail spotting in mice
Douglas Grahn and Walter C. Quevedo, Jr. 106

Progress report: Deuterium oxide intoxication in rats
Effect of deuteration on kidney function
John F. Thomson and Florence J. Klipfel 111

Influence of the endocrine glands on radiation-induced hyperpigmentation in mice
Walter C. Quevedo, Jr., Douglas E. Smith, and Douglas Grahn 113

Radiation protection experiments in mice exposed to fission neutrons
Howard H. Vogel, Jr. and Donn L. Jordan 116

Pilot study of subacute irradiation for future fast neutron and gamma-ray exposures
Donn L. Jordan and Howard H. Vogel, Jr. 121

Moderated neutron flux in the CP-5 biological facility
Norman A. Frigerio and Howard H. Vogel, Jr. 123

The effect of whole-body neutron irradiation on the volitional activity of the mouse
Norman A. Frigerio, Howard H. Vogel, Jr., Nicholas Bink, and Richard Barhorst 127

Recent developments in the theory of neutron-capture therapy
Norman A. Frigerio 129

TABLE OF CONTENTS

Page

On a modification of the power function
Description of body burden from measured retention
Sylvanus A. Tyler. 132

Recovery following injection of nonirradiated protoplasm into amoebae irradiated with fission neutrons
II. Protective effect of centrifuged cell portions
Edward W. Daniels and Howard H. Vogel, Jr. 139

Progress report: Granulocyte life cycle
Mary A. Maloney and Harvey M. Patt. 144

Progress report: Pyresis studies
III. Relationship of degree of fever to antipyresis by sodium salicylate and aurintricarboxylic acid
Marcia White Rosenthal and Joan F. Fried 147

IV. Hematocrit and sedimentation rate during antipyresis
Marcia White Rosenthal and Joan F. Fried 149

Progress report: The use of chelating agents in the treatment of manganese poisoning. II.
Arthur Lindenbaum and William M. Westfall 153

Progress report: The use of chelating agents in the treatment of manganese poisoning. III.
Joan F. Fried, Jack Schubert, and Elizabeth Moretti. 155

Ion exchange and solvent extraction studies of Co(II) and Zn(II) complexes of some organic acids
Jack Schubert, Edmund L. Lind, William M. Westfall, Raymond Pfleger, and Norman C. Li 158

Phagocytosis of granules from disrupted mast cells
Douglas E. Smith and Yevette S. Lewis. 159

Studies on effects of deuterium oxide
V. Growth data for mice
Asher J. Finkel and Dorice M. Czajka 160

VI. Deuterium distribution in mouse tissues
Asher J. Finkel, Joseph J. Katz, Henry L. Crespi, and Dorice M. Czajka 161

TABLE OF CONTENTS

Page

The presence of fission I^{131} in cow's milk
Philip F. Gustafson. 164

Activation products in foodstuffs irradiated with thermal neutrons
Philip F. Gustafson, S. S. Brar, and Austin M. Brues 166

The production of heat by the neutron irradiation of boron-free glass, lime glass and quartz, and its effect upon the condensation of phosphate
Takuya R. Sato and William P. Norris 169

The measurement of Ca^{45} by liquid scintillation methods
Walter E. Kisieleski and Frank Smetana. 175

The measurement of protein turnover in rat liver
III. The effect of dietary protein
Robert W. Swick and Rita A. Martin. 177

IV. The effect of growth
Robert W. Swick and Rita A. Martin. 181

Influence of oxidation products of epinephrine upon the adenosine triphosphatase activity of a uterine muscle preparation
Mario A. Inchiosa, Jr., and N. L. VanDemark 184

Unsaturated fatty acids and cholesterol metabolism
IV. Effect of dietary cholesterol on cholesterol levels and cholesterol ester composition in liver and plasma of rats
Peter D. Klein 188

Hexuronic dehydrogenase of *Agrobacterium tumefaciens*
James E. Zajic 192

Bone tumor integrated death rates
Harry Auerbach 197

Geographic studies in bone tumors
II. Geographic incidence of bone tumors in Illinois
Harry Auerbach 199

TABLE OF CONTENTS

Page

Mortality experience at Argonne National Laboratory
I. Characteristics of the Argonne National Laboratory population
Asher J. Finkel and Harry Auerbach 201

An analysis of inbreeding in the European bison
Herman M. Slatis 203

HEMOLYSIN PRODUCTION IN IRRADIATED RABBITS. PART VII

William H. Taliaferro* and Bernard N. Jaroslow

We have reported that the hemolysin-forming capacity of irradiated (400 r) rabbits can be completely restored (normal peak titer is reached after delay of 6 days) if yeast extract is added when the antigen (1.6×10^9 sheep red cells/kg) is injected one day after irradiation.(1) Since then we have been trying to characterize the "restoration factor." Ribonuclease was reported to be partially effective.(2) This finding led to the investigation of the restorative activity of the nucleic acids and their breakdown products. This activity is measured in terms of the mean peak hemolysin titer of the treated group as compared to this value in unirradiated and irradiated (400 r), untreated animals. Enzymatic digests of the nucleic acids or the enzymes alone partially restored antibody levels, whereas the highly polymerized nucleic acids had absolutely no activity (Table 1).

TABLE 1

Restorative activity of several agents as compared to yeast extract in reference to hemolysin-producing ability

X-ray dose, r	Treatment	No. of rabbits	Mean log peak titer	Geometric mean
0	None	56	3.262 ± 0.040	1830
400	None	59	2.361 ± 0.062	230
400	Yeast extract	25	3.125 ± 0.030	1333
400	DNA incubated with DNase	31	2.725 ± 0.109	531
400	DNase	17	2.531 ± 0.143	340
400	DNA	13	2.481 ± 0.154	303
400	RNA incubated with RNase	15	2.768 ± 0.152	586
400	RNase	10	2.875 ± 0.160	750
400	RNA	9	2.014 ± 0.165	103
400	Kinetin	17	2.791 ± 0.122	618
400	Adenine	9	2.394 ± 0.139	248
400	Adenosine	9	2.333 ± 0.127	216
400	Adenylic acid	6	2.354 ± 0.214	228
400	Crude guanosine	7	2.372 ± 0.067	236

*Department of Microbiology, University of Chicago.

Kinetin (6-aminofurfurylpurine) is a derivative of DNA which has been found to have growth-stimulating activity in plants. When tested in our system, its restorative capacity on antibody production was similar to those of the nucleic acid digests. Adenine (6-aminopurine), adenosine and adenylic acid were also tested, but the results were negative (Table 1). A crude preparation of guanosine was also ineffective.

The restorative activity appears to be associated in part with the breakdown products of nucleic acids. Restoration in the groups treated with nucleic acid digests or kinetin was not as high as in the yeast-treated group, although the other compounds were used in larger amounts than the yeast preparations. We suggest that some factor in yeast mediates the interaction between antigen and nucleic acid derivative that normally occurs in the course of antibody synthesis.

References

1. Jaroslow, B. N., and W. H. Taliaferro. Hemolysin production in irradiated rabbits. Quarterly Report of the Biological and Medical Research Division, Argonne National Laboratory. ANL-5486, p. 8 (1955).

2. Taliaferro, W. H., and B. N. Jaroslow. Hemolysin production in irradiated rabbits. Quarterly Report of the Biological and Medical Research Division, Argonne National Laboratory. ANL-5576, p. 7 (1956).

THE ROLE OF STRUCTURAL DEGRADATION IN THE LOSS OF SEROLOGICAL ACTIVITY OF GAMMA-IRRADIATED OVALBUMIN

Hugo Fricke,* Charles A. Leone,** and Wendell Landmann+

Although it has long been known that ionizing radiations cause denaturation of proteins, as defined by loss of solubility at the isoelectric point, it is yet not known to what extent this denaturation is correlated with loss of biological function. In addition to the denatured constituents, irradiated proteins such as ovalbumin and hemoglobin contain a broad band of structurally injured molecules, characterized by their increased thermal lability with respect to denaturation.(1) Experiments were performed to establish the role played by these various kinds of structural degradation reactions in the loss of serological activity of γ-rayed ovalbumin.

Ovalbumin was irradiated in lyophilized form (8-10% water) in vacuo at 0°C in a homogeneous γ-ray field of 1.5×10^6 r/hr and subsequently completely dissolved in aerated water, brought to pH 7-9 with NaOH, at 0°C. Proteins were characterized serologically by measuring at 0°C, pH 7.2, the precipitations formed from the reaction of various quantities of antigen with a fixed quantity of antinative rabbit serum. The entire range of combining proportions was studied; however, the precipitin curves in Fig. 1 represent only the precipitations formed near the peaks, i.e., from the region of slight antigen excess to the region of slight antiserum excess.

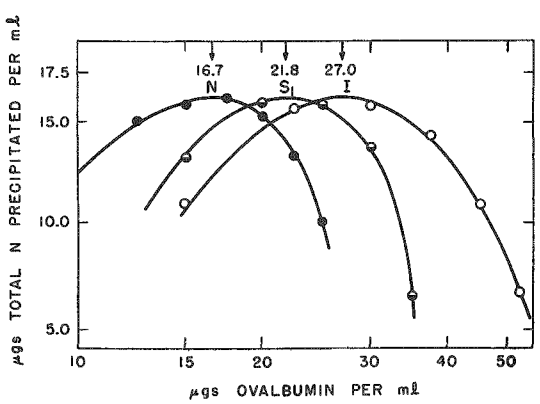

Figure 1

Reaction of anti-native ovalbumin rabbit serum with native ovalbumin, N; irradiated ovalbumin (dose 60 ev/molecule γ-rays, I); and residual protein obtained after removing the irradiation-denatured fraction from I, S_1. The arrows indicate the position of the peaks on the abscissa.

---

*Resident Research Associate 1955-1957 from Cold Spring Harbor, Long Island, New York.

**Resident Research Associate 1955-1956 and Summer 1957 from University of Kansas, Lawrence, Kansas.

+ Resident Research Associate from American Meat Institute Foundation, The University of Chicago.

For ovalbumin preparations irradiated so as to absorb up to 100 electron volts per protein molecule, the effect of irradiation is to shift the precipitin curves parallel to the abscissa toward the side of higher antigen concentrations, with no systematic change in the form of the curves (Fig. 1) as far as can be established with our present techniques. Thus an irradiated ovalbumin system behaves essentially as a mixture of protein molecules which have either completely retained or completely lost their original serological activity. This suggests that the essential underlying mechanism involves structural degradation rather than localized chemical changes in the protein molecule. The fraction of protein molecules that are apparently serologically intact - termed here the serological activity of the system - was obtained as the ratio of the abscissas of the peaks of the precipitin curves for the native and the irradiated system.

It would be easy to understand these observations if the loss of serological activity resulted wholly from denaturation, but this is not the case. The denatured protein was obtained by precipitating it at 0° C, pH 4.85, the approximate isoelectric point of both the radiation-altered and native protein species.(1) Curves representing the amounts of serologically active and nondenatured protein as functions of radiation dosage are shown in Fig. 2. The former curve lies considerably below the latter. Thus, even if the radiation-denatured protein were completely inactive serologically, as further study showed it not to be, it would account for only a fraction of the loss of serological activity. The G values* for initial loss of serological activity and initial denaturation were respectively 1.25 and 0.64.

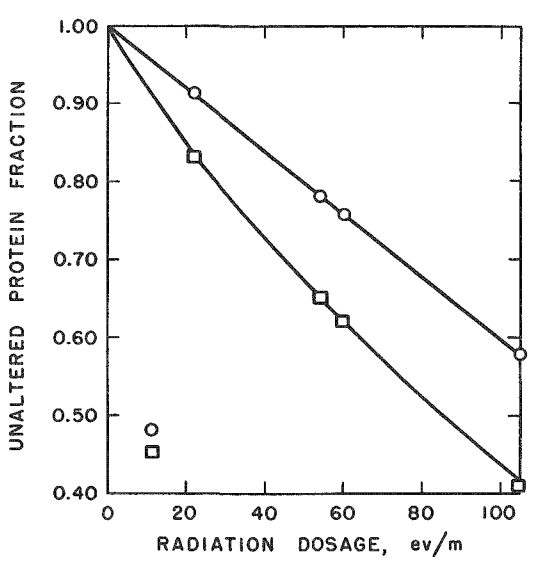

Figure 2

Relationship of radiation dosage to properties of solutions of γ-irradiated ovalbumin. Nondenatured protein fraction, o ; serologically active fraction, □ . Each point represents the average of values obtained from three experiments.

*Number of molecules reacting per 100 ev.

That the loss in serological activity was too large to be accounted for by denaturation was shown also by precipitating the denatured constituents (D) from the irradiated system (I) and measuring the serological activity of the supernatant (S_1). The precipitin curve for S_1 lay a considerable distance to the right of the precipitin curve for the native ovalbumin (N) (Fig. 1).

On the basic assumption that an all-or-none mechanism exists, the serological activity A(D) of the denatured fraction may be calculated from:

$$A(I) = [D] \cdot A(D) + (1 - [D]) \cdot A(S_1) \qquad (1)$$

where A(I) and $A(S_1)$ represent the serological activities of I and S_1 respectively and [D] is the fraction of denatured protein in I. From this equation, A(D) can be calculated from observed quantities. The average value of A(D) thus calculated was A(D) = 0.16 with no apparent dependence on radiation dosage in the range studied. It appears that the serologically active sites were left intact in 16% of the denatured constituents.

In order to establish the serological characteristics of S_1, a portion of the most highly injured proteins was removed by heating S_1 for 6 hr at 50.0°C, pH 7.2. This treatment produced only a trace of denaturation in the native protein but caused an average denaturation of 38% of the protein of S_1 of samples that received a dosage of 60 ev/molecule. The heat-denatured protein was precipitated by adjusting pH to 4.85, and the precipitin curve for the neutralized supernatant S_2 was determined. The form of this curve was the same as that of the native, but its position in the coordinate system relative to that of S_1 was shifted toward the native although it still remained slightly to the right.

Further differential removal of other thermolabile constituents was effected by heating S_2 at 62.0°C, pH 7.2 and precipitating at pH 4.85. After 4 hr of heating, the supernatants of ovalbumin preparations irradiated to receive 30-60 ev/molecule were serologically indistinguishable from similarly heated native ovalbumin. Our observations show that the loss of serological activity, after removal of the denatured protein, is mainly associated with the thermolabile constituents, and particularly those of low stability. By using an analog of Equation 1, we can calculate the serological activity of the fractions removed during the various stages of the heat treatments used. The average value found in three experiments carried out with a dosage of 60 ev/molecule was 0.4 from for the fraction removed at 50°C, pH 7.2, 6 hrs.

Reference

1. Fricke, H. Kinetics of thermal denaturation of X-rayed egg albumin. J. Phys. Chem. 56: 789-795 (1952).

ULTRACENTRIFUGE STUDIES OF GAMMA-IRRADIATED OVALBUMIN

Arthur L. Koch, Wendell Landmann, and Charles A. Leone

Native ovalbumin is a crystalline protein of molecular weight 44,000; it contains one disulfide bond, five sulfhydryl groups and 386 peptide bonds, but no N-terminal amino acid. The chemistry of proteins, particularly ovalbumin, has been reviewed.(1) The presence of sulfhydryl groups can be demonstrated only if the protein has been denatured by physical agents such as heat, surface forces, or radiation, or swollen in homogeneous solution by strong hydrogen-bonding molecules such as urea and guanidine.(1-4) Under oxidizing conditions, gel formation and aggregation follow the exposure of the SH group.(5)

When ovalbumin is irradiated in aqueous solution, examination of the product in the ultracentrifuge shows an increased sedimentation rate, $S_{20,w} = 7.8$, indicating that ovalbumin, like bovine serum albumin,(6) is polymerized by an exposure of the SH groups followed by oxidation to form intermolecular disulfide bridges. This may explain in part the effect of irradiation on the serological characteristics of the protein.(7)

When ovalbumin is irradiated in the dry state, oxidizing radicals do not predominate. The question then arises as to what changes occur in the covalent linkages. In order to gain information pertinent to this question, we have examined in the analytical ultracentrifuge native and irradiated ovalbumin, both before and after performic acid cleavage of disulfide bridges.

Experimental

Dry, twice recrystallized ovalbumin was irradiated at 0° to 4°C under high vacuum in a uniform high-intensity Co^{60} γ-ray field with a dose of 478 ev/molecule, or 11.4×10^7 rep. Another sample was irradiated as a 1% solution with 8.8×10^6 rep. Samples (0.1 g) of native and irradiated protein were subjected to performic acid oxidation by dissolving the samples in 4.0 ml of formic acid and 1.0 ml of 30% H_2O_2. The solution was allowed to stand for 3 hr at room temperature, then diluted to 10.0 ml and dialyzed against three changes of water and two of buffer.

The buffer employed was M/15 phosphate, pH 6.95, containing 0.1 M NaCl. The unoxidized samples were placed in this buffer and then dialyzed against the same buffer.

The samples were examined in the Spinco Model E ultracentrifuge at 59,780 rpm. The temperature of the sample was maintained at 20°C, and the pictures were taken at 16-minute intervals.

The results are shown in Fig. 3. Native ovalbumin has a sedimentation constant $\{S^{1\%}_{20,w}\}$ of 3.33. As the peak is quite sharp the material appears to be quite homogeneous. Upon treatment with performic acid a small amount of a high-molecular-weight aggregate is produced, which quickly sediments. The major change is a slowing of the rate of sedimentation, $S_{20,w} = 1.4$. The symmetry of the peak, considered in conjunction with the known chemical action of performic acid, suggests that the molecule has not been broken down into smaller molecules but that it has unfolded or swelled; this expansion causes an increase in hydrodynamic resistance.

The sample of protein irradiated dry in vacuo was quite insoluble but did contain some small-molecular-weight fragments. This conclusion is drawn from observations that dry irradiation produces trichloroacetic acid-soluble material,(8) that a portion of the Kjeldahl N in the present experiments was dialyzable, and that some material of lower sedimentation rate than the native molecule is evident in the ultracentrifuge diagram.

The forces holding the insoluble aggregate together appear to be mainly electrostatic in nature. The material may be completely dissolved with either dilute alkali or acid. Thus disulfide bond formation does not appear to be important in the aggregation caused by irradiation of the dry protein. A water-soluble product is produced upon performic acid treatment of the irradiated material. The sedimenting peak is broader and moves more slowly, like that of the oxidized native material. In both cases all disulfide bonds had been chemically broken, and further decrease in the sedimentation constant could only be achieved by scission of the peptide chain.

The degradation of the protein appears to be quite probable. If one assumes 32.5 ev per primary ionization, then on the average, 14 such events must have occurred per molecule in the sample, which was irradiated with 478 ev/molecule. Again on the average, if each ionization produced a scission, the average size of the molecule would be reduced to one-fourteenth. The experimental observation is that the sedimentation constant of the dialyzed material is reduced to about one half. Since it is highly probable that these molecules are in random coil configuration, this would correspond to a reduction in molecular weight by a factor of four.(9) The actual factor must be somewhat larger since the smaller fragments have been lost by dialysis.

It seems that exposure of dry ovalbumin to ionizing radiation results in the cleavage of the peptide chains. This process would appear to occur once in about 1 to 3 primary ionization events with the γ-ray emitted by Co^{60}, and it may account for the loss of serological reactivity.(10)

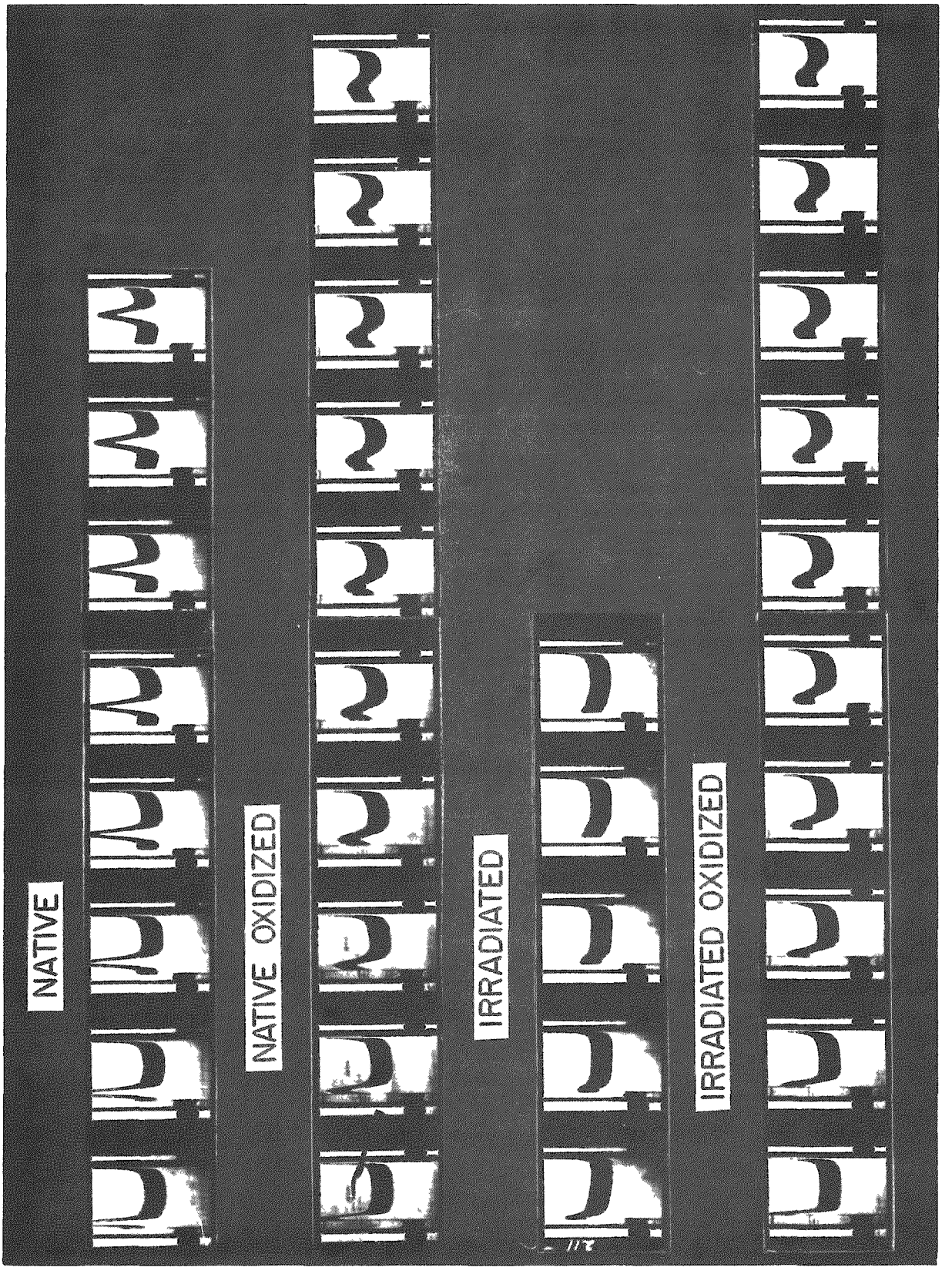

Figure 3. Ultracentrifuge diagrams of native and irradiated ovalbumin, showing effects of oxidation.

References

1. Warner, R. C. Egg proteins, in The Proteins, eds. H. Neurath and K. Bailey, Vol. II, pp. 435-486, Pt. B. Academic Press, New York (1954).

2. Putnam, F. W. Protein denaturation, in The Proteins, eds. H. Neurath and K. Bailey, Vol. I, pp. 807-892, Pt. B. Academic Press, New York (1953).

3. Putnam, F. W. The chemical modification, in The Proteins, eds. H. Neurath and K. Bailey, Vol. I, pp. 893-972, Pt. B. Academic Press, New York (1953).

4. Neurath, H., J. P. Greenstein, F. W. Putnam, and J. O. Erickson. The chemistry of protein denaturation. Chem. Rev. 34:157-265 (1944).

5. Huggins, C., D. F. Tapley, and E. V. Jensen. Sulfhydryl-disulphide relationships in the induction of gels in protein by urea. Nature 167: 592-594 (1951).

6. Barron, E.S.G., and P. Finkelstein. Studies on the mechanism of action of ionizing radiations. X. Effects of X-rays on some physicochemical properties of proteins. Arch. Biochem. Biophys. 41:212-232 (1952).

7. Leone, C. A., and W. Landmann. Effects of gamma rays on the serological properties of ovalbumin. I. Irradiated solutions. Quarterly Report of Biological and Medical Research Division, Argonne National Laboratory. ANL-5655, pp. 5-9 (1956).

8. Landmann, W. Production of peptide fragments by gamma rays in ovalbumin. Abstract No. 141, 132nd meeting of the American Chemical Society, Division of Biological Chemistry, New York, 1957.

9. Flory, P. J., and L. Mandelkern. The frictional coefficient for flexible chain molecules in dilute solutions. J. Chem. Phys. 20:212-14 (1952).

10. Leone, C. A., and J. Vincent. Effects of gamma rays on the serological properties of ovalbumin. II. Irradiated lyophilized protein. Quarterly Report of Biological and Medical Research Division, Argonne National Laboratory. ANL-5655, pp. 10-14 (1956).

PAPER ELECTROPHORETIC ANALYSES OF SERA FROM IRRADIATED, TUBERCULIN-POSITIVE AND TUBERCULIN-NEGATIVE RHESUS MONKEYS

Charles A. Leone,* Anne R. Hartnett,** Robert Christ,***
and Carolee McBeth***

This study describes and compares the changes that were found in successive samples of sera from 25 Rhesus monkeys during both preirradiation and postirradiation periods of observation. The fluctuations and the general postirradiation trends are discussed and interrelated to the positive tuberculin condition of some of the monkeys and to changes reported by others in the electrophoretic patterns of diseased animals and animals subjected to various forms of physiological stress.

Materials and Methods

Monkeys. A total of 25 monkeys (*Rhesus macaccus*) were used in these experiments. They were maintained in individual cages in an air-conditioned kennel and fed a standard ration. The animals were left undisturbed except for the times they were being irradiated or bled. Blood samples were taken periodically by venipuncture in the arm, using aseptic techniques. Sixteen of the monkeys gave positive tests for tuberculosis; they were studied in the same manner as the TB-negative animals.

Irradiation. Bilateral whole-body exposures were employed in all irradiations. During exposures the monkeys were held in a harness that covered the legs and body and permitted the arms to be strapped to the outside. If the animals were suspended in a hammock-like position they remained relatively quiet during an exposure.

X-rays, 250 kv, 15 ma, with 1 mm of Cu and 3 mm of Bakelite filtration (half-value layer, 2.3 mm Cu), were used to give one group of 7 monkeys 600 r (Table 2) in a single exposure at a rate of 5 r/min. The monkeys were placed in an exposure field whose maximum variation was 5%.

Co^{60} γ-rays at 5 r/min were used to give one group of 11 monkeys doses of 60 r every two weeks (Table 2) and one group of 5 monkeys 100 r every week (Table 2). The chronic exposures were continued until the animals died.

---

*Resident Research Associate (1955-1956 and Summer, 1957) from Department of Zoology, University of Kansas, Lawrence, Kansas.

**Student Assistant (Summer) from University of Ottawa, Ottawa, Canada.

***University of Kansas, Lawrence, Kansas.

TABLE 2

Survival of monkeys exposed to X- and γ-irradiation

Exposure	Monkey number	TB	Sex	No. of doses	Total dose, r	Survival days*
X-Rays 600 r	MC4	-	M	1	600	3
	19	-	M	1	600	11
	20	-	M	1	600	39
	21	-	M	1	600	32
	24	-	M	1	600	64
	27	-	M	1	600	39
	30	-	M	1	600	25
Average				1	600	30
γ-Rays, 60 r/2 weeks	1	+	M	12	720	161
	7	+	F	14	840	182
	8	+	F	2	120	21
	9	+	F	3	180	35
	10	+	F	3	180	28
	11	+	F	11	660	147
	12	+	F	7	420	84
	13	-	Preg. F	11	660	140
	16	+	F	7	420	91
	23	+	?	2	120	14
	31	+	?	2	120	14
Average				7	404	83
γ-Rays, 100 r/week	14	+	F	9	900	56
	18	+	M	9	900	56
	22	+	M	5	500	28
	29	+	M	7	700	42
	32	+	M	11	1100	70
Average				8	820	50

*Days after the first exposure to irradiation.

Serum samples. The samples of serum that were compared electrophoretically were derived from slightly heparinized plasmas by freezing the latter at -20° C. Fibrin clots inevitably formed when the plasmas were thawed. Each sample of plasma was frozen within 48 hr after being collected and was kept in this condition until all of the samples from a given monkey had been collected.

Protein determination. A standard curve was plotted using color reactions obtained with biuret reagent and human serum whose protein

content was determined by micro-Kjeldahl analyses of both total and non-protein nitrogen. The values for protein nitrogen were converted to protein on the assumption that the nitrogen was 16% of the total weight of the protein. Dittebrandt's[1] modification of the biuret reagent was employed throughout. Tubes containing the protein and the reagent were incubated at 37° C for 30 min and read in a Coleman Junior Spectrophotometer set at 555 mμ. The reagent-protein mixtures produced color reactions that were stable for periods up to 2 hr after incubation.

Electrophoresis. Serum analyses were made using the Spinco Model "R" paper electrophoresis apparatus and the Spinco Analytrol scanner. Standardized procedures were employed;[2] runs were made with Spinco barbituate buffer B-2 at pH 8.5 for 18 hr at 5 ma of current. Two Model R cells were used in each run. This permitted, for a majority of the monkeys, the simultaneous handling of all samples of serum obtained from a single animal. When more samples were obtained than could be handled by the two cells (i.e. 16 strips), preirradiation samples of sera from these monkeys were included in the second run with the postirradiation samples so that comparative controls were obtained. All strips were placed in a still-air drying oven at 120° C for 30 min. The oven-dried strips were then stained for 6 hr in Spinco Dye B-1, rinsed twice in baths of 5% acetic acid, carefully dried between clean blotters, and returned for 15 min to the drying oven. Fresh stain, rinse and fixing solutions were used to process the strips from each monkey. One hour before scanning the strips in the Analytrol instrument, they were placed for 1 min in a closed container and saturated with vapor from concentrated ammonium hydroxide (28-30% NH_3). Considerable effort was expended to maintain identical conditions of electrophoresis among the serum samples from the 25 experimental monkeys.

Experimental Data

The Analytrol scanner provided curves indicating the relative concentration of the individual serum proteins as they were stained and fixed along the electrophoretic paper strip. The curves were automatically integrated by the scanner which simultaneously recorded "counts" that were proportional to the area under the curve.

Each tracing of serum was divided into four components representing the albumins and the α, β, and γ globulins. No attempt was made to divide the α and β globulins into their subcomponents. In any sample that exhibited hemolysis, the tracing representing the hemoglobin (Hb) was deducted from all calculations derived from the curve.

The albumin to globulin (A/G) ratio was calculated from the scanning counts as follows: $A/G = \frac{\text{albumin count}}{\text{sum of globulins minus Hb counts}}$. The per cent

of each component in a sample of serum was calculated from counts of the total protein minus Hb and the counts for the proteins of each type. The amount of protein represented by the tracing was calculated as follows:

$$\left(\frac{\text{Individual protein count}}{\text{Total count minum Hb count}}\right) \times \left(\begin{array}{c}\text{Total protein}\\ \text{in g/100 ml}\end{array}\right) = \begin{array}{c}\text{Individual protein}\\ \text{in g/100 ml}\end{array} .$$

Plots were made of the amounts of the various component proteins of the sera during the course of the of the experiment. Representative curves for the several kinds of exposures to ionizing irradiations are presented in Figs. 4-7. The observed effects following irradiation may be summarized as follows.

1. In all but three monkeys the total protein decreased after irradiation; of these three, one received 60 r/2 weeks, one 100 r/week and one a single dose of 600 r.

2. In all monkeys except one (100 r/week) the serum albumin decreased after irradiation. The change in albumin was proportionately greater than that observed for the total protein of serum. In most monkeys there was a 50% decrease in albumin from the preirradiation level.

3. In all but three monkeys the α globulin increased steadily following irradiation. The increase in amount of α globulin ranged between 10% and 100%. In those animals not showing a rise the α globulin remained essentially constant.

4. In approximately half of the monkeys the β plus γ globulins decreased slightly during the postirradiation period. In most of the remaining monkeys it increased slightly, and in a few monkeys it was essentially constant.

5. In 10 monkeys the postirradiation β globulins increased slightly; in seven monkeys they decreased slightly; in seven others they remained essentially constant.

6. In 11 monkeys the postirradiation γ globulins decreased slightly; in six they increased slightly; in eight they remained essentially constant.

From data such as those presented in Figs. 4-7 it appeared that the β and γ globulins might be interdependent and complementary to each other. In order to reveal any such relationship, values were determined for the ratio of the single globulin to total globulins for each sample. The ratios, when plotted, had the effect of smoothing out the globulin curves, hence the relationship of each kind of globulin to the others became more apparent. Illustrative curves obtained with values for the globulin ratio are presented in Figs. 9 and 10. From these figures it is clear that the β and γ globulins are complementary to each other because the curves for these globulins are, in every monkey, very nearly mirror images. The curves for the α globulins indicate that these proteins are not metabolically interrelated to the other globulins.

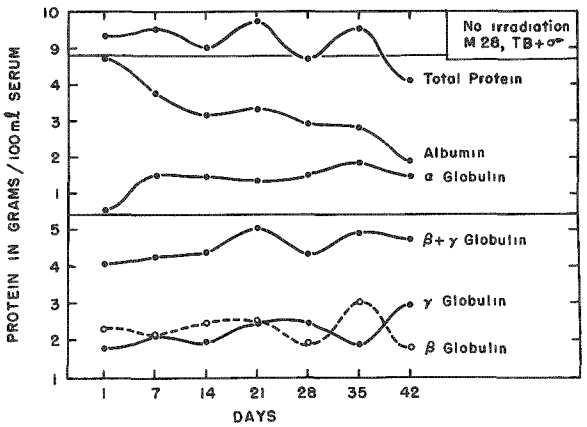

Figure 4. Variations in the levels of the proteins in the serum of an unirradiated monkey (M28).

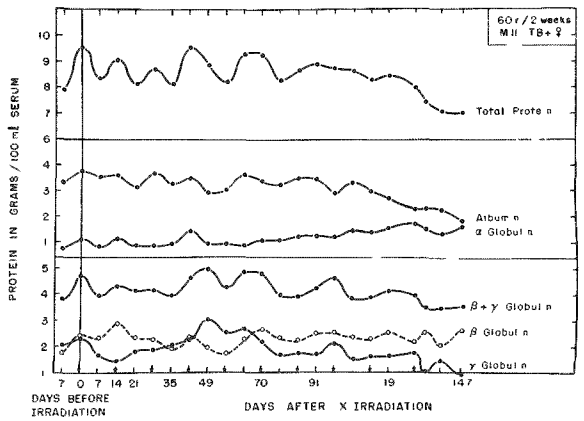

Figure 5. Variations in the levels of the proteins in the serum of a monkey (M11) receiving 60 r of γ-rays/2 weeks. Two samples were obtained prior to irradiation. Blood taken on any day of irradiation indicated on the abscissa, was obtained prior to exposure.

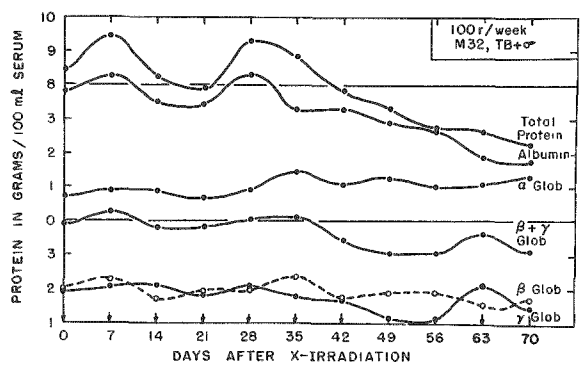

Figure 6. Variations in the levels of the proteins in the serum of a monkey (M32) receiving 100 r of γ-rays/week. Blood taken on any day of irradiation indicated on the abscissa, was obtained prior to exposure.

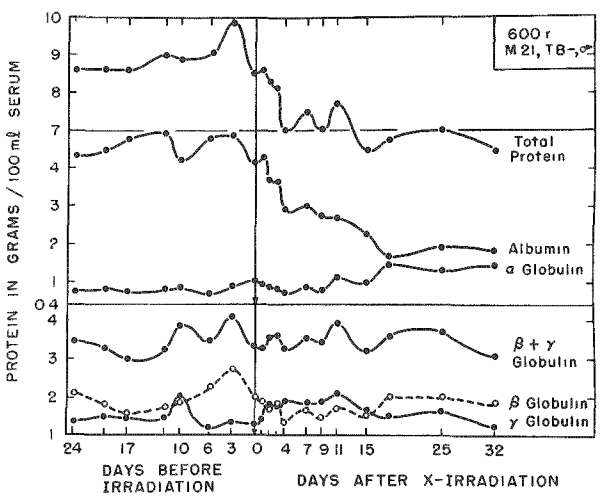

Figure 7. Variations in the levels of the proteins in the serum of a monkey (M21) that received 600 r of X-rays in a single exposure. Blood taken on the day of irradiation, day 0 on the abscissa, was obtained prior to exposure.

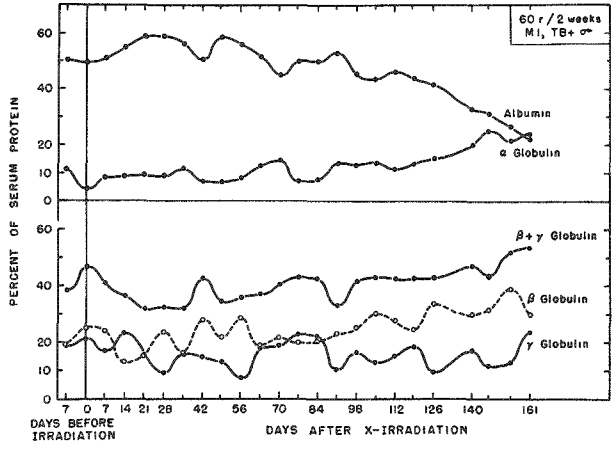

Figure 8. Variations in the proportions of the proteins of the serum of a monkey (M1) receiving 60 r of γ-rays/2 weeks.

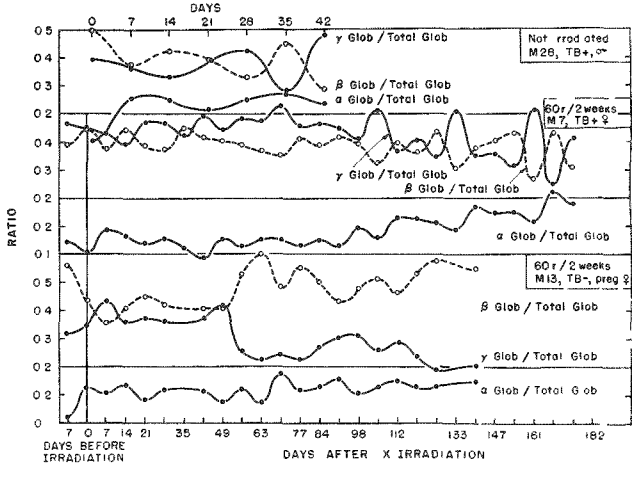

Figure 9. Ratios of each kind of globulin/total globulins in the serum of a monkey (M28) that was not irradiated and the sera of two monkeys (M7 and M13) that received 60 r of γ-rays/2 weeks.

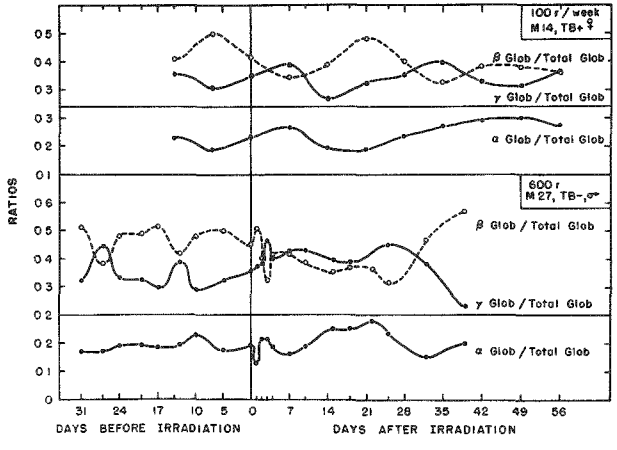

Figure 10. Ratios of each kind of globulin/total globulins in the serum of a monkey (M14) that received 100 r of γ-rays/week and a monkey (M27) that received 600 r of X-rays in a single exposure.

The curves in Figs. 4-7 depict the changes in concentration of the several proteins in the sera. For purposes of comparison values for each component for Monkey M1 (60 r/2 weeks) are presented in Fig. 8 in terms of per cent of total protein. The curves in Figs. 5 and 8 are similar. The per cent plots, by their nature, interrelate all of the values for the components, but while they indicate the true proportionalities, they do not reveal the quantitative aspects of the changes.

Figs. 11 and 12 are plots of the serum A/G ratios of monkeys from each of the X-ray exposure groups. Superimposed upon the cyclic variation of the ratios is a steady decline in the values after irradiation. The concordance of the cycles among the monkeys from each exposure group implies an innate rhythmic metabolic interrelationship between the albumins and the globulins of the sera.

Table 2 is a summary relating radiation dose to the number of days survival after irradiation. Monkeys receiving 60 r/2 weeks on the average were exposed seven times, accumulated a dose of 404 r and survived 83 days. Monkeys receiving 100 r/week on the average were exposed eight times, accumulated a dose of 820 r and survived 50 days. Monkeys that received a single dose of 600 r survived an average of 30 days.

Discussion

The complementary behavior of the β and γ proteins of the serum implies a physiological interrelation between them. Tentatively it is suggested that the site of formation for these two classes of proteins is the same and that the regulatory mechanism is a general, somatic one. The precise stimulus that suppresses the synthesis of one globulin in favor of the other is unknown.

The α globulins behave independently of the β and γ globulins in a quantitative sense Their destiny seems more intimately related to the serum albumins. As the latter begin their general decline following irradiation the former begin to increase in amount. The rise in α globulin (approximately 4 grams %) is not compensatory; the loss of albumin (approximately 16 grams %) exceeds the increase in α globulin.

It is obvious from a study of figures depicting the serum changes in any one monkey that there is considerable fluctuation in the total amount of protein in the serum even in normal animals. The component proteins do not rise and fall proportionately with each change in total protein. The complementary actions of the β and γ globulins coupled with the independent quantitative changes of the α globulins and the albumins establish a picture of continuously altering proportionalities among the components.

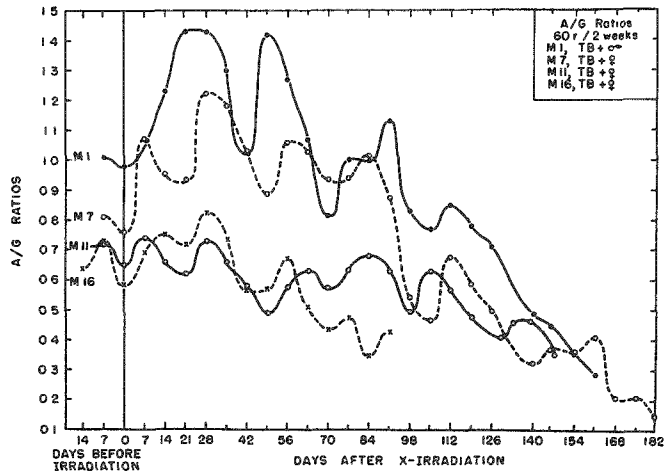

Figure 11. The albumin/globulin (A/G) ratios of four monkeys (M1, M7, M11, M16) that received 60 r of γ-rays/2 weeks until death.

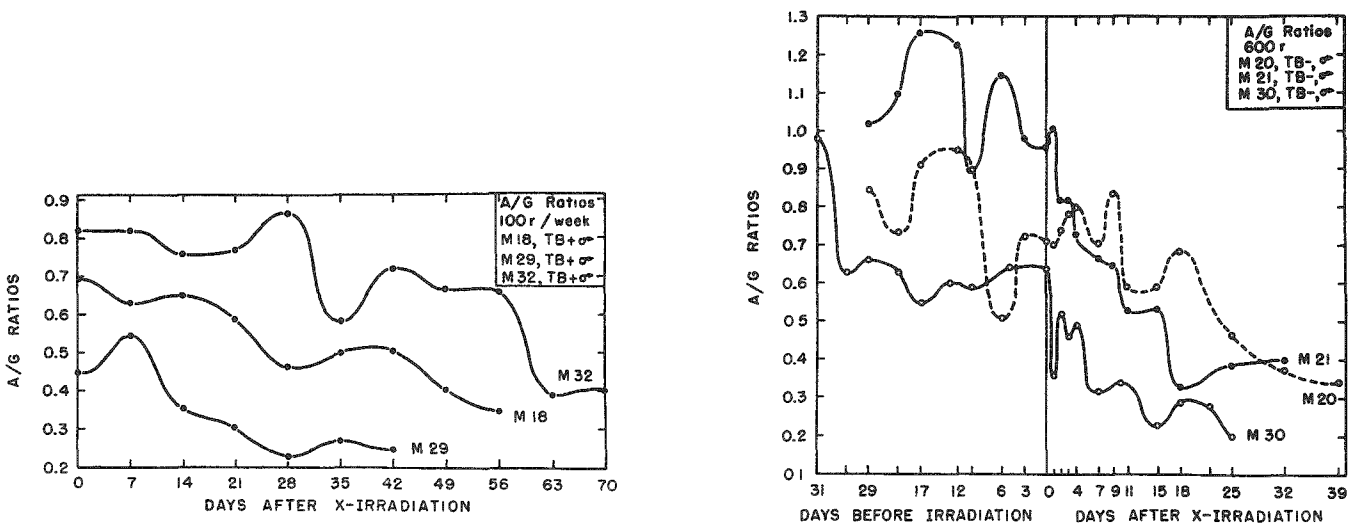

Figure 12. The albumin/globulin (A/G) ratios of three monkeys (M18, M29, M32) that received 100 r of γ-rays/2 weeks until death and of three monkeys (M20, M21, M30) that received 600 r of X-rays in a single exposure.

Both the TB+ and the TB- monkeys appeared to respond to irradiation in the same manner. The decrease in albumin and the increase in α globulin is not a unique response to irradiation. Several workers have reported that tuberculosis in humans induced a decrease in serum albumin and an increase in α globulins. Their observations on the β and γ globulins were contradictory.

Several other infectious and degenerative diseases are known to influence the serum proteins in humans in a manner similar to those described for tuberculosis. Deficiencies in vitamins, niacin and pyridoxine will likewise lead to decreased serum albumin and increased α globulins in monkeys. Various kinds of physiological stress - aging, pregnancy, burns, and low and high temperatures - have been observed to induce the same generalized response of reducing the concentration of serum albumin and increasing the concentration of α globulins.

X-irradiation has been reported to cause a decrease in concentration of serum albumin and an increase in concentration of α globulin in other laboratory animals such as dogs, rabbits, guinea pigs, and rats.

Summary

Successive preirradiation and postirradiation samples of sera from 25 monkeys were studied by means of paper-strip electrophoresis. Eleven TB+ animals received 60 r every two weeks until they died, five TB+ animals received 100 r every week until they died; and seven TB- animals received a single exposure of 600 r. One monkey was not irradiated. In all of the monkeys exposed to X- and γ-rays there was a postirradiation loss of serum albumin and an increase in α globulin. The β and γ globulins fluctuated considerably and were complementary with respect to one another.

References

1. Dittebrandt, M Application of the Wechselbaum biuret reagent to the determination of spinal fluid protein. Am. J. Clin. Pathol. 18:439-441 (1948).

2. Operating Instructions, Spinco Model R Paper Electrophoresis Apparatus. Special Instruments Corporation, Belmont, California.

SOME OBSERVATIONS ON KREBS-2 MOUSE ASCITES CARCINOMA IN RATS

Agnes N. Stroud, Austin M Brues and Beverly M. Richard

We have reported the successful growth of both the Krebs-2 and Ehrlich mouse ascites carcinomas in Sprague-Dawley rats without pretreatment.[1] The results showed an exponential increase, which might be as much as three- or fourfold, in the number of cells over a period of 3 days, with a simultaneous enlargement of the cells and nuclei. Since the phenomenon appears to be associated with an antigen-antibody reaction of the host against the donor cells, we were led to investigate some of the immunological responses induced or altered by various treatments to the host and to the donor cells.

Materials and Methods

The donor tumor cells, for either heterologous or homologous host transfer, were Krebs-2 mouse ascites carcinoma, a nonspecific tumor in mice, with a modal chromosome number of 75.[2] Female Sprague-Dawley rats (125-175 g) and CF No. 1 mice (20-25 g) were used throughout. Transfer of the tumor cells from the donor to the host was made during the 5 or 7 days of the log phase of growth, at which time the ascites yields about 10^8 cells per ml Mice and rats were inoculated intraperitoneally with 10^6 and 10^8 cells, respectively, under aseptic conditions.

Animals of irradiated groups were given a total-body dose of 350 r of X-rays immediately before, or 3 days or more before, tumor cell inoculation. When a combination of ACTH and irradiation was employed, animals were given 3 intraperitoneal injections of ACTH (.05 mg/g body weight) at 24-hr intervals and 350 r of X-rays 24 hr after the last injection, this was followed by tumor cell inoculation. Before tumor cells were irradiated, they were isolated from the tumor-bearing mouse and plated into sterile 100-mm petri dishes in amounts of 8 to 10 cc. The dishes were sealed with Saran Wrap to prevent evaporation, and placed on a continuously rotating wheel under the X-ray tube The conditions of irradiation were: 250 kvp, 15 ma, 0.5 mm Cu plus 3.0 mm Bakelite filter, half-value layer 1.8 mm Cu. The dose rate for both animals and tumor cells was approximately 100 r/min at a distance of 27 inches from the tube.

Cell volumes and nuclear volumes were measured with an eyepiece micrometer after fixation with an aceto-orcein stain; the difference in volume between the fixed and unfixed cells was estimated to be less than 1%. Fifty or more cells were measured routinely. Mitotic indices were

determined in 500 or more aceto-orcein stained cells. Duplicate determinations of cell population were made on each sample, using 2 WBC pipettes and a Neubauer-ruled hemacytometer.

Experimental

Pretreatment of donor cells with X-irradiation. Krebs-2 mouse ascites carcinoma cells increase logarithmically in the rat over a period of two or three days, yielding from a 10^8-cell inoculum, a cell population of 15-20 x 10^8 cells.[1] During this time, cell volumes and nuclear volumes also increase, as much as three- or fourfold (Table 3). The volume ratio of nuclei to cells does not always follow a consistent pattern over this period, but is on the order of about 1:3. Preliminary experiments with solid tumors and point sources of irradiation also demonstrated an increase in cell size,[3,4] which appears to represent growth of cells whose division has been inhibited by radiation. To compare this phenomenon with the enlargement of tumor cells described above, cells were treated with 2 kr or 3 kr of X-irradiation before inoculation into rats or mice. Volumes of the donor cells, with and without prior X-irradiation, are compared in Table 3.

TABLE 3

Cell volume and nuclear volume of Krebs-2 mouse ascites carcinoma cells in rats and mice after X-irradiation of the donor cells

Irradiation dose to cells, r	Cell volume,* μ^3 x 10^2			Nuclear volume,* μ^3 x 10^2		
	Days after inoculation			Days after inoculation		
	0	1	2	0	1	2
	Rats					
0	30	60	93	10	22	22
2000	36	163	146	11	59	56
3000	49	245	306	12	80	108
	Mice					
0	29	35	33	10	11	14
2000	31	127	100	10	37	31
3000	26	139	125	9	42	44

*Each datum represents the mean value for 100 cells.

In rats, irradiation and inoculation resulted in additive increases in nuclear and cell volumes. Increases in cell volume occurring at 1 hr after irradiation, i.e., immediately before inoculation, are noted at 0 time. The ratios between nuclear and cell volumes remained approximately at 1:3 for each dose level and time. Cell and nuclear volumes increased in mice after the similar doses or radiation, but the increment was less at the higher dose levels.

Three days after inoculation of rats with the irradiated tumor cells, very few cells remained in the peritoneal cavities, and most of these were within the normal size range, although the largest attained a size beyond the 48-hr mean values. Leucocytes predominated among the cells seen in the ascitic fluid at this time; this condition is seen also in mice receiving X-irradiated cells. Some cells contained no nuclei, but had many small vesicles ranging in diameter from 1μ to 2μ; they may be equal in number to the modal chromosome number. They did not stain with orcein, carmine or hematoxylin, but were Feulgen-positive. Some cells contained a few micronuclei in addition to the vesicles[5,6]; these appeared to be degenerate since very few were seen at 4 or 5 days after inoculation. At 48 hr the mitotic index was high (4-5%) and most of these dividing cells were in prophase or metaphase, suggesting an inhibition or delay of mitosis resulting in a high mitotic index.[1] Almost all of the mitotic figures present were abnormal; they included clumped metaphases, disorganized prophases, chromosome breaks, and bridges. Occasionally chromosomes are unequally distributed between two daughter cells.

The growth of the irradiated tumor cells after inoculation was studied. In the mouse the cell population increased for 24 hr after irradiation and inoculation. After 48 hr a decline in the population was observed. By the third day and later very few tumor cells were left, but a heavy infiltration of leucocytes had appeared. In the rat, on the other hand, there was no initial population increase of the irradiated donor cells, but rather a steady decline from the original inoculum size (Table 4). Accumulation of ascitic fluid was comparable to that in the control animals, but it continued to increase while the cell population was decreasing.

TABLE 4

Growth of Krebs-2 mouse ascites carcinoma in rats after X-irradiation of the donor cells

Days after inoculation	10^6 Cells*			
	X-ray dose, kr			
	0	1	2	3
0	100	-	100	100
1	260	-	50	35
2	600	-	35	30
3	580	-	< 1	< 1

*Each datum represents the mean of values for 2 rats.

Pretreatment of the host with X-irradiation and/or ACTH. The hypothesis that cell enlargement represents an inflammatory response due to an antigen-antibody reaction of the host to the donor cells was tested by treating rats with X-irradiation and/or ACTH before inoculation with tumor cells. It was anticipated that a previously irradiated host would lose its capacity to develop immunity to the heterologous tumor, and that, as a result, enlargement of cell volume would be minimized. The results are presented in Table 5. Both X-irradiation and ACTH, alone or in combination, minimized the increase in volume of cells and nuclei. Although irradiation of the host resulted in a twofold increase in cell volume after 24 hr, there was no further increase, but rather a decrease at 48 hr and at 72 hr. X-irradiation and ACTH in combination elicited an initial increase of about 100%, with, however, very little change during the 3 days. With ACTH alone, a 50% increase was seen at 2 and 3 days.

TABLE 5

Cell volume and nuclear volume of Krebs-2 mouse ascites carcinoma cells in rats pretreated with X-irradiation and/or ACTH

Treatment	Days			
	0	1	2	3
	Cell volume, $\mu^3 \times 10^2$**			
ACTH*	24.0	24.4	32.2	37.2
X-irradiation	24.0	47.2	35.4	24.8
X-irradiation + ACTH	24.0	46.6	47.2	42.6
	Nuclear volume, $\mu^3 \times 10^2$			
ACTH*	11.8	13.8	11.3	13.2
X-irradiation	11.8	14.7	13.2	15.7
X-irradiation + ACTH	11.8	18.1	14.7	10.5

*3 injections 24 hr apart.

**Each datum represents the mean of 50 or more cells.

From the results it appears that both X-radiation and ACTH, at dosages that check the immune response of the heterologous tumor cells in a foreign host, lessen cell enlargement. In addition to minimizing increases in cell volume, X-irradiation of the rat increased the duration of the growth period of inoculated mouse tumor cells (Table 6). At 6 days

after inoculation, at the time when the cell population has diminished in the nonirradiated rat (i.e., the tumor has regressed), the cell population in the irradiated rat was as much as 40 times that of the inoculum; deaths due to the tumor occurred between 5 and 14 days. Both tumor cell number and accumulation of ascitic fluid were suppressed (Table 6).

TABLE 6

Growth of Krebs-2 mouse ascites carcinoma in rats presented with X-irradiation or water

Treatment	Days				
	0	1	2	3	6
	Cells x 10^8*				
None	1.0	3.0	8.0	12.0	0
X-irradiation, 350 r	1.0	1.3	5.4	6.0	40.0
20 cc water	1.0	-	4.2	6.6	-
	Fluid, ml*				
None	1.0	5.1	12.2	20.3	-
X-irradiation, 350 r	1.0	1.5	5.2	8.4	59.0
20 cc water	1.0	-	2.7	7.2	-

*Each datum represents the mean of values from 2 or more rats.

When rats were irradiated 3 days before tumor cell inoculation, cell numbers exceeded the control values by a factor of two over a 3-day period. Ascitic fluid volume was the same as the control value, or, if more at 24 hr, it had leveled off to control values by 48 and 72 hr. One death in this group was recorded at 5 days. Cell volume increased 3-fold after 24 hr and then remained constant for 3 days, whereas in the controls it had increased 7-fold by 3 days.

When 2 doses of X-ray were given 2 weeks apart and the rats were inoculated 1 week later, they were in all respects similar to the controls. It appears that the reduction in immune response is maintained over this period.

When nontreated rats were put on a water-free diet, concentration of cells and accumulation of fluid were unaffected over a 3-day period; however, if rats were inoculated intraperitoneally with 20 cc of water and

tumor cells were injected 3 days later, the concentration of cell number and ascitic fluid was very similar to that in X-irradiated rats (Table 6). The significance of this finding is not clear.

References

1. Stroud, A. N., A. M. Brues, D. H. Chatterley, and M. Summers. Serial transplantation of Krebs-2 and Ehrlich ascites tumors to rats. Cancer Research 17: 1102-1107 (1957).

2. Hauschka, T. S., B. J. Kvedar, S. T. Grinnell, and D. Amos. Immunoselection of polyploids from predominantly diploid cell populations. Ann. N. Y. Acad. Sci. 63: 683-705 (1956).

3. Brues, A. M., and A. N. Stroud. Continuous irradiation of tumors. Quarterly Report of Biological and Medical Research Division, Argonne National Laboratory. ANL-5332, p. 5 (1954).

4. Brues, A. M., and A. N. Stroud. Radiation effects on tumor nuclei. Quarterly Report of Biological and Medical Research Division, Argonne National Laboratory. ANL-5378, pp. 72-73 (1955).

5. Klein, G., E. Klein, and E. Klein. The viability and the average desoxypentosenucleic acid content of micronuclei-containing cells produced by colchicine treatment in the Ehrlich ascites tumor. Cancer Research 12: 484-489 (1952).

6. Brues, A. M. and E. B. Jackson. The resistance of tumor cells in tissue culture to the growth-inhibiting action of amines. Cancer Research 1: 557-563 (1941).

PROGRESS REPORT: NEW STRAINS AND SPECIES

The Mongolian Gerbil

Robert J. Flynn

In order to gain knowledge concerning their care and breeding, and their possible usefulness for radiobiological studies, one male and two female Mongolian gerbils (Meriones unguiculatus) were obtained (Fig. 13). Within 18 months a sizable colony was produced from these original three animals and a great deal concerning their care, handling, and breeding was learned. When these animals became available commercially,* breeding was discontinued and those on hand were given 300, 500, 700, or 900 r of X-rays (250 kv, 26.89 r/min) in an effort to determine their comparative radiosensitivity. Only two died at the 900 r level and an additional dose of 1050 r (27.76 r/min) was given to all the survivors 55 days after the initial dose.

Figure 13. Mongolian gerbil.

Although the numbers are few and the ages scattered, it appears that the single-dose 30-day LD 50 is in excess of 900 r and probably around 1100-1300 r (Table 7).

*Tumblebrook Farms, Brant Lake, New York.

TABLE 7

Sensitivity to X-irradiation of the Mongolian Gerbil

(*Meriones unguiculatus*)

Group A (12-18 months of age)				Group B (5-7 months of age)			
Age*	Sex	Dose, r	Time of Death**	Age*	Sex	Dose, r	Time of Death**
16	M	900 + 1050	13	7	M	900 + 1050	17
16	M	900 + 1050	15	7	M	900 + 1050	Survived
16	M	900 + 1050	14	7	F	900 + 1050	15
14	F	900	5 †	7	F	900 + 1050	19
13	F	900	12 †	7	F	900 + 1050	19
14	M	700 + 1050	19	7	M	700 + 1050	15
14	M	700 + 1050	19	6	F	700 + 1050	14
13	M	700 + 1050	13	6	F	700 + 1050	20
18	F	700 + 1050	16	6	F	700 + 1050	Survived
16	F	700 + 1050	Survived	6	F	700 + 1050	Survived
18	M	500 + 1050	15	7	M	500 + 1050	Survived
18	M	500 + 1050	17	5	F	500 + 1050	21
13	M	500 + 1050	Survived	5	F	500 + 1050	Survived
13	M	500 + 1050	16	5	F	500 + 1050	22
12	F	500 + 1050	9				
12	F	500 + 1050	10	7	M	300 + 1050	Survived
				7	F	300 + 1050	15
12	M	300 + 1050	12	5	F	300 + 1050	Survived
12	M	300 + 1050	Survived	5	F	300 + 1050	19
12	M	300 + 1050	Survived				
12	F	300 + 1050	Survived				
12	F	300 + 1050	Survived				
12	F	300 + 1050	Survived				

*In months

**In days after final dose

†Died after initial dose

PROGRESS REPORT. DISEASES OF LABORATORY ANIMALS

Studies on the Etiology of Ringtail

Robert J. Flynn

Ringtail is a condition of very young rats initially characterized by constriction and, later, by edema, necrosis, and spontaneous amputation of the tail (Fig. 14). The condition is frequently seen in some animal quarters, yet never observed in others. Certain impressions have been reported concerning its etiology but few experimental data have been published. Genetic factors,(1) humidity,(2) caging,(2) and nutritional effects(3,4) have been implicated.

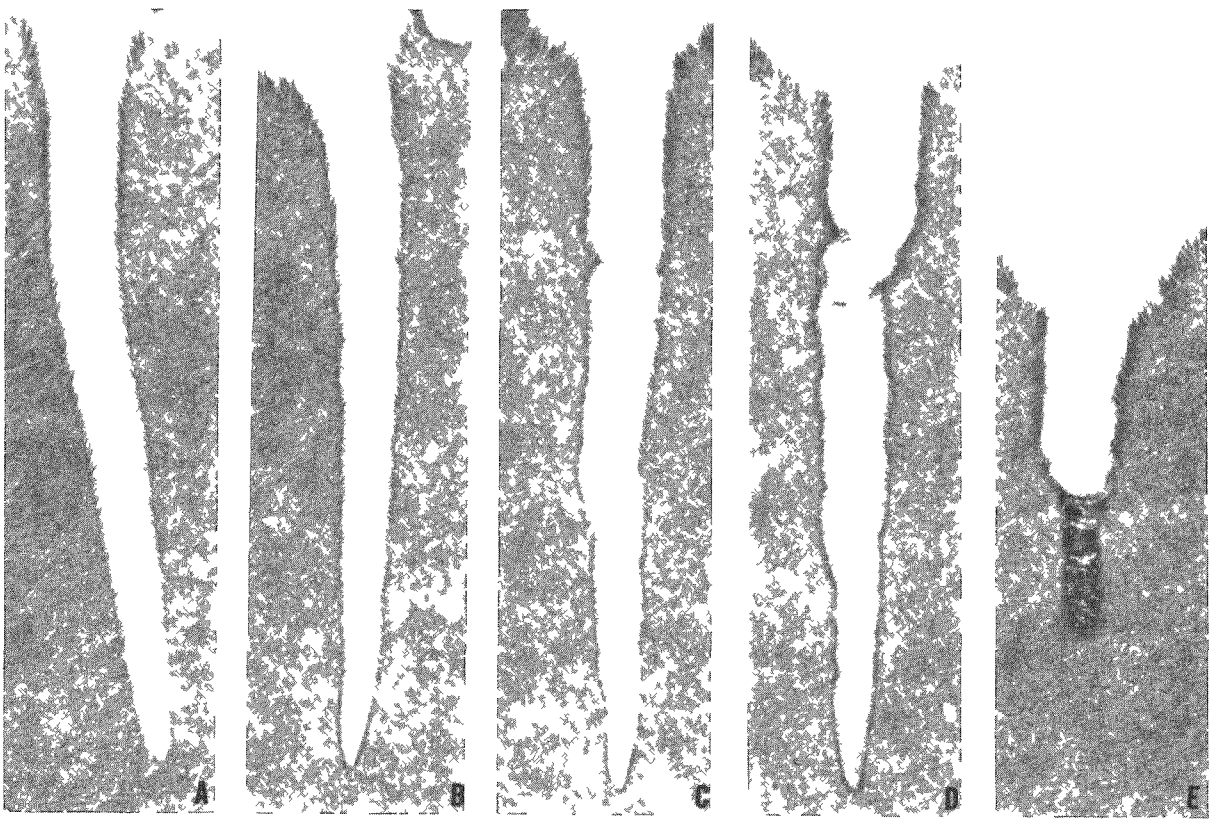

Figure 14. A, normal rat tail, B, pre-ringtail (incomplete constriction), C, ringtail (complete constriction), D, severe ringtail (constriction plus edema); E, irreversible ringtail (necrosis).

Because the experimental evidence was inconclusive, controlled studies were initiated to determine whether or not the condition could be produced experimentally, and if so, to determine the effects and interrelations of variations in humidity, caging, diet, and strain on the incidence and severity of the condition.

Results

The results of a series of experiments show that ringtail can be produced experimentally and that the incidence can be altered by certain variations in the environment.

Under all combinations of conditions, the maximum incidence of ringtail consistently occurred at about one week of age. After the 7-9th day, the majority of affected animals tended to recover spontaneously. Under moderate conditions conducive to the production of ringtail, all but a small percentage of the affected animals were normal by the 14th day and even under extreme conditions, a large percentage were much improved by that time.

The percentage of animals that developed ringtail appeared to be inversely proportional to the relative humidity (R.H.) (Fig. 15). At 20% R.H. the maximum percentage affected was 92.9; at 30% R.H., 86.0; at 40% R.H., 26.3; at 50% R.H., 4.4; and at 60% R.H., 0.0. At 20% R.H., 7.2% of the rats were permanently mutilated by caudal necrosis and spontaneous amputation. At 30% R.H., only one was permanently mutilated and at the higher relative humidities, none.

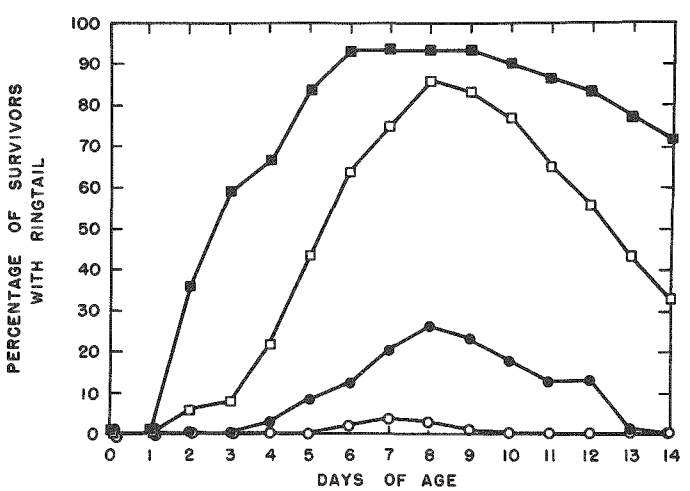

Figure 15. Effects of variations in humidity on incidence of ringtail. Wire-mesh cage, Rockland mouse diet, Sprague-Dawley rat, Temperature 80°F.

■ 20% relative humidity ● 40% relative humidity
□ 30% relative humidity ○ 50% relative humidity

When the rats were born and reared in plastic cages[5] at 20% R.H., the incidence of ringtail was 0.0%; when steel cages[6] were used, the incidence was 92.9%.

The effects of dietary supplementation were also investigated. At 20% R.H., the maximum incidence observed with corn oil supplementation (5 g oil per 100 g diet) was 96.9%, approximately the same as the maximum incidence observed with the unsupplemented Rockland Mouse Diet, 92.9%. Similarly, the addition of corn oil plus compressed yeast and lettuce at 30%, 40%, and 50% R.H. had only a slight effect on the resultant maximum incidences.

Four strains were compared under controlled conditions. Ringtail was produced in all four strains; however, the incidence was much lower in the Long-Evans and Sherman strains (32.6% and 29.4%, respectively) then in the Wistar and Sprague-Dawley strains (78.3% and 82.1%, respectively).

Conclusions

Ringtail can be produced experimentally; the incidence and severity are inversely proportional to the relative humidity.

A caging effect, whether real or merely an expression of the humidity within the cage, and a strain variation, are observable.

Affected animals tend to recover spontaneously. Although dietary supplementation may affect the time of onset or recovery, it does not prevent the condition from occurring and has little effect on the maximum incidence.

References

1. Wooley, G. W., and L. J. Cole. Spontaneous tail amputation in the Norway rat. J. Heredity 29:123-127 (1938).

2. Farris, Edmond J. The rat as an experimental animal. Ch. 2 in The Care and Breeding of Laboratory Animals, Edmond J. Farris, ed. John Wiley and Sons, Inc., New York (1950).

3. Greenman, Milton J., and F. Louise Duhring. Breeding and Care of the Albino Rat for Research Purposes, 2nd ed. The Wistar Institute of Anatomy and Biology, Philadelphia (1931).

4. Guggenhiem, M., and R. Jürgens. Das Schachtelhalmschwanzsymptom bei Saugenden Jungratten und die Beziehungen der ungesättigten Fettsäuren zu den Vitaminen des B-Komplexes. Helv. Physiol. et Pharmacol. Acta 2:417-433 (1944).

5. Flynn, Robert J. Small animal cages. Proc. Animal Care Panel 4:186-188 (1953).

6. Flynn, Robert J. Standard mouse cage. Quarterly Report of the Biological and Medical Research Division, Argonne National Laboratory. ANL-4488, pp. 59-64 (1950).

PROGRESS REPORT: THE USE OF IBM EQUIPMENT TO ANALYZE BIOLOGICAL DATA

Joan M. Gurian

In biological research, the variability of the material frequently makes it necessary to collect great quantities of data in order to describe a phenomenon adequately or to determine the relationship between various causes and effects. Often only a small portion of the information contained in the results of an experiment can be extracted because time and manpower are not available for classification and computation. To aid the experimenter in making maximum use of his experimental results, a program of data processing using IBM equipment has been inaugurated in the Biological and Medical Research Division, in co-operation with the Data-Processing Department of the Accounting Division, where an IBM Type 650 Computer and auxiliary equipment has been made available for scientific problems.

Data to be processed by IBM equipment must be in quantitative form. Some experimental results, for example blood counts, are by nature in this form, others may be quantified easily by assigning numerical values to, e.g. the degree of injury, or, if the data is dichotomous, simply coding yes (1) or no (0). However, certain descriptive data, such as pathology records, are not easily quantified, and a code for such data must be determined through the joint effort of the experimenter and the IBM processor.

Experimental data can be quantified, coded or otherwise prepared for IBM analysis either after collection or when produced. We have adopted the latter procedure whenever feasible since the progress of the experiment is easily followed, partial results are available at any stage, and the final analysis can be completed in a short time after completion of the experiment.

Problems currently being processed in this Division fall into several categories, examples of which will be discussed.

1. Modification of data. Experimental results frequently require extensive modification (adjustment, correction, or standardization) before information pertinent to the biological problem is produced. Survival, for example, is desired in terms of number of time units between treatment and death. However, both treatment and death occur on, let us say, specific dates. These dates are only meaningful in relation to each other, and the number of days elapsed between them must be computed. Such a calculation is simple, but in large experiments it is cumbersome and time consuming. A program to obtain this for each of the three pairs of three dates has been written. If we express the dates as $D_1M_1Y_1$, $D_2M_2Y_2$ and $D_3M_3Y_3$, and the times as T_1, T_2, and T_3 respectively, then the program may be shown schematically as in Fig. 16.

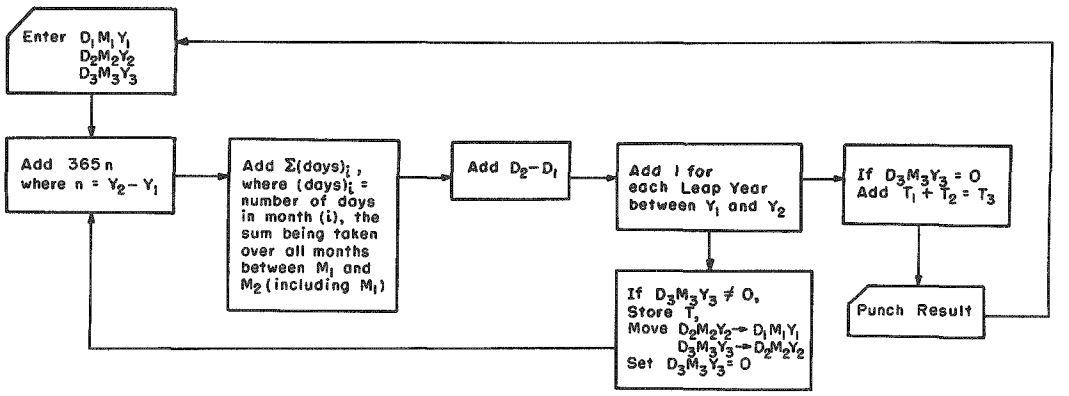

Figure 16. Schematic representation of program for computing elapsed time between two dates.

Another example, currently being processed, is the calculation of the dose received by a specimen irradiated in the spectrograph which is computed from the irradiation delivered, corrected for the effects of lenses, filters, etc. Computing time for each of these programs is approximately 100 sets/minute.

2. Data Reduction and Statistical Analysis. In large-scale experiments, many relationships among the observed or measured variables may be obscured by the vast masses of data that are collected. A reorganization of the data may bring to the fore some causal relationships.

After the data have been transformed into biologically meaningful terms, and a general picture has been obtained, further statistical analysis may be indicated. For example, the determination of an empirical relationship between a pair of variables may be desirable. If this relationship is not linear even under transformation, some hypothesis as to the relationship must be tentatively accepted, and general methods of fitting must be employed to estimate the constants of the expression. Most general methods depend on an iterative process and are easily adapted for processing on the IBM 650, while they may be prohibitively time-consuming if done manually. Usually the adaptation suited for processing can be arranged so that machine instructions are given only once, and only the constants need be changed for each iteration. Such a program has been written to evaluate the constants k and n in the equation $S = 1 - (1 - e^{-kx})^n$, the multi-hit survival curve.

Quantitative experimental results can in many cases be condensed by substitution of sample-statistics (say, the mean and the sample-variance) for the data. For large quantities of data this is time-consuming if done manually (on the desk-calculator or the slide-rule). The labor

in an analysis of variance can also be reduced greatly by use of the IBM 650 since at least the basic quantities, i.e. the sums of squared deviations, can be easily obtained, and thus a simple routine can serve for the analysis of many different experimental designs. A program for the calculation of mean, variance, and standard deviations of various categories and subcategories in a factorial and a hierarchical experimental design has been written. Since the output included the sums of the items and of their squares for each category, the quantities necessary for an analysis of variance are readily available.

Another program in this category is one for the analysis of γ-ray spectra to determine the relative amount of different isotopes present in a mixture of radioactive materials.

Let $f(x)$ = the number of counts from the sample in channel x
$m(x)$ = the number of background counts in channel x
$g_i(x)$ = the number of counts from isotope i in channel x

Then $f(x) = m(x) + \sum_i a_i g_i(x)$, where a_i is the coefficient indicating the relative amount of isotope i in the sample. This is calculated from

$$a_i = \frac{\sum_{j=l_i}^{k_i} \frac{f(x)}{g_{ij}(x)}}{l_i - k_i}$$

, where l_i and k_i are the channels bordering the photopeak of isotope i.

The procedure then is as follows:

1. Subtract background: $f(x) - m(x) = f'(x)$
2. Calculate a_i for $i = 1$
3. Subtract counts due to isotope (1) from all channels:

$$f'(x) - a_1 g_1(x) = f''(x)$$

Repeat steps 2 and 3, inserting the residual $f''(x)$ in step 2, ($i = 2, 3$ ---) until all desired isotopes have been subtracted, or $a_i = 0$. Since $x = 1, 2, 3 \ldots 240$, this is a repetitive procedure, well suited to the electronic computer.

3. Theoretical Calculations. Certain theoretical descriptions of biological systems can lead to large-scale computational projects. These can be easily handled by the IBM 650 computer, and such programs have been written for specific problems in this division.

The programs for the IBM 650 that make up the library of routines in current use by the Biology Division are devised by members of the division or by members of the programming staff of the Data Processing

Department of the Accounting Division, or are obtained from the IBM company and other IBM installations. Usually the programs are the result of collaboration, with alteration of standard programs by members of this division, to fit an individual problem arising in the course of biological experimentation.

From the above examples it may be seen that while IBM equipment does not do anything which, given unlimited time, could not be done using other computational equipment, the utilization of this high-speed equipment makes possible a fuller exploitation of the great masses of basic experimental data collected in biology.

THE INDUCTION OF PHASE SHIFT IN CELLULAR RHYTHMICITY BY FAR ULTRAVIOLET AND ITS RESTORATION BY VISIBLE RADIANT ENERGY

Charles F. Ehret

When nondividing cells of Paramecium bursaria of complementary mating types are mixed together during a sexually reactive phase, a mass agglutination occurs that is known as the mating reaction. This is normally followed by pairing of cells and conjugation of the complementary types. In nature, the reactive phase occurs in the daytime and the nonreactive, or weakly reactive phase, at night. In the laboratory it has been demonstrated that phase shifts can be induced by visible radiant energy,[1,2] that under constant conditions of darkness and temperature an endogenous diurnal rhythm persists,[1,3] and that these relationships hold equally for cells freed of the symbiotic algae that normally inhabit the cytoplasm of this species.[1]

In the course of an investigation of the dose-response relationships for the determination of phase-shift action spectra, it became obvious that radiant energy of the far ultraviolet region of the spectrum was not only highly efficient in inducing phase shifts, but that the efficiency was directly related to the phase stage during which the stimulus was applied. It was further observed that the UV effect was almost entirely photoreversible with visible radiant energy. This paper describes the results of such an experiment.

Methods

Culture methods were essentially similar to those previously described.[1] Chlorella-less* cell populations of P. bursaria stock Wu-5, mating type D, in 250-ml erlenmeyer flasks were transferred at the end of the exponential period of growth into four different light-dark compartments. The flask within each compartment received 150 foot-candles (fc) illumination from a 15 W daylight fluorescent lamp. Each compartment was scheduled according to a photoperiodic cycle consisting of 10 hr of light and 14 hr of darkness. From one compartment to the next, each cycle was unique, with 6-hr spacings between the starts of the photoperiods. By the third day, the mid-reactive phases of each of the four populations was either 6 or 12 hr removed from the other three. This starting condition is represented diagrammatically by the rectangles at the left of each of the graphs in Figs. 17 and 18. Thus at midnight (2400 hours, left end of the

*The cytoplasm of this stock has been entirely freed of the normally symbiotic alga, Chlorella sp.

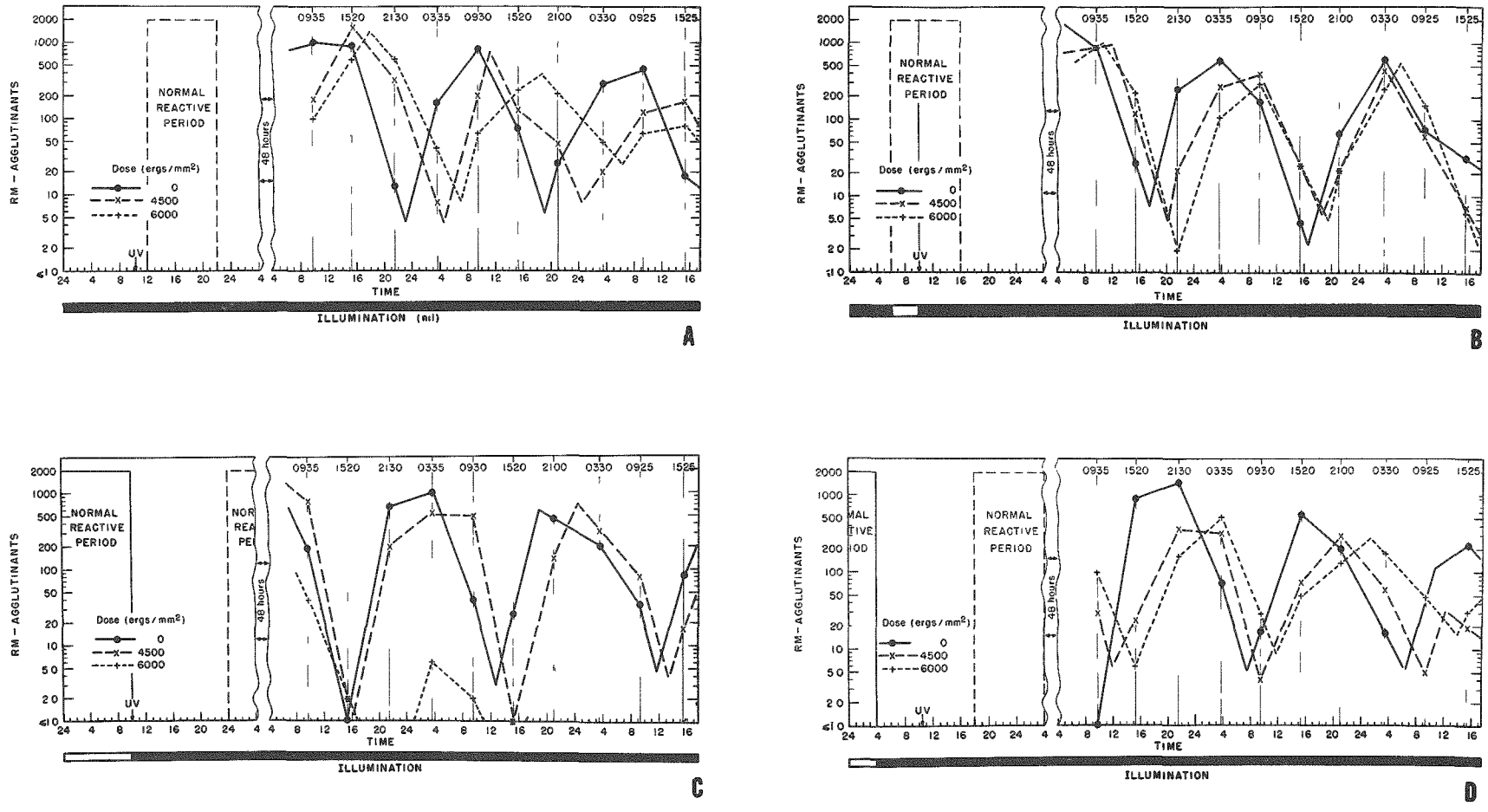

Figure 17. The relationship between ability of experimental paramecia to mate, and the time of day at which the mixture with competent cells of complementary mating type was made. Reaction magnitude of agglutination (RM) was measured ten minutes after mixing. Four categories were irradiated at each of four different phases during a reactive-nonreactive diurnal cycle: A, in the late scotophilic phase; B, just before the middle of the reactive phase; C, at the end of the reactive phase; D, just before the middle of the scotophilic phase.

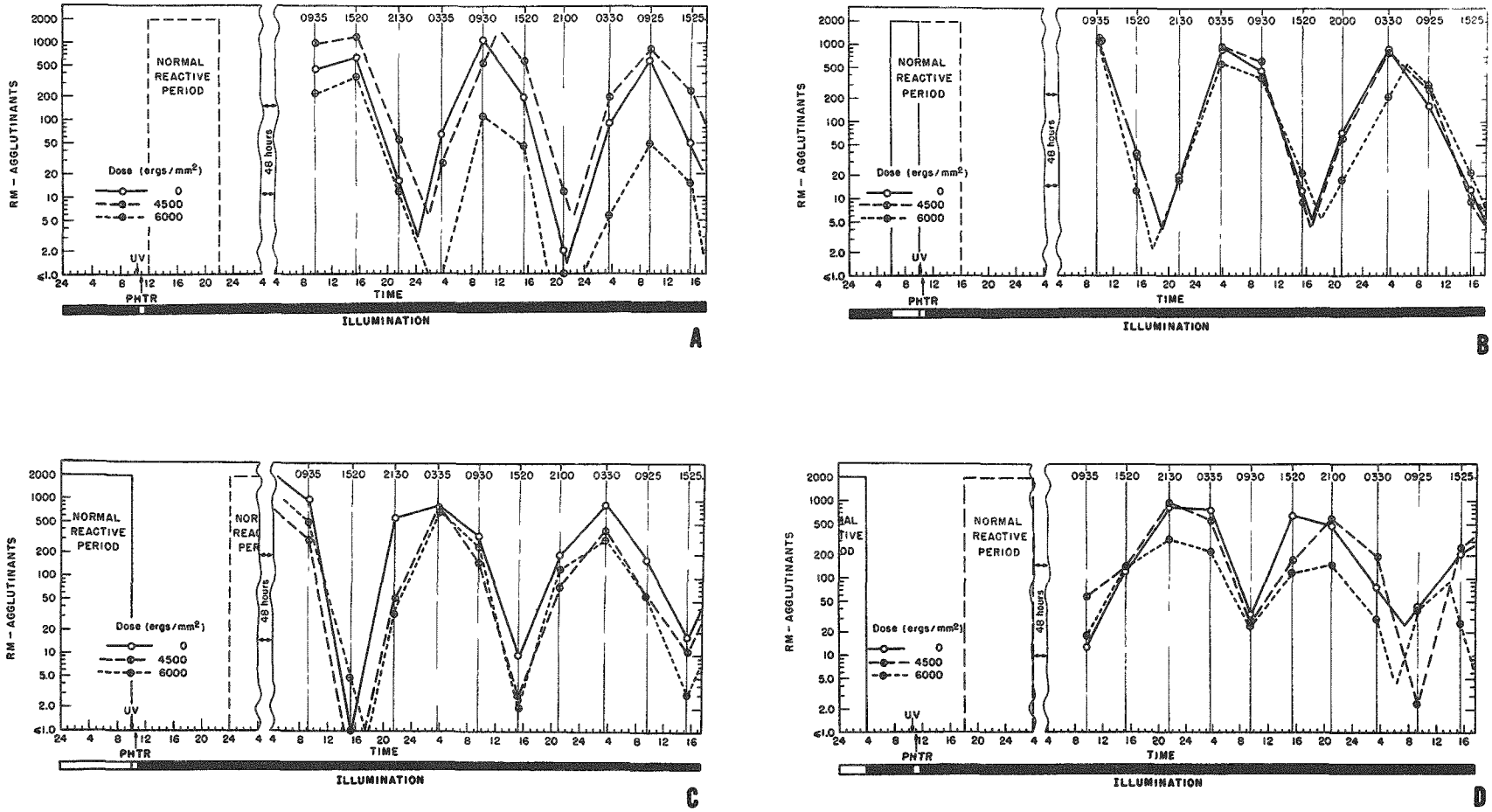

Figure 18. Like Figure 17, except that 420 fc of photoreactivating light was applied 15 minutes after UV dose for one hour.

abscissae) population A was in the early nonreactive or scotophilic phase, population B was in the middle to late scotophilic phase, population C was in the early reactive phase and population D was in the middle to late reactive phase.

At 0945, the four populations were removed from their compartment, and aliquots were transferred to 10-cm petri dishes that served as exposure vessels. A germicidal lamp* was employed as source; the irradiance at 254 mμ was 50 ergs sec^{-1} mm^{-2}, and the exposure times were zero, 90 and 120 seconds. These operations were performed under dim red light, and UV exposures were completed by 1015. After irradiation, the populations were retained in the dark or exposed to photoreactivating (PHTR) light (420 foot-candles (fc), "daylight" fluorescent illumination) for 1 hr. One-ml aliquots of the 24 respective cell populations were transferred under dim red light from the exposure vessels into 240 storage vials. These vials were placed in black envelopes within copper cannisters suspended in a water bath held at 25° C. The first counts (24 vials, 3 on each graph) were made 71 hr after UV exposure (0935), and counts were made at 6-hr intervals for three consecutive days until all 10 sets of the vials were counted. The counts included two measures: 1) the number of experimental cells that participate in the initial agglutination masses formed between the cells in the vials and known reactive test cells[1] of complementary mating type 10 min after mixing; this measure is the reaction magnitude (RM) of agglutination; 2) the number of conjugant pairs formed as a consequence of this mixture, 6 hr after mixing. In each measure it was possible to distinguish between the experimental animals and the testers, because the former were colorless, whereas the latter were green (*Chlorella*-containing cells of mating type A). The contribution of the second measure was to assign an ascending or descending direction to a curve from a given point: this is valid because many conjugants are formed from early reactive period mixtures, whereas few conjugants are formed from late reactive period mixtures. (By this method each intersection of lines that occurs at some place other than at a measured point on the plotted curves was inferred; e.g., the first 2 peaks for the 6000 ergs/mm^2 category, Fig. 17A.)

Results

The effects of exposure to far ultraviolet are shown in Fig. 17. Three general effects are obvious. (a) In each category there is an endogenous rhythmicity of reactivity with cycles of approximately 23 hours' duration. (b) There is apparent phase shift to the right (delay) that is UV dose-dependent. (c) The amplitudes (RM) of the response curves are only slightly affected by low doses of UV. (Higher doses, correlated with some cell death, cause an extreme depression of maxima and a slight elevation of minima.[3])

*15 W Westinghouse Sterilamp G15T8.

The results of subsequent exposure of ultraviolet-irradiated cells to visible irradiances are shown in Fig. 18; (a) The approximately diurnal rhythmicity (23 hours) is again evident. (b) There are not conspicuous phase shifts experienced by treated groups independently of the controls. (c) The response curves are either not at all, or only slightly, depressed, and there is a slight elevation of minima in curve D.

A further analysis of these results shows that there are three rather general superimposing effects that can be distinguished from the more specific UV-plus-dark and UV-plus-light effects on the cellular mechanism. The superimposing effects are (a) an endogenous 23-hr rhythm, (b) the initial exposure of all categories to dim light and (c) the effect of photoreactivating light itself on controls. In Table 8 such an analysis is summarized, and the consequent minimum and maximum sensitivity phases are inferred from it. It should be noted in the table that in categories 17A and 17B the controls are 2.5 hr earlier than expected. This is compatible both in direction and degree with the shift expectations that ensue from foreshortening of the photoperiod[1] in 17B, and from a dim light stimulus applied during the late scotophilic phase in 17A.[2] It is probable that the stimulus in this case was the dim red light to which the cultures were exposed at the start of the experiment. However, despite these slight control irregularities, the ultraviolet effect is conspicuous.

TABLE 8

An analysis of UV-induced phase shift to distinguish between the normal light effect, the UV effect and the photoreversing effect

The figures are extrapolated from the data of UV categories A-D and corresponding dark controls (Fig. 17) and UV + light categories A-D and corresponding light controls (Fig. 18). The expected time of the reaction peak (column 3) is calculated for each category on the basis of a 23-hour cycle, four days after the last photoperiod experienced before the start of the experiment. Observed time (column 4) refers to the actual peak closest to the expected one. The difference in hours between these values is entered as an early or late shift in columns 5 and 6. The average shifts induced by UV are entered in columns 7 and 8 as hours later than the observed peak (column 4).

Code			Nonirradiated Controls					Irradiated	
			Time of reaction peak			Shift (from 3)		UV-Induced shift (from 4)	
								4500 ergs mm^{-2}	6000 ergs mm^{-2}
(1) Fig.	Graph	PHTR*	(2) Last photoperiod	(3) Expected	(4) Observed	(5) Hours	(6) Directions	(7) Hours	(8) Hours
17	A	-	1700	1300	1030	2.5	early	3.8	7.1
18	A	+	1700	→	1130	1.5	early	0.8	0.0
17	B	-	1100	0700	0430	2.5	early	2.5	3.5
18	B	+	1100	→	0530	1.5	early	0.0	0.7
17	C	-	0500	0100	0100	0	on time	3.0	4.0
18	C	+	0500	→	0350	2.8	late	0.0	0.0
17	D	-	2300	1900	1900	0	on time	5.0	8.5
18	D	+	2300	→	2200	3.0	late	1.0	1.0

*Exposed (+) or not exposed (-) to 1 hour "photoreactivating" (PHTR) light.

In both 17A and 17B the irradiated categories are late whether compared with the controls as they are (early, column 4) or as they should have been without phase shift ("on time," column 3). We can further conclude from this that UV-induced phase-delay is not entirely (if at all) due to some failure of the cells to respond to a phase-shifting stimulus.

In 17C the controls are on time, indicating no response to a short dim light stimulus in the very early scotophilic phase; the irradiated group is late and clearly sensitive to phase delay by UV. In 17D the controls are on time, which is compatible with an interruption of the mid-scotophilic phase by dim light(2) (Before this time, the shift is late; after it the shift is early.) The irradiated categories are conspicuously late; however, even here the magnitude of the delay is possibly influenced by pre-treatment with dim red light since the subsequent exposure to white light at this time (18D below) produces an unexpected synergism.

The photoreactivated categories can similarly be compared: it appears that each of the control and UV-irradiated populations that have been illuminated after UV-irradiation reacts synchronously. Was this because the UV delays were prevented or because illumination maximized delays in each instance? In three cases this distinction is possible. In 18A and 18B light applied before or at the beginning of the normal photoperiod induces the reaction to occur ahead of schedule. These are not so early as 17A and 17B controls above because the stronger stimulus occurred an hour later. Nevertheless, the UV-irradiated categories in 18A and 18B are just as early as their light controls, although they should have been at least 1.0 to 4.5 hr later than even the 17A and 17B dark controls had photoreactivation not occurred.

In 18D the controls are late, which is unexpected since illumination in the late scotophilic phase usually shortens the phase; however, when added to red light mid-scotophilic interruption (17D above) the effect appears to be that of an early or prolonged scotophile interruption, and the phase shift is delay. Compatible with this interpretation is the broadening effect of a slightly heterogenous cell population. However, the UV-irradiation categories show only an hour greater delay, whereas they would have been at least 2 to 5.5 hr later had photoreactivation not occurred.

These distinctions cannot be made in 18C in which the UV-irradiated categories are no later than the controls, but were as late as they would have been without light, although possibly more synchronous. It is conceivable that the UV-induced phase delay was photoreversed and a photo-induced phase delay substituted for it, but this experiment cannot decide that issue.

Discussion

This demonstration that phase shifts in cellular rhythmicity can be induced by ultraviolet irradiation should prove encouraging to the investigator who hopes to find clock escapements for the rhythm-controlling timepieces at the cellular level. It is of further interest that the UV-induced damage is photoreversible. This brings the phenomenon into line with a large number of diverse biological mechanisms, none of which in the past has been directly associated with rhythms. The high efficiency of ultraviolet light, both in absolute energy and in time for induction, must ultimately be compared with induction efficiencies of the longer wavelengths that are generally associated with phase shift but not usually with either nucleic acid absorption or photoreactivation. Separate avenues of phase shift induction may thus be employed by visible and by far ultraviolet radiant energy within the cell. In the preliminary speculations, the conspicuous intranuclear and nucleolar[3,4] effects of far ultraviolet light should not go unnoticed.

While little is known about the chemistry or biosynthesis of mating substance, the present results can be described within the framework of the heuristic scheme previously adopted for Paramecium.[1] In that terminology, the times at which cells are most sensitive to phase shift are those at the middle and end of the scotophilic phase, when mating-substance precursor is being synthesized and during the time just prior to the conversion of such precursors to mating substance.

Summary

1. Phase shifts in cellular rhythmicity in Paramecium can be induced by low doses of ultraviolet irradiation.

2. Stages most sensitive to induction are the middle and late portions of the scotophilic phase.

3. Phase-shift induction by UV is photoreversible by radiant energy from the visible region of the spectrum.

References

1. Ehret, C. F., An analysis of the role of electromagnetic radiations in the mating reaction of Paramecium bursaria. Physiol. Zool 26:274-300 (1953).

2. Ehret, C. F., The effects of pre- and post-illumination on the scotophilic recovery phase of the Paramecium bursaria mating reaction. Anat. Record 122: 456-457 (1955).

3. Ehret, C. F., The photoreactivability of sexual activity and rhythmicity in Paramecium bursaria. Radiation Research 3:222-223 (1955).

4. Kimball, R. F. and N. Gaither, The influence of light upon the action of ultraviolet in Paramecium aurelia. J. Cellular Comp. Physiol. 37:211-233 (1951).

PROGRESS REPORT: COLONY-FORMATION INHIBITION OF A T5-RESISTANT VARIANT OF *ESCHERICHIA COLI* BY THE BACTERIOPHAGE T5

Harold E. Bendigkeit and Herbert E. Kubitschek

Two T5-resistant mutants of *E. coli* strain B/1,t, designated E and L, were described in a previous report.[1] Studies have been undertaken to determine the nature of colony-formation inhibition of the L variant by bacteriophage T5.

The division rates of E, L, and parental strains appear identical in the absence of T5. In the presence of appropriate concentrations of T5, a growth inhibition of the L variant has been observed in both liquid and semisolid media.

To assay the inhibitory activity in semisolid media, L cells are seeded in nutrient agar in the presence or absence of T5, and colonies are counted at 18 hr and again after 3 days' incubation at 37°C. Colony counts do not increase after 3 days. Two effects are noticeable from the results:

1. Inactivation. At concentrations greater than 5×10^9 T5 particles/ml there is a decrease in colony counts measured at 3 days. The effect (Fig. 19) is dependent upon the concentration of active T5.
2. Delay in colony appearance. With a standard inoculum of 100 L cells per petri dish, all colonies are countable within 18 hr when T5 concentrations less than 10^7/ml are used. At T5 concentrations greater than 5×10^8/ml no colonies appear at 18 hr, but all colonies have appeared by 3 days.

In an effort to determine whether the delay is caused by T5 particles or by some other component of the suspension obtained in T5 production, the concentrations of active T5 were altered. Treatment by heat, ultraviolet light, sonic vibration, centrifugation, and adsorption to sensitive bacteria were utilized separately or in combinations. In all cases, the inhibitory activity of resulting suspensions was predictable directly from the concentration of active T5 remaining (Fig. 20). Since this result is independent of the method of treatment, it implies that the inhibitory activity of T5 suspensions resides in the active T5 particles, not in another component of the suspensions.

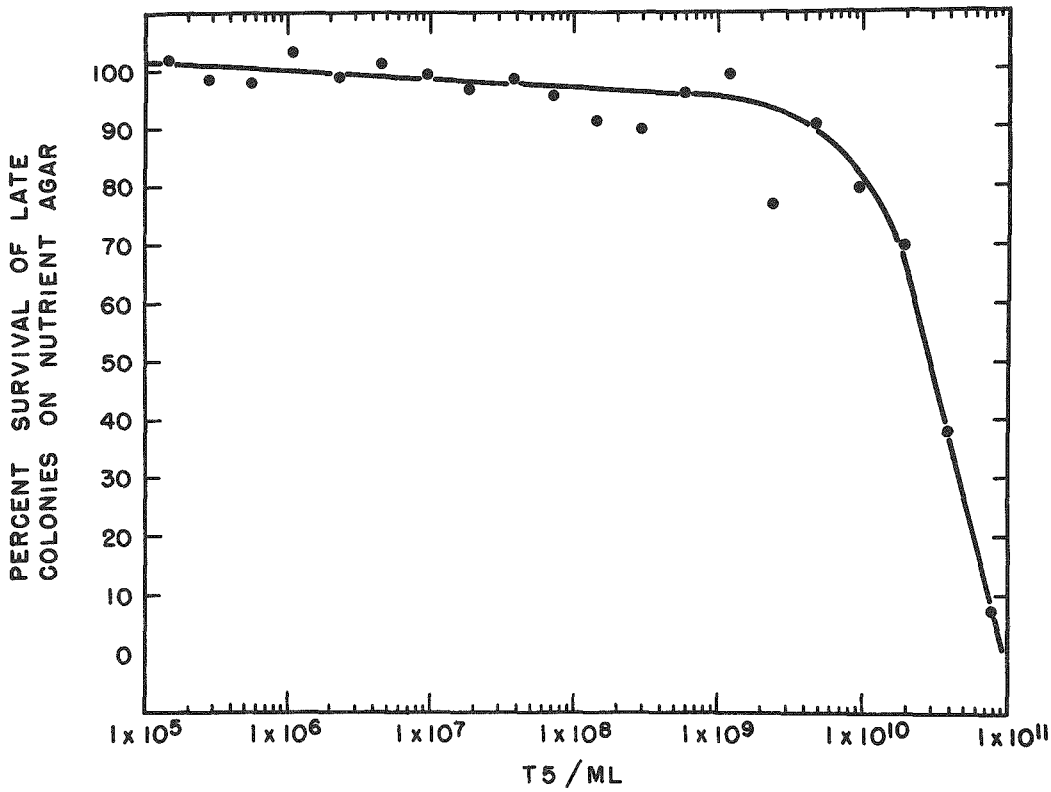

Figure 19. Colony survival in the presence of different concentrations of phage.

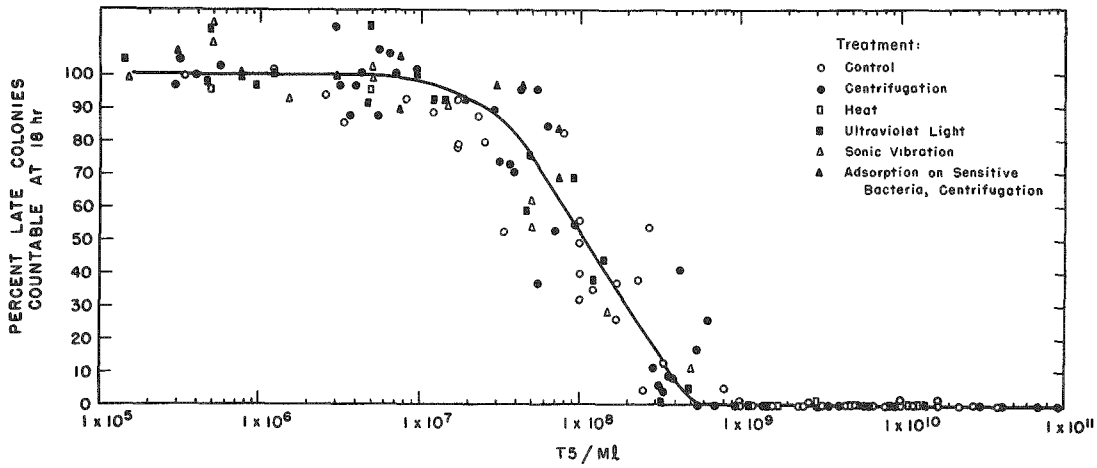

Figure 20. The fraction of colonies appearing within 18 hours as a function of phage concentration.

Reference

1. Kubitschek, H. E. and H. E. Bendigkeit. A new variant for T5-resistance in Escherichia coli. Quarterly Report of Biological and Medical Research Division, Argonne National Laboratory. ANL-5576, p. 21 (1956).

TOXICITY OF Sr^{90} AND OF Ca^{45} IN MICE

III. Effect of Sr^{90} Upon Life Span and Neoplasms of Bone and the Blood-forming Tissues

Miriam P. Finkel, Birute O. Biskis, and Gertrude M. Scribner

Previous reports in this series concerning the study of the long-term toxicity of Sr^{90} in CF No. 1 female mice have described the general pattern of the experiment and the results during the first 300 days[1] and have evaluated the data collected by the 625th day after injection.[2] The experiment was terminated at 1045 days, when the last animal died. Analyses of the morbidity data and some phases of the histopathologic studies have now been completed.

Table 9 lists the dose levels and gives the size of each group. An isotonic equilibrium mixture of Sr^{90} and Y^{90} chloride, at pH 5-6, had been injected into a tail vein at the start of the experiment.

TABLE 9

Dose levels and population sizes

Group	Number of animals	Injected dose		$\overline{M}$ expected retained dose at 400 days (μc/kg)
		total μc	μc/g	
POX-1	15	224	9.33	1166
POX-2	30	168	7.0	875
POX-3 } PO-1 }	45	106	4.5	561
PO-2	30	50	2.2	275
PO-3	45	20.4	0.88	110
PO-4	45	10.2	0.44	55
PO-5	60	4.6	0.20	25
PO-6	75	2.0	0.088	11
PO-7	90	1.0	0.044	5.5
PO-8	105	0.21	0.0089	1.1
PO-9	120	0.10	0.0045	0.56
PO-10	150	0.029	0.0013	0.16
POP	150	0	0	0
Total	960			

The dosage was based on the average weight of the entire population of 960 animals, which had been completely randomized one week before injection. At high levels only a few animals were needed because the

effects were expected to appear rapidly and be unequivocal; at low levels many animals were required because the effects were expected to appear late and be more difficult to recognize. It was intended that the highest dose reach or exceed the amount necessary to kill 50% of the population in 30 days (30-day LD_{50}) and that the lowest dose be so low that the treated animals would be indistinguishable from the control animals (the indifference dose). Originally, 4.5 $\mu c/g$ (group number PO-1) was the highest level; POX-1, 2, and 3 were added when this proved to be below the 30-day LD_{50}. The last column in Table 9 gives the average expected retained doses 400 days after injection, at which time approximately 12.5% of the injected dose remains.(3) At 600 days, which was the average survival time of the control animals, about 11% remains. The lowest dose level thus resulted in a body burden that was roughly equivalent to 10 times the currently accepted maximum permissible level for personnel engaged in atomic energy work, or to 100 times the level set for the general population.

Survival

The mortality data are presented as survival curves in Fig. 21 and as life-expectancy curves in Fig. 22. In both figures the 5 lowest dose groups have been combined in a shaded area because there were no consistent differences among them, and curves of their individual values are an indistinguishable network of recrossing lines. The control population had the highest percentage of survivors through 700 days and demonstrated the greatest life expectancy through 350 days.

Two related questions of fundamental importance in evaluating the toxicity of low levels of irradiation are whether there is a linear relationship between dose and effect and whether there is a threshold dose below which there is no effect. Survival data can be examined from this point of view, as illustrated in Fig. 23, where both the logarithm of time to 50% mortality and the logarithm of the average survival time have been plotted against the logarithm of the dose. These two curves are very similar because neither acute epidemic nor chronic infections, which can result in temporary high mortality rates among segments of the population, occurred. Through 100 days the curves reflect acute and subacute irradiation death; through 500 days they primarily reflect death from tumors. At levels below 0.1 $\mu c/g$ the treated animals died, on the average, sooner than the control animals, but their deaths were not associated obviously with any particular disease. Although these three portions of the curve separately may suggest linearity between dose and response, the entire curve cannot be described by a simple linear function.

The second important feature of Fig. 23 is the apparent threshold for the life-shortening effect at an injected dose of about 0.0005 $\mu c/g$, which is roughly equivalent to 3.5 times the maximum permissible body burden for people engaged in atomic energy work and 35 times that recommended

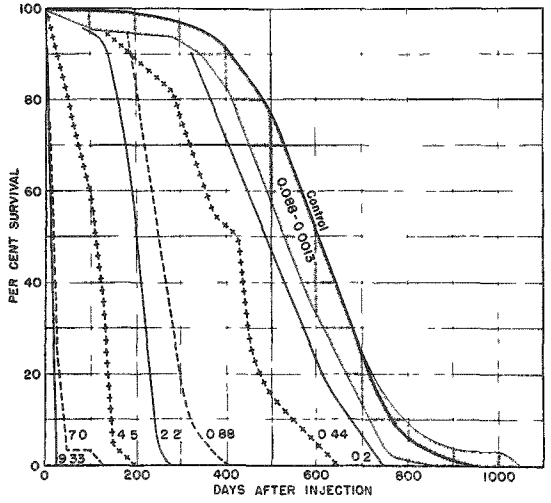

Figure 21. Survival after intravenous injection of Sr^{90} (Y^{90}).

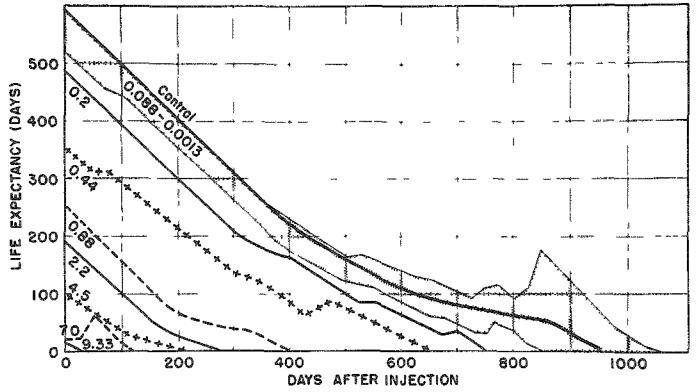

Figure 22. Life expectancy after intravenous administration of Sr^{90} (Y^{90}).

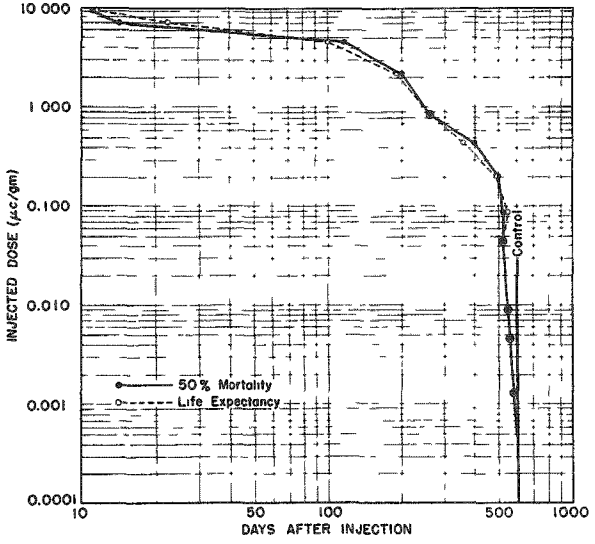

Figure 23. The median and mean survival times after intravenous injection of Sr^{90} (Y^{90}).

for the general population. As we speculate in this realm, however, we must point out that, although the life shortening noted after the injection of 0.044 $\mu c/g$ was so great that its probability of occurring by chance was only 1 in 100, the life shortening noted after 0.0089 $\mu c/g$, the next lower dose, was not significant ($P = 0.1$). The differences at the two lowest levels were even less significant. A difference as small as that observed at the lowest dose would be significant at the 1% confidence level if it had been based upon 1393 treated animals compared with the same number of control animals. The next point, at 0.0045 $\mu c/g$, similarly would require 286 animals in each group for it to be considered to differ significantly. Thus, although a straight extension of the curve suggests an apparent threshold at an injected dose of 0.0005 $\mu c/g$, a significant difference in life span was not seen below an injected dose of 0.044 $\mu c/g$.

Tumors of and around Bone

One of the characteristic sequelae of poisoning with Sr^{90} is the appearance of skeletal tumors. Since mouse bones are very small compared to the range of the β-ray emitted by the Y^{90} daughter of Sr^{90}, it is conceivable that in this species tumors appear in tissues adjacent to bone as well. For example, a mouse femur is only about 1.5 mm in diameter whereas the maximum range of the Y^{90} β-ray in tissue is approximately 10 mm, and its average range is 1.2 mm. The incidence of animals with various tumors that might be attributed to the isotope are tabulated in Table 10. There was a pronounced association of dose with both osteogenic sarcomas and hemangioendotheliomas of bone marrow and a suggested association with epidermoid carcinomas of the oral cavity. Fibrosarcomas adjacent to bone and benign bony tumors were not influenced by radiostrontium except insofar as their total incidence was decreased at levels that resulted in markedly decreased survival time.

Many animals had more than one osteogenic sarcoma, and multiple tumors were the rule among those that had received 0.44 $\mu c/g$ or more. As many as 13 tumors were detected in one animal, and probably serial sectioning of the entire skeleton would reveal many more. The distribution of tumors among the animals of each dosage group was tested for randomness by comparing the observed frequencies of tumors per mouse with a Poisson distribution. A non-random distribution would indicate that cases of multiple tumors were due either to the spread of a single tumor to other skeletal sites or to the presence of particularly sensitive animals that responded with many tumors instead of one. The observed frequencies fit the calculated frequencies so well that the tumors appear to be randomly distributed among the animals. For this reason it is felt that the number of tumors is a more accurate statistic than the number of tumor-bearing animals.

TABLE 10

Incidence of animals with tumors (%)

Injected dose (μc/g)	Osteogenic sarcoma (121)* Osteochondrosarcoma (1)*	Hemangioendothelioma of bone marrow (36)*	Epidermoid carcinoma of oral cavity (10)*	Fibrosarcoma around bone (5).* Giant cell tumor of disc (1)*	Osteoma (125).* Osteochondroma (3).* Odontoma (1)* (?) Caudal fibroma (7)*
4.5	0	0	0	0	0
2.2	63.3	3.3	0	0	0
0.88	97.8	11.1	2.2	0	0
0.44	71.1	13.3	2.2	0	8.8
0.20	13.3	8.3	1.7	0	13.3
0.088	4.0	6.7	1.3	1.3	20.0
0.044	5.6	0.3	3.3	0	14.3
0.0089	0	1.9	0	1.9	17.2
0.0045	3.3	2.5	0.8	0.8	19.1
0.0013	2.0	2.0	0.7	0.7	19.3
Control	2.0	2.0	0.7	0.7	17.3

*Number of animals

In Fig. 24 the dashed line plots the logarithm of the total incidence of tumor-bearing mice against the logarithm of the dose; the solid line shows the average probability of dying with a malignant bone tumor. The latter value is obtained by averaging the ratios "number of tumors to come per number of animals still alive," calculated at 25-day intervals. The control values are indicated by the horizontal dashed and solid lines. As in the case of the survival data, the resulting dose-response curves are not linear, and there is an apparent threshold below which the treated animals are indistinguishable from the control animals. The lowest dose that resulted in a significantly higher number of osteogenic sarcomas was 0.044 μc/g, the same level that resulted in a significant difference in survival. At the next lower level (0.0089 μc/g) there were no malignant tumors of the bony tissues.

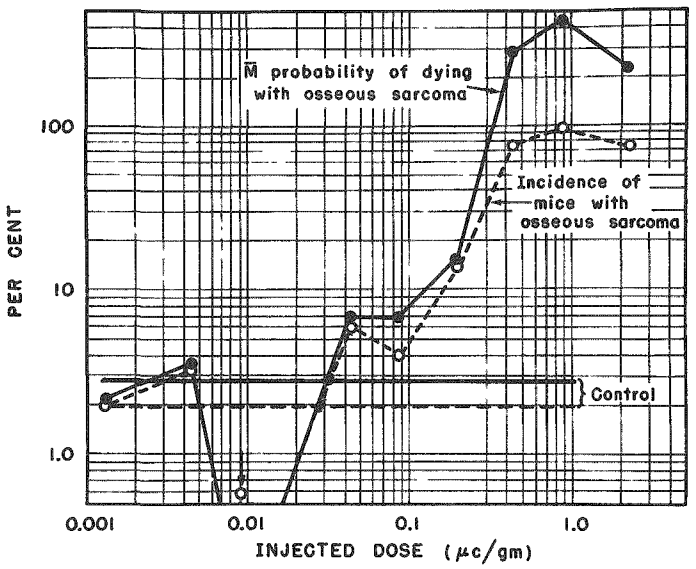

Fig. 24

Morbidity expectation and total incidence of mice with osteogenic sarcomas after intravenous administration of Sr^{90} (Y^{90}).

Tumors of the Blood-forming Tissues

Another family of neoplasms occurring in the mouse that are influenced by irradiation are those that show certain similarities to the leukemias of man. These tumors have been designated by a variety of names, among which are mouse leukemias, lymphomas, lymphoid tumors, thymic tumors, and reticular tumors. "Tumors of the blood-forming tissues" is cumbersome, but it has the advantages of greater accuracy and decreased susceptibility to criticism. In Fig. 25 the logarithm of the morbidity rate with these tumors has been plotted against time.

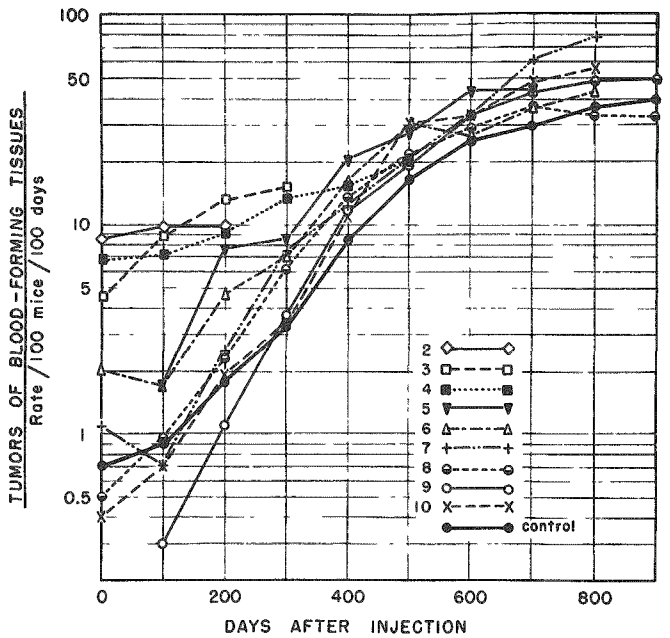

Fig. 25

Rate of morbidity with tumors of the blood-forming tissues after intravenous administration of Sr^{90} (Y^{90}). (See Table 9)

PO-2
PO-3
PO-4
PO-5
PO-6
PO-7
PO-8
PO-9
PO-10
Control

It is at once evident that the untreated CF No. 1 female mouse displays a very high incidence of this disease and that the morbidity rate increases with age. It is also evident that the disease appeared earlier among the animals of the higher dosage groups (0.088 $\mu c/g$ and above), but unscrambling the results at lower levels is difficult. Since the impression was gained that irradiation with Sr^{90} causes the disease to become manifest earlier than would occur naturally, the data were examined from this point of view. In Fig. 26 the number of days from injection to the time when 20% of the population had died with tumors of the blood-forming tissues is plotted against the logarithm of the dose. The control animals reached this 20% incidence 565 days after the beginning of the experiment. The two lowest points on the curve are not significantly different from the control value; the point at 0.0089 $\mu c/g$ is significant at the 1% confidence level. This is one-fifth of the lowest dose that resulted in a significant difference in life span and in incidence of osteogenic sarcomas.

A plot of the percentage decrease in time to a 20% incidence of reticular tumors cannot be described adequately by a simple linear function or by any of a number of mathematical transformations. However, the three lowest values that are significantly different from the control value (at 0.088, 0.044, and 0.0089 $\mu c/g$) do lie along a straight line (Fig. 27).

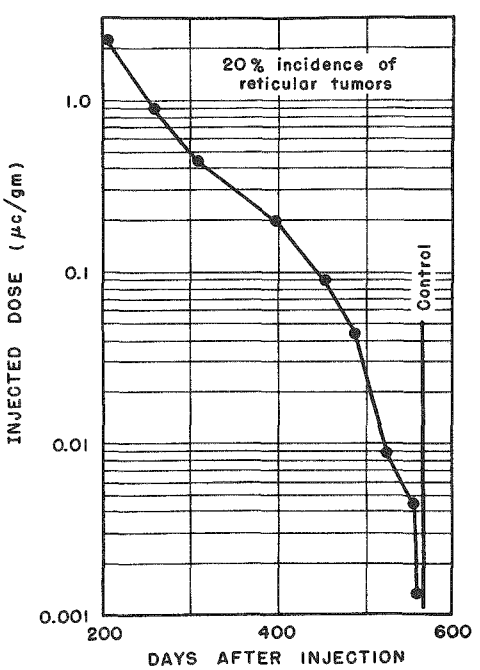

Fig. 26

Time required to reach 20% incidence of tumors of the blood-forming tissues after intravenous administration of Sr^{90} (Y^{90}).

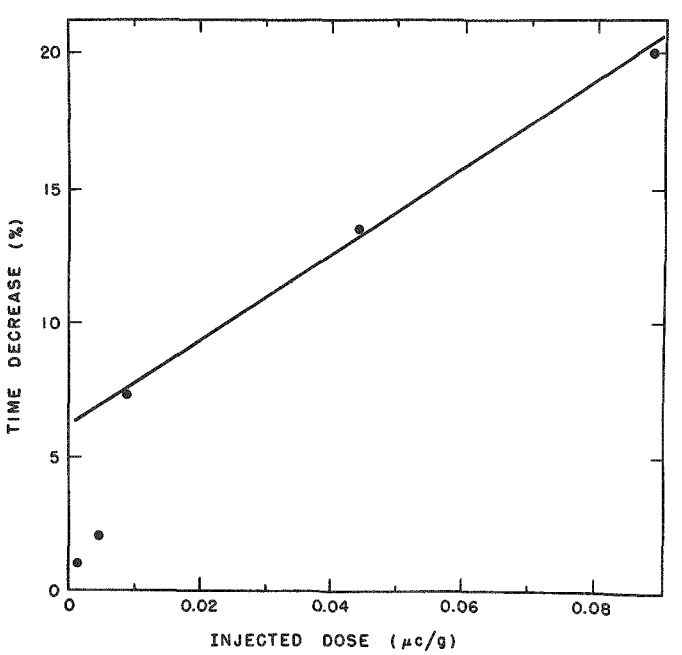

Fig. 27

Percentage decrease in time (based on control population) required to reach a 20% incidence of tumors of the blood-forming tissues after intravenous administration of Sr^{90} (Y^{90}).

The values of the two lowest dose levels (at 0.0045 and 0.0013 $\mu c/g$) which do not differ significantly from the control value, were examined to determine whether they fell within the statistical range of an extension of this straight line. They were found to lie outside of this range. Thus, these data indicate that a threshold dose must be exceeded before there is a measurable change in the course of tumors of the blood-forming tissues.

Discussion and Summary

Many interesting portions of this experiment have yet to be examined and evaluated, but analyses of the data concerning mortality and morbidity with neoplasms of bone and blood-forming tissues are approaching completion.

Neither the average life expectancy nor the time to 50% mortality plotted against the dose resulted in curves that could be described adequately by a simple linear function. At the three lowest levels the differences in survival between the experimental and the control populations were within the range of expected variation. A statistically significant difference in life expectancy was not seen below an injected dose of 0.044 $\mu c/g$; this is roughly equivalent to a body burden of 350 $\mu c/man$.

The data on osteogenic sarcomas similarly failed to demonstrate a linear dose-response curve, and the number of such neoplasms among the 3 lowest dosage groups fell within the control range. Thus life span and malignant tumors of bone appear to be equally sensitive indicators of radiation damage. Neoplastic change of the blood-forming tissues, however, proved to be more sensitive criterion of injury. Although the total incidence of reticular tumors was not markedly influenced by radiostrontium, these neoplasms appeared earlier as the dose increased. The time required to reach a 20% incidence was significantly shorter among the animals that had received 0.0089 $\mu c/g$ than it was among the control animals. This injected dose resulted in a body burden of approximately 1 $\mu c/kg$, which is roughly equivalent to 70 $\mu c/man$. Below this level the treated animals were indistinguishable from their controls.

Since it has not been possible to demonstrate a linear relationship between dose and response, the use of straight line extrapolations from fragmentary data is contraindicated. In addition, the fact that there were no differences in life span or neoplasms of bone and blood-forming tissues among the control population and the groups that had received the lowest doses suggests that there is a threshold, and consequently a true "indifference" dose, for pathologic change as measured in the total mammalian organism.

Acknowledgement

We are greatly indebted to J. Gurian for performing the statistical tests.

References

1. Finkel, M. P. and G. M. Scribner. Toxicity of strontium-90 and of calcium-45 in mice. I. Status of experiments 200-300 days after injection. Quarterly Report of Biological and Medical Research Division, Argonne National Laboratory. ANL-5456, p. 36-37 (1955).

2. Finkel, M. P. and G. M. Scribner. Toxicity of strontium-90 and of calcium-45 in mice. II. Status of experiments 625 days after injection. Quarterly Report of Biological and Medical Research Division, Argonne National Laboratory. ANL-5597, p. 16-20 (1956).

3. Finkel, M. P., B. J. Tellekson, J. Lestina, and B. O. Biskis. The influence of dosage pattern upon the toxicity of Sr^{90} in mice. I. Preliminary experiment and 212-day survey of the long-term study. Quarterly Report of Biological and Medical Research Division, Argonne National Laboratory. ANL-5732, p. 21-31 (1957).

XANTHINE CONCENTRATION AND XANTHINE OXIDASE ACTIVITY IN CHICKEN LIVER HOMOGENATES IN THE INITIAL POSTIRRADIATION PERIOD

S. Phyllis Stearner, Margaret H. Sanderson, and Emily J. Christian

In the initial postirradiation period, the actively circulating blood volume in the chicken liver decreases markedly.[1] The formation of uric acid from ammonia takes place entirely in the liver in this species, and a significant decrease in functional activity may result in accumulation of ammonia or intermediate products in the conversion to uric acid. The measurement of the uric acid precursors, xanthine and hypoxanthine, and the xanthine oxidase activity present in the liver should give some insight into this aspect of liver function.

We report here the xanthine oxidase activity and xanthine concentration in the livers of normal and X-irradiated chickens. Three- to 4-day chicks and 6-month-old roosters were exposed to 1000 r and 1200 r of X-rays, respectively, delivered at about 40 r/min. Birds were sacrificed 4-5 hours after irradiation to obtain liver samples. Hypoxanthine-xanthine concentration and xanthine oxidase activity were determined using the following procedure. Approximately 1 g of tissue was homogenized in cold phosphate buffer pH 7.3. Appropriate quantities of xanthine, xanthine oxidase, and/or buffer were added to 100-mg aliquots of homogenate and the volume made up to 4 ml. All suspension mixtures were incubated with agitation at 40° C for 1 hr and the increase in uric acid concentration measured. The amount of xanthine converted during the period of incubation indicates the amount of enzyme activity. On the other hand, accumulation of hypoxanthine suggests either insufficient xanthine oxidase activity or the lack of some intermediate substance.

Results

The liver of both irradiated and nonirradiated chickens contained excess xanthine oxidase activity and could readily convert additional xanthine to uric acid. Chick liver showed a higher enzyme activity per gram liver tissue than did that of the rooster, and irradiation produced no significant change (Table 11). All livers contained some xanthine, indicated by an increase in uric acid during the incubation period. There was no difference between control and irradiated chicks and only a small increase in irradiated roosters. The postirradiation increase in uric acid concentration in liver and kidneys is related to the increase in blood urate concentration that occurs at this time.

TABLE 11

Effect of X-irradiation on xanthine oxidase activity and xanthine and uric acid concentration

	Chick*		Rooster*	
	Control	Irradiated	Control	Irradiated
Excess xanthine oxidase activity: mg of added xanthine converted to uric acid per gram of liver	8.8 (4)	7.9 (5)	2.0 (3)	3.1 (4)
Xanthine concentration. mg/g liver	0.737 (5)	0.734 (9)	0.267 (3)	0.395 (4)
Uric acid concentration:				
mg/g liver	0.458 (5)	0.713 (9)	0.489 (3)	0.617 (4)
mg/g kidney	0.731 (3)	10.507 (5)	0.736 (2)	1.474 (2)

*Number of animals in each group is indicated in parentheses.

All evidence indicates that there is no early radiation disturbance of hepatic function for conversion of hypoxanthine to uric acid. Some hepatic functions may be more radiosensitive, however, and accumulation of other intermediate metabolites has not been investigated. Possible radiosensitive enzyme systems in chicken liver should also be considered.

Reference

1. Stearner, S. P., M. H. Sanderson, E. J. Christian, and A. M. Brues. Evidence of circulatory failure in the early radiation response of the chicken. Am. J. Physiol., in press.

PROGRESS REPORT: THE HOMOCYSTEINE TRANSMETHYLASE SYSTEM

Stanley K. Shapiro and David A. Yphantis

Previous reports have described the transmethylation of homocysteine with the methyl donors S-methyl-L-methionine and S-adenosyl-L-methionine.[1,2] In order to gain some insight into the mechanism of transmethylation, purification of the enzyme(s) was felt to be essential. To facilitate this project a new method for the assay of enzymatic activity has been developed.

Assays are performed by incubating a mixture of the enzyme, L-homocysteine and S-methyl-L-methionine ($C^{14}H_3$) at 35° C for a few minutes. An aliquot is placed on a short ion exchange column (2 X 0.5 cm of Dowex 50 X 4) in Li^+ form. The labeled substrate (S-methyl-L-methionine) is retained quantitatively on the column, while the labeled product of the reaction, methionine, may be collected quantitatively by washing the column with small aliquots of distilled water. The washings (1 ml) are collected in a polyethylene bottle, scintillator fluid is added, and the activity is measured in a scintillation counter.

In principle the method depends only on a simple method to separate quantitatively the labeled substrate from the labeled product. With our former assay for methionine [1] a typical assay required 5 to 6 hrs. With the use of this tracer technique it is now possible to complete such an assay in 15 min. The assay may be made over 25 times as sensitive in the determination of enzymatic activity.

Good yields of enzyme may be obtained in several ways. Yeast cells or bacterial cells disrupted by sonic vibration yield active extracts. For the preparation of large batches of enzyme from baker's yeast, it has been most convenient to suspend the cells in an equal volume of water and freeze the suspension in liquid nitrogen. The mixture is then thawed rapidly, refrozen and again thawed. The supernatant of the centrifuged suspension serves as the crude enzyme source.

Partial purification of this crude extract has been accomplished. After incubation for 1 hr with ribonuclease the crude enzyme solution is centrifuged and dialyzed against a low concentration of phosphate buffer. The solution is placed on a chromatography column of hydroxylapatite at pH 6.8.[3] About 60% of the activity is recovered in a fraction assaying 15-20 times the specific activity, based on protein concentration, of the crude enzyme.

References

1. Shapiro, S. K. Biosynthesis of methionine from homocysteine and S-methylmethionine in bacteria. J. Bacteriol. 72:730-735 (1956).

2. Shapiro, S. K. Progress report. The biosynthesis of methionine in bacteria. A new transmethylation. Quarterly Report of Biological and Medical Research Division, Argonne National Laboratory. ANL - 5655, pp. 59-60 (1956).

3. Tiselius, A., S. Hjerter and O. Levin. Protein chromatography on calcium phosphate columns. Arch. Biochem. and Biophys. 65:132-155 (1956).

THE METABOLIC RELATION BETWEEN ADENINE AND SULFUR AMINO ACIDS

The Stability and Hydrolysis of S-Adenosylmethionine

Leo W. Parks and F. Schlenk

Recent improvements in the methods for biosynthesis and isolation of S-adenosylmethionine [1,2] have stimulated extensive experimentation with this compound. Detailed information on its stability under various biochemical conditions is a prerequisite to microbiological, nutritional, and enzymatic research involving this substance. Not only is it desirable to have an estimate of the residual amount of S-adenosylmethionine at any given time during an experiment, but in many instances it is necessary also to know what fragments may accrue. Erroneous results may be surmised, especially in microbiological studies with mutants, if the response to hydrolytic products is mistaken for an effect of the parent substance. Experiments were carried out, therefore, on the stability of S-adenosylmethionine under the conditions of biological experimentation. Our study soon revealed that several hydrolytic processes occur simultaneously. To gain insight into the conditions which favor individual reactions, extremes of pH and temperature were included in this investigation. The latter phase of our work revealed conditions for splitting methionine from the molecule and for hydrolysis to adenine and a hitherto unknown fragment, S-ribosylmethionine. Directions for preparation and a description of some of the properties of this new compound are given.

Our data extend the earlier observations of Cantoni, Baddiley, and Jamieson [3,4] on the hydrolysis of S-adenosylmethionine; they observed the formation of adenine by acid hydrolysis and of methylthioadenosine and homoserine by heating in neutral solution.

Methods and Results

The preparation of S-adenosylmethionine from yeast, as well as suitable analytical techniques, have been described in our earlier reports.[1,2]. Minor details and modifications will be noted in connection with the experiments. Dimethyladenosylthetin and 5'-methylthioribose were synthesized from 5'-methylthioadenosine.[5,6,7]

Stability under physiological conditions. The decline in the concentration of S-adenosylmethionine (6 μM/ml) under conditions resembling those of biochemical experimentation was studied by incubation in 0.05 M phosphate buffer at 30° C in the presence of a small amount of toluene as

a preservative. Samples were withdrawn at intervals for the determination of residual S-adenosylmethionine by means of a Dowex 50 column.[1] Fig. 28 shows the results. The initial pH values are specified; the gradual abolition of the sulfonium configuration, according to $R_1(R_2)S^+R_3 + H_2O \longrightarrow R_1SR_2 + R_3OH + H^+$, gave an increase in acidity to pH 8.2, 7.0, and 6.0, respectively. Paper chromatographic survey of simultaneous samples revealed the identity and approximate concentration of split products. The results of ultraviolet scanning and ninhydrin tests are listed in Table 12.

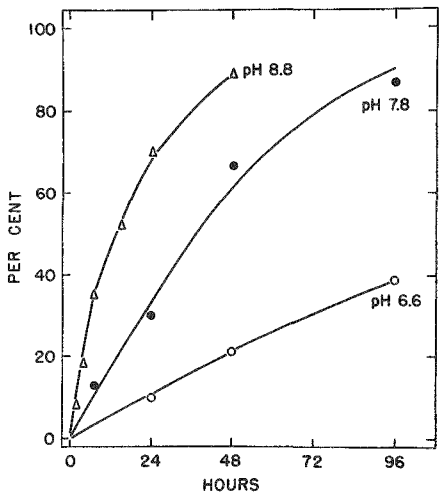

Fig. 28. The destruction of S-adenosylmethionine in buffer solutions at 30° C.

Observations of the material incubated at weakly alkaline reaction indicated a novel hydrolytic mechanism leading to methionine and adenine. To gain information on this point an extension of the hydrolytic studies into the acid and alkaline range and a comparison with related compounds appeared desirable.

Acid hydrolysis. S-adenosylmethionine is rather stable in strong acids at low temperature.[2] A comparison was made of its glycosidic bond with those of adenosine and 5'-methylthioadenosine in 0.1 N HCl at 100° C. Using the release of adenine as the criterion of hydrolysis, no striking differences in the rates of acid hydrolysis are apparent.

TABLE 12

Hydrolytic products of S-adenosylmethionine

Products obtained	pH of hydrolysates		
	6.0*	7.0*	8.2**
S-Adenosylmethionine	+++	±	±
5'-Methylthioadenosine	++	++	+
Adenine	±	+	++
Homoserine	++	++	+
Methionine	±	+	++

*Incubation at 30° C for 96 hr.
**Incubation at 30° C for 48 hr.

Alkaline hydrolysis. Paper chromatography of hydrolysates of S-adenosylmethionine obtained with 0.1 N NaOH at the temperature of a boiling water bath revealed adenine and methionine as the main products; these were accompanied by smaller amounts of homoserine, methylthioadenosine, methylthioribose and presumably some other split products. When the hydrolysis was conducted at room temperature only two products of hydrolysis were evident. The identification of adenine and the presence of only one other major split product suggested that the latter might be S-ribosylmethionine. This was confirmed by the analysis of eluates from large scale paper chromatograms.

Comparison with dimethyladenosylthetin. The extreme lability of the glycosidic bond in S-adenosylmethionine toward alkali appeared to be a special effect of the sulfonium configuration in the molecule. In view of the novelty of this observation, it was desirable to amplify the information on this point. A related compound, dimethyladenosylthetin,

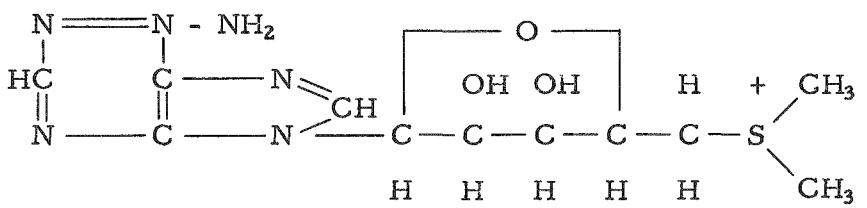

(Dimethyladenosylthetin)

was available for this purpose. This compound showed sensitivity to alkali in a fashion similar to S-adenosylmethionine (see Fig. 29). Adenine, which resulted from the hydrolysis, was readily identified by paper chromatography.

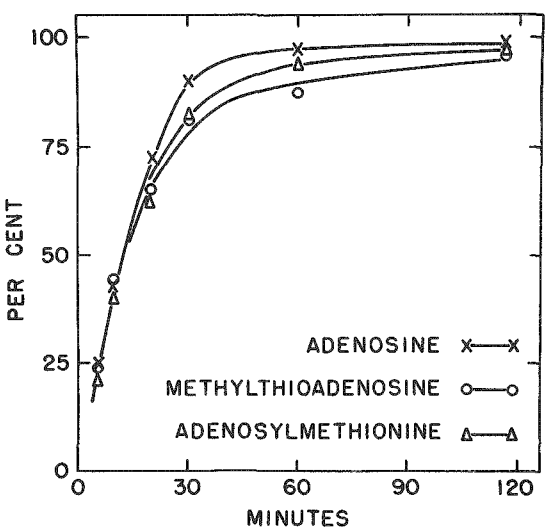

Figure 29. The splitting of adenine from S-adenosylmethionine, adenosine, and 5'-methylthioadenosine by 0.1 N NCl in a boiling water bath.

Analysis and properties of S-ribosylmethionine. S-ribosylmethionine may be prepared in high purity from S-adenosylmethionine by alkaline hydrolysis under mild conditions.[7] No traces of adenine or adenine derivatives can be found in the preparations by paper chromatography or spectrophotometry. S-ribosylmethionine is readily detected on paper chromatograms by the ninhydrin spray, while the platinum iodide reagent[8] is less sensitive. In butanol-water-acetic acid (60:25:15, v/v) the R_f is 0.1; in ethanol-water-acetic acid (65:34:1, v/v) the R_f is 0.35.

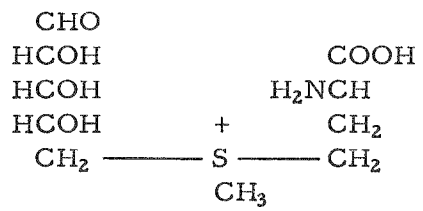

S-ribosylmethionine

The structure of S-ribosylmethionine is inferred mainly from the composition and configuration of its parent substance, S-adenosylmethionine, and from the observation that under the hydrolytic conditions specified here adenine is the only other principal fragment. Unfortunately, S-ribosylmethionine proved refractory to isolation in the dry or crystallized state. Thus it became necessary to establish a measure of the concentration of the compound in solution by a suitable analytical test. Ultraviolet spectrophotometry, which serves for this purpose in experimentation with S-adenosylmethionine, cannot be used for lack of a specific light-absorbing group in the molecule of S-ribosylmethionine. Pentose determination by the orcinol reagent was found to serve as measure of the concentration of S-ribosylmethionine, provided that the identity and uniformity of the product are ascertained by concomitant paper chromatography.

A preparation of S-ribosylmethionine, from which adenine had been removed, contained 7.8 μM/ml as determined by the orcinol reaction. Hydrolysis of 1 ml at pH 5.3 for 30 min at 100° C yielded 7.2 μM methylthioribose [9] and 8.5 μM homoserine.[10] Experiments with L-amino acid oxidase[1] showed that 11.0 μM of the preparation was inert as a substrate while methionine was oxidized almost completely. Heating in 0.1 N NaOH destroyed the sulfonium group and produced methionine in 65% yield as determined by the amino acid oxidase technique.[1]

Discussion

It may be assumed from our data that the loss of S-adenosylmethionine caused by its chemical lability remains small during the short periods of incubation in enzymatic studies. In nutritional and microbiological investigations the lability may be a complicating factor, and in all types of experiments involving intact cells, tissue homogenates, or crude enzyme preparations, the additional rapid enzymatic destruction has to be considered.

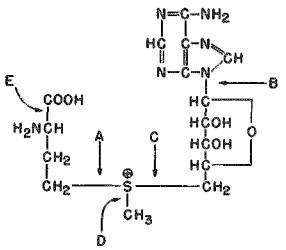

Fig. 30. Various ways of hydrolysis of S-adenosylmethionine. A discussion is given in the text.

The experiments on hydrolysis are illustrated in Fig. 30, in which various modes of splitting are indicated. The earlier observations[3,4] on the formation of methylthioadenosine and homoserine (split A) have been confirmed; heating at pH > 4 or in neutral solution for 30 min gives nearly quantitative results. More rigorous treatment with acid leads to further degradation of methylthioadenosine (split B) resulting in adenine and methylthioribose.

Methionine can be obtained by brief heating in alkali (split C); we have not been able to detect adenosine which would be the other fragment expected from this split. Control experiments with adenosine, heated with alkali under the same conditions, proved its stability. Therefore, adenosine could not be considered as a product nor as an intermediate compound in the alkaline hydrolysis of S-adenosylmethionine. The quantitative formation of adenine by alkali suggested that split B precedes split C. This has been confirmed by alkaline hydrolysis at low temperature. Under these conditions, split C becomes negligible compared with B; adenine and S-ribosylmethionine are formed. The designation of the latter product as S-ribosylmethionine is based on the following observations; precipitability and chromatographic behavior as an entity, the orcinol response characteristic of pentoses, alkaline hydrolysis leading to methionine with destruction of the pentose, splitting by weak acid to methylthioribose and homoserine, and the identification of these compounds by paper chromatography. The sulfonium character is implied from the structure of the parent compound whose characteristics of stability and hydrolytic behavior are retained in the molecule. Like other sulfonium compounds, S-ribosylmethionine is resistant to amino acid oxidase.

The extreme lability of the glycosidic bond in S-adenosylmethionine has no analogy in ribose nucleoside and nucleotide chemistry with the exception of the nicotinamide ribose linkage in the nicotinamide nucleotides:[11] here, the pyridinium nitrogen changes to the trivalent state when nicotinamide is liberated by alkali. It was surmised at first that, by an intramolecular rearrangement of S-adenosylmethionine, the methyl group might be shifted from the sulfur atom to nitrogen atom 9 of the adenine with resultant labilization of the flycosidic bond. However, 9-methyladenine and S-ribosylhomocysteine would then be expected as fragments; they were not found in our hydrolysates. In view of the stability of adenosine and methylthioadenosine toward alkali, it became clear that the presence of the sulfonium group in S-adenosylmethionine must be responsible for the lability of the adenine ribose linkage in alkaline medium. Confidence in this concept was gained by the observation of almost identical behavior of the related sulfonium compound, dimethyladenosylthetin. Such an effect of the

sulfonium group on a linkage which is removed by several interatomic bonds from the activating site has not been observed before. It is noteworthy that the construction of a molecular model of S-adenosylmethionine shows proximity of the sulfonium group to the glycosidic bond. Furthermore, a search of the literature on sulfonium compounds revealed a somewhat related observation by Rydon and his coworkers.[12] They found that 2-aroyloxyethyldimethylsulfonium compounds readily undergo alkaline fission, mainly as follows:

$$Ar.CO_2CH_2CH_2S^+(CH_3)_2 + NaOH \longrightarrow Ar.\ CO_2Na + HOCH_2CH_2S^+(CH_3)_2 \quad .$$

To a lesser extent irreversible hydrolysis occurred:

$$Ar.CO_2CH_2S^+(CH_3)_2 + NaOH \longrightarrow Ar.CO_2Na + HOCH_2CH_2S^+(CH_3)_2 \quad .$$

In S-adenosylmethionine the attack is on a C - N bond rather than a C - O bond, and the split is predominantly of the irreversible hydrolytic type. Splitting of S-adenosylmethionine by enzyme action at site D and site E[3,13] has been observed (see Fig. 30). No analogous chemical hydrolyses have been detected in our studies.

The authors wish to acknowledge the technical assistance of Mrs. S. Stanford.

References

1. Schlenk, F. and R. E. DePalma. The preparation of S-adenosylmethionine. J. Biol. Chem., in press.

2. Schlenk, F., and R. E. DePalma. The formation of S-adenosylmethionine in yeast. J. Biol. Chem., in press.

3. Cantoni, G. L. S-adenosylmethionine; A new intermediate formed enzymatically from L-methionine and adenosinetriphosphate. J. Biol. Chem. 204:403-416 (1953).

4. Baddiley, J., G. L. Cantoni, and G. A. Jamieson. Structural observations on "Active Methionine." J. Chem. Soc. 1953: 2662-2664.

5. Smith, R. L., E. E. Anderson, Jr., R. N. Overland, and F. Schlenk. The occurrence, formation and isolation of thiomethyladenosine. Arch. Biochem. and Biophys. 42:72-82 (1953).

6. Toennies, G., and J. J. Kolb. Methionine studies. VII. Sulfonium derivatives. J. Am. Chem. Soc. 67:849-851 (1945).

7. Parks, L. W., and F. Schlenk. The stability and hydrolysis of S-adenosylmethionine; isolation of S-ribosylmethionine. J. Biol. Chem., in press.

8. Toennies, G., and J. J. Kolb. Techniques and reagents for paper chromatography. Anal. Chem. 23:823-826 (1951).

9. Smith, R. L., and F. Schlenk. Determination of adenine thiomethylriboside and 5-thiomethylribose, and their differentiation from methionine. Arch. Biochem. and Biophys. 38:159-165 (1952).

10. Moore, S., and W. H. Stein. Photometric ninhydrin method for use in the chromatography of amino acids. J. Biol. Chem. 176:367-388 (1948).

11. Schlenk, F. Codehydrogenases I and II and Apoenzymes, in Sumner, J. B., and Myrbäck, K., The Enzymes. Vol. II, Academic Press, New York, p. 250 (1951).

12. Mamalis, P., and H. N. Rydon. Alkaline fission of 2-aroyloxyethyldimethylsulfonium iodides: The evaluation of Hammett's substituent constants for some o-substituents. J. Chem. Soc. 1955: 1049-1065.

13. Tabor, H., S. M. Rosenthal, and C. W. Tabor. The role of putrescine and methionine in the enzymatic synthesis of spermidine in *Escherichia coli* extracts. J. Am. Chem. Soc. 79-2978-2979 (1957).

THE BIOSYNTHESIS OF S-ADENOSYLMETHIONINE BY YEAST MUTANTS

I The Adenine Requirement for Synthesis

Irving Yall

S-Adenosylmethionine* has been found to be synthesized in good yield by various common yeasts such as Torulopsis utilis and Saccharomyces cerevisiae.[1] The aim of this project was to test strains of yeast that are good AM producers but that require one or more of the AM constituents for growth, in order to determine the pathways of AM formation within the cell.

Materials and Methods

The organism used was an adenine- or hypoxanthine-requiring pink mutant (strain SC-10-80-3-5) of S. cerevisiae.** The inoculum was prepared by growing the yeast on a rotary shaker for 24 hr in 30 ml of the synthetic medium of Roman,[2] contained in 125-ml erlenmeyer flasks at about 27°C. The cells were harvested by centrifugation, washed twice in sterile isotonic saline and resuspended in saline. The suspensions were used to inoculate 100 ml of the synthetic medium contained in 500-ml erlenmeyer flasks. For the growth experiments the medium was made up without adenine. The growth factor to be tested and L-methionine (4 μM/ml) were added. The cells were allowed to grow in this medium for 40 hr, with shaking, at 27°C. The yield of cells was measured by dry weight determination. The amount of AM formed was determined by the Dowex 50 method of Schlenk and DePalma.[3] The reversion rate of this mutant was quite low in that no growth was observed in flasks of synthetic medium without either adenine or hypoxanthine after 7 days of incubation.

All the supplements used in this study, except where otherwise specified, were obtained from the California Foundation for Biochemical Research, Los Angeles. The AM and MTA were prepared in this laboratory and were purified by chromatographic methods. Hypoxanthine-2 C^{14} and adenosine-8 C^{14} were obtained from Schwarz Laboratories, Inc., Mount Vernon, New York.

---

*Abbreviations used: S-adenosylmethionine, AM; methylthioadenosine, MTA; inosinic acid, IMP; adenylic acid, AMP; adenosine triphosphate, ATP; adenosine diphosphate, ADP.

**Kindly furnished by Dr. F. P. Hungate, General Electric Co., Richland, Washington.

Experimental

Figure 31 shows the effect of varying concentrations of adenine, ranging from 1 to 10 μM/100 ml of medium, on growth and on AM production of the organism. It appears that within the range of adenine concentration tried, no minimal amount of adenine is needed for AM production when an excess of L-methionine is present. If there is sufficient adenine to support growth, some of it is diverted to the synthesis of AM.

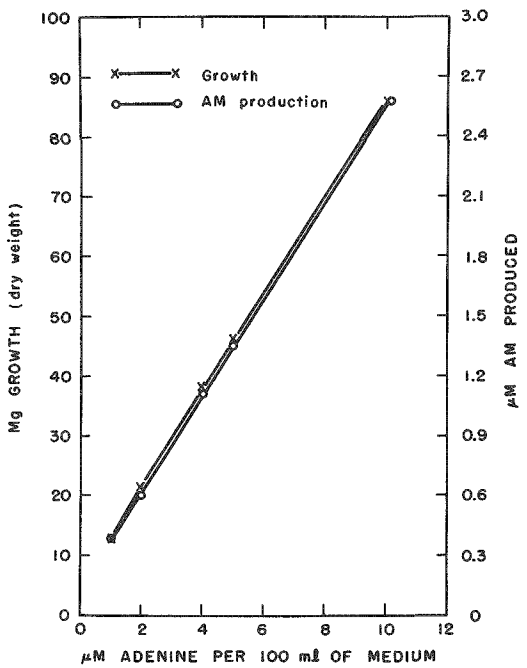

Fig. 31. Adenine concentration versus growth and production of S-adenosylmethionine.

Table 13 shows the effect of various supplements substituted for adenine on growth and AM production of the organism. Of the compounds tried, only hypoxanthine and AM itself supported growth. That hypoxanthine was used for the production of AM was shown by the ultraviolet absorption spectrum of the isolated compound which showed a maximum at 260 mμ in neutral solution; other tests confirmed its identity with AM.

When the mutant was allowed to metabolize hypoxanthine-2 C^{14}, radioactive AM was obtained in good yield.

In view of the possibility that adenosine might not enter the cell in sufficient quantity to allow growth to take place, studies were made to determine whether adenosine-8 C^{14} (at the level of 10 μM/100 ml of medium) was capable of penetrating into the cells of the parent strain SC-10 during growth. Approximately 30% of the adenosine-8 C^{14} originally introduced disappeared from the medium after 40 hr of cell growth. This amount would be sufficient for growth of the adenine-requiring mutant if adenosine

could be used as a substitute for adenine. There is, of course, the possibility that the cell permeability of the mutant may differ from that of the parent strain.

Table 13

Effect of supplements on growth and AM production of strain SC-10-80-3-5

Supplement*	Increase in dry weight, mg	Total AM production, μM	AM production, μM/50 mg dry weight
Adenine	70.0	3.30	2.36
Hypoxanthine	75.4	3.18	2.12
Adenosine	0	0	0
AMP	0	0	0
ADP	0	0	0
ATP	0	0	0
MTA	0	0	0
AM	17.5	0.66	1.88
Guanine	0	0	0
Xanthine	0	0	0
None	0	0	0

*All supplements were at the level of 10 μM/100 ml of medium; 400 μM of L-methionine were added to each flask. The organisms were allowed to grow for 40 hr.

Discussion

The fact that neither guanine nor xanthine could substitute for adenine or hypoxanthine indicates the absence of the purine transformation reaction of Abrams and Bentley[4] and Gehrig and Magasanik.[5] The ability of AM to serve as a growth factor may indicate the presence of an enzyme system capable of splitting the adenine-ribose linkage in the AM molecule to yield adenine and S-ribosylmethionine. Excluding considerations of permeability, the organism does not seem to be able to split the adenine-ribose linkage of adenosine or MTA. Parks and Schlenk[6] have found that AM at a pH of approximately 9 will split readily to form adenine and S-ribosylmethionine, while MTA and similar compounds will not. It is possible that the strain inherent in the configuration of the AM molecule is sufficient to permit some specific system in the organism to split off adenine although it is unable to cleave the linkages in related compounds.

A pathway from hypoxanthine to AM which would avoid the adenosine step might involve adenylosuccinic acid. Carter and Cohen[7] have purified an enzyme from yeast which converts adenylosuccinic acid to AMP and fumaric acid.

$$\text{Hypoxanthine} \longrightarrow \text{IMP} \xrightarrow[\text{+ aspartic acid}]{} \text{adenylosuccinic acid}$$

$$\xrightarrow[\text{adenylosuccinase}]{} \text{AMP} \longrightarrow \text{ATP}$$

The ATP formed would presumably condense with methionine in the reaction of Cantoni[8] to form AM.

It is possible that this organism converts adenine to hypoxanthine, which then goes through the reaction described above.

References

1. Schlenk, F. and R. E. DePalma. The formation of S-adenosylmethionine in yeast. J. Biol. Chem. 229:1037-1050 (1957).

2. Roman, H. L. A system selective for mutations affecting the synthesis of adenine in yeast. Compt. rend. Lab. Carlsberg, Ser. physiol. 26:299-314 (1956).

3. Schlenk, F. and R. E. DePalma. The preparation of S-adenosylmethionine. J. Biol. Chem. 229:1051-1057 (1958).

4. Abrams, R. and M. Bentley. Transformation of inosinic acid to adenylic and guanylic acids in a soluble enzyme system. J. Am. Chem. Soc. 77:4179-4180 (1955).

5. Gehrig, L. B. and B. Magasanik. Biosynthesis of nucleic acid guanine: The enzymic conversion of inosine-5'-phosphate to xanthosine-5'-phosphate. J. Am. Chem. Soc. 77:4685-4686. (1955).

6. Parks, L. W. and F. Schlenk. The stability and hydrolysis of S-adenosylmethionine; isolation of S-ribosylmethionine. J. Biol. Chem., in press.

7. Carter, C. E. and L. H. Cohen. The preparation and properties of adenylosuccinase and adenylosuccinic acid. J. Biol. Chem. 222:17-30 (1956).

8. Cantoni, G. L. Synthesis and transfer of the labile methyl group, in McElroy, W. D. and B. Glass, Phosphorous Metabolism, Vol. 2, p. 129-152. Johns Hopkins University Press, Baltimore (1952).

S-ADENOSYLMETHIONINE AS A GROWTH FACTOR SUBSTITUTE FOR AN ADENINE-REQUIRING YEAST MUTANT

Irving Yall

It has been reported[1] that an adenine- or hypoxanthine-requiring mutant of Saccharomyces cerevisiae (strain SC-10-80-3-5) is able to grow in the presence of S-adenosylmethionine (AM) without an additional purine supplement. This paper reports a series of experiments performed with AM labeled in various positions, which were intended to show how this compound is utilized by the organism.

Materials and Methods

S-Adenosylmethionine-S^{35} was prepared as follows. Active dry yeast (Fleischmann, 250 mg) was placed in 100 ml of 0.2 M phosphate buffer in a 500 ml erlenmeyer flask and shaken at a temperature of about 28° C for about 16 hr. Following the period of starvation, 15 g of glucose, 400 μM of L-aspartic acid, and approximately 1 millicurie of $Na_2S^{35}O_4$ were added to the flask. Sterile techniques were not used. The cells were shaken and after 24 hr were harvested by centrifugation and washed twice with cold distilled water. The cells were extracted with perchloric acid and the AM-S^{35} was isolated and purified by the procedure of Schlenk and DePalma.[2] Approximately 100 microcuries of AM-S^{35} were obtained by this procedure.

S-Adenosylmethionine-2-C^{14} was obtained by allowing the organism to metabolize hypoxanthine-2-C^{14} and isolating the resulting labeled AM; AM($C^{14}H_3$) was obtained by adding methionine ($C^{14}H_3$) as the AM inducer.[3] The conditions for growth of the organisms were as described previously.[1]

Experimental

The results obtained when strains SC-10 (the parent strain) and SC-10-80-3-5 were exposed to labeled AM, with or without 400 μM of L-methionine, are presented in Table 14.

The adenine- or hypoxanthine-requiring mutant utilizes AM readily as a substitute for these growth factors both in the presence and absence of excess L-methionine although, in the presence of excess methionine, some AM remains intact. That the complete molecule is retained is indicated by the fact that molecules initially labeled in the adenine portion, the methyl group, and the sulfur of the methionine portion of the molecule were recovered with the original specific activities.

TABLE 14

Effect of L-methionine on the utilization of S-adenosylmethionine by strains of Saccharomyces cerevisiae

Organism strain	AM introduced, μM	Specific activity of AM introduced, cpm/μM	AM recovered, μM		Specific activity of AM recovered, cpm/μM	
			No methionine added	Methionine added	No methionine added	Methionine added
SC-10	AM-S^{35} 8.5	47,000	0.51	4.25	50,000	14,000
SC-10-80-3-5	AM-S^{35} 3.6	56,000	0.35	0.70	7,500	56,300
SC-10-80-3-5	AM-$C^{14}H_3$ 7.1	11,500	0.37	0.57	-*	12,500
SC-10-80-3-5	AN-2-C^{14} 4.1	67,000	0.32	0.60	-*	65,000

*No detectible activity.

The parent strain, with no purine requirement, also utilizes the AM-S^{35} readily. Without excess L-methionine, it will retain some of the original AM, and it does not synthesize any additional amounts. In the presence of excess L-methionine, the organism will synthesize additional AM as shown by the decrease in specific activity of the reisolated AM-S^{35}.

The fate of S^{35} resulting from the breakdown of AM-S^{35} by the mutant organisms depends on whether excess L-methionine is present. In the experiments conducted in the absence of excess L-methionine, a considerable portion of the S^{35} was incorporated into the cellular constituents. In the presence of excess L-methionine, most of the S^{35} was converted to inorganic sulfur.

Discussion

Since AM substitutes for the adenine or hypoxanthine requirement of the mutant, it was anticipated that the organism might possess a system capable of splitting AM to adenine and S-ribosylmethionine, as has been shown to occur *in vitro* at pH 9 by Parks and Schlenk.(4) Previous data(1) have shown that if sufficient adenine is present to permit growth (0.01-0.1 μM adenine/ml), then some of it is diverted towards the production of AM, provided that excess L-methionine is present. Since the reisolated AM had the same specific activity as that originally introduced, no additional AM could have been synthesized during the period of cell growth. It is possible that the AM is supplying a factor other than adenine. A second possibility is that the AM equilibrium within the mutant cell is such that, when AM is supplied as a growth factor, enough remains intact

within the cell to reverse the equilibrium of formation and thus to prevent the de novo synthesis of AM; hence the available adenine (split from the AM) is diverted toward other cellular processes. Both of these possibilities are being investigated.

References

1. Yall, I. Progress report: The biosynthesis of S-adenosylmethionine by yeast mutants. I. The adenine requirement for synthesis. This report, p.71

2. Schlenk, F. and R. E. DePalma. The preparation of S-adenosylmethionine. J. Biol. Chem. 229:1051-1057 (1957).

3. Schlenk, F. and R. E. DePalma. The formation of S-adenosylmethionine in yeast. J. Biol. Chem. 229:1037-1050 (1957)

4. Parks, L. W. and F. Schlenk. The stability and hydrolysis of S-adenosylmethionine; isolation of S-ribosylmethionine. J. Biol. Chem., in press.

ELECTRONIC COUNTING AND SIZING OF BACTERIA

Herbert E. Kubitschek

The Coulter counter, designed for red blood cells, has been modified to count and size bacteria. This has been accomplished by the construction of an aperture 10 μ in diameter in a glass sheet about 50 μ thick, and by the addition of an electronic circuit to allow direct counting of the number of bacteria within a narrow size range (differential analyzer). With the 10-μ aperture the counter will count and size nonconducting particles with volumes between 0.25 μ^3 and 4 μ^3. Larger apertures will count correspondingly larger particles.

The passage of a particle through the aperture should generate an electric pulse height proportional to the volume of the bacterium. This relation is under study with the use of graded polystyrene latex spheres. Figure 32 shows approximate linearity in a preliminary measurement using 1.17-μ spheres. The three peaks correspond to pulse heights observed when one, two, and three particles, respectively, are within the aperture. At low counting rates, the resolution of the counter is about 5% for 1-μ particles.

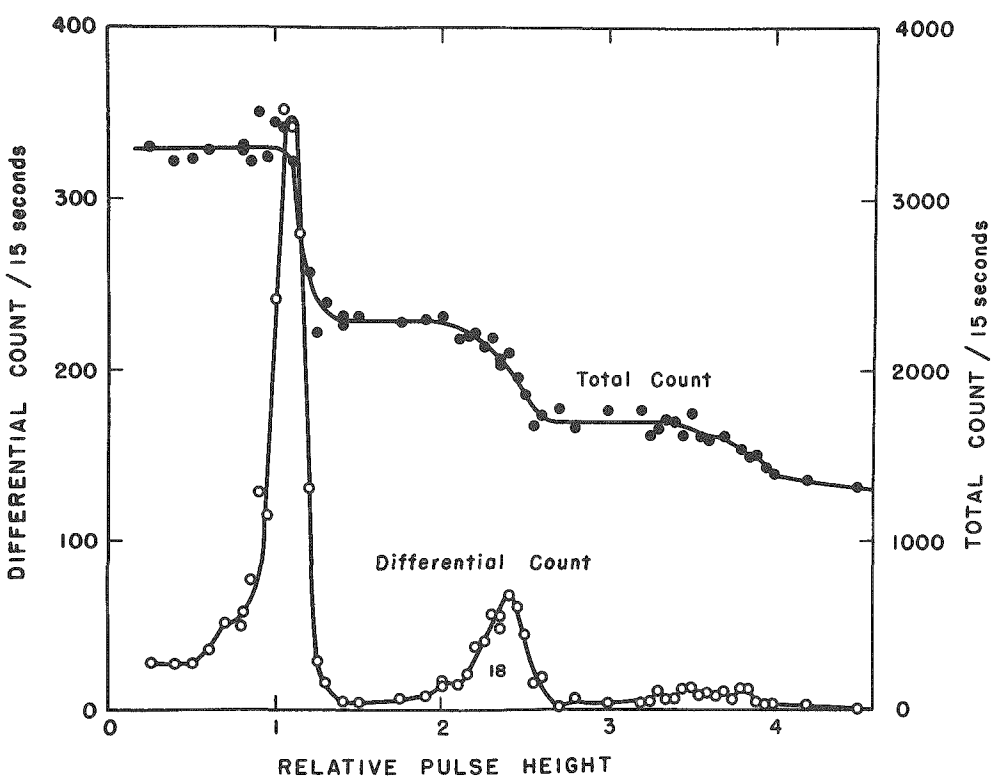

Figure 32. Counting rates as a function of pulse height for 1.17-μ spheres.

3-AMINO-1,2,4-TRIAZOLE

VII. Effect on Liver Catalase of Repeated Injections of Aminotriazole, and of Aminotriazole in the Drinking Water

Robert N. Feinstein

For reasons to be discussed in later reports, it was desired to maintain a prolonged low level of liver catalase activity in mice; 3-amino-1,2,4-triazole (AT), which has been shown[1-3] to lower the liver catalase activity of animals precipitously, seemed most suitable. The AT was administered in two ways: (a) by repeated intraperitoneal injections, and (b) by solution in the sole source of drinking water. The latter is far more desirable because of ease of administration to large numbers of animals and, more important, because a more even intake should assure a more constant, low level of catalase activity. The serious difficulty has arisen, however, that mice strongly reject solutions of AT even more dilute than 0.5%, a concentration at which the taste of the solute is barely detectable to the human taster.

Fluid consumption decreased from an average of approximately 0.25 ml of water per mouse per hour to an average of 0.11 ml of 0.5% AT. During a 7-day period, 20 mice drinking water averaged a loss of body weight of 0.2 grams, while 20 mice drinking the AT solution averaged a loss of 2.9 grams. In longer experiments with smaller numbers of mice, it became apparent that mice would die (presumably of dehydration) rather than drink more of the AT solutions. A wide variety of flavors and seasonings has been tested in an attempt to mask the unfavorable taste; none has been completely successful.

It is of interest that even with the low consumption of AT, effects on liver catalase are significant, as indicated by Table 15. Unfortunately, however, liver catalase level is so nonspecific as a parameter that we cannot be sure the dehydration itself was not at least partially responsible for the drop in enzyme activity.

Intraperitoneal AT, in rats[1,2] at 1 g/kg and in mice[3] at 2.25 g/kg, has been shown to have at least one very consistent effect in repeated experiments: 24 hr after administration, the liver catalase has returned to approximately 35% of the normal value. An attempt was therefore made to attain a constant level of liver catalase activity no higher than this, by repeated injection of the agent.

Figure 33 indicates that the effect of repeated injections of AT is not cumulative; liver catalase is affected according to the time and dose of the last injection, at least under the conditions of time and dosage employed.

TABLE 15

Effect of oral injection of 3-amino-1,2,4-triazole (AT) on liver catalase activity of mice

Drinking fluid	Average consumption, ml/mouse/hr	Liver catalase, perborate units/g	
		at 3 days	at 8 days
H_2O	0.25	814 ±62	857 ±62
0.5% AT	0.10	185 ±40	236 ±19

Figures for liquid consumption are based on groups of 14-20 CF No. 1 ♀ mice, initially averaging 28.9 g in weight. Three mice were sacrificed from each group for each set of catalase assays. Catalase data are mean and average deviation from the mean.

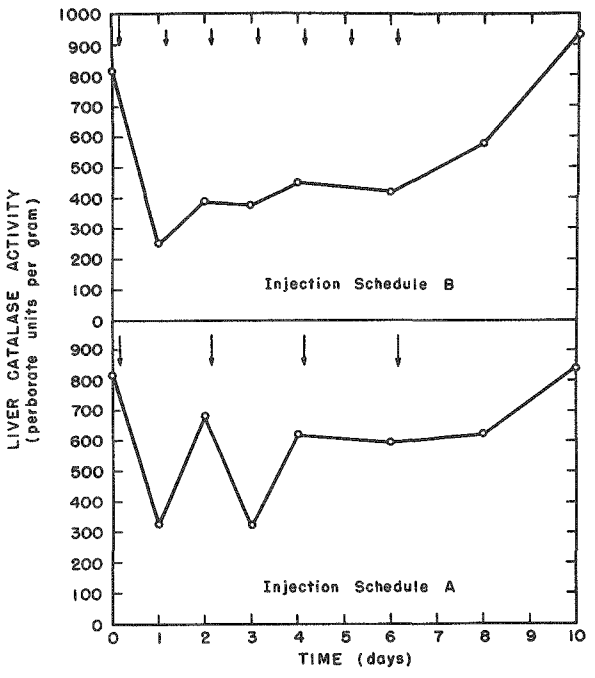

Figure 33. Effect of repeated intraperitoneal injection of 3-amino-1, 2, 4-triazole (AT) on liver catalase of mice. Large arrows indicate injection of 1000 mg/kg; small arrows indicate injection of 200 mg/kg. Each point represents the average of three individual mouse livers.

References

1. Heim, W. G., D. Appleman, and H. T. Pyfrom. Production of catalase changes in animals with 3-amino-1,2,4-triazole. Science 122:693-694 (1955).

2. Heim, W. G., D. Appleman, and H. T. Pyfrom. Effects of 3-amino-1,2,4-triazole (AT) on catalase and other compounds. Am. J. Physiol. 186:19-23 (1956).

3. Feinstein, R. N., S. Berliner, and F. O. Green. 3-Amino-1,2,4-triazole. II. Effects on tissue catalase: possible similarity to tumor growth. Quarterly Report of Biological and Medical Research Division, Argonne National Laboratory. ANL-5655, pp. 110-117 (1956).

3-AMINO-1,2,4-TRIAZOLE

VIII. Differential Effect on the Catalase of Erythrocytes and of Liver

Robert N. Feinstein

It was demonstrated by Heim, Appleman, and Pyfrom,[1] and later confirmed[2,3] that the injection of 3-amino-1,2,4-triazole (AT) results in a striking reduction of the catalase activity of the liver and other solid tissues, but not that of the erythrocyte. As pointed out by Heim *et al.*,[1] this observation is of particular interest because the effect is the same as that produced by the growth of a tumor.[3,4] An explanation of the differential effect in the case of injected AT may therefore be of interest as a possible explanation of the parallel phenomenon in the case of tumor growth.

Methods and Results

Catalase was assayed by the perborate method;[5] in the case of solid tissues, this was done on whole homogenates. The AT was analyzed by a method recently described elsewhere.[6] Animals were CF No. 1 female mice and male Maguran rats. They received a standard laboratory diet *ad libitum*. The AT was prepared from a commercial product and purified before use.

It has been found (Table 16) that AT reduces the catalase activity of liver homogenates upon incubation and also reduces the catalase activity of blood cells which have been laked by the addition of water, but it does not reduce the catalase activity of packed blood cells suspended in isotonic saline.

TABLE 16

In vitro effect of AT on liver and erythrocyte catalase

Tissue	Treatment	Catalase activity, PU*/ml		
		Initial	2 hr	4 hr
Mouse liver	Homogenized with water	1.67	0.74	0.02
Rat blood cells	Laked with water	1.98	1.63	1.28
Rat blood cells	Suspended in isotonic saline	1.91	1.89	2.00

*PU = perborate units.

AT was present at 0.02 M. Incubation was at 37°C.

The obvious implication of this experiment - that AT fails to act on erythrocyte catalase in vivo because of a simple lack of penetration of the red cell - is made uncertain by the fact that the liver homogenate, prepared with distilled water, represents a mixture of intact and disintegrated cells. Since it is impossible to prepare solid tissues in such a way that there is not at least some cellular destruction, it was decided to approach the question with an in vivo technique that was not dependent on the extent of destruction of cells.

An AT solution (10%) prepared by dissolving directly in heparin solution (Liquaemin sodium, Organon, 1000 USP units of heparin (10 mg) per ml) was injected in this form at a dosage of 1 g/kg body weight. In control animals, heparin solution alone was injected. In this way, completely clot-free blood was obtained. This seems to be essential, since it has been found that even minute clot fragments apparently retain significant amounts of AT. At the same time the animal was bled by cutting the throat, and the liver was removed. The blood cells were separated by centrifugation and washed twice with cold isotonic saline. The liver was homogenized, and the blood cells were laked with distilled water. The AT content of the blood cells, the plasma, and the liver homogenate was then determined. Table 17 indicates clearly that the blood cells contain far less AT than does the plasma or the liver.

TABLE 17

Distribution of injected 3-amino-1,2,4-triazole (AT) in rat liver and blood

Tissue	AT content, mg/g or mg/ml
Liver	1.19
Plasma	1.13
Washed blood cells	0.14

AT was injected intraperitoneally at the rate of 1.0 g/kg, dissolved in heparin solution. Blood was withdrawn, and the liver was removed 30 min after injection. Three rats were injected with AT in heparin solution, and 3 with heparin solution alone. Values were averaged, and the small amount of AT-like chromogen detected in the control tissues was subtracted from the color values obtained in the case of the AT-injected rats.

Discussion

If the suggested explanation for the differential effect of AT on the catalase of blood cells and of solid tissues may be projected to the corresponding effects due to the presence of a tumor, it might be hypothesized that the tumor elaborates an agent, similar to AT in its effects although

not necessarily similar in its chemistry, which enters the plasma and thence the solid tissues freely, but is incapable of penetrating the erythrocyte. It is planned to examine the "toxohormone" of Nakahara and Fukuoka(7) from this point of view.

References

1. Heim, W. G., D. Appleman, and H. T. Pyfrom. Production of catalase changes in animals with 3-amino-1,2,4-triazole. Science 122:693-4 (1955).

2. Heim, W. G., D. Appleman, and H. T. Pyfrom. Effects of 3-amino-1,2,4-triazole (AT) on catalase and other compounds. Am. J. Physiol. 186:19-23 (1956).

3. Feinstein, R. N., S. Berliner, and F. O. Green. Mechanism of inhibition of catalase by 3-amino-1,2,4-triazole. Arch. Biochem. and Biophys., in press.

4. Greenstein, J. P. Biochemistry of Cancer. Academic Press, New York (1954).

5. Feinstein, R. N. Perborate as substrate in a new assay of catalase. J. Biol. Chem. 180:1197-1202 (1949).

6. Green, F. O., and R. N. Feinstein. Quantitative estimation of 3-amino-1,2,4-triazole. Anal. Chem. 29:1658-1660 (1957).

7. Nakahara, W., and F. Fukuoka. Toxohormone: a characteristic substance produced by cancer tissue. Gann 40:45-69 (1949).

PROGRESS REPORT: DENSITY GRADIENT CENTRIFUGATION

Polyvinylpyrrolidone-Sucrose Gradients

John F. Thomson and Florence J. Klipfel

In previous experiments on separation of subcellular components of rat liver by gradient differential centrifugation, we prepared gradient tubes from sucrose solutions of varying concentration.(1) The calculation of the distribution of particle sizes associated with a specific enzyme activity was thus complicated not only by density and viscosity gradients, but also by osmotic pressure gradients, for which at best a semiarbitrary correction could be made.(2) The usefulness of polyvinylpyrrolidone (PVP) in the preparation of cytoplasmic particulates for biochemical and cytologic studies suggested the possibility of varying the concentration of PVP to produce a density gradient without materially altering the osmotic pressure.

Gradient tubes were prepared by layering solutions of 0.25 M sucrose containing between 6 and 18% PVP. Tissues were homogenized in 0.25 M sucrose containing 5% PVP. The homogenate was layered onto the gradient column and the tubes were then centrifuged in a Lourdes centrifuge with a swinging rotor. Layers were removed and assayed for various enzymes. Measurements of viscosities and densities of the PVP-sucrose solutions were made so that the particle size distributions could be determined as described previously.(1)

The distributions of rat liver succinic dehydrogenase and rat thymus cytochrome oxidase are presented in Fig. 34.

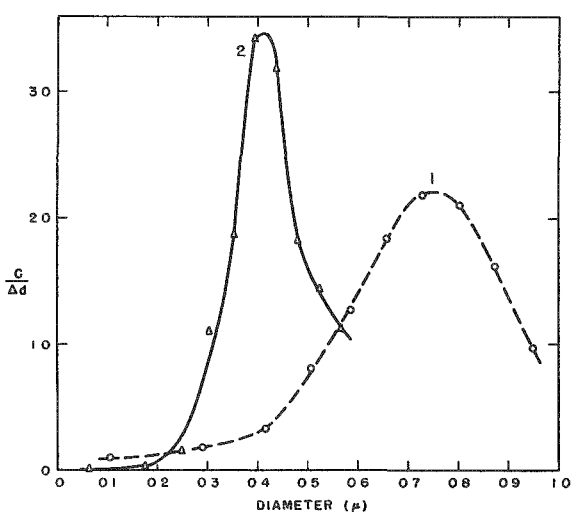

Figure 34. Curve 1, distribution of succinic dehydrogenase activity of rat liver. Centrifuged at 6000 rpm for 1 hr. Curve 2, distribution of cytochrome oxidase activity of rat thymus. Centrifuged at 10, 000 rpm for 1 hr.

References

1. Thomson, J. F., and E. T. Mikuta. Enzymatic activity of cytoplasmic particulates of rat liver isolated by gradient centrifugation. Arch. Biochem. Biophys. 51:487-98 (1954).

2. Thomson, J. F., and F. J. Klipfel. Further studies on cytoplasmic particulates isolated by gradient centrifugation. Arch. Biochem. Biophys. 70:234-238 (1957).

NEW ELECTRON MICROSCOPIC OBSERVATIONS ON FIBRILLOGENESIS IN THE REGENERATING ACHILLES TENDON OF NORMAL, SCORBUTIC, AND RECOVERING GUINEA PIGS

F. Wassermann

Recently Policard and Collet,(1) reporting on their studies of experimental fibrosis, reviewed our present knowledge about fibrillogenesis. These authors found their own electron microscopic observations in complete agreement with those of Porter,(2) Jackson,(3), and Wassermann,(4) whose studies concerned fiber formation in tissue culture, embryonic tissues and the regenerating tendon. It is now generally accepted that, as the French authors write, the primary fibrils are found "dans la zone de contact entre cellule et milieu ambiant; soit dans la couchetout à fait superficielle de l'élément, soit dans le milieu intercellulaire, mais au contact même de la cellule." However, the formation of the primary fibrils themselves and their growth and maturation within the intercellular milieu requires still further investigation.

Material and Methods

In our present studies we are using the regenerating Achilles' tendon of the guinea pig in which fibrillogenesis can be prevented or initiated by withdrawal or readministration, respectively, of ascorbic acid. Tenotomy was performed in 250-350 g guinea pigs as previously described for rats.(4) The material was taken at various intervals after the operation from normal and scorbutic animals and from animals at various stages of recovery from experimental scorbutus. The procedures for preparing ultrathin sections have been described.(4)

The fibroblast. The failure of the tissue to form intercellular structures in the absence of ascorbic acid has been ascribed to the injury which the fibroblasts supposedly suffer in scurvy. Although this opinion was based on light microscopic observations concerning cell and nuclear size and the degree of basophilia of the cytoplasm, no cytologic descriptions were available to distinguish the injured fibroblast from the normal.(5,p.308) The electron microscopic picture of fibroblasts from scorbutic guinea pigs shows for the first time how characteristically vitamin C deficiency affects the cell. Figure 35 presents a "scorbutic" fibroblast 12 days after tenotomy, in which the most characteristic feature is what appears in the section to be extensive vacuolation of the cytoplasm. The vacuoles, which may reach considerably greater sizes than the largest ones seen in the cell of Fig. 35, contain a material which precipitates in strands. The clearly outlined walls of the vacuoles are often seen to be set with microsomal granules; this suggests that the vacuoles originate from the endoplasmic reticulum which is missing as such in these cells.

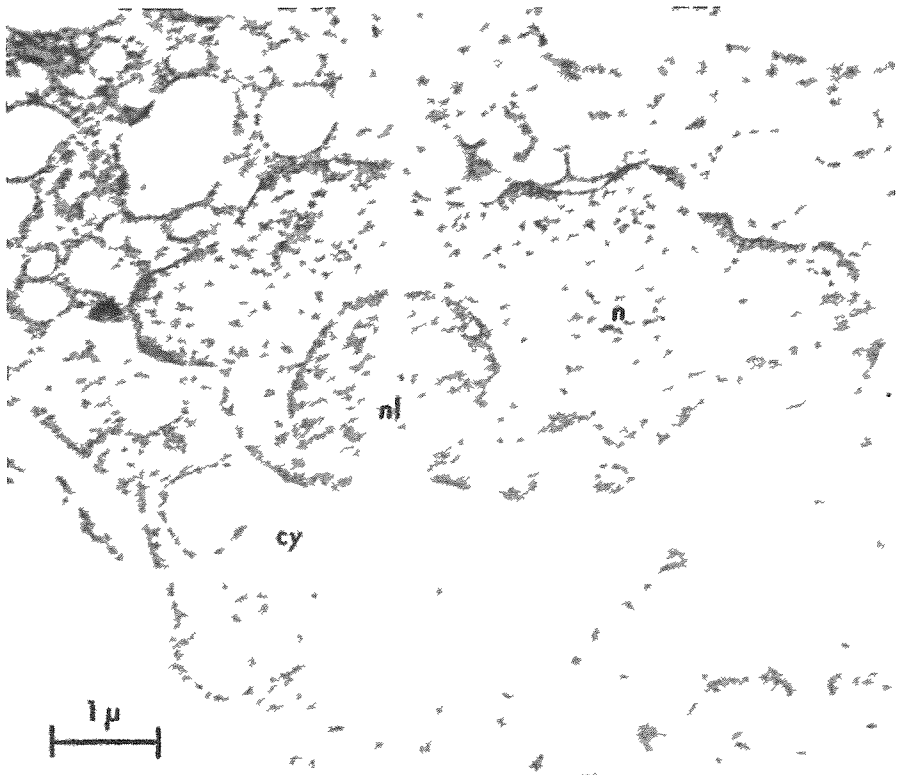

Figure 35. Fibroblast from the regenerating tendon of a scorbutic guinea pig 12 days after tenotomy, n, nucleus, nl, nucleolus. Notice the large vacuoles in the cytoplasm (cy) containing a precipitated material. At the walls of the vacuoles microsomes are attached.

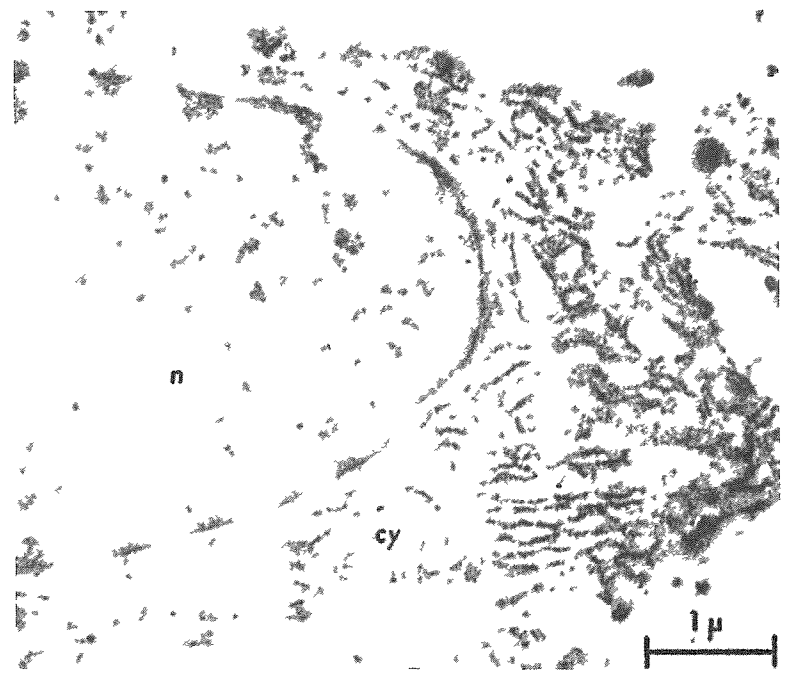

Figure 36. Fibroblast from the regenerating tendon of a scorbutic guinea pig which after tenotomy received within 7 days 3 subcutaneous injections of 20 mg ascorbic acid in addition to vitamin C-containing diet; n, nucleus, cy, cytoplasm. Notice that the endoplasmic reticulum has been restored.

The groundplasm between the vacuoles contains many small vacuoles and granules of various sizes. Mitochondria may or may not be present in a particular section, but they are certainly not absent from the scorbutic fibroblasts. The nucleus, although smaller than that of a healthy fibroblast and usually of irregular shape, does not differ markedly in structure from its normal counterpart. The nucleolus in such fibroblasts does not show the characteristic composition of an electron-dense material with a kind of ground substance, and it is sharply set off against the nuclear structure; this may well be significant as we are dealing with a cell whose protein-producing activity may be interrupted or altered. The scorbutic changes of the fibroblast seem to be completely reversible The fibroblast in Fig. 36 was obtained from an animal which, after tenotomy, was allowed to recover from scorbutus for 8 days. The endoplasmic reticulum has been restored and the groundplasm no longer contains the small vacuoles seen in the scorbutic cell. The nucleus is large and shows a smooth surface.

Fibrillogenesis. In a healthy animal the fibroblastic activity may be expected to begin about 2 weeks after tenotomy. A striking feature of the fibroblast at that time (Fig. 37) is the presence of a marginal zone of cytoplasm which is entirely free of endoplasmic lamellae and mitochondria.

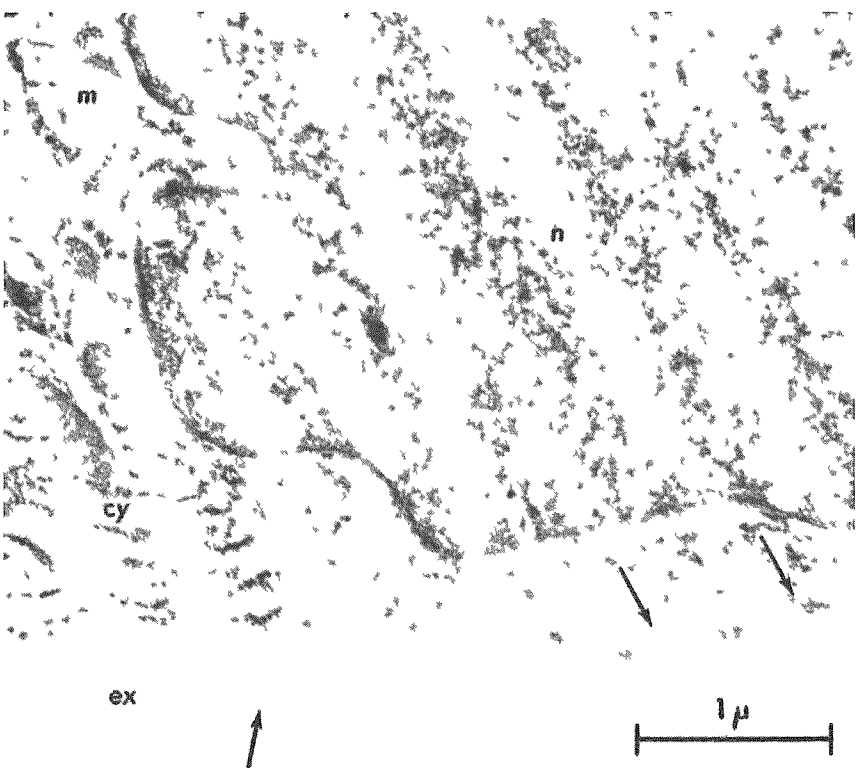

Figure 37. Part of fibroblast from a healthy guinea pig 16 days after tenotomy; n, nucleus; cy, cytoplasm, ex, exoplasm; m, mitochondria. Notice the exoplasmic zone in which at some places an orientation of fine structures parallel to the surface of the cell can be observed.

It corresponds to the exoplasm known to exist in various kinds of cells. While no demarcation can be seen between endo- and exoplasm, the latter forms a well-defined surface in young fibroblasts. In the exoplasm in Fig. 37 one observes slight but clear indications of an orientation, parallel to the surface of the cell, of very fine fibrillar structures. The fibroblast was obtained from the regenerating tendon of a healthy animal 16 days after tenotomy, i.e., at the time of onset of fibroblastic activity. Such early inconspicuous structures become meaningful when one sees them more numerous and much more distinct in other fibroblasts at the beginning of fibrillogenesis, especially in cases where the process was initiated by injections of ascorbic acid at a time when the fibroblasts had already invaded the area of regeneration. Such a case is presented in Fig. 38A. The endoplasmic spaces, still very large, show that the scorbutic changes have not been reversed in this cell. However, its outer zone has assumed the character of the exoplasm and contains numerous very fine fibrils of widths of about 50 A. In somewhat later stages the cell surface is no longer clearly defined as in Fig. 38A but is lost in bundles of primary fibrils which seem to have become disengaged from the cell. In Fig. 38B relatively dense fibrils of this kind have been slightly separated from the exoplasm probably by the cutting knife. Such distortions, which we cannot avoid at present, bring some uncertainty into the interpretation of electron micrographs. They are, however, compensated to some degree by taking into account the experimental conditions which produced the situation seen in the micrograph.

Growth of microfibrils. Although these and earlier observations indicate that fibrillogenesis begins within the cytoplasm of the fibroblast, it is necessary to assume that the primary fibrils so produced and then released by the cell must take up procollagenous material from the ground substance, otherwise they could not grow outside the cells, increasing their widths as they do from about 200 to 1000 A or more.(5, p. 329) Up to now examination of the ground substance with the electron microscope has showed only that it is not amorphous.(4) None of the structures observed in the ground substance could be identified with any material that would account for the accretion of the collagenous fibrils. Our new material taken from the guinea pig, especially under the condition of stimulated fibrillogenesis, shows for the first time fine fibrils situated between young collagenous microfibrils in a relationship which strongly suggests that the fine fibrils represent the procollagenous material in the ground substance. A representative picture of this kind is shown in Fig. 39A.

Periodic activity of the fibroblast. The growing microfibrils in Fig. 39A are located in the ground substance. Adjacent fibroblasts such as that in Fig. 39B often show a well-defined surface. The period of the exoplasmic zone as shown in Fig. 39A apparently is past; the situation suggests that the cell after producing a certain amount of fibrils ceases to continue its fibroblastic activity. The conclusion seems unavoidable that the fibroblast after a period of activity assumes the character of the fibrocyte without

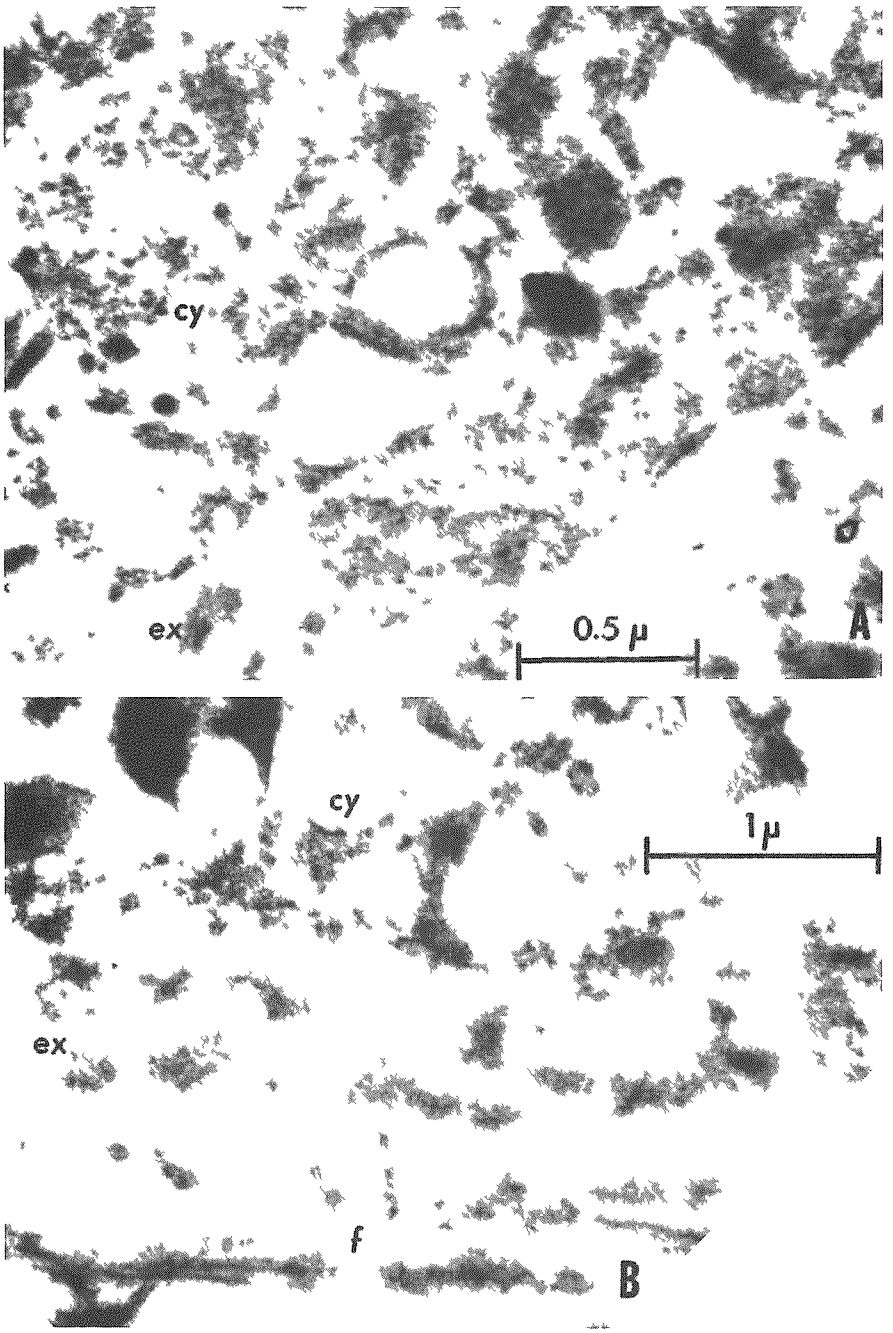

Figure 38A. Part of cytoplasm (cy) of a fibroblast from the regenerating tendon of a scorbutic guinea pig which after tenotomy was recovering from the deficiency. Notice the numerous microfibrils in the exoplasm (ex).

Figure 38B. The situation is similar to that in A in that fibrillogenesis was also stimulated by injections of ascorbic acid and vitamin C-containing diet; however, the beginning of fibrillogenesis is somewhat farther advanced, insofar as well-defined primary fibrils are present in the outermost zone of the cell in parallel arrangement.
Symbols = cy, cytoplasm; ex, exoplasm; f, fibril.

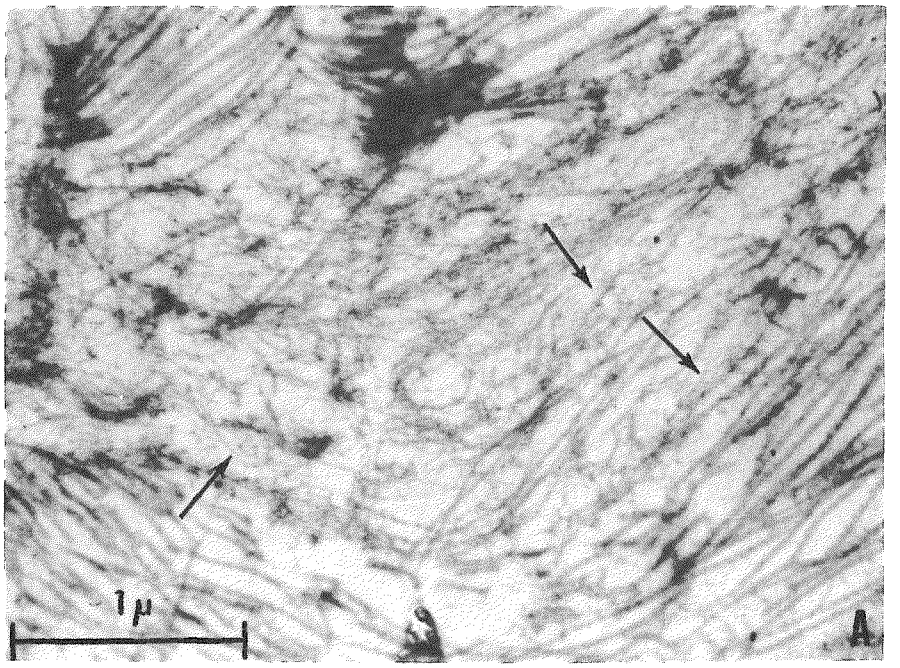

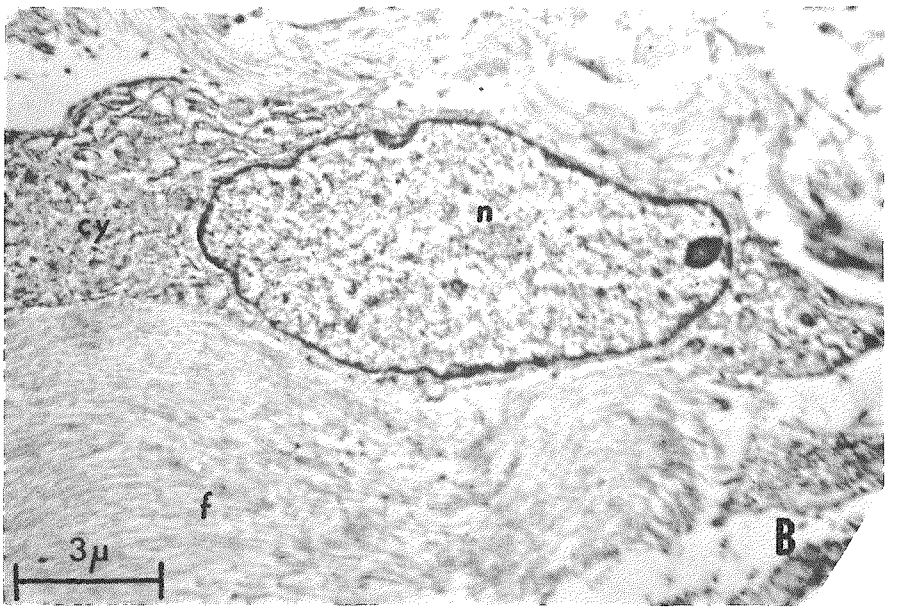

Figure 39A. Intercellular material from the regenerating tendon of a guinea pig recovering from scurvy. Between the well-defined collagenous microfibrils can be seen extremely fine fibrils (arrows) which are considered to represent procollagenous material in the ground substance.

Figure 39B. Fibroblast from the regenerating tendon of a guinea pig which was allowed a period of recovery of 7 days. The cytoplasmic structure is completely restored. The fibrils adjacent to the cell are 250 to 300 A thick and are supposed to have been formed during the period of recovery. However, the fibroblast shows no sign of activity at the surface and is clearly separated from the fibrils. The situation suggests that this cell, after a period of activity, has ceased to produce fibrils. Symbol = n, nucleus; cy, cytoplasm; f, fibrils.

losing its fibroblastic potency. The analogy with the osteoblast is obvious. Although most students of connective tissue would probably subscribe to this conclusion, no attention has been given in the studies on fibrillogenesis to a limited or, as far as embryonic tissues are concerned, a periodic activity of the fibroblast. If, through neglect of this point, one fails to recognize the difference between active fibroblasts and fibroblasts that are in this sense inactive, one cannot interpret correctly the cell-fibril relationships during the formation of collagenous fibers.

Summary. The present studies on fibrillogenesis in the regenerating tendon of the guinea pig under normal and experimentally controlled conditions not only confirmed the results of previous investigators including this author, but enlarged our knowledge. The new findings are as follows.

1. The failure of the tissue to produce intercellular material in the absence of ascorbic acid is paralleled by characteristic changes in the fibroblast. During recovery from scurvy these are reversed to normal.
2. The beginning of fibroblastic activity consists of the differentiation of an exoplasmic zone in the fibroblast. In this zone the first fibrillar structures appear.
3. Between the growing collagenous microfibrils of the ground substance are very fine fibrils, which further studies may show to be identical with procollagenous material.
4. Some fibroblasts in young connective tissue can be found in a state of inactivity. This fact must be taken into account in order to interpret electron micrographs correctly with regard to the relationships between cells and fibrils.

References

1. Policard, A. and A. Collet. La genese des fibrilles collagenes et le debuts de la Fibrose evisages au point de vue inframicroscopique. La Biologie Medicale 45, 16 pp., 1956.

2. Porter, K. R. Repair processes in connective tissues, in Second Conference on Connective Tissues, New York Josiah Macy, Jr. Foundation 1952.

3. Jackson, S. F. The formation of connective and skeletal tissues. Proc. Roy. Soc. Lond. Ser. B. Biol. Sci. 142:536-548 (1954).

4. Wassermann, F. Fibrillogenesis in the regenerating rat tendon with special reference to growth and composition of the collagenous fibril. Am. J. Anat. 94:399-438 (1954).

5. Wassermann, F. The intercellular components of connective tissue: Origin, structure and interrelationship of fibers and ground substance. Erg. der Anatomie 35:240-333 (1956).

PROGRESS REPORT: GAMMA RAY TOXICITY PROGRAM

Response of Mice to Conditioning Doses of Whole-body Irradiation

George A. Sacher and Douglas Grahn

Mice exposed to 0.11 r/day of radium γ-rays for the duration of life were observed to have a greater mean after survival than their controls.[1,2] More complete analysis of these data has shown that this effect is due to a lower mortality in the irradiated mice during the first 3-6 months of exposure although late in life the mortality rate of the 0.11 r/day mice is greater than the control.[3] The analysis also demonstrated that the same phenomenon existed at daily exposure levels of 1.1, 2.2, 4.4 and 8.8 r/day, and that the duration of the depressed mortality rate became shorter as daily dose increased. The same response is noted in the present γ-ray toxicity studies at 6 r/day.

These observations indicate that following the start of exposure there is a brief period when accumulated injury is not being expressed, but, instead, there is an improved survival value. It is unlikely that the protracted low-level exposure has a direct beneficial action. We favor the hypothesis that the improved survival is a compensatory or conditioned response to a stimulus arising from a low level of radiation injury. Under our experimental conditions, this compensation appears to express itself in the form of an enhanced defense against infection. It is predominantly infectious disease mortality that occurs in the early period in both control and irradiated mice, and death from this cause is lower in the irradiated group.

These data on improved survival under low levels of irradiation constitute the major evidence for the existence of a threshold dose (the dose below which no biological effect can be measured). If the improved survival arises from a response to low-grade injury, the threshold dose concept is not appropriate. There is need for further evaluation of this problem because the degree of improved survival is quite variable.

We are currently endeavoring to produce and evaluate this conditioned response. Mice (100 days of age) are subject to a daily exposure of approximately 0.6 r/day for varying periods of time, then tested, along with unirradiated controls, by exposure to either a high daily dose of Co^{60} γ-radiation or a single acutely lethal dose of 200 kvp X-rays. In the first test procedure, mean after survival (MAS) is the end point; in the second, per cent mortality in the first 30 days after exposure is determined. Table 18 gives a summary of the results to date on LAF_1 and $C3H_f$/He mice.

TABLE 18

Acute radiation response of LAF_1 and $C3H_f$ mice after protracted low-level irradiation started at 100 days of age

Strain	No. of animals	Conditioning exposure, r/day	Duration of conditioning, days	Test dose, r/day	MAS, days	30-Day mortality, %
Daily-dose test series						
LAF_1	18	0	45	170	21.9	
LAF_1	18	0.6	45	170	21.0	
LAF_1	24	0	90	170	23.9	
LAF_1	24	0.6	90	170	24.0	
LAF_1	24	0	160	170	23.5	
LAF_1	24	0.6	160	170	24.3	
LAF_1	24	0	225	170	24.8	
LAF_1	24	0.6	225	170	20.4	
LAF_1	12	0	325	170	25.3	
LAF_1	12	0.6	325	170	24.6	
$C3H_f$	42	0	50-150	97-125	31.1	
$C3H_f$	42	0.6	50-150	97-125	31.3	
Single-dose test series						
LAF_1	23	0	50	750		75
LAF_1	23	0.6	50	750		74
LAF_1	45	0	100	750		67
LAF_1	48	0.6	100	750		35
LAF_1	46	0	140	750		61
LAF_1	47	0.6	140	750		34
LAF_1	22	0	200	800		91
LAF_1	22	0.6	200	800		64
$C3H_f$	35	0	100-200	650-700		40
$C3H_f$	36	0.6	100-200	650-700		56

In the LAF_1, the test exposure of 170 r/day gives negative results with respect to improved survival for the first 5-6 months. The single-dose test on the LAF_1 gives more promising results. Improved resistance to acutely lethal irradiation is seen after 100, 140, and 200 days of conditioning.

Data for the $C3H_f$ strain are pooled because of the small test samples employed. Here, again, the daily-dose test procedure gives negative results although no detrimental effect of the conditioning dose is detectable. The single-dose test shows the conditioned $C3H_f$ mice to have a

slightly greater sensitivity. While the data are still quite limited, the possibility of a genetic interaction in the conditioned response is indicated.

Data on age changes in radioresistance have indicated that a progressive increase in resistance normally occurs during the same interval in which this conditioned response is expressed (see, for example, the MAS values in Table 18 for the unconditioned 170-r/day series in the LAF_1 mice). The possibility of a relationship between normal maturation and the capacity to develop improved survival value must be explored. In this connection, the contrast in the LAF_1 series between the responses to the single-dose and daily-dose test procedures needs further investigation. The daily dose test condition was made part of the present study because of prior evidence that the increase of radioresistance with age is of the same magnitude whether measured by single exposures or by daily exposures in the 125-170 r/day range. Mice conditioned with small daily gamma exposures showed improved survival only under the single-dose test condition. This suggests that the increased radioresistance brought about by small daily γ-ray exposures is not entirely equivalent to the increase of radioresistance with age.

Ultimately, the response of conditioned mice to various sublethal stresses should be studied in order to obtain data on the physiological basis of the improved survival.

References

1. Lorenz, E. Some biologic effects of long continued irradiation. Am. J. Roentgenol. 63:176-185 (1950).

2. Lorenz, E., J. W. Hollcroft, E. Miller, C. C. Congdon, and R. Schweisthal. Long term effects of acute and chronic irradiation in mice. I. Survival and tumor incidence following chronic irradiation of 0.11 r per day. J. Nat. Cancer Inst. 15:1049-1058 (1955).

3. Sacher, G. A. On the statistical nature of mortality, with especial reference to chronic radiation mortality. Radiology 67:250-257 (1956).

PROGRESS REPORT: GAMMA RAY TOXICITY PROGRAM

Thymic Lymphomas in Mice Exposed to Low-Dose Daily Co^{60} Gamma Irradiation

Samuel Lesher, George A. Sacher, Douglas Grahn, and Joan M. Gurian

This is a preliminary report on the incidence of thymic lymphoma in LAF_1 male and female mice exposed to continuous daily γ-irradiation. Thymic involvement can be established at gross autopsy; other types of leukemias will be reported after completion of histopathological diagnoses.

Mice at 100 days of age are entered into the low-level γ-chamber in replications consisting of equal numbers of males and females to minimize the possible variability between shipments. Only completed replications have been analyzed. The data are summarized in Table 19 and Fig. 40. The incidence is significantly higher in the females.

TABLE 19

Summary of data showing for both male and female LAF_1 mice the total number of mice in each experimental group, mean survival, numbers of mice with thymic lymphomas and per cent incidence in each group

Radiation dose r/day	No mice		Mean survival, days		Thymic lymphomas		Incidence, %	
	♀	♂	♀	♂	♀	♂	♀	♂
0	71	72	634 5	420 2	3	1	4 2	1 4
6	75	75	529 8	462 8	11	4	14 7	5 3
12	102	102	405 8	361 8	22	7	21 6	6 9
24	126	126	269 0	251 0	32	19	25 4	15 1
32	135	135	217 8	205 5	39	22	28 9	16 3
43	150	150	155 9	149 8	35	20	23 3	13 3
49	135	135	134 1	126 9	17	8	12 6	5 9
56	120	120	104 2	102 1	7	2	5 8	1 7

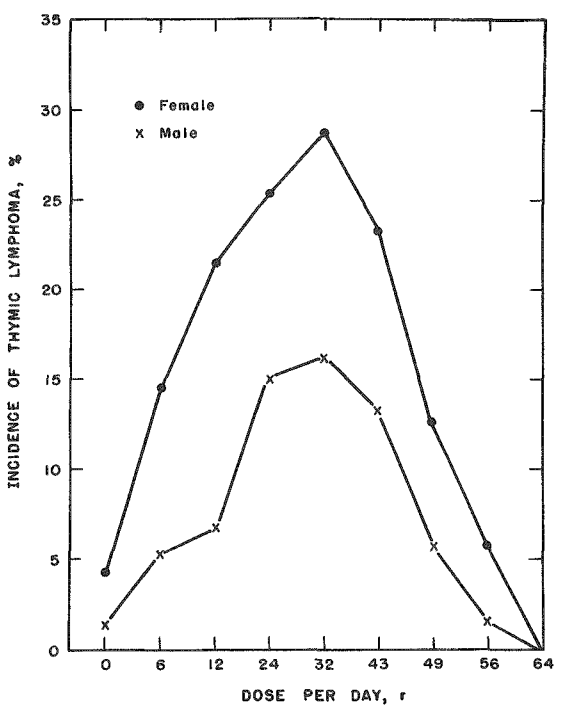

Figure 40. Thymic lymphoma incidence vs. dose.

PROGRESS REPORT: GAMMA RAY TOXICITY PROGRAM

A Preliminary Report on a Histopathological Study of the Mouse Duodenum after Starvation

Samuel Lesher and Anthony Sallese

After exposure to lethal doses of ionizing radiation, the mouse very early becomes lethargic and stops eating. It is thought that starvation and inanition may produce changes in the small intestine that closely resemble those produced by irradiation. To our knowledge the problem has not been examined since Sun[1] published the results of a rather superficial investigation of the effects of starvation and refeeding on the mouse duodenum. He described rather pronounced lesions which occurred at the tips of the villi after 40 hr of starvation, but neglected to describe the mice he used other than to say that they weighed from 10 to 14 g.

In this preliminary re-examination of the histological changes produced by starvation, equal numbers of 100-day-old male and female LAF_1 mice were separated into two groups; the first without food and water, the second without food but with free access to water. The mice were separated as to sex and maintained in wire-bottom cages.

Four animals, one male and one female from each group were sacrificed at each of 4 successive intervals (24, 48, 72, and 96 hr after the beginning of the starvation period), and segments of duodenum immediately distal to the pyloric sphincter were fixed and prepared for study. By 48 hr the entire intestine was devoid of food and feces. The first deaths occurred on the 4th day, when 2 of the remaining 12 mice died. The peak in deaths occurred on the 5th day, when 7 of the remaining 8 died; one survived to the 6th day. Peristaltic movement must have increased tremendously between the second sacrifice at 48 hr and the third at 72 hr, since intussusception involving two-thirds of the colon was observed in 3 of 4 mice.

Histologically the duodenum of the starved animals at 24, 48, and 72 hr was normal in every respect and could not be distinguished from the duodenum of healthy unstarved mice (Fig. 41). At 96 and 122 hr the histological picture of the duodenum from the starved mice differed only from that of the unstarved by a decrease in stainability of the cells near the tip of the villi. In none of the mice did starvation produce the type of lesions described by Sun.

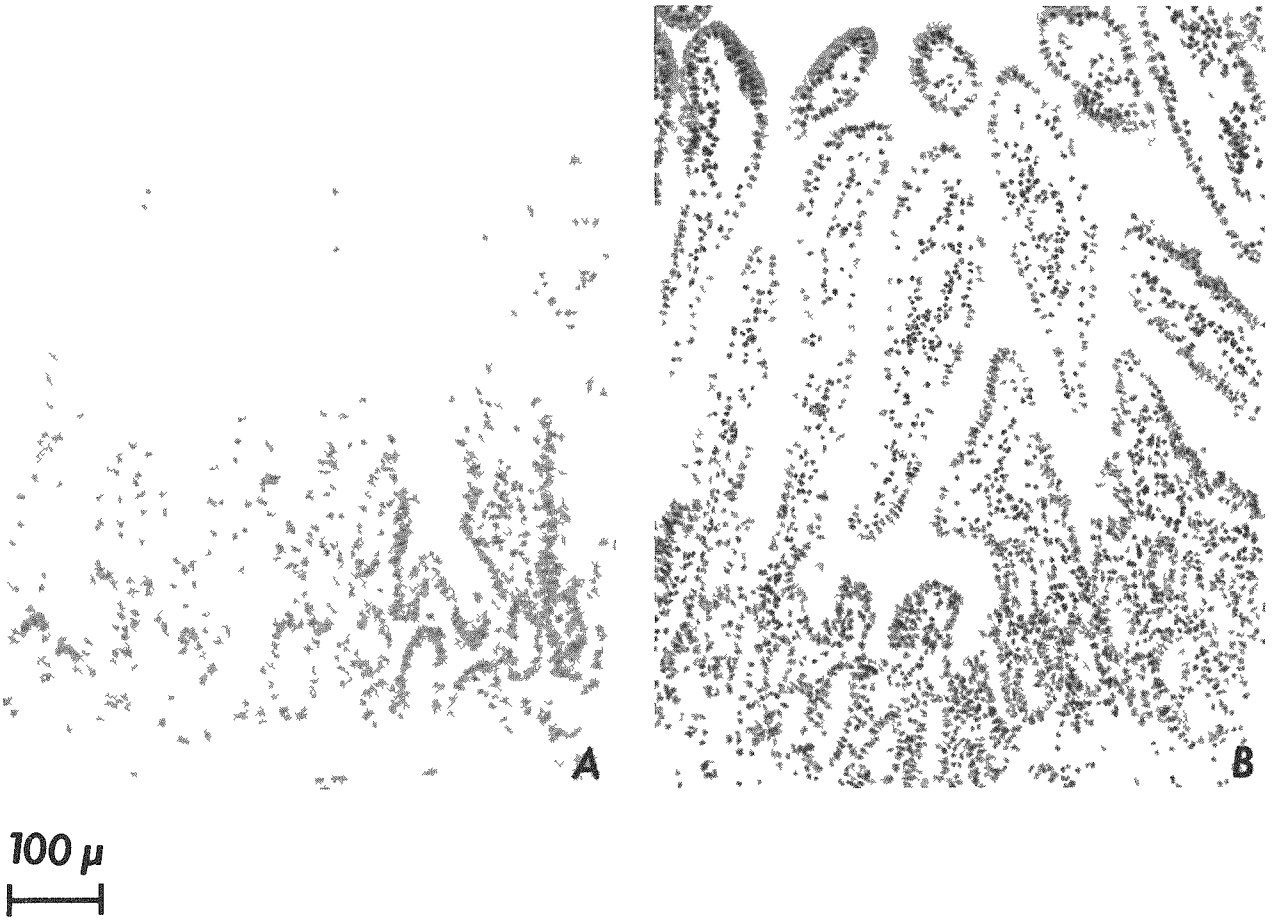

Figure 41 A, duodenum of normal mouse. B, duodenum after 72 hr without food and water. No evidence of structural change or cytological damage. Hematoxylin and eosin stain.

Reference

1. Sun, T. P., Histophysiological study of the epithelial changes in the small intestine of the albino mouse after starvation and refeeding., Anat. Rec. 34: 341-349 (1927).

A COMPARATIVE HISTOLOGICAL STUDY OF DUODENAL DAMAGE PRODUCED BY FISSION NEUTRONS AND Co^{60} GAMMA RAYS

Samuel Lesher and Howard H. Vogel, Jr.

During the past several years, experiments have been carried out to test the relative effectiveness of Co^{60} γ-rays and fission neutrons on a number of biological objects.(1) One of the comparative criteria utilized was the acute lethal action on mice exposed to single doses of these two radiations. Following exposures to fission neutrons, mice showed a much earlier mode of mortality than after comparable irradiation with Co^{60} γ-rays.(2) A specific intestinal radiation syndrome leading to death in 3 to 5 days has been described in several species of laboratory animals following exposure to large doses (1500 to 10,000/r) of X-rays.(3) It seemed of interest to determine whether or not the early mortality characteristically following fission neutrons was also produced by intestinal damage.

Materials and Methods

Two groups of female CF No. 1 mice were exposed to doses sufficiently high to kill 90% in a 30-day period: 350 rads fission neutrons or 1050 r gamma rays. All exposures were carried out in a gamma-neutron radiation chamber at the CP-5 research reactor.(4) The methods of exposure were similar to those already described for the CP-3 reactor.(2) The dose rate of fission neutrons at the animal exposure position, with CP-5 operating at 2000 kw, was approximately 7.5 rads/min including 10-15% of contaminating γ-radiation. The intensity of Co^{60} γ-rays used in these exposures was approximately 14 r/min. The single exposures to each radiation varied from 45 to 75 min.

Two neutron- and two γ-irradiated mice were sacrificed at $\frac{1}{2}$, 2, 3, 5, 10, 15, 22, 24, 30, 36, 46, 48, 54, 72, 96, 120, 144, 168, 192, 216, and 240 hr after irradiation. In addition, 2 γ-irradiated mice were killed at 12, 14, 16, and 20 days after exposure. In a second experiment mice similarly irradiated were sacrificed when they became moribund.

From each mouse two pieces of duodenum in the segment adjacent to the pyloric sphincter were removed and fixed in Tellyesniczky's solution. One piece was sectioned longitudinally and the other transversely. Five-micron sections from each block were stained with Delafield's hematoxylin and eosin and studied for structural changes. Additional adjacent sections were also stained with toluidine blue, the PAS reaction and Feulgen reaction.

Observations

Crypt nuclei are damaged both by fission neutrons and γ-rays within the first half hour following exposure. At this time mitotic figures are completely absent. The degree and type of damage for the first 10 hr is essentially the same in both experimental groups with the early damage being confined to the crypts in the form of intensely basophilic karyolytic bodies and enlarged nuclei. These early changes are similar to those described by Lesher[5] following exposure to continuous γ-irradiation in the high acute range.

Mitotic figures are detectible in the duodenal crypts of the γ-irradiated mice by 10 hr. The mitotic rate reaches a relatively high level by the end of the first day. There is little chromosomal damage in the crypts of the γ-irradiated mice. The early onset of mitosis and the subsequent high rate leads to the replacement of damaged crypt cells before the crypts become disorganized and disintegrate. By 48 hr repair exceeds damage, and by 96 hr most of the crypts appear normal. Although the villi become shorter through the loss of cells at the extrusion zone, their repair is complete by 144 hr. The first γ-irradiated mice die on the 8th day at which time the duodenum appears normal microscopically.

The first mitotic figures are seen in the crypts of the neutron-irradiated mice at 22 hr. Many of the chromosomes observed during the metaphase to anaphase period are severely damaged and few dividing nuclei appear capable of forming new viable cells. Chromosome fragments, bridges, and whole pyknotic nuclei are common. From the first day on, there is a distinct difference in the degree of damage and the rate of recovery between the neutron- and γ-irradiated groups (Fig. 42).

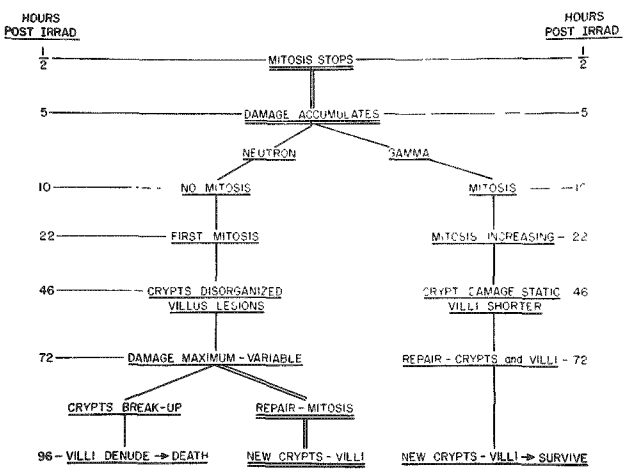

Figure 42. A diagrammatic presentation which emphasizes the differences in degree of damage and time of recovery of two series of CF No. 1 female mice exposed to fission neutrons and γ-rays.

The duodenal crypts of the neutron groups become disorganized and by 48 hr begin to breakup into isolated cell nests. At about the same time lesions appear at the tips of the villi as excessive numbers of cells are extruded at the villar tips. Without new cells from the crypts to replace those extruded, the villi become progressively shorter and by 72 hr most are less than half their normal length.

In the crypts there is an increase in the number of mitoses by 72 hr and new crypts form. Where the original crypt has disintegrated completely, masses of chromatin fragments accumulate in the crypt spaces. In approximately 50% of the mice, new crypts are slow in forming and mucosal membrane begins to slough off. This occurs at $3\frac{1}{2}$ to 5 days after irradiation. As the denuding of villi progresses, the villar connective tissue framework collapses forming a series of low cellular mounds in the area originally occupied by two or more separate villi. The cytoplasm of the epithelial cells is highly vacuolated and the nuclei are extremely irregular in shape and for the most part pyknotic. When the duodenum reaches this stage of degeneration, recovery is impossible and the mouse dies. In other mice of the neutron series, new crypts form before the crypts collapse and a few new cells move up along the base of the villi. In these mice repair keeps pace with or exceeds damage and the animals may live beyond the critical early period.

Duodenal sections of mice sacrificed when moribund and as near death as possible were studied to determine the extent of recovery. All mice exposed to γ-rays lived at least 8 days; in every case the duodenal, villar covering was intact and intestinal recovery was essentially complete. In mice exposed to fission neutrons and sacrificed when moribund at $3\frac{1}{2}$ to 6 days, the epithelial membrane covering the villi was severely damaged and denuding was well advanced. Lesions were common, and hemorrhage was excessive.

The duodenum of nonmoribund mice sacrificed at 5 and $5\frac{1}{2}$ days was in various stages of repair. In some cases the crypts were reorganized, mitotic rate was high, and new cells had begun to push up the sides of the villi closing off the radiation-produced lesions. In others, the villi had collapsed, blocking the movement of cells from the crypts. In the latter, bizarre, hyperplastic cell configurations had formed in the crypt region. There was considerable variability in the extent of duodenal recovery in the large number of mice examined in the 4- to 6-day period. Histologically they fall into three classes:

1. Villi are completely collapsed and partially or completely denuded, mice are near death.

2. Villi are collapsed but for the most part covered. Crypts are reorganized, and mitotic rate is high; however, with crypts blocked, movement of cells becomes disorderly and without direction. Death is probable.

3. Villi are short but new cells are moving up from the crypts to form a new epithelial covering. The mice are lethargic but should survive the original intestinal damage.

The duodenum of neutron-irradiated mice dying or sacrificed six days or longer following exposure were in advanced stages of recovery, and all serious lesions had been sealed with new epithelial cells.

Summary

The deaths occurring in the period $3\frac{1}{2}$ to 6 days after irradiation are accounted for by the complete destruction of the crypts and the subsequent extensive loss of the epithelial covering of the villi in the duodenum of at least half of the mice exposed to fission neutrons (350 rads, whole-body). Although the duodenum of the γ-irradiated mice (1050 r, whole-body) is severely damaged, recovery is complete, and all mice survive well beyond the 6th day.

Two important differences between the neutron- and γ-irradiated tissues were noted. First, mitotic inhibition is longer lasting following neutron irradiation. Mitosis is resumed in about 10 hr following γ-irradiation but is delayed for about 22 hr after neutron irradiation. Secondly, there is greater chromosome damage after neutron irradiation; a high percentage of the mitotic figures observed in the duodenum of mice sacrificed during the second and third day contain lagging and detached chromosome fragments and chromosome bridges. As a result of the excessive chromosome damage, very few of the early mitotic figures are capable of forming viable daughter cells. The great number of pyknotic nuclei found in the duodenal crypts of neutron-irradiated mice during the critical period from 22 to 84 hr supports this hypothesis. Few new cells are available to form new crypts; hence the mucosal membrane cannot be replaced before collapse and denuding of the villi occur.

References

1. Clark, J. W., D. L. Jordan, and H. H. Vogel, Jr. Biological effects of fast neutrons and gamma rays. Am. J. Roentgenol. 77: 524-530 (1957).

2. Vogel, H. H., Jr., J. W. Clark, and D. L. Jordan. Comparative mortality following single whole-body exposures of mice to fission neutrons and Co^{60} gamma rays. Radiology 68: 386-398 (1957).

3. Quastler, H., The nature of intestinal radiation death. Radiation Research 4: 303-320 (1956).

4. Vogel, H. H., Jr., R. A. Blomgren, and N. J. G. Bohlin. Gamma-neutron radiation chamber for radiobiological studies. Nucleonics II, 29-31 (1953).

5. Lesher, S., Cytologic changes in the mouse intestine under daily exposure to gamma rays., J. Nat. Cancer Inst. 19: 419-449 (1957).

VARIABILITY IN THE EXPRESSION OF TAIL SPOTTING IN MICE

Douglas Grahn and Walter C. Quevedo, Jr.

Although tail spotting is a common occurrence in pigmented mice, the genetic basis of this phenomenon has not been fully characterized. Grüneberg[1] gave evidence that it was due to a recessive gene that lacked full penetrance when homozygous, but had minor expression when heterozygous. Barrows,[2] in a selection experiment, suggested that tail spotting was due to a complex of genes, or what we now call a polygenic system.

Studies on tail spotting have often involved the C57BL strain which normally shows a high incidence of spotting (e.g., 91.4% in our C57BL/6 strain). This strain was reciprocally crossed with strain BALB/c (an albino) for genetic studies in acute and chronic radiation toxicity. The appearance of tail spotting in the F_1 led us to record the characteristic routinely in both F_1 and F_2 generations. The two reciprocal crosses in the hybrid generations are listed as the BC, from the C57BL dam, and the CB, from the BALB dam.

White tail spotting has various manifestations: tipping, banding, mottling and any combination of these; however, in this analysis, all forms of expression are pooled in one category.

Table 20 gives the principal results in the F_1 generation. The overall incidence of tail spotting is 62%, but a large and significant difference exists between the two reciprocal crosses. The BC F_1 shows over 80% spotting, nearly twice that of the CB F_1; it is, however, significantly below the C57BL parent value of 91%.

TABLE 20

White tail spotting incidence in BALB/c C57BL/6 F_1 hybrids

Reciprocal Cross	♀	No. of animals	♂	No. of animals	♀ + ♂	No. of animals
BC F_1	80.1	357	82.6	299	81.3	656
CB F_1	45.5	301	38.3	339	41.7	640
Comb. reciprocals	64.3	658	59.1	638	61.7	1296

There is a slight but insignificant sex difference, and no significant deviation indicative of sex linkage. Litter size has no influence, but the incidence of tail spotting increases linearly with advancing maternal age in both reciprocal crosses. The rate of increase differs for the two crosses; it is +16.6% for each 100 days of maternal age in the CB F_1 and +5.4% per 100 days in the BC F_1. This relationship is curious, since no maternal age effect is noted in the inbred C57BL parent.

A variance analysis of the F_1 data indicates that about 60% of the total variation is due to a difference between the two reciprocal crosses (a difference of maternal environment), 6% between dams within reciprocal cross and 34% between litters within dams. About one-fifth of the latter, or 7%, is attributable to differences in maternal age.

In the F_2 (Table 21) an average incidence of 56% is observed. Reciprocal cross and sex differences are not significant although deviations from equality are in the same direction as noted in the F_1. Maternal age effects are not apparent and there is no difference between dams within reciprocal cross. Apparently the F_1 dam provides a more uniform prenatal environment as compared to the inbred parents since much of the variability noted in the F_1 is not detected in the F_2.

TABLE 21

White tail spotting incidence in BALB/c:
C57BL/6 F_2 hybrids

Reciprocal cross	♀	No. of animals	♂	No. of animals	♀ + ♂	No. of animals
BC F_2	63.6	261	56.2	272	59.8	533
CB F_2	54.9	304	50.2	261	52.7	565
Comb. reciprocals	58.9	565	53.3	533	56.2	1098

The F_2 generation segregates five coat color types: black agouti, brown agouti, black, brown and albino. The incidence of tail spotting for the several color types is given in Table 22. Significant differences exist in all comparisons indicated, but a greater effect is associated with black than with agouti. Black and agouti combined also produce a greater effect than either one by itself. A simple additive genetic hypothesis could account for the variation noted among the color segregants.

TABLE 22

White tail spotting incidence in coat color segregants of BALB/c: C57BL/6 F_2

Coat color	% spotting	No. of animals	Chi square	Degrees of freedom	P
Bl. agouti	63.8	597	35.97	3	<.01
Black	52.3	197			
Brn. agouti	46.3	218			
Brown	37.2	86			
All blacks	61.0	794	26.04	1	<.01
All browns	43.8	304			
All agoutis	59.1	815	10.99	1	<.01
All non-agoutis	47.7	283			

On the basis of the findings in the BALB:C57BL hybrid data, several additional crosses have been made with the black agouti $C3H_f$/He strain. In our experience, this strain has not shown any evidence of tail spotting. The following crosses are in production: BALB x C3H F_1 and F_2, C57BL x C3H F_1 and F_2, C3H x C57BL F_1 and F_2. Some backcrossing is also being carried out, but no data are available at this time. Preliminary results from the crosses with C3H are given in Table 23.

TABLE 23

White tail spotting incidence in $C3H_f$/He hybrids

Cross	Generation				F_2 color types		
	F_1	No. of animals	F_2	No. of animals	Black agouti	Brown agouti	Black
BALB/c x $C3H_f$	2.3%	89	25.5%	298	24.2%	29.3%	-
C57BL x $C3H_f$	10.4%	96	32.5%	360	36.9%	-	21.0%
$C3H_f$ x C57BL	5.0%	140	30.4%	289	30.8%	-	29.4%

These data strongly suggest that the tail-spotting gene is carried by both the BALB and the C57BL strains. The appearance of tail spotting in the F_2 at a level near 25% approximates expectation for a 3:1 genetic segregation of a recessive gene. It is not completely recessive, however, since some expression is seen in the F_1 mice, which can be presumed to be heterozygous.

While the BALB:C3H F_2 data are nearly perfect for a recessive gene, the F_2 mice from the C57BL parent show an excess of spotting. Similarly, the F_1 mice from the black parent have a higher incidence of spotting than the F_1 from the BALB. These data support the postulate that, although both strains BALB and C57BL appear to carry the same major recessive gene for spotting, the C57BL mouse carries more, or stronger, modifying factors. This would also explain why the BC F_1 showed a significantly lower spotting incidence than the C57BL parent, even though both are homozygous for spotting and have the same maternal environment. The BALB contribution to the BC F_1 apparently acts to reduce or "dilute" the effect of the modifying factors from the C57BL.

The BALB:C3H F_2 color segregants show a similar spotting incidence. Since the black gene in this cross comes from the C3H parent, the previously noted enhancing effect of black in the BC and CB F_2 may have been the result of a modifier linked with the black gene brought in from the C57BL parent rather than the result of a pleiotropic effect of the black gene itself. In the C57BL:C3H F_2 segregants, the data are equivocal. One reciprocal cross shows an enhancing effect for agouti, as seen in the BC and CB F_2, but the other does not. Here, again, the segregating gene is from the C3H strain.

Unpublished observations by Allen[3] are in close agreement with the general findings regarding maternal influences, the existence of a major recessive gene for tail spotting and a differing effectiveness of modifiers in the BALB and C57BL strains. She also concluded that strains BALB and C57BL carry the tail-spotting gene, that strain A is another carrier, but strain AKR has the dominant allele. The gene is listed by the symbol tsp by Allen. From available data, the following strains are tsp/tsp: A, BALB/c, C57BL and C57L. Strains with the dominant gene (Tsp/Tsp) are: C3H, CBA and AKR.

In summary, tail spotting is a function of a major recessive gene that has variable expressivity, that lacks full penetrance when homozygous, and that exercises some expression when heterozygous. These observations are in full agreement with Grüneberg's conclusions.[1]

When homozygous (C57BL, BC and CB F_1 and F_2), the penetrance of tail spotting varies with the maternal environment, maternal age and innate genetic modifiers. In view of this, the penetrance of the gene could be increased by selection, particularly since the accumulation of effective genetic modifiers would undoubtedly act to enhance the contribution of the maternal environment. Such results would lead to the assumption that a polygenic system is responsible, as suggested by Barrows.[2]

References

1. Grüneberg, H. Inheritance of tail tip pigmentation in the house mouse. J. Genet. 33:343-345 (1936).

2. Barrows, E. F. Selection for tail spotting in the house mouse. J. Exptl. Zool. 80:107-111 (1939).

3. Allen, S. L. Effect of genetic and maternal environment upon tail spotting in mice, unpublished observations (1957).

PROGRESS REPORT: DEUTERIUM OXIDE INTOXICATION IN RATS

Effect of Deuteration on Kidney Function

John F. Thomson and Florence J. Klipfel

In the preceding report[1] data were presented demonstrating decreases in glomerular filtration rate (creatinine clearance, C_{Cr}) and renal plasma flow (p-aminohippurate clearance, C_{PAH}) in rats drinking heavy water. It was pointed out that the normal values for C_{PAH} were considerably lower than those reported in the literature, and it seemed probable that the amount of PAH administered yielded plasma levels of PAH above that which saturates the tubules; with lower doses of PAH, the terminal plasma values were so low that absurdly high clearance values were obtained. We have achieved in normal rats reproducible results, consonant with literature values, by injecting subcutaneously two doses of PAH, each dose 150 mg/kg, as a 1.5% solution in 2% sodium sulfate. The second injection was made 50 min after the first one. Urine was collected during the next 50 min.

We have subsequently repeated and extended our observations on the effects of deuteration on renal function. Eight female Sprague-Dawley rats, about 7 months old, were given 50% D_2O to drink ad libitum. Measurements of C_{Cr} and C_{PAH} were made three times before D_2O was given and six times during a 38-day period when the rats were drinking D_2O. After 3 of the rats died, the others were given H_2O to drink, and the studies were repeated 1 and 5 days after restoration to tap water.

The data are summarized in Table 24. Within 9 days, C_{Cr}, C_{PAH}, and urine output had decreased significantly, and by the 36th day were reduced to about 40% of the control values. The recovery after restoration to H_2O was remarkably fast. Even 1 day after removal from D_2O the urine flow was essentially normal, C_{Cr} was 80% of normal, and C_{PAH} was 60% of normal; after 5 days on ordinary water all were actually slightly above the initial values. At no time during the study was a difference evident between the rats that died and those that ultimately survived.

Since both the glomerular filtration rate and the renal plasma flow decreased at nearly the same rate and to the same extent with increasing levels of D_2O, it seems likely that there was no specific injury to the kidney per se. The elevated concentration of urea and NPN and the decreased concentrations of plasma protein and glucose in the blood of moribund rats[2] are strongly suggestive of adrenal insufficiency since these changes were quantitatively similar to those seen in adrenalectomized rats. It has been shown in a variety of species that reduction of renal function occurs after adrenalectomy [see Smith[3] for review]. Thus it is possible that one of

the reasons for the toxicity of D_2O is a disturbance of adrenal function. In agreement with this supposition are the observations that the adrenals increase in size by as much as 50% in deuterated rats, and that hypophysectomized animals, with atrophic adrenals, show toxic effects at much lower levels of D_2O.[2]

TABLE 24

Effect of D_2O on kidney function in rats

Days on D_2O	Plasma D_2O, %	No. of rats	Body weight, g	Ml/min/100 cm^2 surface area					
				Urine Flow		CCr		CPAH	
				Av	S.E.	Av	S.E.	Av	S.E.
-50	-	7	246	0.033	0.003	0.521	0.050	2.57	0.20
-43	-	8	251	0.027	0.003	0.616	0.025	2.22	0.06
-2	-	8	266	0.031	0.002	0.521	0.027	2.54	0.20
Av before D_2O	-	23	-	0.030	0.002	0.551	0.022	2.43	0.10
3	9.7	8	261	0.022	0.002	0.592	0.036	2.50	0.17
9	18.2	8	265	0.015	0.001	0.396	0.028	1.53	0.19
15	20.6	8	263	0.014	0.001	0.372	0.037	1.71	0.17
22	23.2	8	260	0.017	0.002	0.283	0.045	1.25	0.11
29	26.0	8	258	0.017	0.003	0.249	0.039	1.52	0.23
36	28.3	6	249	0.013	0.002	0.228	0.017	0.92	0.21
After H_2O									
1	19.8	5	254	0.026	0.004	0.434	0.039	1.42	0.24
5	< 5	4	250	0.032	0.005	0.628	0.012	2.60	0.29

References

1. Thomson, J. F., and F. J. Klipfel. Deuterium oxide intoxication in rats. Effect of deuteration on renal function. Semiannual Report of Biological and Medical Research Division, Argonne National Laboratory. ANL-5732, pp. 84-88 (1957).

2. Katz, J. J., H. L. Crespi, R. J. Hasterlik, J. F. Thomson, and A. J. Finkel. Some observations on biologic effects of deuterium, with special reference to effects on neoplastic processes. J. Nat. Cancer Inst. 18:641-59 (1957).

3. Smith, H. W. The Kidney. pp. 361-365. Oxford University Press (1951).

INFLUENCE OF THE ENDOCRINE GLANDS ON RADIATION-INDUCED HYPERPIGMENTATION IN MICE

Walter C. Quevedo, Jr., Douglas E. Smith, and Douglas Grahn

When pigmented mice are exposed daily to gamma radiation (6 r/day to 410 r/day), the skin of the extremities becomes progressively darkened.[1,2] The hyperpigmentation induced by radiation is characterized by an increased epidermal melanization resulting from the enhanced activity of melanocytes within the basal layer of the epidermis.[1-3] Shielding experiments have demonstrated that a direct exposure of epidermal melanocytes to radiation is required to elicit hyperpigmentation.[1] The increased rate of melanogenesis within irradiated melanocytes is attributed to the removal of inhibitory sulfhydryl (-SH) groups and the consequent release of the pigmentogenic enzyme tyrosinase.[4] Although hormones are known to play an important role in the regulation of mammalian pigmentation,[5,6] the extent to which radiation-induced darkening is also dependent on their action remains to be elucidated. To test the possibility of an endocrine-radiation interaction during hyperpigmentation, the hormonal status of mice was varied either by surgical removal of certain endocrine glands prior to irradiation or by the introduction of supplementary doses of hormones into intact animals concurrent with irradiation. The present report summarizes briefly the findings thus far.

Experimental

C57BL and LAF_1 mice (3-6 months old) of both sexes were employed throughout. Pigmentation changes were studied in the plantar surfaces of the hind feet which have been shown to be ideally suited for this purpose.[1] All mice received total body doses of either 97 r/day or 125 r/day of γ-rays from a Co^{60} source. At these daily doses intact mice generally survive from 4 to 7 weeks. Definite hyperpigmentation is observed by approximately 9 days of exposure and progressively increases thereafter, so that by 25 days the plantar surfaces are intensely darkened. By employing an arbitrary grading system as a measure of increased pigmentation during this period, a comparison of the progress of hyperpigmentation was made between intact mice and mice of altered endocrine status. In addition, observations were made on a smaller number of animals exposed daily to ultraviolet irradiation.

Castration. Thirty-two C57BL and LAF_1 mice of both sexes castrated from 3 weeks to 3 months prior to irradiation subsequently developed hyperpigmentation at approximately the same rate as did the controls; both achieved the maximum grade of pigmentation by 25 days of exposure to γ-radiation. A similar failure of castration to affect in any obvious fashion

the progress of hyperpigmentation was observed when castrated and control mice were exposed daily to ultraviolet radiation. After 16 daily exposures to UV, both intact and castrated mice showed similar degrees of tanning in the plantar surfaces of the feet.

Adrenalectomy. Daily exposure to γ-radiation was initiated from 1 to 3 days after removal of the adrenal glands. All adrenalectomized mice received sodium chloride (0.9%) in the drinking water. Although early mortality was observed, 14 of 18 operated LAF_1 and C57BL mice survived for 9 days or longer. In these mice hyperpigmentation apparently developed at the normal rate; at death, the adrenalectomized mice were as darkly pigmented as intact control mice exposed to γ-radiation for comparable periods of time.

Supplementary cortisone. Among the LAF_1 mice receiving daily γ-irradiation together with 2.5 to 6.0 mg/day of cortisone acetate, a striking suppression of darkening was observed in addition to an early mortality. Of 21 mice so treated only 7 survived from 9 to 12 days. Whereas by 9 days the control mice showed a definite darkening, the cortisone-treated mice surviving beyond 9 days failed to darken. The majority of 15 LAF_1 mice treated with 1.25 mg/day of cortisone survived longer than those receiving larger doses and developed hyperpigmentation. However, throughout the period of observation the cortisone-treated mice were consistently graded as being less pigmented than the controls.

Supplementary adrenocorticotropin (ACTH). Twenty-four LAF_1 and C57BL mice exposed to daily γ-irradiation and injected daily with from 1 to 4 U.S.P. units of Corticotropin-Gel (Wilson) became hyperpigmented at essentially the same rate as did the controls. All mice survived throughout the period of observation, which varied from 16 to 28 days.

Summary and Conclusions. The failure of castration to influence significantly the development of hyperpigmentation in irradiated mice is in contrast to the reports of very poor tanning responses in male and female human castrates exposed to ultraviolet light.[6] At present, no definitive statement can be made as to the nature of the inhibition imposed by cortisone on the melanin formation triggered by γ-radiation. It is possible that cortisone does not act directly on melanocytes but indirectly by suppressing the release of essential hormones from the pituitary gland.[5] Hypophysectomized animals are currently being studied to test for the possible contributions of pituitary hormones to radiation-induced hyperpigmentation. The failure of ACTH to inhibit pigment formation is surprising since ACTH acts to promote the release of cortisone-like compounds by the adrenal cortex. Possibly the rapid inactivation of exogenous ACTH[7] or the contamination of ACTH preparations by other pituitary hormones[5,8] may account for its apparent ineffectiveness. The results obtained thus far, except in the case of large doses of exogenous

cortisone, suggest that the occurrence of hyperpigmentation during daily irradiation may be largely independent of hormonal control. Obviously, however, the validity of such a conclusion will depend heavily on the results obtained with irradiated, hypophysectomized animals.

References

1. Quevedo, W. C., Jr., and D. Grahn. Hyperpigmentation in mice. I. Effect of chronic γ-irradiation. Quarterly Report of Biological and Medical Research Division, Argonne National Laboratory. ANL-5696, pp. 57-63 (1957).

2. Quevedo, W. C., Jr., and D. Grahn. Hyperpigmentation in mice. II. Influence of ultraviolet radiation and further observations on the effect of chronic X- and gamma-radiation. Semiannual Report of Biological and Medical Research Division, Argonne National Laboratory. ANL-5732, pp. 93-94 (1957).

3. Ellinger, F. The Biologic Fundamentals of Radiation Therapy. Elsevier Publishing Company, New York (1941).

4. Flesch, P., and S. Rothman. Role of sulfhydryl compounds in pigmentation. Science 108:505-506 (1948).

5. Lerner, A. B., K. Shizume, and I. Bunding. The mechanism of endocrine control of melanin pigmentation. J. Clin. Endocrinol. Metabolism 14:1463-1490 (1954).

6. Deutsch, S., and H. Mescon. Melanin pigmentation and its endocrine control. New Engl. J. Med. 257:222-226, 268-272 (1957).

7. Baker, B. L., D. J. Ingle, and C. H. Li. The histology of the lymphoid organs of rats treated with adrenocorticotropin. Am. J. Anat. 88:313-350 (1951).

8. Pickford, G. E., and B. Kosto. Hormonal induction of melanogenesis in in hypophysectomized killifish (Fundulus heteroclitus). Endocrinology 61:177-196 (1957).

RADIATION PROTECTION EXPERIMENTS IN MICE EXPOSED TO FISSION NEUTRONS

Howard H. Vogel, Jr. and Donn L. Jordan

1. Comparative Effects of Single, Postirradiation Intravenous Injection of Homologous Bone Marrow Cells in Mice Irradiated with Lethal Doses of Fission Neutrons and Co^{60} γ-Rays

CF No. 1 female mice, 6 to 8 weeks of age, were exposed to a single dose of fission neutrons or of Co^{60} γ-rays sufficiently high so that 95-100% would die within 30 days. The exposures were carried out in the gamma-neutron radiation chamber[1] at the CP-5 research reactor. Ninety-four mice were exposed to 360 rads of fission neutrons in 100 min with the reactor operating at 1000 kw; 69 additional mice were exposed to a single dose of 1082 r of Co^{60} γ-rays delivered at an intensity of 13.3 r/min. Each series of irradiated mice was then subdivided into two groups, the first receiving an intravenous injection via the tail vein of 0.2 cc bone-marrow cells in Tyrode's solution, the second half receiving 0.2 cc of Tyrode's solution only. All injections were completed within a few hours following irradiation.

The bone-marrow cells were obtained from the femora of other CF No. 1 female mice of approximately the same age as the irradiated animals. The donor mice were sacrificed with ether, and both femurs were dissected free. The head of each femur was then cut off, and the cells were washed out of the marrow cavity into a small glass dish with a small amount of sterile Tyrode's solution, by means of a hypodermic needle. For every irradiated mouse that received a bone-marrow injection, one donor mouse was sacrificed, and each bone-marrow injection contained the equivalent of the cellular contents from two femurs.

The results of this experiment are illustrated in Fig. 43. It is clear from the cumulative mortality indicated for the γ-irradiated mice that the single intravenous injection of bone-marrow cells gave definite protection. All of the 34 irradiated controls died within 10 days after exposure. In contrast, only 15 of the 35 mice (43%) that received bone-marrow cells died during the 30-day period following irradiation. The protective action of these cells following irradiation with fission neutrons is much less evident. For 7 or 8 days after exposure, no protection by the marrow cells is evident. However, there is evidence of marrow-protection in the neutron-irradiated mice after the first week, and the 30-day lethality is decreased.

Cytological studies of the duodenum of neutron-irradiated mice have shown that the early 4-9 day mortality, characteristically seen after irradiation with fission neutrons, is correlated with severe damage and partial denudation of the intestinal mucosa.[2] Mice irradiated with Co^{60} γ-rays, within the acute lethal dose range, do not die from this intestinal syndrome. Although their intestinal cells show damage following exposure, recovery is rapid, and the intestinal lining appears well repaired within 3 to 4 days after irradiation. It seems probable, therefore, that bone-marrow cells failed to protect neutron-irradiated mice during the first week after exposure because these animals were dying as a result of intestinal damage against which the bone-marrow cells were ineffective. In contrast, X- or γ-irradiated mice are well protected by bone-marrow cells because their hematopoietic systems are stimulated to prevent death from the usual "hematological syndrome."

2. The Synergistic Action of Intravenous Bone-Marrow Cells and Streptomycin in Protecting Neutron-Irradiated Mice

Since it has been demonstrated that an antibiotic such as streptomycin can protect neutron-irradiated mice for at least 10 days after exposure,[3] it seemed possible that a combination of marrow cells and streptomycin might result in better protection than either agent alone. It was thought that the antibiotic would keep some of the irradiated mice alive beyond the period of the intestinal syndrome, and that the bone-marrow cells could then assume their protective role in helping to prevent the later deaths associated with the destruction of the blood-forming elements.

Approximately 130 CF No. 1 female mice were irradiated with 350 rads of fission neutrons at CP-5. The reactor was operated at 2000 kw, twice the power of the first experiment, so that the second exposure was carried out in 46 min, at a dose rate of 7.5 rads/min. The irradiated mice were divided into four equal groups as follows:

Group I (32 mice) received a single intravenous injection of bone-marrow cells (0.2 cc in Tyrode's solution) within a few hours after exposure.

Group II (32 mice) received a single intravenous injection of bone-marrow cells and, in addition, received daily subcutaneous injections of streptomycin (5 mg in 0.5 cc physiological saline) for the first 12 days after irradiation.

Group III (32 mice) received a single intravenous injection of Tyrode's solution (0.2 cc) and daily streptomycin injections, as above.

Group IV (30 mice) received a single intravenous injection of Tyrode's solution plus daily subcutaneous injections of 0.5 cc physiological saline solution.

A fifth group of 32 mice served as unirradiated controls.

The results of this experiment (Fig. 44) tend to support the hypothesis. Although daily streptomycin therapy alone (Group III) protected the irradiated mice for at least 9 days, protection was not evident thereafter; the 30-day mortality figure (75%) was not greatly reduced from that of the saline-injected irradiated mice of Group IV (87%). A single bone- marrow injection (Group I) reduced the 30-day mortality to only 25%. Most of these deaths occurred during the first 8 days after exposure, during the period of intestinal damage. When both agents were combined (Group II), a synergistic protective action was observed; only 3 mice of the 32 irradiated (9%) died within the 30-day period, in contrast to approximately 90% in Group IV, which received neither therapeutic agent.

3. Isologous Bone-Marrow Injections

Although the results of the first experiment showed protection when 30-day mortality was used as the criterion, (Fig. 43), the irradiated mice should be followed for longer periods in order to study possible incompatibility reactions between host and donor cells. Thus, of the 33 mice that survived the 30-day period in the γ-ray and neutron exposures illustrated in Fig. 43, 22 died between the 30th and 90th days after irradiation. After single acute exposures to these radiations, there are usually few deaths between the 30th and 100th days. This phenomenon of delayed deaths after homologous bone-marrow injections parallels the reactions following heterologous transfer of rat cells to the mouse.

The CF No. 1 mouse used in the first two experiments, and obtained commercially from Carworth Farms, is not a pure inbred line. Several skin transplants have been attempted between individual mice of this strain and invariably these homotransplants showed destruction within a 2-week period. This is good evidence that the genes are not identical and that the bone-marrow cells used are therefore homologous rather than isologous.

In order to determine whether the delayed deaths could be eliminated by using isologous rather than homologous bone marrow, a third experiment was carried out using C57BL/6 black mice, a closely inbred strain. A total of 36 mice was irradiated with 350 rads fission neutrons. Half of these were given isologous bone-marrow cells from other C57 black donors in a single intravenous injection after irradiation and were also injected daily for 12 days with streptomycin. The other half received a single intravenous injection of Tyrode's solution and daily subcutaneous injections of saline.

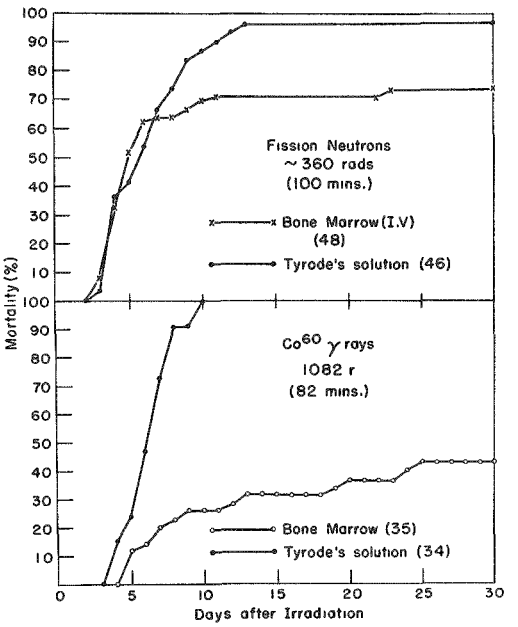

Figure 43. Comparative effects of single, postirradiation intravenous injection of homologous bone-marrow cells in mice irradiated with lethal doses of fission neutrons and $Co^{60}\gamma$-rays.

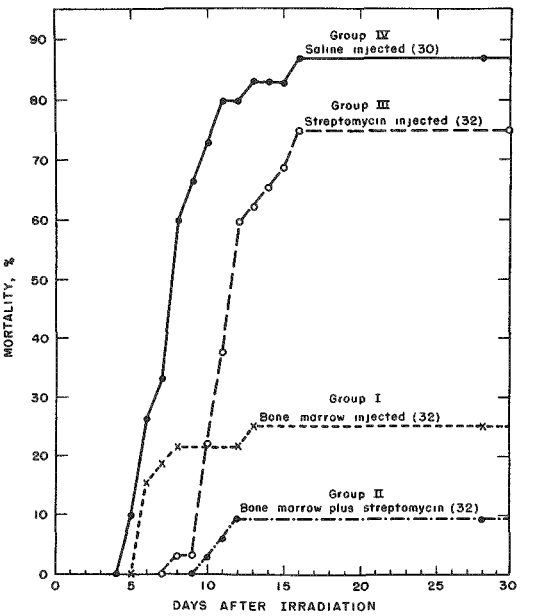

Figure 44. Comparative protective effects of postirradiation treatment with (a) streptomycin, (b) homologous bone-marrow cells, and (c) both agents combined. CF No. 1 female mice irradiated with single dose of 350 rads of fission neutrons at CP-5. Duration of exposure 46 min.

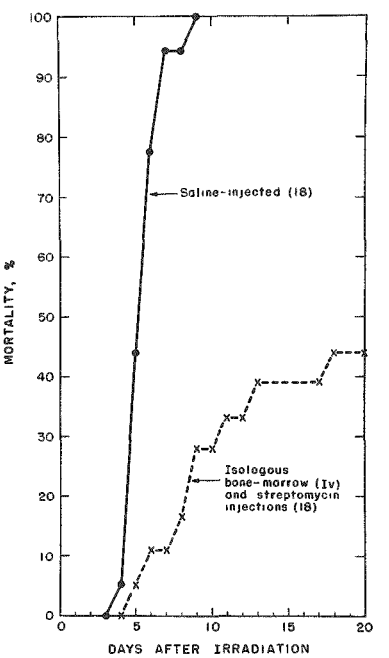

Figure 45. Postirradiation treatment of C57 black mice with combined therapy of streptomycin injections and isologous bone-marrow cells. Irradiation 350 rads of fission neutrons at CP-5. Duration of exposure 46 min.

Of the 18 mice in the second group, all had died by day 9 (Fig. 45). Mice of the first group were protected somewhat by the combination of bone marrow and streptomycin although the protection was not as marked as in the CF No. 1 mice. The 9-day LD_{100} was reduced to an apparent 9-day LD_{28}. In the acute 30-day period, 8 of the 18 mice died. It will be of interest to see if any of the 30-day survivors show the "delayed death" in the 30- to 90-day period, as has been found after the use of both homologous and heterologous bone-marrow cells.

References

1. Vogel, H. H., Jr., R. Blomgren, and N. Bohlin. The gamma-neutron radiation chamber for radiobiological studies. Nucleonics 11: (3) 28-31 (1953).

2. Lesher, S., and H. H. Vogel, Jr. A comparative histological study of duodenal damage produced by fission neutrons and Co^{60} gamma-rays. This report, pp. 101.

3. Hammond, C., H. H. Vogel, Jr., J. W. Clark, D. B. Cooper, and C. P. Miller. The effect of streptomycin therapy on mice irradiated with fast neutrons. Radiation Research 2:354-360 (1955).

PILOT STUDY OF SUBACUTE IRRADIATION FOR FUTURE FAST NEUTRON AND GAMMA-RAY EXPOSURES

Donn L. Jordan and Howard H. Vogel, Jr.

Use of the thermal column of the CP-5 reactor for the Neutron Toxicity Program is restricted to relatively short periods, in keeping with a schedule of use by several investigators. Thus long-term irradiations in a low-dose range present a problem of planning for investigations of chronic dose effects. The present pilot study is in progress to evaluate the effects of a series of fractionated doses from the 30-day LD_{100} acute dose ranges of fission neutrons and γ-rays through the subacute area to a very low total dose. The information should be useful in planning a larger experiment in the chronic area.

The schedule of exposures to fission neutrons is given in Table 25. A total of 198 CF No. 1 mice was used. Each group was given 13 exposures at a constant dose rate (4.6 rad/min), but the exposure time for each successive group was increased by a factor of 2 to yield total doses ranging from 29 to 908 rad.

TABLE 25

Schedule of exposures to fission neutrons

Group	Number of animals	Total exposure time* min	Dose per exposure, rad	Total dose, rad
A	18	209	69.9	908
B	36	104	36.0	468
C	18	52	17.5	227
D	36	26	9.0	117
E	18	13	4.4	57
F	36	6.5	2.2	29
Control	36	0	0	0

*13 exposures

For Co^{60} γ-rays, a similar schedule of exposures was applied to 158 mice at 13.5 ± 0.4 r per minute, with the maximum dose group at 2811 r (Table 26).

TABLE 26

Schedule of exposure to γ-rays

Group	Number of animals	Total exposure time,* min	Dose per exposure, r	Total dose, r
A	18	209	216.3	2811
B	24	104	111.5	1450
C	18	52	54.1	703
D	24	26	27.9	362
E	18	13	13.5	176
F	24	6.5	6.9	91
Control	32	0	0	0

*13 exposures

The animals in Group A of each irradiation category showed the mortality pattern associated with acute single exposures. The survivors are being observed to determine survival time and incidences of cataracts, lymphomas, and other tumors.

MODERATED NEUTRON FLUX IN THE CP-5 BIOLOGICAL FACILITY

Norman A. Frigerio and Howard H. Vogel, Jr.

In neutron toxicity studies involving energies greater than thermal, moderation both within the organism and in the shielding appears to be inevitable. The degree to which these moderated neutrons affect the results can be shown to be a function of the spectrum of incident neutrons and the geometry peculiar to each facility. Recent studies[1,2] have suggested that neutrons in the epithermal region (0.1 to 100,000 ev) may be of considerable biological importance and may have higher RBE values than those obtained with high-energy or purely thermal neutrons.

Such elevated RBE values are theoretically reasonable in view of the probability that epithermal neutrons occasion biological damage through both activation and collision processes. High resonance cross sections are available in the epithermal region for many of the biologically common nuclides.[3] Furthermore, the maximum bond energy of biological compounds (5 ev) is exceeded by the majority of epithermal collision processes which occur in tissue, particularly since the collision cross sections for most biological nuclides increase with decreasing neutron energy. In order to determine the epithermal neutron flux for the calculation of biological effectiveness, a series of activation studies has been made, and values for thermal and high-energy neutron flux were obtained simultaneously for comparison.

Thermal neutron flux was estimated by measurement of the activation and cadmium ratio of 10-mg gold foils. These were counted on a sodium iodide scintillation counter and compared with standard gold foils which had been calibrated against fission counters in a known thermal neutron flux.

High-energy neutrons were estimated by activation of standard sulfur discs which were then counted in a calibrated GM end-window counter.* From the known cross sections of sulfur and the high-energy spectrum of the CP-5 biological facility,[4] it has been estimated that the sulfur-activating neutrons represent 7.4% of the total flux in the region 0.1 to 10 Mev. The same value has also been obtained by a different method.[5]

In estimating the epithermal neutron flux in the region 0.1 to 100,000 ev, use was made of the "slowing down density" treatment of Hughes.[6] If a dE/E spectrum[6] is assumed, a reasonable assumption for the uranium matrix and graphite, water and concrete lattice of the

*Counting was done by E. Tochilin, U. S. Naval Radiation Defense Laboratory, San Francisco.

facility, the flux in any single decade of neutron energy, $(nv)_E$, may be expressed in terms of the thermal flux, $(nv)_{2200}$, by the expression

$$(nv)_E = \frac{(nv)_{2200}\ \sigma_{2200}\ \ln_e 10}{(R_{Cd}-1)\int_{0.07}^{\infty} \sigma_a \frac{dE}{E}}$$

where σ_{2200} is the thermal cross section,

R_{Cd} the cadmium ratio and

$\int_{0.07}^{\infty} \sigma_a \frac{dE}{E}$ the activation integral.

Samples for activation, either uncovered or encased in 0.03-inch cadmium foil, were exposed for 2 hr in the CP-5 biological facility.(7) Power was maintained at two megawatts, and the boral shutter before the uranium converter plate was set at "full open" position. Samples were irradiated within plastic mouse phantoms and surrounded by a full load of phantoms to simulate standard conditions for the exposure of animals. Samples were then counted with a GM end-window counter, counting being continued until the desired, active, nuclide had been positively identified and interference from other nuclides had been eliminated. The gold foils were identical with those employed for estimation of the thermal flux. The copper samples were 220-mg foils, 33 μ in thickness. The sodium and iodine were employed as 220-mg pressed discs of chemically pure, anhydrous sodium carbonate and para-iodobenzoic acid respectively; the discs were 0.9 mm high and 13 mm in diameter.

Results are presented in Table 27. Reproducibility was found to be excellent, but consistent discrepancies with respect to epithermal neutron flux appeared among the different nuclides. These discrepancies very probably reflect uncertainties in the available values of cross sections and of corrections for the 0.07 to 0.4 ev integral.(8) It is evident, however, that the total fluxes in each of the three major energy regions are of the same order of magnitude and that the epithermal flux is nearly equal to that of the high-energy neutrons.

This high value for the epithermal neutron flux suggests that discrepancies in RBE values among the various neutron irradiation facilities may well be due, in part, to differences in flux of moderated neutrons, especially in view of the insensitivity of the usual ionization dosimetry to neutrons in this energy region.(9) In this connection it is also suggestive that, in the three facilities for which data are available(5,6,9,10,11,12) the apparent RBE for 30-day mouse lethality is inversely proportional to the R_{Cd} for Cu^{64}.

TABLE 27

Neutron flux in the CP-5 biological irradiation facility

Nuclide	R_{Cd}	Flux, neutrons x $10^{-7}/cm^2/sec$				
		Thermal	Direct sulfur	Derived fast	Epithermal, per decade*	Total epithermal
Na^{24}	5.7	1.8	0.37	4.9	5.8	3.5
Cu^{64}	4.7	1.8	0.37	4.9	5.4	3.2
I^{128}	1.3	1.8	0.37	4.9	7.4	4.4
Au^{198}	1.6	1.8	0.37	4.9	4.9	3.0

*Neutrons x $10^{-6}/cm^2/sec$.

References

1. Rossi, H., private communication.

2. Storer, J. B., P. S. Harris, J. E. Furchner, and W. H. Langham. The relative biological effectiveness of various ionizing radiations in mammalian systems. Radiation Research 6:188-288 (1957).

3. Hughes, D. J. Neutron cross sections. Brookhaven National Laboratory Report. BNL-325 (1955).

4. Vogel, H. H., Jr., D. L. Jordan, G. Kohler, E. Tochilin, and B. W. Shumway. Neutron spectrum within the biological radiation chamber at CP-5. Semiannual Report of the Biological and Medical Research Division, Argonne National Laboratory. ANL-5732, pp. 110-112 (1957).

5. Handloser, J. S., and N. Delihas. Neutron flux within the Brookhaven biological facility. Brookhaven National Laboratory Report. BNL-386 (1955).

6. Hughes, D. J., Pile Neutron Research. pp. 58-64. Addison-Wesley, Cambridge, Mass. (1953).

7. Vogel, H. H., Jr., J. W. Clark, and D. L. Jordan. Modification of the gamma-neutron radiation chamber for use at the Argonne Research Reactor. Quarterly Report of Biological and Medical Research Division, Argonne National Laboratory. ANL-5288, pp. 35-36 (1954).

8. Hughes, D. J., Pile Neutron Research. pp. 139-142. Addison-Wesley, Cambridge, Mass. (1953).

9. Sheppard, C. W., M. Slater, and G. J. Atta. A theory for heterogeneous ion chambers and neutron response of Victoreen dosimeters. Radiation Research 7: 342-356 (1957).

10. Walton, H., Jr. Thermal contribution to a fast neutron exposure. Quarterly Report of Biological and Medical Research Division, Argonne National Laboratory. ANL-5378, pp. 121-122 (1955).

11. Delihas, N., and H. J. Curtis. The relative biological effectiveness of fission neutrons for the production of acute mortality in mice. Radiation Research 8: 166-180 (1958).

12. Curtis, H. J., personal communication.

THE EFFECT OF WHOLE-BODY NEUTRON IRRADIATION ON THE VOLITIONAL ACTIVITY OF THE MOUSE

Norman A. Frigerio, Howard H. Vogel, Jr., Nicholas Bink, and Richard Barhorst

In the course of a study of the sequelae of whole-body radiation of the intact mammal, it seemed of interest to develop methods of determining physiological effects without destruction of the subject. The measurement of volitional activity as an indication of radiation-induced malaise[1] appeared promising, and a preliminary experiment was conducted to determine the applicability of the method to animals irradiated with fission neutrons.

Fourteen CF No. 1 female mice, 5 weeks old, each weighing 25 g, were placed in standard 14-inch activity wheels equipped with direction-insensitive revolution counters. Before use the wheels were adjusted to constant starting and rolling friction and were calibrated for moment of inertia according to the method of Lacey.[2] The attached cages were cleaned and food and water were renewed weekly. Temperature and humidity were maintained at 75°F and 50%, respectively, and an automatic light cycle, 10 hours on, 14 off, was employed. It was observed that, due to the nocturnal nature of these mice, over 97% of the activity recorded in any one day occurred during the dark cycle. Accordingly the short time required for cage cleaning during the light cycle had virtually no effect on the observed activity.

After 57 days of acclimatization, 7 mice were chosen at random and irradiated at CP-5 with a sublethal dose of 183 rads of fission neutrons, using the procedures described previously.[3] After irradiation, they were returned immediately to their cages. The remaining 7 mice were sham-irradiated in the same manner. The volitional activity of the irradiated animals relative to that of the controls is shown in Fig. 46. Each point represents the ratio between average values of the two groups. The activity of one of the irradiated animals decreased continuously and sharply, reaching zero on the 63rd day, 6 days after irradiation. This animal eventually died on the 71st day, and its activity has been omitted in the construction of the curve after the 56th day. A very sharp drop in volitional activity is apparent immediately after irradiation; this is followed by a period of erratic increases and decreases after which the values eventually approach those of the control group. A final decrease relative to control values is associated with increasing age. Since a very similar pattern is obtained with X-irradiated rats,[1] it seems likely that the pattern of radiation-induced malaise is independent of the nature of the ionizing radiation employed, unlike the modes of lethality.[4]

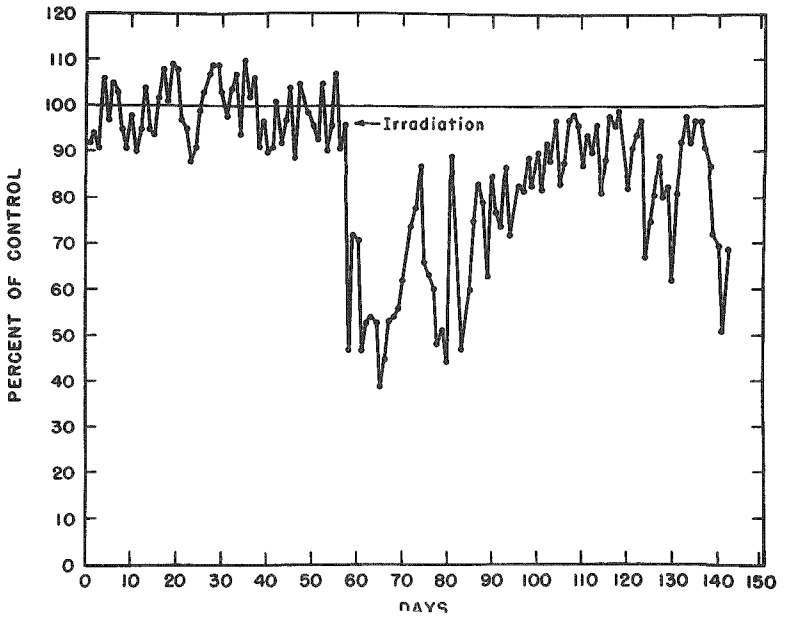

Figure 46. Volitional activity measured in CF No. 1 mice irradiated with a single sublethal dose of fission neutrons.

Because of complications introduced by individual differences, motivation, and estrus cycle, it would seem advisable to employ much larger numbers of animals in future experiments of this type in order to assure a higher degree of statistical validity.

References

1. Jones, D. C., D. J. Kimmeldrof, D. O. Rubadeau, G. K. Osborn, and T. J. Castanera. Effect of X-irradiation on performance of volitional activity by the adult male rat. Am. J. Physiol. 177:243-250 (1954).

2. Lacey, O. L. A procedure for calibration of activity wheels. Am. J. Psychol. 57:412-415 (1944).

3. Vogel, H. H. Jr., R. A. Blomgren, and N. J. G. Bohlin. Gamma-neutron chamber for radiobiological studies. Nucleonics 11 (3) : 28-31 (1953).

4. Vogel, H. H. Jr., J. W. Clark, and D. L. Jordan. The daily probability of death in fast neutron and Co^{60} gamma-irradiated CF#1 female mice. Quarterly Report of Biological and Medical Research Division, Argonne National Laboratory. ANL - 5378, p. 118-120 (1955).

RECENT DEVELOPMENTS IN THE THEORY OF NEUTRON-CAPTURE THERAPY

Norman A. Frigerio

Interest in neutron-capture therapy has centered, to date, on the use of the Li^6 and B^{10} (n,α) reactions.(1) This has been due primarily to two facts: they possess high thermal cross sections, and the reaction products have very short ranges and high ionization densities. Results have been encouraging, but difficulties of a chemical and physiological nature remain unsolved for these two nuclides. Ionic lithium or boron localize poorly in tumors, and lithium compounds which do not release ionized lithium under physiological conditions have not yet been synthesized. Boronic acid derivatives of the acid azo dyes such as Evans Blue and trypan blue(2) have given promising results.(3) However, our recent experience with these compounds has been that concentration of the dye in vivo is not accompanied by concentration of the boron, which appears to be hydrolyzed to free boric acid by enzymes present in the organism before a high differential concentration can be achieved in the neoplasm.

In considering alternatives to these nuclides, the U^{233} and U^{235} (n,f) reactions appeared particularly promising. Their instantaneous energy yield is of the order of 200 Mev per process, some 90 times as great as that of the B^{10} (n,α) reaction. In addition, thermal and epithermal(4) cross sections are quite high, and over 90% of the energy yield appears as short-range, densely ionizing particles. Of the potentially fissionable nuclides, these alone possess sufficiently low specific activities so that considerable body burdens might be tolerated without fear of extensive radiation injury.

From consideration of the properties of the blood-brain barrier(5) it appeared that effective localization of activatable nuclides in brain tumors, as well as low toxicity to normal cells, might be achieved by the use of resonance-stabilized heterocyclic compounds of high molecular weight, especially those of high negative charge density. Accordingly, a series of uranium and other actinide and lanthanide compounds of this type has been synthesized by us and screened for chemical toxicity and tumor localization. These compounds include metal phthalocyanines, porphyrins and Schiff base complexes.

To date the most successful of these compounds have been the sulfonated phthalocyanines. The minimum lethal dose (intravenous) for mice is over 1000 mg/kg, and doses in this range are without apparent effect on the health or breeding ability of the recipient mice or of their

offspring. Localization in brain tumors has been striking, with differential concentrations of 50 and over having been achieved routinely. In addition, these compounds are highly colored, greatly simplifying location of the tumors.

In consequence of these favorable characteristics, analogs of the compounds containing nonfissionable nuclides have also been synthesized and are being studied as possible radiological contrast media. Methods developed for their synthesis have included fusion with phthalonitrile, metathesis with dilithium phthalocyanine and reaction with sulfonated phthalamide. The phthalocyanines of uranium, thorium, lanthanum, gadolinium and neodymium have been prepared. They are deep blue or green solids possessing strong purple reflexes; apparently they contain one atom of metal per phthalocyanine residue. They decompose in vacuo at 350 to 500°C to yield the metal-free phthalocyanine as a sublimate. The unsulfonated compounds are soluble only in concentrated sulfuric and fluosulfonic acids, from which they may be precipitated by dilution; such treatment results in slow decomposition of some of these compounds.

It is apparent from consideration of certain parameters of the neutron-capture process in mammals that the useful nuclear reactions need not depend on thermal activation or prompt particle emission. Among those reactions in resonance region that yield particle-emitting nuclides, there are many of acceptably high cross section. For β-emitting nuclides of short half-life in mammals of moderate size, expressions have been derived which show that dose distribution effectively approximates that from the available (n,α) reactions. Radiation damage by neutrons of low energy is due primarily to the activation of N, H, B, and Cl in the tissues. Since the activation cross sections of these elements follow the $1/v$ law, their activation will be much less in the epithermal than in the thermal region. Therefore, epithermal neutrons can be used to activate selectively those nuclides with strong resonances, without incurring this type of radiation damage. Neutrons of suitable energy can be obtained by filtration of moderated fission neutrons with nuclides of high thermal absorption cross section such as Li^6. Thus epithermal activation of the natural I^{127} in thyroid neoplasms might result in very effective therapy without incurring the whole-body dose inevitable with I^{131} treatment. Here, too, it would be possible to treat neoplasms which, having lost their ability to take up iodine, are unresponsive to injected I^{131}. So long as they retained any natural iodine, they would remain vulnerable to epithermal activation.

The general synthesis of nontoxic, heterocyclic compounds of high molecular weight containing activatable nuclides, coupled with epithermal activation, makes possible many extensions of neutron-capture therapy. Nontoxic solutions or colloidal suspensions, chemically modified for

maximum physiological localization, might be administered freely and activated to any desired degree in situ. Considerable freedom in choice of nuclide is possible with these compounds, permitting use either for therapy or for diagnosis. In the latter case, positron emitters would be particularly useful since the annihilation radiations accompanying their decay may be conveniently located with coincidence detectors.[6]

References

1. Farr, L. E., W. H. Sweet, J. S. Robertson, C. G. Foster, H. B. Locksley, D. L. Sutherland, M. L. Mendelsohn, and E. E. Stickley. Neutron-capture therapy with boron in the treatment of glioblastoma multiforme. Am. J. Roentgenol. 71:279-293 (1954).

2. Snyder, H. R., and S. L. Meisel. Synthesis of azo boronic acids. II. Dyes from tetrazotized benzidine-2,2'-diboronic acid. J. Am. Chem. Soc. 70:774-776 (1948).

3. Kruger, P. G. Boron uptake in mouse brain neoplasm. Radiation Research 3:1-17 (1955).

4. Frigerio, N. A., and H. H. Vogel, Jr. Moderated neutron flux in the CP-5 biological facility. This report pp. 123.

5. Friedemann, U. Blood-brain barrier. Physiol. Rev. 22:125 (1942).

6. Sweet, W. H., and G. L. Brownell. Localization of intracranial lesions by scanning with positron-emitting arsenic. J. Am. Med. Assoc. 157:1183-1188 (1955).

ON A MODIFICATION OF THE POWER FUNCTION

Description of Body Burden from Measured Retention

Sylvanus A. Tyler

The "gross retention"* in humans and in animals of several radioactive isotopes after a single administration, has frequently been described empirically by the power function,

$$R_s'(t) = At^{-b}, \qquad 0 < b < 1 \tag{1}$$

where $R_s'(t)$ is the amount of the delivered material retained at time t, and A and b are constants.[1,2,3,4] Though it is generally felt that this description is in no way indicative of mechanism, its popularity as a statistical tool is a consequence of (a) the ease with which estimates of the characterizing constants are obtained and (b) the numerical stability they possess. The disquieting disadvantage of this empirical model is its behavior at t = 0 which is irreconcilable with the physical requirement that initial retention must be finite. In this note, a slight modification of Equation 1 is presented that is both free of this difficulty and asymptotically equivalent to Equation 1. The behavior of this model for repeated and continuous administrations is examined and compared with experimental findings.

Proposed Modification

Assume that the single dose, retention function is given by

$$R_s(t) = \begin{cases} \dfrac{R_0\alpha^b}{(t+\alpha)^b}, & t \geq 0;\ \alpha,\ b \text{ constants},\ 0 < b < 1,\ 0 < \alpha \leq 1. \\ 0 \text{ otherwise}, \end{cases} \tag{2}$$

where R_0 is the amount administered. Equation 2 is equal to R_0 at t = 0, and asymptotically approaches Equation 1 as time increases. The instantaneous rate of excretion and the coefficient of elimination (CE) are thus given by Equations 3 and 4.

$$-\frac{d\,R_s(t)}{dt} = \frac{R_0 b\alpha^b}{(t+\alpha)^{b+1}} \tag{3}$$

---

*"Gross retention," as used here, refers to the total quantity of the administered substance remaining in the body, including both the original element and the products remaining after decay. "Net retention" we define as a measure of the residual labeled substance present in the body.

$$CE = \frac{-d\,R_s(t)}{dt} \Big/ R_s(t) = \frac{b}{t + \alpha} \tag{4}$$

Total insult (integrated retention, $I_s(t)$) sustained from a single administration of a toxic material at any time t after administration is

$$I_s(t) = \int_0^t R_s(v)dv = \frac{R_0 \alpha^b}{1 - b} \left[(t + \alpha)^{1-b} - \alpha^{1-b} \right] \quad . \tag{5}$$

The correctness of Equation 5 requires that decay in toxicity over the interval investigated be negligible.

The extension to the case of repeated, single administrations is immediate. Suppose an amount of radioactive material D is delivered in n + 1 fractions of amounts d_i at times t_i, i = 0, 1, 2, ... n, $D = \sum_{i=0}^{n} d_i, t_0 = 0,\ t_i < t_{i+1}$. Then under the assumption that the proportion retained at any time t is a function of the time elapsed from administration and is independent of the preceding number of administered fractions, the amount retained ($R_d(t)$) at any time t is given by

$$R_d(t) = \alpha^b \sum_{j=0}^{p} \frac{d_j}{(t - t_j + \alpha)^b}, \quad t \neq t_j$$

$$\begin{cases} R_d(t_i-) = \alpha^b \sum_{j=0}^{p} \dfrac{d_j}{(t_i - t_j + \alpha)^b}, \quad R_d(0-) = 0 \\ R_d(t_i+) = R_d(t_i-) + d_i \end{cases} \tag{6}$$

where p is equal to the subscript j of the t_j immediately preceding t. The total insult sustained at time t is found by integrating Equation 6 over the required time range. The function $R_d(t)$ under repeated administration possesses jump discontinuities at times t_i. Thus, at these times the retention function has two values - one is the limit of the function from the left ($R_d(t_i-)$); the other is the corresponding limit value from the right ($R_d(t_i+)$). Piecewise continuity of $R_d(t)$ is, of course, required.

If administration is continuous at a rate q per unit time to time τ, the amount retained at any time $t \geq \tau$ and the total insult sustained are expressed by Equations 7 and 8.

$$R_c(t) = \int_0^{\tau} \frac{q\,\alpha^b\,dv}{(t - v + \alpha)^b} = \frac{q\,\alpha^b}{1 - b} \left[(t + \alpha)^{1-b} - (t + \alpha - \tau)^{1-b} \right] \quad . \tag{7}$$

$$I_c(t) = q\alpha^b \int_0^{\tau} \left\{ \int_0^{t-\omega} (v+\alpha)^{-b}\, dv \right\} d\omega$$

$$= \frac{q\alpha^b}{1-b} \left\{ \frac{(t+\alpha)^{2-b}}{2-b} - \frac{(t-\tau+\alpha)^{2-b}}{2-b} - \alpha^{1-b}\tau \right\} . \qquad (8)$$

Several questions can be answered on the basis of the above results.

1. At what rate under continuous administration will there be retained at some time τ an amount equal to the retention after a single administration of initial amount R_0?

2. What relationship exists between the continuous administration rate and the single administration amount that will produce equal insult at time τ?

The answer to question 1 is obtained by equating Equations 2 and 7.

$$q = \frac{R_0(1-b)}{t + \quad - \alpha^{1-b}(t+\alpha)^b} \qquad (9)$$

By putting $I_s(\tau) = I_c(\tau)$ we get

$$\frac{q}{R_0} = \frac{(\tau+\alpha)^{1-b} - \quad {}^{1-b}}{\frac{(\tau+\alpha)^{2-b}}{2-b} - \frac{\alpha^{2-b}}{2-b} - \alpha^{1-b}\tau} , \qquad (10)$$

the relationship requested in question 2.

Estimation of Constants

For sufficiently large t, the approximating equation (Equation 1) can be used to estimate the values of the constants α^b and b. If recording times of the retention values are assumed to be error-free and the number of recordings at each time point is equal, the weighted least squares procedure[5] on the log transforms of the variables will yield efficient estimates of both the constants and their associated errors. The appropriate weighting factor for each transformed retention value is the retention value itself.*

* Statistical analyses of replicated retention data from several animal experiments indicate that the variance of retained amounts is approximately proportional to the average amount retained.

$$\hat{\alpha}^2[R(t)] \doteq R(t) \qquad \text{(i)}$$

Let $W_1(t)$ represent the weight of the retention value (R(t)) and $W_2(t)$ represent the weight of the log-transform (log R(t)). Then, as a consequence of the variable transformation (6)

$$W_2(t) = k\, R^2(t)\, W_1(t);\ k \text{ a positive constant} \qquad \text{(ii)}$$

Thus, by (i) and (ii).

$$W_2(t) \sim R(t) \ . \qquad \text{(iii)}$$

Provided the errors of the characterizing constants of the retention function are small, the linear truncation of the formula for propagated errors in n variables* will permit determination of the errors associated with the estimates of α, R(t) and I(t). When a suitable portion of the t values are not large enough to justify use of Equation 1 as the approximating model, estimates of the constants may sometimes be determined by using Equation 2 directly and employing the general method of fitting nonlinear equations.(7) The estimation procedure, in this case, requires extensive computations.

Comment

"Gross retention" and "net retention" are approximately equivalent over times for which the decay of the administered material is negligibly small. However, when decay is significant within the period investigated, Equations 5 and 8 are not appropriate and the "net retention" function must be determined. The retention relations can no longer be expressed as elementary functions; thus, approximating techniques and graphical methods are required to effect solutions. Suppose we are given the single dose "gross retention" function (Equation 2) and a decay constant k. Our defining expression for the "net retention" ($R_s''(t)$) following a single administration becomes

$$R_s''(t) = R_s'(t)\, e^{-kt} = \frac{R_0 \alpha^b}{(t+\alpha)^b}\, e^{-kt};\ t \geq 0,\ 0 < b < 1$$

$$0 \text{ otherwise}, \qquad \alpha,\ R_0,\ k \text{ positive constants} \tag{11}$$

and Equations 3, 4, 5, and 6 must be altered in like manner.

Example**

As an example of the employment of Equation 2 as model, we shall use data from a pilot experiment conducted for the purpose of investigating the relative influence of the administered dosage and the retained dosage on late pathological changes noted in mice injected with Sr^{90}.(8)

CF No. 1 female mice, approximately 70 days old at the beginning of the experiment, were injected in the tail vein with Sr^{90} (in equilibrium with Y^{90}) as a chloride in normal saline at pH 5.5. Single injections at

*When the error in x_i (i=1,2,...n) is small,

$$\hat{\sigma}^2[f(x_1,x_2,\ldots x_n)] \doteq \sum_{i=1}^{n} \frac{\partial f}{\partial x_i}\, \hat{\sigma}^2(x_i)$$

**We are greatly indebted to Dr. Miriam Finkel of this division for kindly placing at our disposal the data used in this example.

three dosage levels were given, and in addition, 5 equal fractions at 7-day intervals and 20 equal fractions 5 days a week for 4 weeks (Table 28) were administered at one of the single dosage levels. The amount of Sr^{90} retained in the living animals was determined by measuring the bremsstrahlung produced by the beta emanations of the Y^{90} daughter. Results of this experiment are shown in Fig. 47. A measure of the retained amount was taken just before and approximately 24 hr after injection. Since the time period of interest here is exceedingly short compared with the half-time of Sr^{90}, all of the relationships established for "gross retention" are applicable. Also, the single dose data (Fig. 47) permits the use of approximating Equation 1. Thus the linear, log-log form of Equation 1 with $A = R_0 \alpha^b$,

$$\log \left[\frac{R_s'(t)}{R_0} \right] = \log (\alpha^b) - b \log t \quad , \tag{12}$$

is used as model and the weighted, least squares estimates of the log-log transforms of the mean fractional retention - time pairs at all time points except day 1 are determined (Table 29). Substituting these estimates of α and b in Equation 6 with $d_j = 0.1\ \mu c/g$, $j = 0,1,2,3,4$, the retention $R_d(t)$ was determined; the function $\frac{R_d(t)}{\sum_{j=0}^{4} d_j}$ is plotted in Fig. 48 and compared with the experimental measurements. A χ^2_{12} test of the goodness of fit gives a probability of occurrence by chance of the observed differences roughly equal to 0.80.

TABLE 28

Injection schedule*

Total dose $\mu c/g$	Number of injections	Dose per injection $\mu c/g$	Number of animals injected
1.0	1	1.0	10
0.5	1	0.5	10
0.25	1	0.25	10
0.5	5	0.1	10
0.5	20	0.025	10

*Taken from reference (8), Table 3, p. 22 by permission of authors.

The validity of the continuous model as an approximation was tested using as criteria the retention results from the 20-fraction experiment. Equation 7 was used as model and the function $R_c(t)/q\tau$ is plotted in Fig. 49. Values of the experimentally determined constants used are τ = 28 days and q = 0.017857 μc/g/day. By χ^2_{13}, the predicted retention values are compatible with the corresponding experimental measures (probability > 0.99).

TABLE 29

Constants of the single-dose retention function

No. of pairs	b	$\hat{\sigma}_b$	$\log(\alpha b)$	$\hat{\sigma}_{\log \alpha b}$	αb	$\hat{\sigma}_{\alpha b}$	α	$\hat{\sigma}_\alpha$
10	0.320	0.003	-0.0943	0.0124	0.805	0.023	0.507	0.014

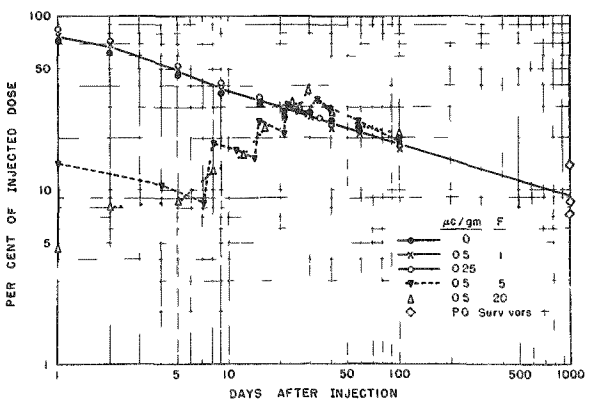

Figure 47. Body burden as a function of dosage pattern and time. F = number of fractions. Reproduced from Fig. 6, p. 24 of the report of Finkel et al.(8)

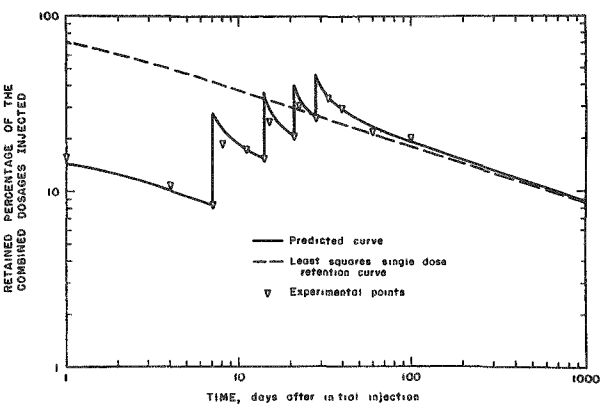

Figure 48. Comparison of predicted and experimental values for the 5-fraction experiment.

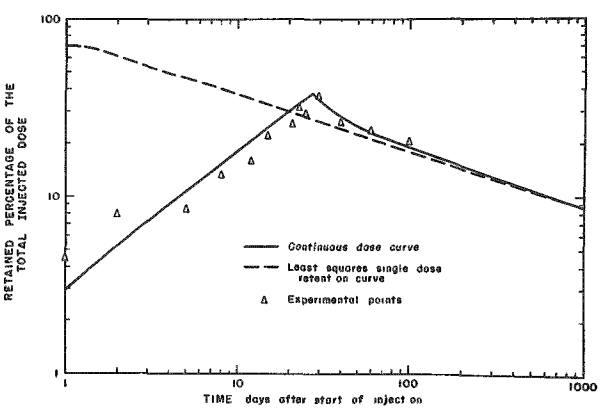

Figure 49. Continuous-dose approximation to the 20-fraction experiment.

Summary

A modification of the power function as an empirical model of retention following a single administration of radioactive tracers is presented. It is shown that this model (a) satisfies the imposed initial conditions of retention experiments, (b) is readily extended to fractionated and continuously administered dosage patterns, and (c) is supported by experimental data.

References

1. Sacher, G The excretion, retention, distribution and clinical effects of strontium-89 in the dog. Part II. Statistical analysis of excretion and retention of strontium-89 for individual dogs. University of Chicago Metallurgical Laboratory Report CH-3866 (1946).

2. Norris, W.P., T.W. Speckman, and P.F. Gustafson. Studies of the metabolism of radium in man. Am. J. Roentgenol. 73:785-802 (1955).

3. Langham, W.H. Determination of internally deposited radioactive isotopes from excretion analyses. Am. Ind. Hyg. Assoc. Quart. 17: 305 (1956).

4. Healy, J.W. The calculation of maximum permissible concentration for long-lived radioisotopes. Radiation Research 4:367-372 (1956)

5. Mather, K. Statistical analysis in biology, 2nd ed., pp. 248-251, Interscience Publishers Inc. N.Y. (1947).

6. Deming, W.E. Statistical Adjustment of Data. John Wiley and Sons, Inc., N.Y. (1948).

7 Scarborough, J. B. Numerical Mathematical Analysis, 3rd ed., pp. 463-469, The Johns Hopkins Press, Baltimore (1955).

8. Finkel, M P., B. J. Tellekson, J. Lestina, and B. O. Biskis. The influence of dosage pattern upon the toxicity of Sr^{90} in mice. I. Preliminary experiment and 212-day survey of the long-term study. Semiannual Report of Biological and Medical Research Division, Argonne National Laboratory. ANL-5732, pp. 21-31 (1957).

RECOVERY FOLLOWING INJECTION OF NONIRRADIATED PROTOPLASM INTO AMOEBAE IRRADIATED WITH FISSION NEUTRONS

II. Protective effect of centrifuged cell portions

Edward W. Daniels and Howard H. Vogel, Jr.

In previous studies it was shown that exposure to about 15 krep of fission neutrons is sufficient to kill all of a population of the giant amoeba *Pelomyxa illinoisensis* within 10 days.(1) However, even when this dose was doubled, 91% of the irradiated cells survived when nonirradiated homologous protoplasm was added by microfusion.(2) In the present report further work is discussed which was designed to help answer the questions: (a) What are the necessary components in the nonirradiated donor protoplasm which are essential for recovery in supralethally neutron-irradiated cells? (b) Are these the same as those required by X-irradiated amoebae for recovery? (c) Where in the cell is the critical site of radiation damage and is this at the same locus regardless of whether X-rays or fission neutrons are used? It is tentatively assumed that if the therapeutic agent in nonirradiated protoplasm can be isolated, this will represent in crude form the critical site of radiation damage in exposed cells.

In the present work centrifuged portions of nonirradiated cells were put into supralethally neutron-irradiated amoebae so that separate strata of intracellular components could be individually analyzed for therapeutic capability. Also, an experiment is presented here which was designed to determine whether the survival pattern after exposure to the two radiations, X-rays and fission neutrons, involves damage and/or recovery of the same component. In this study X-irradiated protoplasm was tested as a protective agent in neutron-irradiated cells.

Experimental

Methods of centrifugation and microfusion have been described previously.(3) Fig. 50 shows normal *P. illinoisensis* before and after centrifugation at varying gravitational forces all of which were applied for a period of 10 minutes. At 715 *g* (Fig. 50 B) the nuclei, food vacuoles, heavy spherical bodies, most of the crystal-like components and most mitochondria migrate toward the centrifugal pole into the heavy half of the cell. At the same time, the fat globules, liquid-containing vacuoles, and some crystal vacuoles migrate toward the centripetal (light) pole. The optically clear cytoplasm migrates according to its density. Evidence of this is gained by observations on the location of the different layers of visible particulate components. Centrifugation at 3000 *g* (Fig. 50 C) brings about more complete concentration of the mitochondria and fine (0.1 - 0.3 μ) particulates into the heavy half of the cell, while the nuclei remain in approximately the same position.

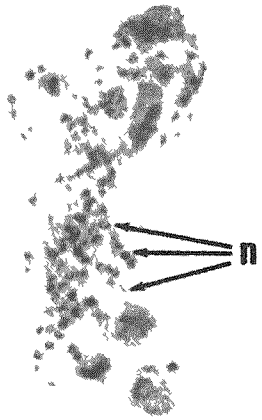

A

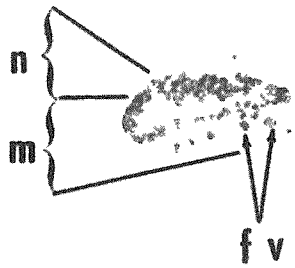

B

A. Noncentrifuged cell, fixed in Schaudinn's fluid and stained with Delafield's hematoxylin. Many nuclei (n) are shown randomly distributed.

B. Five-micron section from a cell after centrifugation for 10 min at 715 g. Fixed in osmium tetroxide and stained with aniline acid-fuchsin. Nuclei (n) and mitochondria (m) are stratified in the heavy half of the cell. The nuclear stratum also contains mitochondria. Arrows (fv) point to food vacuoles which lie centrifugally from the nuclei.

C

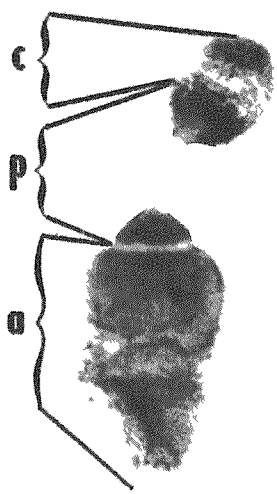

D

100 μ

C. Whole cell centrifuged 10 min at 3000 g. Fixed and stained as in A. Nuclear stratum is shown at (n); microscopic examination showed no nuclei above or below this stratum. Very few food vacuoles seen in this specimen.

D. Whole cell centrifuged for 10 min at 6700 g. Fixed and stained as in A. Cytoplasm at centripetal portion (a) contains no nuclei. The nuclei are confined to the portion designated as (b). This portion was nearly pulled into two parts by the centrifugal force. All except a few nuclei are located in the lower part of section (b). Many food vacuoles which can be seen in section (c).

Figure 50. Pelomyxa illinoisensis before and after centrifugation. In B, C, and D, the centrifugal poles are toward the bottom of the page.

Centrifugation at 6700 g (Fig. 50 D) moves significantly more of the fine particulates out of the light third of the cell into the middle and heavy thirds while the positions of the other visible components are changed very little. Some food vacuoles migrate to the extreme heavy pole as the 6700 g force is applied. These vary in size, shape and density, whereas the more uniform nuclei remain in a fixed position.

The nonirradiated, stratified cells were cut into light, middle and heavy thirds. Addition of the middle or heavy thirds of cells centrifuged at 3000 or 6700 g prevented death in 89% to 96% of supralethally neutron-irradiated recipients, as shown in Table 30. Only a relatively small quantity of donor protoplasm from the middle third, and even less from the heavy-third portions, was sufficient to bring about recovery in the irradiated cells. The heavy-third portions were the most difficult to fuse since they tended to disintegrate when stabbed with a microneedle. When this occurred, the cell membrane usually burst and liberated the contents of the cell portion into the culture medium. Survival data from successfully fused cells agree with those obtained previously, following the fusion of supralethally X-irradiated P. illinoisensis either with whole protoplasm(4) or with centrifuged halves of nonirradiated cells(5). In unfused cells, death occurred in 4 or 5 days after lethal irradiation (Table 30).

TABLE 30

Percent survival and mean cell division times of supralethally-irradiated amoebae given different donor cell portions

Experimental procedures	Number of cells	Survival, %	Irradiation to first cell division, days	First to second cell division, days	Second to third cell division, days
Nonirradiated, nonfused controls	45	100	2.2 ± 0.2*	2.3 ± 0.1	2.4 ± 0.2
Neutron-irradiated, nonfused controls	158	0			
Neutron-irradiated cells fused with nonirradiated noncentrifuged portions of amoebae	33	91	4.0 ± 0.3	2.3 ± 0.4	2.2 ± 0.2
Nonirradiated, centrifuged (3000 g) cell portions fused into neutron-irradiated cells					
Centripetal third	28	54	4.6 ± 0.5	2.0 ± 0.3	2.3 ± 0.4
Middle third	24	92	5.5 ± 0.6	2.4 ± 0.3	2.3 ± 0.3
Centrifugal third	26	96	5.6 ± 0.5	2.4 ± 0.2	2.1 ± 0.2
Nonirradiated, centrifuged (6700 g) cell portions fused into neutron-irradiated cells					
Centripetal third	23	13	3.0 ± 0.6	1.8 ± 0.8	3.3 ± 0.8
Middle third	26	89	4.6 ± 0.4	2.2 ± 0.2	1.8 ± 0.1
Centrifugal third	22	96	5.1 ± 0.2	2.6 ± 0.3	1.3 ± 0.3

*All values ± standard error.

Following the transfer of cytoplasm from the light third into the neutron-irradiated cell, death frequently occurred at the usual 4- or 5-day postirradiation period, sometimes even after the transfer, within 1 day of exposure, of the entire contents of a light third cell portion. About half (54%) of the supralethally neutron-irradiated cells lived following fusion with light third portion from cells centrifuged at 3000 g. Light portions from cells centrifuged at 6700 g prevented death in only 13% of treated cells. Thus, the component(s) required for recovery appear to be most concentrated in the heavy third, next most concentrated in the middle third and least concentrated in the light-third portion.

The majority of the irradiated, fused cells divided at least once within 10 days of exposure. The mean times of those divisions which occurred are presented in Table 30. The mean time required for the first cell divisions after supralethal neutron exposure (and microfusion) is about twice that required by the nonirradiated, nonfused controls. This delay occurred whether the nonirradiated protoplasm was from a noncentrifuged cell or from the light, middle or heavy-third portion of a centrifuged cell. The second and third mean cell divisions were not delayed in any of the experimentally fused groups in which nonirradiated protoplasm was used.

Fusion of X-irradiated Protoplasm into Neutron-irradiated Cells

Supralethally X-irradiated protoplasmic systems will not prevent death or promote cell division if introduced by fusion into other supralethally X-irradiated cells. The same effect was obtained when 21 supralethally neutron-irradiated cells were fused with portions of supralethally X-irradiated cells. The transfer of substantial quantities of X-irradiated protoplasm into the neutron-irradiated cells was clearly seen. Death in these fused cells occurred at approximately the same time (5.0 ± 0.1 days) as death in 164 X-irradiated cells (4.6 ± 0.1 days). The conclusion seems inescapable that there is nothing in supralethally X-irradiated systems which will prevent death in cells exposed to supralethal doses of fission neutrons. In other words, the X-radiation renders the therapeutic component(s) of nonirradiated systems incapable of preventing death in lethally neutron-irradiated cells, and *vice versa*.

References

1. Daniels, E. W., and H. H. Vogel, Jr. Survival of giant amoebae after single exposures to Co^{60} gamma rays and fission neutrons. Semi-annual Report, Biological and Medical Research Division, Argonne National Laboratory. ANL-5732, pp. 123-127 (1957).

2. Daniels, E. W., and H. H. Vogel, Jr. Recovery following injection of nonirradiated protoplasm into amoebae irradiated with fission neutrons. Semiannual Report, Biological and Medical Research Division, Argonne National Laboratory. ANL-5732, p. 128 (1957)

3. Daniels, E. W. Cell division in the giant amoeba, Pelomyxa carolinensis, following X-irradiation. II. Analysis of therapeutic effects after fusion with nonirradiated cell portions. J. Exptl. Zool. 127: 427-462 (1954).

4. Daniels, E. W. X-irradiation of the giant amoeba, Pelomyxa illinoisensis. I. Survival and cell division following exposure. Therapeutic effects of whole protoplasm. J. Exptl. Zool. 130:183-197 (1955).

5. Daniels, E. W. Recovery from lethal X-radiation injury in amoebae after injection of centrifugal portions of nonirradiated cells. Radiation Research 5:604-605 (1956).

PROGRESS REPORT: GRANULOCYTE LIFE CYCLE

Mary A. Maloney and Harvey M. Patt

Possible mechanisms for control of granulocyte formation are being considered against the background of the granulocyte life cycle. Information of this sort is pertinent to interpretation of various perturbations of the granulocyte system including those induced by irradiation. The data of Ottesen[1] and of Kline and Cliffton[2] on P^{32} incorporation in the DNA of leucocytes in man indicate that labeled cells appear in the circulation within 4-5 days after isotope administration. A 3-day transit time in marrow has been estimated by Osgood[3] from in vitro observations of marrow suspensions and by Patt[4] from consideration of mitotic activity. A more precise appraisal of the chronology of granulocyte development in the normal steady state and under the influence of radiation and other factors is possible by means of radioautography. Such studies with tritiated thymidine in dogs are in progress. As discussed by Taylor et al.,[5] a high degree of selectivity is possible with tritiated thymidine because of the specific incorporation of thymidine into DNA and the short range of the tritium β particles.

Tritiated thymidine with a radiochemical purity of 90-100% and a specific activity of 390 mc/millimole was obtained from Schwarz Laboratories, Mount Vernon, New York. Thus far, two dogs have been injected intravenously with the tritiated nucleoside (No. 1, female beagle, 3.8 years old, 80 μc per kg; No. 2, male beagle, 1.5 years old, 100 μc per kg). Bone marrow and peripheral blood studies were carried out at frequent intervals during the first 2 days, and daily for 2 weeks. Marrow samples were obtained by aspiration from the femur under local anesthesia. The marrow, usually 0.8 ml, was drawn into an equal volume of homologous heparinized plasma. Total nucleated cell counts were made on each sample, and the fat and myeloid-erythroid layers were estimated after centrifugation. Two sets of marrow slides were prepared. One set was treated with Wright's stain, the other was used for radioautographs and subsequent staining with a modified Giemsa stain.[6] This was done to compare the distribution of cell types and mitoses on the stained radioautograph with that on the conventional slide. Peripheral blood studies consisted of total and differential leucocyte counts, hematocrit, and blood volume. As in the case of marrow, two sets of slides were used for differential analysis and radioautography.

Technique for preparation of radioautographs. Clean glass slides were coated with 0.5% egg albumin and then with 0.05% chrome alum. Care was taken to make thin films of marrow and blood so that the cells were on the slide in one cell thickness. The preparations were fixed in absolute methyl alcohol for 45 minutes. British Kodak fine grain autoradiographic film (AR 10) was floated on 1% glycerine in double distilled water at 18° C, allowed to stretch to maximum size, and hung on the slide. The slides were

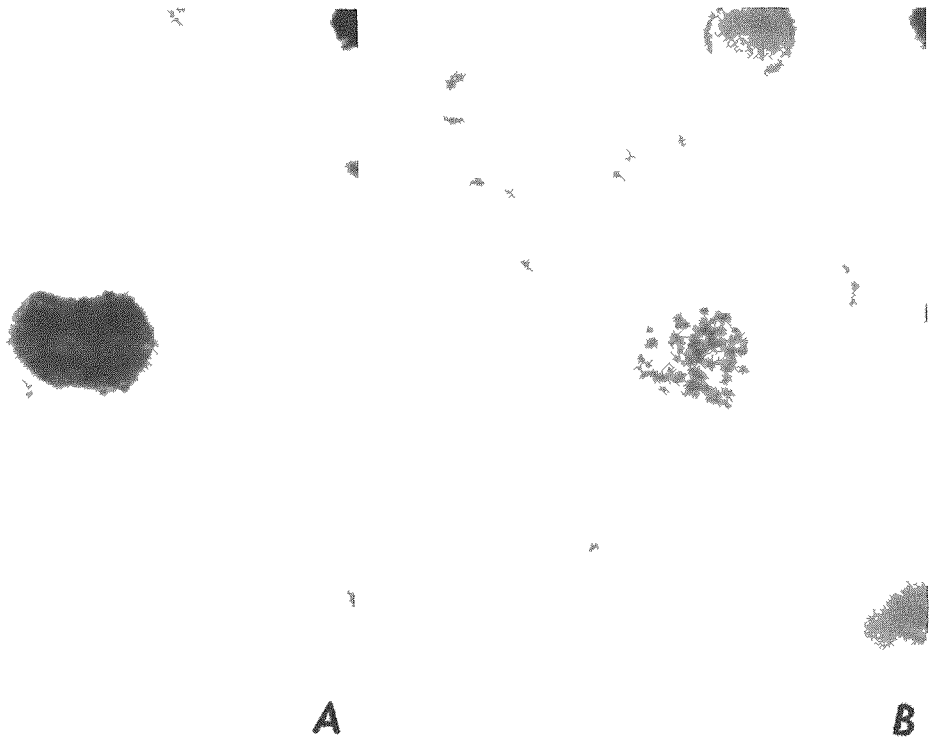

A. Myelocyte in bone marrow.

B. Radioautograph of the same cell.

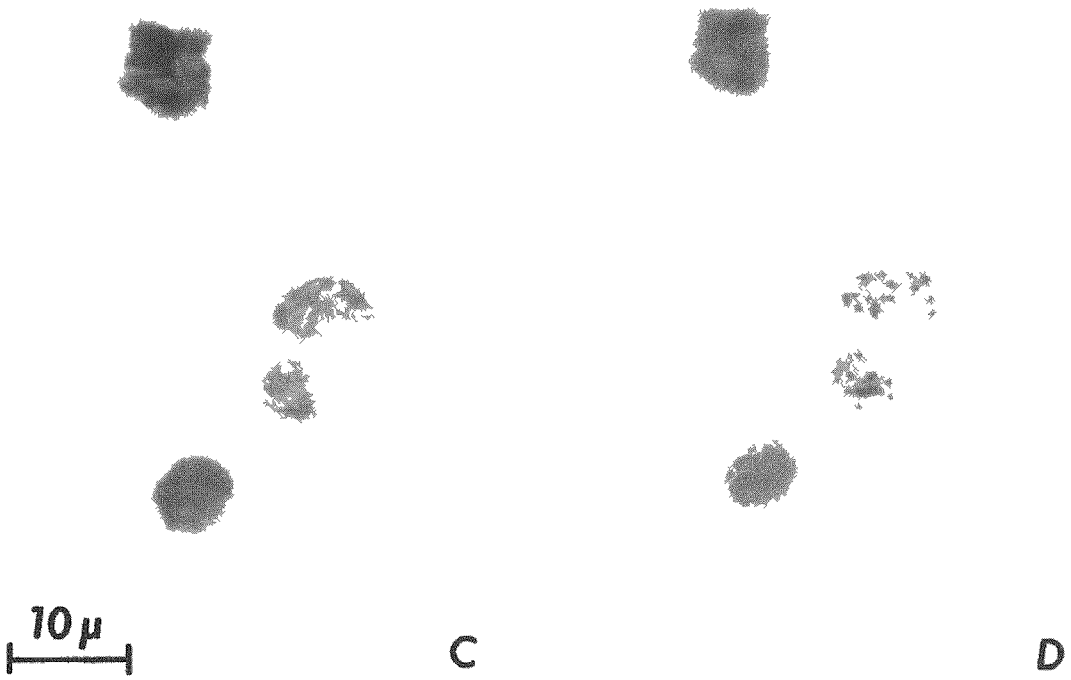

C. Myelocyte telophase in bone marrow.

D. Radioautograph of the same cell.

Figure 51

air dried and stored with calcium chloride in black slide boxes covered with light sensitive tape. These operations were performed in a dark room with minimal use of a safe light (Wratten No. 2). After storage for 6 weeks in a refrigerator, the slides were developed for 4 min (Kodak D-19), washed in distilled water, fixed for 10 min (Kodak acid fixer), and finally washed in running tap water for 1 hr. Developing, fixing and washing were carried out at 18° C. After the slides were air-dried, they were stained with a modified Giemsa stain at pH 5.75 for 30 min at room temperature and washed in pH 5.75 buffer for 3 min. Figure 51 illustrates the quality of radioautographs that have been obtained with this technique.*

Although the various analyses have not been completed, preliminary results indicate that the label appears first in the immature cells of both the myeloid and erythroid series (myeloblast, myelocyte and erythroblast). The distribution of tagged cells seems to progress in an orderly manner from the less to the more differentiated forms with time after injection of tritiated thymidine. Labeled neutrophils can be detected in the bone marrow by 36 hr, and in the peripheral blood by 3 to 4 days. An indication of the rapidity of cell turnover is given by the fact that densely-labeled telephases are found in the marrow within 4 hr after injection of the tritiated thymidine.

References

1. Ottesen, J. On the age of human white cells in peripheral blood. Acta Physiol. Scand. 32:75-93 (1954)

2. Kline, J. L. and Cliffton, P. E., Life span of leucocytes in man. J. Appl. Physiol. 5:79-84 (1952).

3. Osgood, E. E. Number and distribution of human hemic cells. Blood 9: 1141-1154 (1954).

4. Patt, H. M. A consideration of myeloid-erythroid balance in man. Blood 12:777-787 (1957).

5. Taylor, J. H., Woods, P.S. and Hughes, W. L. The organization and duplication of chromosomes as revealed by autoradiographic studies using tritium - labeled thymidine. Proc. Natl. Acad. Sci. U.S. 43:122-128 (1957).

6. Gude, W. D., Upton, A. C., and Odell, T. T., Jr. Giemsa staining of autoradiograms prepared with stripping film. Stain Technol. 30:161-162 (1955).

---

*The authors gratefully acknowledge the interest and advice of Dr. W. P. Norris and Mr. W. E. Kisieleski in the preparation of the radioautographs.

PROGRESS REPORT: PYRESIS STUDIES

III. Relationship of Degree of Fever to Antipyresis by Sodium Salicylate and Aurintricarboxylic Acid

Marcia White Rosenthal and Joan F. Fried

The body temperature of normal adult female Sprague-Dawley rats normally varies from 36.6 to 39.8° C, with a normal frequency distribution and a mean of 38.1° C. The injection of yeast produces a rise of 0.9° C to a mean temperature of 39.0° C. (Fig. 52). This fever is interesting from several aspects - it varies almost as widely as the normal temperature, it does not exceed the highest normal temperatures, and the temperature reached is independent of the initial body temperature, i.e., the mean fever is always the same regardless of the initial temperature.

The earlier experiments in this series have been carefully controlled with regard to the variation in temperatures of fevered animals; each experimental group contained rats with a representative range of fevers. Analysis of the antipyretic effect of sodium salicylate and of aurintricarboxylic acid (ATA) on this yeast-induced pyrexia suggested differences between the action of the two substances related to the initial degree of fever. To clarify this suggestion, the following experiment was performed. About 18 hr after subcutaneous injection of 3 ml of a 15% suspension of dried baker's yeast in saline, when the induced fever was high and had reached a plateau, rats were divided into 2 groups, those with high fevers (mean 39° C) and those with low fevers (mean 38.5° C), with no overlap of individual temperatures between groups. Treatment with sodium salicylate reduced the fever, whether initially high or low, to the same temperature ($P = >>0.5$ in a comparison of the two treated groups at 1 hr after treatment). Injection of ATA, on the other hand, reduced the fever by a specific decrement so that the animals with high initial temperatures remained significantly above the animals of the low group for 2 hr after treatment ($P = <.01 > .001$) (Fig. 53). This finding suggests that the antipyretic action of these two related substances may be accomplished by different mechanisms.

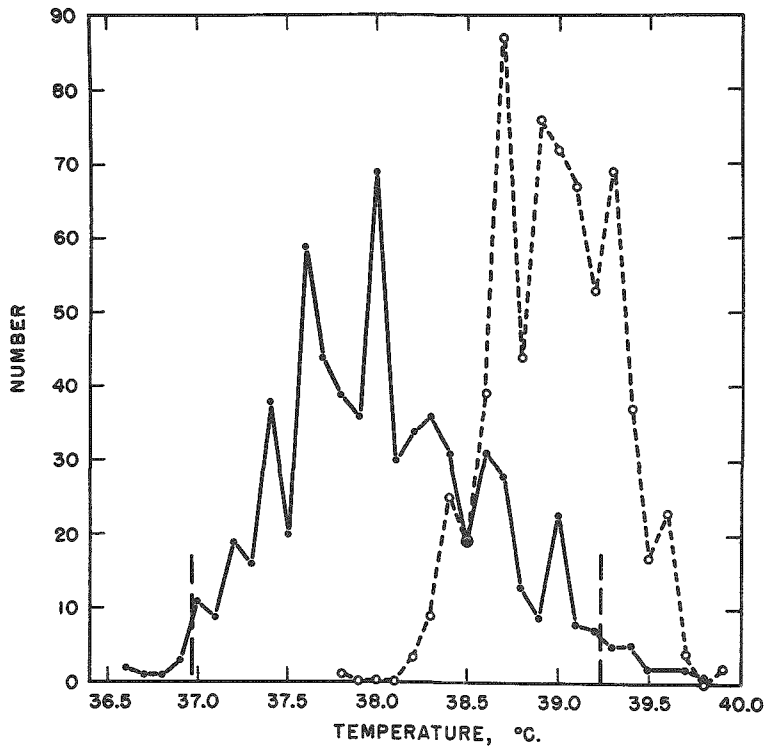

Figure 52. Solid line represents the frequency distribution of normal rectal temperatures of 651 unselected stock rats, measured from 1:30 to 3:00 p.m. Dashed line shows distribution of temperatures of 648 rats about 17 hr after subcutaneous injection of 3 ml of a 15% suspension of baker's yeast in saline solution. Normal temperatures of these rats followed a distribution curve similar to that shown at the left, except that rats with normal temperatures below 37.0° C or above 39.2° C were excluded from the experiment.

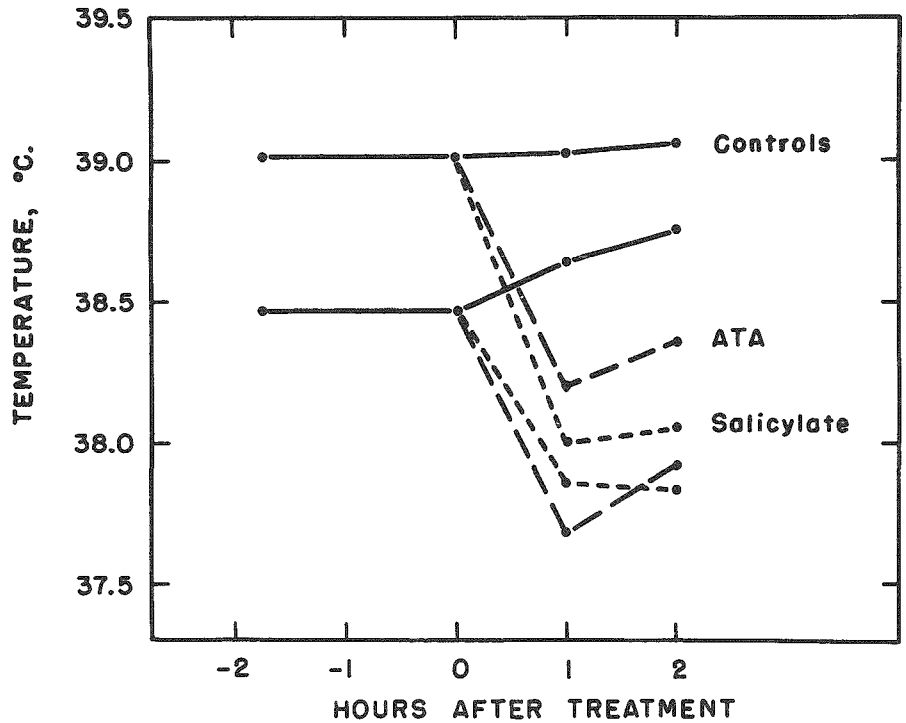

Figure 53. Comparison of antipyretic effect of ATA and sodium salicylate on rats with high and low fevers. Dosages were 125 mg/kg of either compound, injected intravenously 20 hr after yeast administration. Controls received an equivalent volume of saline. Each point represents the mean rectal temperature of the following numbers of rats: ATA-treated, 10 each: salicylate-treated, 7 and 8; saline-treated, 10 each.

PROGRESS REPORT: PYRESIS STUDIES

IV. Hematocrit and Sedimentation Rate During Antipyresis

Marcia White Rosenthal and Joan F. Fried

The antipyretic effect of the salicylates is generally considered to be accomplished by heat elimination through increased peripheral blood flow and hyperpnea. The suggestion has also been made that the analgesic action of salicylates in rheumatic disease is brought about by a loss of water from affected joints and transport of this water in the plasma to the kidney.[1] This mechanism of water removal would presumably be reflected in a lowering of the hematocrit value. Such a change has been reported in the blood of rats undergoing salicylate antipyresis.[2] Hematocrit studies have therefore been performed as a part of the experimental comparison of antipyresis by sodium salicylate and aurintricarboxylic acid (ATA). Further, the known reduction of sedimentation rate by the salicylates in treatment of rheumatic fever led to a study of sedimentation rates using the same blood samples.

Fevers were produced in 3-1/2-month old female Sprague-Dawley rats by our standard technique of subcutaneous injection of 3 ml of a 15% suspension of baker's yeast in saline solution. Blood was withdrawn after cardiac puncture into a heparinized syringe, and placed in stoppered Wintrobe hematocrit tubes. The settling of the cells was observed at frequent intervals for at least 2-1/2 hr, and a final reading was taken at 24 hr. Then the tubes were centrifuged for 1 hr at 2900 rpm, and hematocrit readings were made.

The packed red-blood-cell volume of rats about 20 hr after yeast injection, when their fevers were high, was the same as that of uninjected controls (Table 31). Further, sodium salicylate treatment at a fully effective antipyretic dose did not affect these hematocrits. ATA, on the other hand, caused a significant increase in packed red-blood-cell volume 1 hr after its injection into rats with yeast-induced fevers, at the time of maximal reduction of the fever. These results suggest that the antipyretic effect of ATA and probably of sodium salicylate in our experimental system is not associated with hydremia and that the basic mechanisms involved need further elucidation.

Although the sedimentation rate of individual rats showed considerable variation, the results are clear-cut enough to permit the following summary. The sedimentation rate of normal uninjected rats was slow; after 5-6 hr the red blood cells had settled only 2-4 mm, and they showed no further drop after 24 hr. Both the rate and the degree of sedimentation increased significantly when the fever was high (analyzed 18-22 hr after yeast

TABLE 31

Effect of sodium salicylate and ATA* on hematocrits of rats with yeast-induced fevers

Treatment	Number of rats	Time of blood withdrawal, hr after therapy	RBC (mean), %	S.E.	P
Uninjected controls	5	-	53.5	0.9	>.05
Yeast, no treatment	5	-	52.0	0.5	
Yeast + saline	13	1	54.7	0.6	>>.05
Yeast + salicylate	12	1	53.9	0.3	
Yeast + saline	8	2	52.9	1.1	>>.05
Yeast + salicylate	10	2	54.2	0.9	
Yeast + saline	13	1	54.7	0.6	<<.001
Yeast + ATA	6	1	62.1	0.9	

*Doses: 125 mg/kg of sodium salicylate or of ATA (as the ammonium salt) injected intravenously about 18 hr after yeast administration. The yeast and saline controls received an equivalent volume of saline solution.

injection). Most of the drop occurred from 45 min to 2 hr after withdrawal of the blood. Intravenous injection of sodium salicylate (125 mg/kg), or of an equivalent volume of saline solution, did not influence this increased sedimentation rate in any way. Statistical analysis of the drop in red blood cells did not reveal any significant difference between means of groups of rats receiving yeast only, yeast plus saline, or yeast plus sodium salicylate, either at 80 min, when the rate of drop was highest, or at 2-1/2 hr when the sedimentation was essentially complete (Table 32). Injection of 125 mg/kg of

ATA at 1 hr before blood withdrawal, however, prevented any measurable separation of blood cells and plasma for at least 5 hr. Twenty-four hours later only a 0.5 mm drop of red blood cells was observed in the tubes.

TABLE 32

Effect of antipyretic doses* of sodium salicylate and ATA on sedimentation of RBC's of rats with yeast-induced fevers

Treatment	Number of rats	Time of blood withdrawal, hr after therapy	RBC sedimentation					
			80 min after sampling			2-1/2 hr after sampling		
			Mean, mm	S.E.	P	Mean, mm	S.E.	P
Uninjected controls	5	-	0.4	0.1	<.05 >.02	1.1	0.3	<.01 >.001
Yeast, no treatment	5	-	8.8	3.2		19.0	4.0	
Yeast + saline	13	1	7.5	1.0	>> .05	17.4	2.5	>>.05
Yeast + salicylate	13	1	6.5	0.8		16.8	1.4	
Yeast + saline	8	2	11.2	2.7	>> .05	21.6	3.9	> .05
Yeast + salicylate	10	2	8.7	1.7		14.7	3.0	
Yeast + saline	13	1	7.5	1.0	<< .001	16.8	1.4	<<.001
Yeast + ATA	8	1	trace	-		trace	-	

*Doses: 125 mg/kg of sodium salicylate or of ATA, or an equivalent volume of saline, injected intravenously about 18 hr after yeast administration.

In summary, the experimental introduction of yeast into the rat produces the typical inflammatory effects of increased sedimentation rate and pyresis, but at least during the time interval sampled, it does not cause blood concentration. The administration of sodium salicylate in this experimental system results in reduction of fever but has no effect upon either sedimentation rate or hematocrit. ATA not only reduces the fever but in addition markedly reduces the sedimentation rate. It increases, rather than decreases, the ratio of blood cells to blood plasma.

Sodium salicylate therapy in rheumatic fever is conducted on a schedule of daily administrations of the drug at doses of about 125 mg/kg per injection. The plasma level of salicylate during the period of treatment rises slowly, building to a maximum in about eight days. The typical reduction of the sedimentation rate does not manifest itself until this time.[1] The failure of sodium salicylate to lower the sedimentation rate in our experiments probably results from the fact that adequate plasma levels cannot

be attained after a single injection. The pronounced reduction of sedimentation rate by ATA, even in our test system, and its structural similarity to sodium salicylate, indicate that this compound deserves further investigation as a possible antirheumatic agent.

References

1. Reid, J., R. D. Watson, and D. H. Sproull. The mode of action of salicylate in acute rheumatic fever. Quart. J. Med. 19:1-19 (1950).

2. Crabtree, R. E., J. B. Data, and J. E. Christian. A study of the carbon-14 content of blood after the oral administration of C^{14}-carboxyl acetylsalicylic acid to nonfevered and fevered rats. J. Am. Pharm. Assoc., Sci. Ed., 45:667-669 (1956).

PROGRESS REPORT: THE USE OF CHELATING AGENTS IN THE TREATMENT OF MANGANESE POISONING II.

Arthur Lindenbaum and William M. Westfall

In recent years the development of the polyamino acid chelating agents has led to the widespread use of one of these, ethylenediaminetetraacetic acid (EDTA) as a therapeutic agent in the treatment of metal poisoning. However, the ability of EDTA to combine with, and inactivate, many metal ions in the body is impaired by its relatively high affinity for calcium.

Other compounds of the polyamino type are now available. One of these, diethyleneaminetriaminepentaacetic acid (DTPA)*, has been shown[1,2,3] to have a greater comparative affinity for the manganous ion than does EDTA:

Cation	Log $K_{M\text{-}DTPA}$	Log $K_{M\text{-}EDTA}$
Ca^{++}	10.6, 9.98	10.6
Mn^{++}	15.1	13.4

Experimental

Preliminary to determining the therapeutic value of this compound in the treatment of manganese poisoning, the relative binding of DTPA and EDTA with calcium and manganese was studied *in vitro* over the general pH range of physiological interest. This was done by means of a titration method[4] in which the increase in the hydrogen ion concentration resulting from chelate formation was measured potentiometrically during titration with 0.100 *M* NaOH. Each solution titrated consisted of 100 ml which was 0.1 *N* in NaCl and 0.001 *M* in chelating agent (acid form) with or without an equimolar concentration of metal chloride.

Results and Discussion

The titration data were converted to equivalents of hydrogen ion released per mole of chelating agent. The results are shown in Figure 54, from which it may be seen that in the pH range 4.5-7.4 the relative extent of formation of the manganous chelate as compared with that of the calcium chelate is greater for DTPA than for EDTA. If it may be correctly assumed

*Supplied through the courtesy of the Alrose Division of the Geigy Chemical Corporation under the designation "Chel 330."

that toxic concentrations of manganese accumulate intracellularly and that DTPA in both chelated and unchelated form can penetrate cell walls, this finding suggests that DTPA may have greater therapeutic effectiveness than EDTA. In view of the above considerations further studies in vivo with DTPA have been made and the results are presented elsewhere in this report.(5)

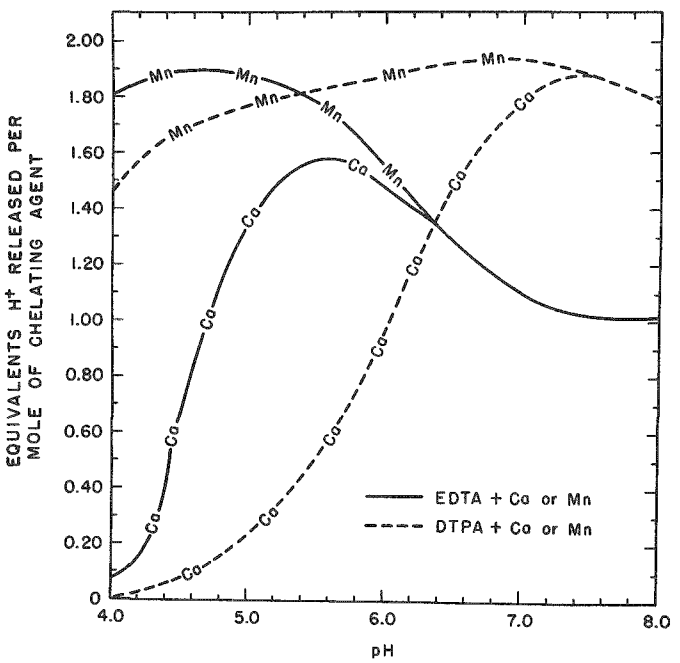

Figure 54
Titration of calcium and manganese complexes of EDTA and DTPA with 0.100 M NaOH.

References

1. Wānninen, E. Diethylenetriaminepentaacetic acid, a new complex-forming substance. Suomen Kemistilehti 28 B:146-152 (1955).

2. Kroll, H. Personal communication.

3. Lindenbaum, A., and J. Schubert. Progress Report: Radioelement removal. II. Quarterly Report of Biological and Medical Research Division, Argonne National Laboratory. ANL-5655, p. 130 (1956).

4. Martell, A. E., and M. Calvin, Chemistry of the Metal Chelate Compounds, pp. 39-43. New York, Prentice-Hall, Inc. (1952).

5. Fried, J. F., J. Schubert, and E. Moretti. Progress Report: The use of chelating agents in the treatment of manganese poisoning. III. This report, p. 155.

PROGRESS REPORT: THE USE OF CHELATING AGENTS IN THE TREATMENT OF MANGANESE POISONING. III

Joan F. Fried, Jack Schubert, and Elizabeth Moretti

Ethylenediaminetetraacetic acid (EDTA) has been tested in the treatment of acute manganism of laboratory animals[1,2] and has been suggested for clinical use in the industrial disease.[3] A consideration of the chemistry of the structurally related compound, diethylenetriaminepentaacetic acid (DTPA), indicated that it might be of equal or greater value in this respect. Accordingly, the compounds were compared in three types of experiments: (a) toxicity studies using the calcium chelates of the two; (b) survival studies on rats given an LD_{90} of manganese gluconate and treated at varying times afterward with either CaEDTA, CaDTPA or saline; and (c) survival studies on rats given the manganese chelates of EDTA and DTPA.

Methods

Female Sprague-Dawley rats between 70 and 135 days of age and weighing 190-280 g were used; animals of equal age were selected for each experimental group. Manganese was administered intraperitoneally as a 3.5% solution of manganous gluconate, pH 6.2, at 27 mg/kg as Mn, a dose which had previously been determined by toxicity studies to be the 30-day LD_{90} value. The calcium and manganous chelates of EDTA and DTPA were prepared by neutralizing the acid or sodium salt with NaOH, adding calcium or manganous gluconate in 1:1 molar ratio of metal to chelating agent, and adjusting the concentration to 0.16 M and the pH to 7.2. CaEDTA and CaDTPA were injected into a tail vein or intraperitoneally in equimolar ratio at levels of from 105 to 2000 mg/kg; doses of these compounds, wherever given, are expressed as the acid form of the chelating agent. MnEDTA and MnDTPA were injected intraperitoneally in doses providing 130 to 260 mg/kg as Mn. All survival data given are on a 30-day basis, but surviving animals were kept under observation for 90 days.

Results

Toxicity studies. Intraperitoneal administration of CaDTPA at a level of 2000 mg/kg resulted in 90% survival, while at a corresponding equimolar level of CaEDTA of 1490 mg/kg survival was 100% (20 rats per group). However, 70% of the CaDTPA-injected animals at this dose level developed paralysis of the hind limbs on approximately the 6th day after injection. At a slightly lower level (1830 mg/kg) of CaDTPA no deaths or paralyses occurred. Intravenous administration of CaDTPA in amounts up to 250 mg/kg produced no toxic effects.

Survival studies. In Table 33, the effects of CaEDTA and CaDTPA in manganese poisoning are compared. It can be seen that the maximal time interval for effective treatment was nearly $3\frac{1}{2}$ hr for CaDTPA, and slightly less for CaEDTA; both compounds were partially effective when given as late as 5 hr after Mn.

TABLE 33

Therapeutic effect of equimolar levels of CaDTPA (158 mg/kg) and CaEDTA (118 mg/kg), intravenously, after an LD_{90} of manganese gluconate (27 mg/kg)

Time of treatment	Survival, %*		
	CaDTPA	CaEDTA	Saline**
Immediately before Mn	100	100	11†
1 hr after Mn	100	100	20†
2 hr after Mn	-	90	10†
$3\frac{1}{2}$ hr after Mn	90	70	10†
5 hr after Mn	45.5†	55†	10†

*10 or more animals per group.
**Saline was given in equivalent volume.
†Average time to death of nonsurvivors was 1.5 days for the CaDTPA-treated, 0.7 days for the CaEDTA treated, and 0.8 days for the saline controls.

In another experiment, the minimum effective dose for complete protection against an LD_{90} dose of manganese, when given 1 hr after the manganese, was found to be 115 mg/kg for each of the two compounds.

Survival data from rats given the manganese chelates of DTPA and EDTA intraperitoneally are shown in Table 34. When manganese is administered as the DTPA chelate, a higher dose may be given without toxic effects than when it is administered as the EDTA chelate.

Discussion

Both CaEDTA and CaDTPA have been found to be beneficial in the treatment of experimental acute manganese poisoning. However, CaDTPA appears to be slightly more effective, in that (a) smaller amounts, on a molar basis, were needed; (b) when given at $3\frac{1}{2}$ hr after manganese, the protective effect of CaDTPA was still nearly complete whereas for CaEDTA it had diminished somewhat; and (c) the survival time of animals treated with CaDTPA at 5 hr after manganese was about twice that of CaEDTA-treated and control animals. The manganese chelate survival studies and

TABLE 34

Survival of rats given manganese chelates of DTPA and EDTA

Dose of Mn, mg/kg	Survival, %	
	MnDTPA	MnEDTA
130	100 (10)*	100 (10)
162.5	100 (6)	83 (6)
195	100 (17)	70 (17)
225	94 (16)	60 (10)
245	73 (15)	67 (15)

*Numbers of animals injected are in parentheses.

titration data obtained in our laboratory [4] indicate that the enhanced effectiveness of CaDTPA may be due to the greater stability of MnDTPA at intracellular pH levels.

References

1. Kosai, M. F. and A. J. Boyle. Ethylenediaminetetraacetic acid in manganese poisoning of rats. Ind. Med and Surg., 25:1-3 (1956).

2. Rodier, J., R. Mallet, and L. Rodi. Étude de l'action détoxicant de l'éthylénediaminetétraacétate de calcium dans l'intoxication expérimentale par le manganese. Arch. maladies profess. med. travail et sécurité sociale. 15:210-224 (1954).

3. Peñalver, R. Diagnosis and treatment of manganese intoxication. A.M.A. Arch. Ind. Health. 16:64-68 (1957).

4. Lindenbaum, A., and W. M. Westfall. Progress report: The use of chelating agents in the treatment of manganese poisoning. II. This report, pp. 153.

ION EXCHANGE AND SOLVENT EXTRACTION STUDIES ON Co(II) AND Zn(II) COMPLEXES OF SOME ORGANIC ACIDS

Jack Schubert, Edmund L. Lind,* William M. Westfall, Raymond Pfleger,** and Normal C. Li**

Abstract

The stability of the Co(II) and Zn(II) complexes of bioxalate, oxalate, citrate and glycolate have been determined by the use of Co^{60} and Zn^{65} in conjunction with the methods of ion exchange and solvent extraction. A decrease in both the stability of the glycolate complexes and the ion-exchange distribution coefficients of the tracer metals with increase in ionic strength was demonstrated. An important assumption in the use of the ion-exchange method for complex study is that the uptake of the complex itself by the cation exchanger is nil or very small relative to the uncomplexed cation. This was demonstrated directly for the Mg(II) complex of oxalate by means of oxalate labeled with C^{14}. In ion-exchange experiments the uptake of Co(II) and Zn(II) is higher in the presence of imidazole than in its absence, while in corresponding solvent-extraction experiments, the opposite is true. These results indicate that the +2 imidazole complexes themselves are taken up by the cation exchanger, and show that the ion-exchange and solvent-extraction experiments complement each other in the study of metal complexes.

*Resident Research Associate from Central Washington College of Education.

**Duquesne University.

PHAGOCYTOSIS OF GRANULES FROM DISRUPTED MAST CELLS

Douglas E. Smith and Yevette S. Lewis

Abstract

Microscopic examination was made of the fate of the cytoplasmic granules of mesenteric mast cells disrupted by intraperitoneal injection of distilled water or 48/80* into the rat. Both fixed and living tissues were employed. Similar microscopic examinations were carried out on the "abnormal" or degenerated mast cells of several tissues from control and treated (X-radiation, ACTH or cortisone) rats and hamsters.

Treatment with distilled water completely disrupted the mast cells of the mesentery, while other cells appeared to be undamaged. Fibroblasts, macrophages and leucocytes were observed to take up and dispose of the granules shed from the disrupted mast cells. These phagocytes were quite similar in appearance to the "abnormal" or degenerated mast cells previously described as occurring in normal and treated animals.

It was concluded that "abnormal" or degenerated mast cells are in reality, phagocytes which have taken up the granules of disrupted mast cells.

---

*A polymer of N-methylhomoanisylamine and formaldehyde, supplied through the courtesy of Dr. Edwin J. de Beer of Wellcome Research Laboratories.

STUDIES ON EFFECTS OF DEUTERIUM OXIDE

V. Growth Data for Mice

Asher J. Finkel and Dorice M. Czajka

Data were collected in several long-range experiments on the body weights of young adult CF No. 1 female mice maintained on drinking water of constant deuterium oxide concentrations at various levels. The mice were fed Rockland mouse diet in pellet form, and both the solid food and the drinking water were available ad libitum. The animals were sacrificed periodically for deuterium analyses of body fluids and tissues.

Body weights of surviving animals were averaged and these means were divided by the mean weight of the initial population at each deuterium level. The data plotted at 10-day intervals are presented in Figure 55, which also gives the numbers of mice averaged at each point. Mice maintained on 40 atom per cent deuterium lost about 25% of the initial body weight over a period of three months. During this same period mice on 30 atom per cent deuterium grew at least as rapidly as did control mice but thereafter grew somewhat more slowly. Mice on 25 atom per cent deuterium consistently maintained a slightly higher weight level relative to this starting weight than did the control group.

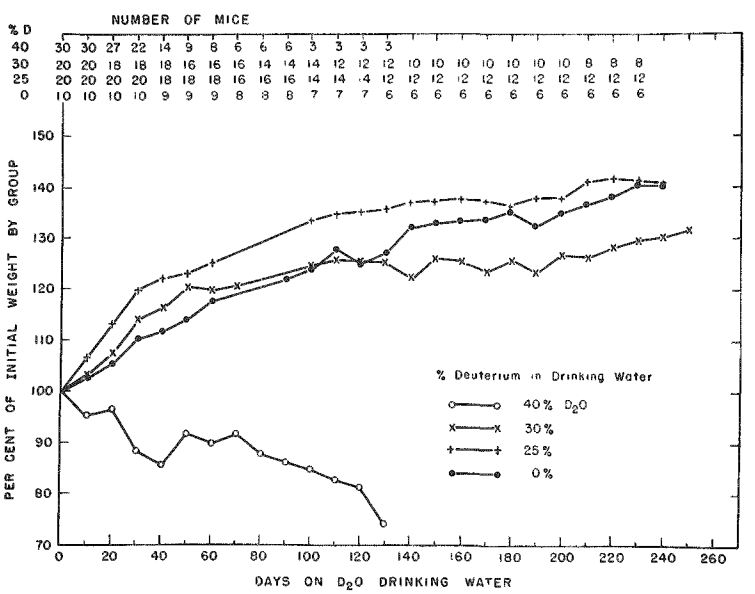

Figure 55

Growth of young CF No. 1 female mice maintained on various levels of deuterium oxide.

These data demonstrate that mice can be maintained for long periods of time on drinking water containing at least 25, and possibly even 30 atom per cent deuterium without adversely affecting body weight.

STUDIES ON EFFECTS OF DEUTERIUM OXIDE

VI. Deuterium Distribution in Mouse Tissues

Asher J. Finkel, Joseph J. Katz,* Henry L. Crespi,* and Dorice M. Czajka

Basic to an understanding of the deuterium isotope effect is the general question of deuterium-hydrogen proportions in the aqueous and solid phases of tissues of deuterated animals. Further, there is the specific problem of whether any tissue fixes deuterium to an extent greater than the concentration of the isotope in body fluids and tissue water.

Young adult female CF No. 1 mice were maintained in several series for varying periods of time on 25, 30, or 40 atom per cent deuterium oxide in the drinking water. The animals were sacrificed periodically, and the liver, kidney, spleen, and brain were removed for analysis. Water obtained by distillation of these tissues was analyzed for deuterium content and the deuterium incorporated in body compounds was determined by analysis of water obtained by combustion of these desiccated tissues.

The data are summarized in Table 35 where the mean values represent data from 2 to 10 mice. It can be seen that by the 11th day the distillable water has reached a deuterium content that is very close to the maximum.

TABLE 35

Per cent deuterium in water from mouse tissues

Day	Liver - Kidney - Spleen		Brain	
	Distillation deuterium	Combustion deuterium	Distillation deuterium	Combustion deuterium
	A. 25 atom per cent deuterium drinking water			
11	16.5	5.3	-	-
42	16.0	7.1	15.2	4.6
92	15.7	7.6	15.9	5.9
102	16.9	8.5	-	-
108	15.1	7.3	14.9	5.4
127	17.2	7.6	17.9	6.1
201	17.9	8.1	19.1	7.5
	B. 30 atom per cent deuterium drinking water			
11	19.4	6.0	20.6	3.1
26	22.9	8.9	23.3	4.6
45	20.1	8.5	-	-
74	19.1	9.0	19.2	6.0
102	16.6	7.8	15.1	7.6
136	18.9	8.4	19.9	8.2
	C. 40 atom per cent deuterium drinking water (tentative)			
11	26.9	6.9	27.0	4.7
21	26.1	9.3	26.6	5.4
32	27.5	9.7	28.1	6.6
42	27.5	10.2	28.1	6.8
61	27.9	10.4	28.7	7.6

*Chemistry Division

This result is consistent with that previously reported for urine deuterium, where by the 11th day the level had reached 95 atom per cent of the equilibrium value.(1) Liver, kidney, and spleen data were combined because they were indistinguishable from each other. Further, the mean distillable deuterium values for these tissues, as well as brain, at each level are very close to 66 atom per cent of the deuterium level of the drinking water.

The incorporated deuterium, consisting of that fixed in nonexchangeable positions in body compounds plus that which is readily exchangeable, increases in accordance with a pattern that depends, in large part, on the deuterium level in the drinking water (Figure 56). Brain incorporates deuterium at a much lower level than liver, kidney, and spleen. Figure 57 shows the percentage incorporation of deuterium in relation to the levels in the tissue fluids. The data for the 25 atom per cent and 30 atom per cent drinking water series are practically superimposable, and a solitary point calculated from whole mouse data from a comparable 15 per cent series(2) also falls on the curve. Again the curve for the abdominal organs differs from that for brain.

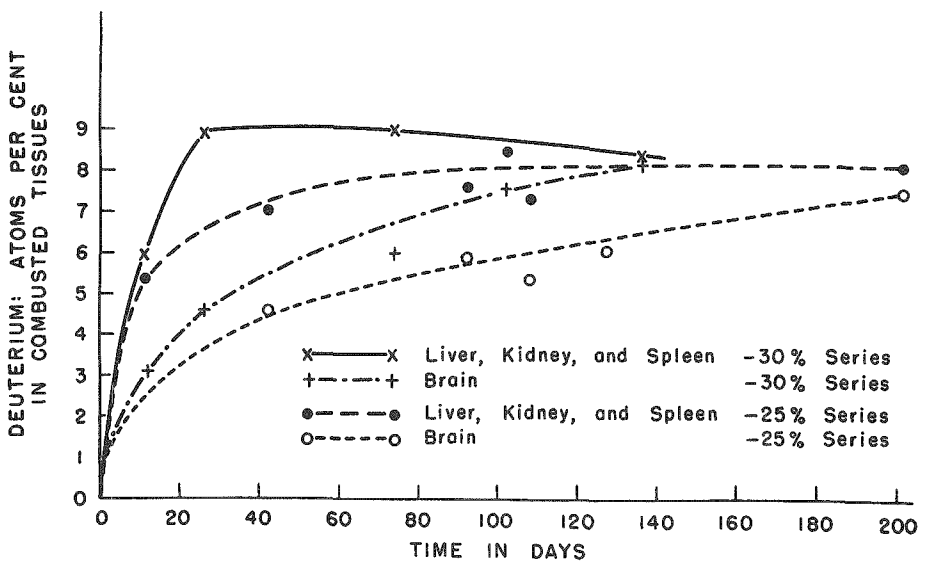

Figure 56. Incorporation of deuterium into mouse tissues: atom % deuterium recovered by combustion of dry tissues is shown for serial sacrifice series. Data for liver, kidney and spleen are combined.

The amount of deuterium incorporated into body tissues when mice are supplied with deuterated drinking water reaches a value of from 40 to 50 per cent of the deuterium in the tissue fluids. These results indicate that none of the tissues studied has any unusual affinity for deuterium and that these experiments, with concentrations of heavy water as high as mice will tolerate, are in general agreement with earlier studies where smaller amounts of deuterium were employed.

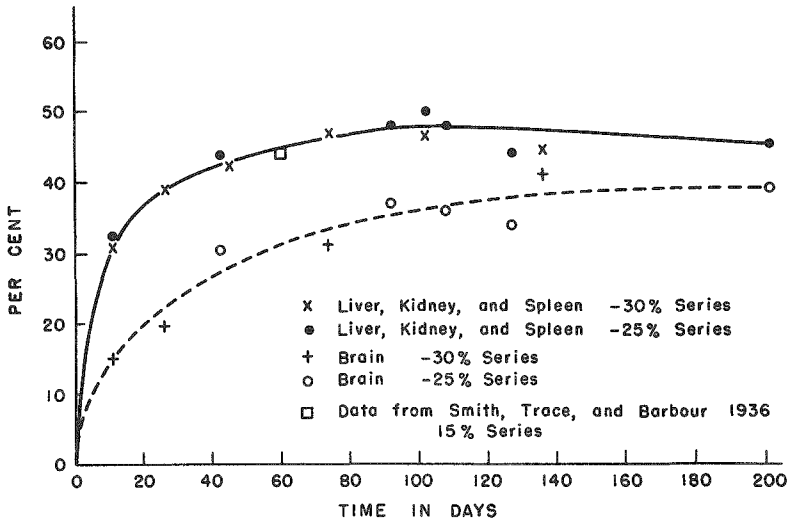

Figure 57. Percentage incorporation of deuterium into mouse tissues in relation to the levels in the tissue fluids.

References

1. Finkel, A. J., D. M. Czajka, H. L. Crespi, and Dolores W. Symon. Studies on Effects of Deuterium Oxide. I. The course of deuteration of mice. Quarterly Report of Biological and Medical Research Division, Argonne National Laboratory. ANL-5696, pp 68-70 (1956).

2. Smith, P. K., J. Trace, and H. G. Barbour. The fate of deuterium in the mammalian body, J. Biol. Chem. 116:371-376 (1936).

THE PRESENCE OF FISSION I^{131} IN COW'S MILK

Philip F. Gustafson

During late July and early August of 1957, in vivo γ-ray counting of persons with no history of radioactive contamination showed elevated counting rates which were traced to I^{131} present primarily in the thyroid. Counting of two adults and one child in the Biology steel room, using a 2 in. diameter by 2 in. thick NaI crystal and an Argonne type 256-channel analyzer, showed total thyroid values of 0.13 and 0.15 mμc (millimicrocurie) of I^{131} for the adults and 0.41 mμc for the child.

The fact that such concentration of I^{131} occurred rather abruptly led to an examination of possible routes of entry into the human system. One gallon of laboratory drinking water, counted for 17 hr failed to show any sign of I^{131} or other fission-product activities. On the suggestion of Dr. A. M. Brues one gallon of milk was counted for 17 hr, and a respectable I^{131} spectrum was obtained as illustrated in Figure 58. After correction for the contribution due to K^{40}, comparison with values for one gallon of water to which a known quantity of I^{131} has been added, showed the presence of 2.6 mμc I^{131} per gallon of milk, or 0.069 mμc I^{131}/100 ml of milk.

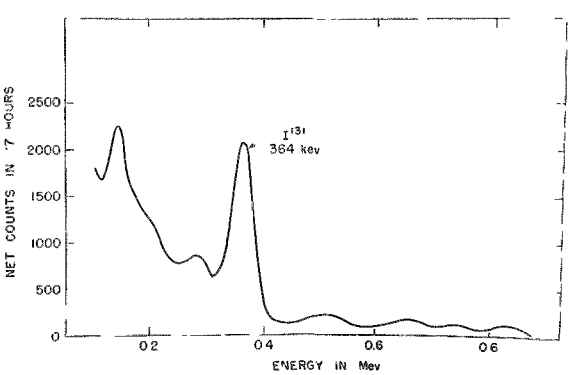

Figure 58 Gamma-ray spectrum of milk (8/5/57) showing the presence of I^{131}.

Comar[1] mentions the negative results of direct assay for I^{131} in 100-ml samples of milk carried out by his group. His estimated values for I^{131} in milk, based on radioiodine content of human thyroids on autopsy, range from 0.002 to 0.2 mμc/100 ml. The observed value of 0.069 mμc/100 ml is in accord with this estimate.

Due to the 8-day half-life of I^{131} no appreciable build-up of this radioisotope is possible in vivo. The observed value of 0.4 mμc in a child's thyroid, may indicate a value as high as 0.04 mμc/g of thyroid which is about 3×10^{-3} of the tolerance level.[2]

References

1. Comar, C. L., Bernard F. Trum, U.S.G. Kuhn III, R. H. Wasserman, M. M. Nold, and J. C. Schooley. Thyroid radioactivity after nuclear weapons tests. Science 126:16-18 (1957)

2. U. S. National Committee on Radiation Protection. Maximum permissible amounts of radioisotopes in the human body and maximum permissible concentrations in air and water. Natl. Bur. Standards (U.S.) Handbook 52 (1953).

ACTIVATION PRODUCTS IN FOODSTUFFS IRRADIATED WITH THERMAL NEUTRONS

Philip F. Gustafson, S. S. Brar, and Austin M. Brues

Whether or not pile irradiation involving thermal neutron absorption may be a safe method of food sterilization depends on the amounts of long-lived radioisotopes resulting from this procedure. To investigate this question, representative samples of meat, fish, poultry, fruit and vegetables supplied through the Quartermaster Corps, U.S. Army, were irradiated in 300-g quantities in the thermal column of the Argonaut reactor. The foods were placed in commercially available refrigerator dishes, wrapped in polyethylene sheeting, and placed in the thermal column for about 2 hr. The total thermal flux incident upon and passing through each sample was measured by gold foils of known weight placed on the top, bottom, and middle of each container. The average flux was 5.2×10^{12} n/cm^2.

Gamma-ray counting was carried out using a 5" x 4" NaI crystal and associated electronic equipment, including a 256-channel analyzer. Thus, spectral data, as well as net counts, were obtained. The first measurements were made 2 days after irradiation, at which time the induced activities of the foods and accompanying containers were low enough to allow safe handling.

The bulk of the gamma-activity at this time was due to Na^{24} as indicated both by spectral characteristics and by decay time; K^{42} must obviously have been present at this time but was not observed since the intensity of the 1.49-Mev γ-ray from K^{42} is between 1% and 10% that of either γ-ray from Na^{24}, assuming equal concentrations of the two elements in the irradiated material. Estimates of Na^{24} activity at the end of irradiation were 27 to 33 μc/kg for the animal tissues, 6.6 μc/kg for fruit (peaches), and 24 μc/kg for vegetables (carrots). Two weeks after irradiation the animal tissue samples had a net counting rate equivalent to 7×10^{-11} curie Ra/sample or about 2×10^{-10} curie Ra/kg. No discrete structure was apparent in the net spectra. In the region of 1.12 Mev (Zn^{65} photopeak) the net counts indicated that not more than 6×10^{-11} curie could be present. The fruit and vegetable samples showed no net count 2 weeks after irradiation.

Beta-ray counting of infinitely thick samples of the same materials showed activity decreasing with the half-life of P^{32}. Extrapolating back to the time of irradiation, values of the order of 2.4 μc/kg of induced P^{32} were indicated in the animal tissues. There was no measurable β activity in the fruit or vegetable samples.

On the assumption that food is irradiated under such conditions that a total flux of 10^9 slow neutrons has been received (an amount which should be adequate for sterilization), and taking the maximum values for the meat

samples as maximal for any diet so sterilized, we may tabulate the radioisotope concentrations as in Table 36, which also gives the permissible concentrations for potable water.

TABLE 36

Maximum radioactivities induced in food irradiated with 10^9 n/cm^2*

	t = 0	t = 2 weeks	t = 100 days	Industrial permissible water conc.	1/30 of permissible water conc.
Na^{24}	6.3×10^{-6}	10^{-12}	-	8×10^{-3}	2.7×10^{-4}
K^{42}	2.5×10^{-6}	10^{-14}	-	10×10^{-3}	3.3×10^{-4}
P^{32}	4.6×10^{-7}	2.4×10^{-7}	4.4×10^{-9}	2×10^{-4}	6.7×10^{-6}
S^{35}(Cl)	4.5×10^{-8}	3.7×10^{-8}	2.1×10^{-8}	5×10^{-3}	1.3×10^{-4}
Ca^{45}	4.4×10^{-11}	4.0×10^{-11}	2.8×10^{-11}	5×10^{-4}	1.3×10^{-5}
Total gamma	-	2.2×10^{-7}	-		
Natural K^{40}	about 10^{-3}				

*Data are expressed as μc/g. It is assumed that ratios of K: Na: Cl: Ca in the food are as 36: 10: 16: 4.2

Taking 1/30 of the industrial permissible radiation level as acceptable for the whole population, it is seen that total food intake 2 weeks after irradiation would be safe within a factor of about 30, and that if the food were to cool for 100 days, the factor would be in excess of 100.

TABLE 37

Approximate radiation dose rate in food irradiated with 10^9 n/cm^2

	Dose, mrads/year		
	"Cooling" time		
	0	2 weeks	100 days
Na^{24}	70	10^{-4}	-
K^{42}	65	2×10^{-6}	-
P^{32}	6.6	3.4	6×10^{-2}
S^{35}	0.06	0.05	3×10^{-2}

Another way of calculating risk would be to estimate the radiation dose to the body if it should come to equal that within an infinite volume of the meat consumed - which should, in general, be limiting. This appears, roughly approximated, in Table 37.

Under this assumption, total dose rate after 2 weeks' cooling time will be less than 1/5 of that from natural K^{40} values for tissue (about 1/50 of natural background radiation) and after 100 days will be about 1/1000 of background. It would appear from this that pile sterilization of foodstuffs is feasible if a reasonable cooling time (a few days) is allowed. It is noted that S^{35} (from chlorine) eventually may become the limiting factor.

Further studies, using higher thermal fluxes, will be carried out to determine what rare elements of high-activation cross section may appear in foodstuffs, and the form in which S^{35} appears after its production in foodstuffs by the n,p reaction on Cl^{35}.

Summary

Measurements of radioactivity of typical foodstuffs after pile irradiation, and of the particular isotopes concerned, indicate that sterilization in a flux of 10^9 thermal neutrons is an entirely safe procedure, particularly if a few days' cooling is allowed. After 100 days' cooling the radioactivity of typical foodstuffs is negligible by any criteria.

THE PRODUCTION OF HEAT BY THE NEUTRON IRRADIATION OF BORON-FREE GLASS, LIME GLASS AND QUARTZ, AND ITS EFFECT UPON THE CONDENSATION OF PHOSPHATE

Takuya R. Sato and William P. Norris

Recently, electrochromatographic analysis of neutron-irradiated phosphate has revealed that great care must be exercised in the selection of containers for materials to be activated with neutrons in the reactor. When we first irradiated phosphates with neutrons, we found that anhydrous disodium acid phosphate, Na_2HPO_4, was sometimes completely converted into pyrophosphate, $Na_4P_2O_7$. This condensation effect was finally traced to the nature of the glass containers. With containers of pure quartz, there was no alteration of the phosphate, but with those of lime glass and of so-called boron-free glass (that contain about 2.0% and 0.2% of boric oxide, respectively) there was complete conversion of phosphate to pyrophosphate.

The effect of lime glass and of boron-free glass upon the condensation of Na_2HPO_4 in the reactor is similar to the action of heat upon Na_2HPO_4. Boron atoms have about 7000 times greater capacity for absorption of neutrons than the silicon, oxygen and calcium of the glass itself, yet all these elements have about the same neutron-binding energy. This suggested that neutron absorption by boron in lime glass and in boron-free glass might provide sufficient energy to heat the glass and the enclosed phosphate.

In view of the possible significance of these observations for the interpretation of the effects produced by neutron irradiation, we have now explored more exhaustively the heat produced by neutron irradiation of various containers. The shape of the containers has been varied, and they have been irradiated with and without samples of Na_2HPO_4.

Materials and Methods

Measurement of container temperature. The glass tubes employed for the irradiation were pure silica (quartz, Corning Glass Company), boron-free glass (Corning 7280) and lime glass (Corning). Three different tubes were prepared from each glass as follows: empty tubes, 1 x 10 cm, sealed at one end, without any sample; tubes + Na_2HPO_4, 1 x 10 cm, with a commercial anhydrous preparation of Na_2HPO_4; and capillary tubes, 1 x 10 cm, one end of which had been melted into a thick-walled capillary with the end sealed; outer diameter 10 mm, inner diameter 2 mm, length 2 cm. The amount of Na_2HPO_4 in each quartz and boron-free glass tube was 0.2 g, that in the lime glass 0.4 g. The thermocouples consisted of a No. 28 gauge,

chromel-alumel (duplex thermocouple, Leeds and Northrup Company); the thermocouple junctions were spot welded. These thermocouples were suspended near the sealed ends of the empty tubes, in the capillary of the capillary tubes, and in the powdered crystals in the tubes + Na_2HPO_4. The insulated lead wires to the thermocouples were secured tightly by means of a cork stopper. These wires, which were about 12 feet long, were spot welded to copper wire, and the chromel-copper junction served as the cold junction.

The glass containers with the thermocouples were placed in standard aluminum cans (3 cm in diameter, 14 cm long). The cans were covered and lowered into the vertical thimbles of the Argonne reactor CP-5, which had been turned off for this loading operation. The containers were placed in the region in which the neutron flux was, after "run up," about 2×10^{13} n/sec, and the γ-radiation was roughly 500,000 r/min. From "shut off," the reactor was "run up" under automatic control to full power in about 25 min.

For the measurements, the copper wire leads were connected to a Leeds and Northrup 10-point thermocouple selector switch so that 9 different thermocouples could be connected quickly in succession to a Brown potentiometer. The potentiometer had a pen-travel distance of 12 inches (100 scale divisions) per 10 millivolts. A variable resistance was connected in parallel with the potentiometer to decrease the scale deflection one-fourth the original distance

The chromel-alumel thermocouples were standardized at the melting point of ice (0°) and the boiling of water (100°). The voltage output with a cold junction at 0° and the hot junction at 100° was measured with a Leeds and Northrup millivolt potentiometer, and the output voltage was compared with that of the Brown Instrument Company's standard chromel-alumel chart to arrive at a corresponding temperature value. The output voltage of the thermocouples was noted on the Brown recording potentiometer to which the output of each thermocouple was connected in succession. In this way, the temperature of the glass containers was determined as a function of time.

Analysis of irradiated phosphate. The products formed by the irradiation of phosphate in containers of different kinds of glass were separated by electrochromatography For this purpose, 0.0142-g portions of the irradiated salts were transferred to 10-ml volumetric flasks and dissolved in water to form 0.01 formula weight solutions. The various oxyacids contained in these solutions were separated by electrochromatography in a soft, acid-washed commercial filter paper moistened with 0.1 M acetic acid.

For the detection and location of the radioactive products, radioautographs were made with Kodak No Screen X-ray film. The separated

substances were identified by reference to the migration of authentic non-radioactive preparations submitted on the same sheet of filter paper.

For the identification of the radioactive phosphorus compounds separated by electrical migration, authentic, nonradioactive phosphorus compounds were submitted to electrical migration in moist paper and located by neutron activation, or alternatively, radioactive tracers were employed. For the activation, the paper was dried, placed on a sheet of polyethylene, and the two sheets were rolled together, providing a cylinder about 2 inches in diameter. This rolled paper was wrapped in another sheet of polyethylene and placed in the thermal column of the reactor for two days at a neutron flux of approximately 10^{12} neutrons per sec. When removed from the reactor, the paper was permitted to "cool" for some 7 to 14 days to reduce the background of the paper itself. A radioautograph of this paper was then made using Kodak No Screen X-ray film.

Results

Variation of temperature of the glass containers with time is shown in Fig. 59. The temperature of quartz, boron-free glass and lime glass containers rose rapidly and leveled off after 25-30 min. At the start, after "shut-off," all the thermocouples gave the same reading of 50°C in the vertical thimbles of the reactor, thus indicating that all the thermocouples were performing consistently.

The three quartz containers yielded the same temperature curve, which reached a constant temperature of about 155°C. The boron-free glass containers reached higher temperatures: the capillary tube, 398°C; the empty tube, 368°C; and the tube + Na_2HPO_4, 350°C. The temperature of the lime glass containers reached very high temperatures: the capillary tube, 555°C; the empty tube, 537°C; and the tube with 0.4 g Na_2HPO_4, 499°C.

A typical electrochromatogram of Na_2HPO_4 samples after exposure to neutrons for 6 hr in different kinds of glass is reproduced in Fig. 60. Simultaneous electrical migration of Oak Ridge $H_3P^{32}O_4$ proved that the principal radioactive product formed in the quartz tube was phosphate ($P^{32}O_4^{\equiv}$). In boron-free glass and lime glass tubes, the principal radioactive product was pyrophosphate ($P_2O_7^{\equiv}$), identified by comparison with authentic nonradioactive pyrophosphate which was located by neutron activation of the electrochromatogram.

If the pyrophosphate in the boron-free and lime glass tubes was formed by heat, the entire sample, not only the radioactive species, should have been converted to pyrophosphate. To test this, the electrochromatogram that provided the autograph shown in Fig. 60 was allowed to stand

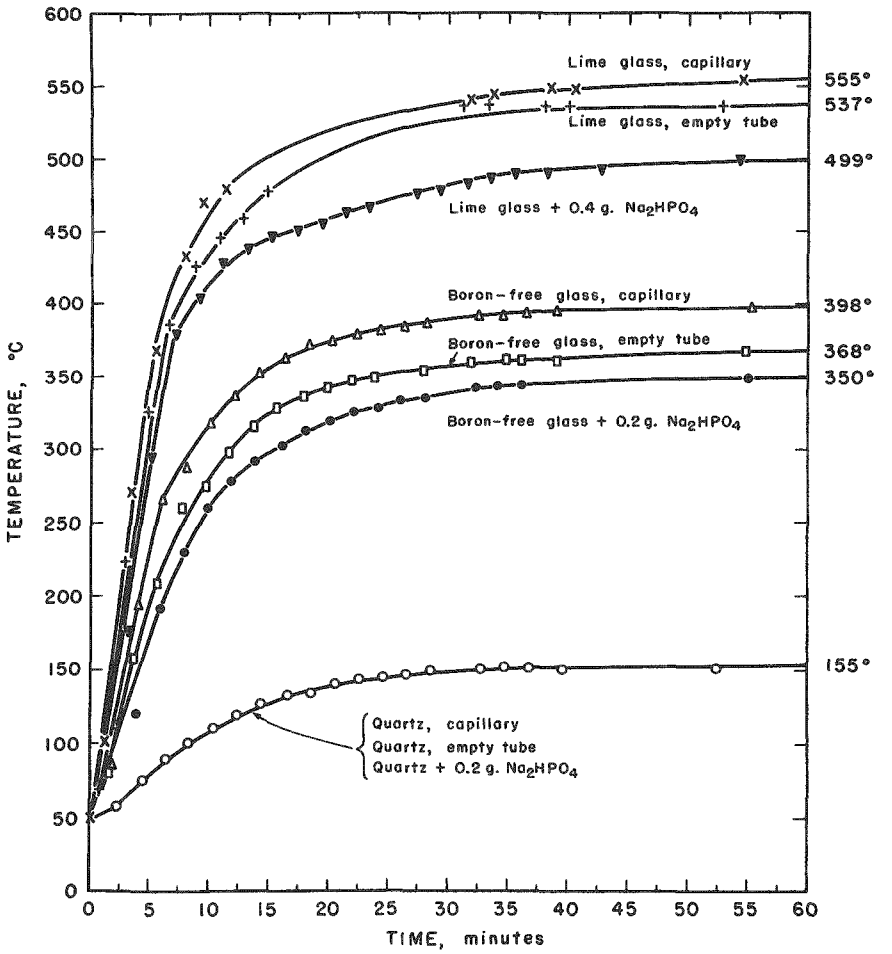

Figure 59. Temperature of glass containers exposed to neutrons in the CP-5 reactor as a function of time.

until most of the radioactivity had decayed. The paper was then exposed to neutrons, allowed to cool for two weeks to reduce the background, and another autograph was made. As shown in Fig. 61 the activity was located in the same region as before (compare with Fig. 60), thus demonstrating that the phosphate in quartz tubes had remained phosphate, whereas the phosphate in boron-free glass and in lime glass had been converted entirely into pyrophosphate.

Discussion

The rates of temperature rise shown in Fig. 59 indicate that the temperature increase resulted from the interaction of neutrons with elements of the glass containers. This temperature rise can be correlated with the boron content of the glass, with the large cross section of boron for neutrons, and with the great energy of the $B(n,\alpha)Li$ reaction.

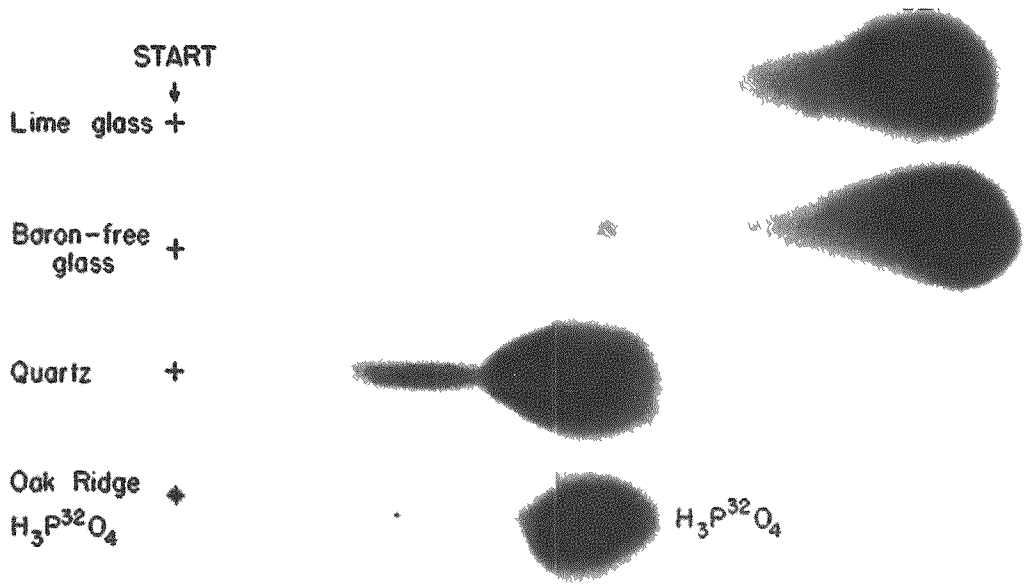

Figure 60. Neutron activation products of Na_2HPO_4 irradiated in glass containers in air. Radioautograph of radioactive products separated by electrochromatography after neutron irradiation of Na_2HPO_4 in lime glass, boron-free glass and quartz in air. Background solution 0.1 M acetic acid, time 2 hr, D.C. potential about 12 v/cm.

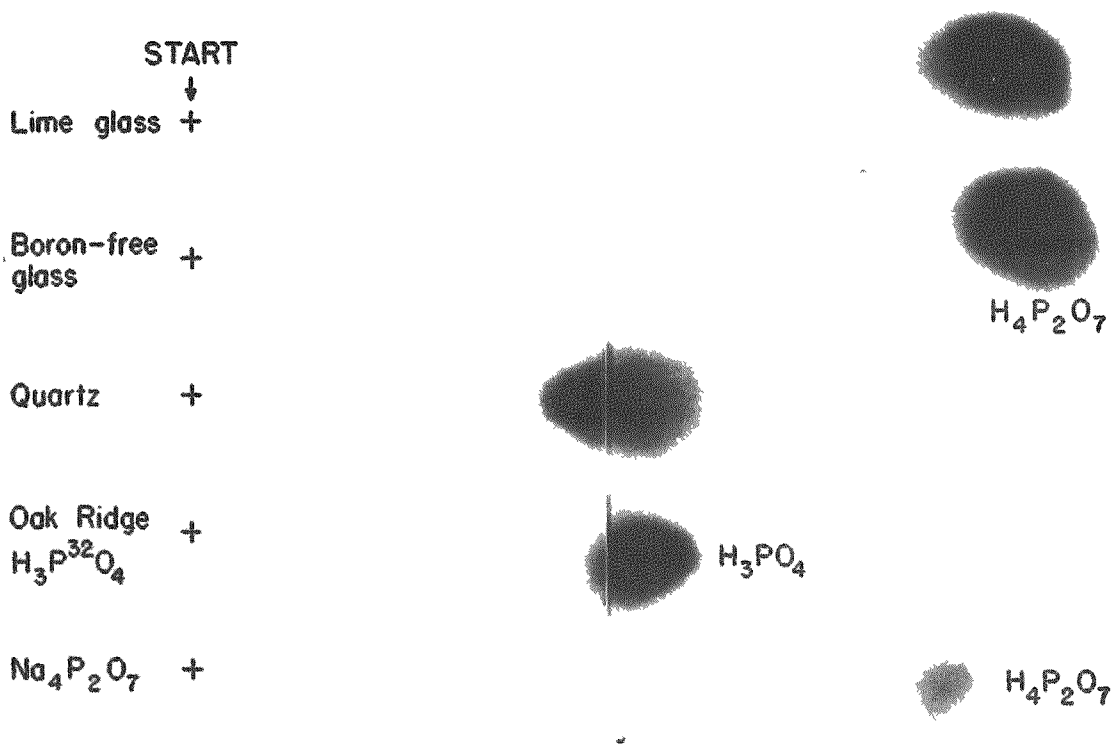

Figure 61. Neutron activation products of Na_2HPO_4 separated by electrochromatography and reactivated by neutron irradiation of the electrochromatogram. The electrochromatogram that provided the autograph shown in Fig. 60 was permitted to stand until the activity decayed. It was then exposed to neutrons at a flux of 10^{12} n/sec for 48 hr and allowed to stand for 2 weeks. The autograph was made with Kodak No Screen X-ray film.

The similarity of temperatures of the three quartz glass containers indicates that heat production and heat transfer were not affected by the presence of Na_2HPO_4 in the quartz glass tube. Electrochromatographic analysis of the phosphate (Fig. 60) proves that there was no thermal conversion of Na_2HPO_4 to pyrophosphate in the quartz tubes.

The three tubes of boron-free glass did not reach the same temperatures, as shown in Fig. 59. Whether or not these different temperatures can be attributed to the mass of the glass, to the thermal conductivity of the crystalline phosphate, or to other factors, has yet to be established. The same considerations apply to the three tubes of lime glass.

The results shown in Fig. 59 indicate that the boron-free and lime glass tubes reached temperatures that were high enough to convert phosphate into pyrophosphate. The conversion of Na_2HPO_4 into pyrophosphate is an endothermic reaction, proceeding at a rapid rate in the temperature range of 360-400° C. This temperature was reached by the boron-free glass and was greatly exceeded in the lime glass, (Fig. 59) indicating that the heating effect originated in the glass and not in the phosphate, itself.

The rate of heating of the glass containers is indicated by the slope of the curves in Fig. 59. Several conditions contributed to this rate of heating. The first was the heat capacity of the tubes themselves and of the contained phosphate. Another was the gradually increasing neutron flux as the reactor was brought to full power during the first 25 min. When the curves leveled off, the heat production was balanced by the heat loss by thermal conductivity.

The authors wish to acknowledge the assistance of Mr. Eugene Synder during a part of this work.

MEASUREMENT OF Ca^{45} BY LIQUID SCINTILLATION METHODS

Walter E. Kisieleski and Frank Smetana

Liquid scintillation counting has proved to be a convenient, sensitive, and rapid method for the routine measurement of organic and aqueous solutions containing tritium, C^{14}, and S^{35}. The ability of liquid phosphors to respond with excellent sensitivity to low-energy β-emitters suggests that they may be applicable to higher-energy β-emitters as well as γ- and α-emitters. With low-energy β-emitters such as C^{14} and tritium, the isotope can be incorporated into gaseous compounds for gas-phase counting. Ca^{45}, on the other hand, can only be counted in the solid phase; liquid scintillation counting affords an alternative method of measurement which eliminates the problems of self-absorption and scatter.

Measurements of Ca^{45} have been made utilizing the techniques of liquid scintillation counting as previously described.(1) Using a liquid scintillator composed of 4 g/liter of 2,5-diphenyloxazole in a solution of 70% toluene and 30% absolute alcohol, Ca^{45} can be measured with an efficiency of 45% at a background of 50 cpm. With these counting characteristics Ca^{45} can be measured routinely in a solution containing 500 mg/ml of $CaCl_2$ at a lower limit of 3×10^{-4} μc/ml.

Samples for the measurement of Ca^{45} are prepared by dissolving up to 0.2 ml of an aqueous solution of $CaCl_2$ in 10 ml of the liquid scintillator. The samples are contained either in 5-dram glass vials or in 1-oz polyethylene bottles, and the measurements are made with a Packard Tri-Carb Spectrometer.

The optimum electronic characteristics with regard to photomultiplier voltage and amplifier gain for Ca^{45} were determined by plotting a series of curves showing the effect of photomultiplier voltage on pulse height distribution (Figure 62). From this series of curves, it was established that the optimum operating characteristics for the measurement of Ca^{45} in the Tri-Carb Spectrometer are photomultiplier voltage, 1050 v; discriminator voltage width, 10 to 75 v; and maximum gain on the amplifiers. Under these conditions the counting rate varies less than 5% over a photomultiplier voltage that ranges between 1000 and 1100 volts.

The over-all precision of the method was determined by measuring 10 samples each containing 0.1 ml of a calibrated solution of Ca^{45} plus the liquid scintillator. The standard deviation of these measurements was found to be $\pm$ 1.1% as against an expected standard deviation, based on counting statistics, of $\pm$ 0.7%. The results were essentially the same in the 5-dram glass vials and in the polyethylene bottles.

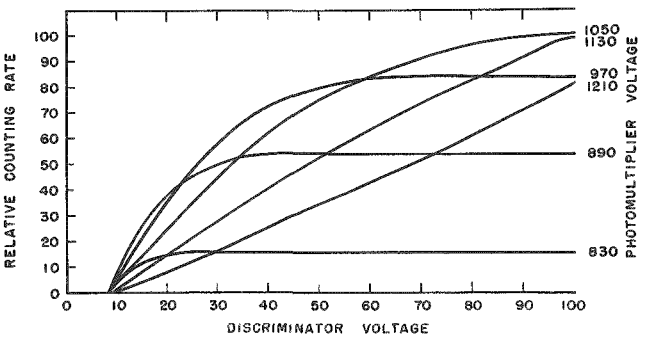

Figure 62. Relative counting efficiency versus photomultiplier and discriminator voltage.

In considering the background contributions, it was determined that the liquid scintillator contributes approximately 2 cpm/ml and the 5-dram glass vial alone gives a background count of 20 cpm. The background of the polyethylene bottles is about 10% less than that of the glass vials with about an equal increase in efficiency under the same conditions. Because of the low cost of polyethylene bottles, they may find use in routine low-level counting where a disposable bottle would be desirable.

The method is being applied to the measurement of Ca^{45} in biological materials, especially bone. Certain quenching phenomena associated with these measurements will be reported shortly.

Reference

1. Kisieleski, W. E., and F. Smetana. Liquid scintillation counting of low-energy β-emitters. Quarterly Report of Biological and Medical Research Division, Argonne National Laboratory. ANL-5426, pp. 125-128 (1955).

THE MEASUREMENT OF PROTEIN TURNOVER IN RAT LIVER

III. The Effect of Dietary Protein

Robert W. Swick and Rita A. Martin

Solomon and Tarver[1] attempted to reconcile the disparity in the estimates of liver protein turnover calculated from data obtained by a single exposure to tracer materials. They suggested that the discrepancies might be due to differences in the protein content of the several experimental diets. As evidence, they measured the loss of methionine-S^{35} from various tissue proteins including liver over a period of 4 days and found that the disappearance was accelerated when the animals were fed a diet containing 45-50% of casein. That the increased rate of loss of isotope was not due to a washing-out effect was shown when methionine added to a low casein diet failed to affect the rate of disappearance of isotope. They used two time periods, from 3 hr to 4 days in one experiment and from 1 day to 5 days in a second, in order to show that their data were not the result of selecting the right time period. However, there were some rather large differences in the disappearance of isotopes between the two experiments. The use of an arbitrary time for the initial point on their curves may not be valid since it may not represent the same relative position on each specific activity curve.

The present report describes the effects of varying the level and the type of amino acid source on the renewal rate of liver protein as measured by the incorporation of isotopic CO_2 into the guanidine group of arginine. It will be shown that the level of protein intake has little or no effect on the turnover of liver protein but that the spectrum of amino acids offered may have a slight effect on the turnover rate.

Methods

Adult female rats were fed various diets containing $CaC^{14}O_3$ in a continuous manner as described previously.[2] The amino acid sources used were a mixture of essential amino acids plus additional nitrogen in the form of ammonium citrate, casein and a casein hydrolysate. The levels are shown in Table 38. In one experiment, 5 cc of blood were withdrawn by cardiac puncture immediately before exposure to the tracer diet. After an exposure of 2 days, all animals were sacrificed and liver protein arginine was isolated and degraded enzymatically. The specific activity of the guanidine carbon as well as that of excreted urea measured as before.[2,3]

TABLE 38

Effect of diet on the renewal rate of liver protein
(2-day exposure)

Amino acid source	Fraction replaced per day*
20% essential amino acid mixture	0.24, 0.25
10% essential amino acid mixture	0.26, 0.27, 0.25, 0.27
2% essential amino acid mixture	0.29, 0.35, 0.32, 0.40
50% casein	0.23, 0.24, 0.22, 0.25
18% casein	0.20, 0.23, 0.22, 0.25
12% casein	0.23, 0.32
2% casein	0.24, 0.31
Casein hydrolysate equiv. to 18% casein plus 0.2% dl-tryptophan	0.21, 0.24
18% casein**	0.22, 0.25

*Each value represents data obtained from one animal.

**5 cc of blood were removed from each of these animals at the beginning of the exposure period.

Results

The rise in specific activity of the excreted urea reached a plateau at about the same time, 18 ± 3 hr, regardless of the diet fed; hence, it appeared unnecessary to determine the rising curve of activity for each experimental group. It is more reasonable to expect that the specific activity of the guanidine moiety of free hepatic arginine reaches its equilibrium value almost instantaneously than that it follows the time course represented by excreted urea. The merits of this assumption have been discussed.[3] Therefore, the rise in specific activity of the guanidine group of liver protein arginine was assumed to be described by a single exponential function. The data were fitted to Equation 3 of Reference(3), and the replacement rate was calculated (Table 38).

It is immediately apparent that, as long as they are adequate, neither the level nor the type of amino acid source has much effect on the rate of renewal of liver protein as measured by a 2-day experiment. During this period, isotope is incorporated predominantly into those proteins which are presumed to be the most labile, i.e. those that have the fastest turnover rates and hence those most likely to show differences due to dietary or metabolic variation. Since there is so little difference between dietary groups receiving adequate amounts of the essential amino acids (e.g., 10 and 20% of essential amino acid mixture and 12, 18 and 50% of casein), one may conclude that the level of protein intake has no effect on the turnover rate of liver protein.

The turnover rates of the proteins in rats fed a diet containing only the essential amino acids appear to differ slightly from those in which the diet contained all of the amino acids, whether as intact protein or as a protein hydrolysate. The turnover rate of hepatic proteins of the former rats exceeded that of the latter groups by about 10%. It is interesting to note that the ratio of liver weight to body weight in animals fed the essential amino acid mixture was also about 10% higher than in those fed casein.

The turnover rate of liver protein in animals fed inadequate amounts of the essential amino acids, i.e. 2% of the mixture or of casein, appeared to be faster than in those given an adequate supply. This is contrary to what one would expect. The more labile proteins, those with the faster turnover rates, would be the ones which would be expected to decrease in amount in the deficiency state, thus resulting in a slower apparent renewal rate.

In an extension of the earlier work, Steinbock and Tarver[4] found that the disappearance of S^{35}-labeled methionine from plasma albumin was definitely associated with the protein content of the diet. The half-life of plasma albumin ranged from 17 days in rats fed no protein to 2.9 days in animals given 65% protein. However, Hubay et al.[5], using I^{131} labeled plasma albumin, could find no effect of nutritional status on the rate of disappearance of isotope from the blood of patients. It has been suggested that much of the protein synthesized by the liver is plasma albumin, and indeed, the amount of albumin formed daily as calculated by others would account for most of the protein synthesized at the rates presented here. However, when roughly one-third of the circulating albumin was removed by bleeding, there was no subsequent rise in the liver turnover rate (last item in Table 38). If this albumin depletion were going to produce a measurable effect, it should have been apparent within the experimental period chosen.

Either the estimates of rate of synthesis of the albumin are excessive or the liver is producing albumin at a maximum rate at all times.

It is hoped that examination of the plasma albumin from these animals will facilitate interpretation of these data.

References

1. Solomon, G., and H. Tarver. The effect of diet on the rate of loss of labeled amino acid from tissue proteins. J. Biol. Chem. 195:447-452 (1952).

2. Swick, R. W., and D. T. Handa. The distribution of fixed carbon in amino acids. J. Biol. Chem. 218:577-585 (1956).

3. Swick, R. W., Measurement of protein turnover in rat liver. J. Biol. Chem., in press.

4. Steinbock, H. L. and H. Tarver. Plasma protein. V. The effect of the protein content of the diet on turnover. J. Biol. Chem. 209:127-132 (1954).

5. Hubay, C. A., H. Krieger, W. D. Holden, and T. Hancock. Effect of protein depletion on rate of disappearance of radioactive protein from the blood stream. Proc. Soc. Exptl. Biol. Med. 78:402-406 (1951).

THE MEASUREMENT OF PROTEIN TURNOVER IN RAT LIVER

IV. The Effect of Growth

Robert W. Swick and Rita A. Martin

Buchanan and Nakao[1] studied the effects of growth on carbon turnover in an attempt to explain the greater uptake of isotope in growing systems as compared to nongrowing systems observed by others after a single dose of tracer material. They measured the total carbon turnover of growing and nongrowing animals continuously exposed to isotopic CO_2 and concluded that the rapid uptake observed in growing systems is a result of the rapid synthesis of materials in equilibrium with the isotope, plus the normal turnover of components already synthesized. The present work is an elaboration of their experiments, wherein the incorporation of $C^{14}O_2$ into the guanidine group of arginine isolated from the liver proteins of growing rats was measured and compared with that in adult animals.

Methods

Weanling female rats were fed a diet containing 18% of casein as the protein source and $CaC^{14}O_3$ at hourly intervals as described previously.[2] After 4 days' exposure, the animals were sacrificed, and the livers were removed and weighed. Arginine was isolated from the total liver proteins, and the specific activity of the guanidine group and of excreted urea was determined as CO_2 after enzymatic degradation.[2,3]

The initial liver weights of the experimental rats were estimated by calculating the regression of liver weight against body weight from a group of rats of comparable weight and history; these rats were sacrificed at the time the experimental animals were placed on the feeding regimen.

The livers of the young rats which grew during the exposure period may be considered to be composed of two fractions: that liver which existed at the start of the exposure period and that liver which was formed during the experiment. Since the specific activity of the guanidine group of free arginine is assumed to reach its equilibrium value almost immediately after exposure to isotope,[3] all of the arginine incorporated into the liver protein formed during the experimental period will have the same specific activity as free arginine as measured by excreted urea. Therefore, the specific activity of the arginine isolated from the whole liver will be the weighted average of the new liver protein of known specific activity and the "old" liver of unknown specific activity. If the amount of new liver protein can be estimated from the growth of the liver, then the specific activity of the "old" liver protein may be calculated. The calculated specific activity of "old" protein is then fitted into Equation 3 of Reference (3), and its renewal rate is computed.

Results

Table 39 shows the estimated growth of the liver during the exposure period, the observed specific activity of the liver protein relative to urea, and the calculated specific activity of that fraction of liver which existed at the beginning of the experiment. Table 40 gives the calculated rates of renewal of the "old" proteins and, for comparison, the rates of renewal observed in adult rats treated for a similar length of time.[3] The wider range of the values for the weanlings partly results from the error in estimating the initial liver weight of the young animals.

TABLE 39

Growth of liver and specific activity of guanidine groups of arginine of liver protein

Each value represents data obtained from a single animal

Initial weight of liver (est.), g	Final weight of liver, g	New liver formed, % of total	Observed specific activity in total liver,* cpm/mM	Calculated specific activity in "old" liver,* cpm/mM
2.17	2.99	27	76.7	67.9
2.17	2.87	25	79.1	72.2
2.65	2.81	6	68.5	66.5
2.65	2.96	10	67.3	63.5
2.00	2.69	26	65.1	53.1
1.90	2.55	25	66.3	54.8

*Specific activity of urea = 100

TABLE 40

Effect of growth on liver protein turnover

Each value represents data obtained from a single animal

Rats	Fraction replaced per day
Weanlings	0.28, 0.32, 0.27, 0.25, 0.19, 0.20
Adults	0.24, 0.24, 0.25, 0.26

It appears clear that turnover takes place in the presence of growth at a rate comparable to that in adult animals. In fact turnover is so rapid relative to growth that it accounts for 82-97% of the isotope incorporated. The separation of growth and turnover probably should be attempted in some organ or system where the two are occurring at more nearly the same rate. Since turnover in the absence of growth involves both synthesis and degradation, the estimate of turnover is given either by the rate of synthesis or by the rate of degradation. The similarity of renewal rates observed in adult and growing rats suggests that growth occurs in the presence of a normal turnover rate. Therefore growth probably results from an increased rate of synthesis and not from an inhibition of the degradative processes. These data are in accord with the findings of Buchanan and Nakao.[1]

References

1. Buchanan, D. L., and A. Nakao. Effect of growth and body size on fixed carbon turnover. J. Biol. Chem. 200:407-416 (1953).

2. Swick, R. W., and D. T. Handa. The distribution of fixed carbon in amino acids. J. Biol. Chem. 218:577-585 (1956).

3. Swick, R. W., Measurement of protein turnover in rat liver. J. Biol. Chem., in press.

INFLUENCE OF OXIDATION PRODUCTS OF EPINEPHRINE UPON THE ADENOSINE TRIPHOSPHATASE ACTIVITY OF A UTERINE MUSCLE PREPARATION

Mario A. Inchiosa, Jr., and N. L. VanDemark*

These investigations were undertaken as part of an attempt to gain information concerning the biochemical changes accompanying the stimulation of uterine contractility by epinephrine. The typical physiological response of the nonpregnant uterus to epinephrine in most species appears to be diphasic, with an initial contractile response followed by a longer period of inhibition.(1) In the present study it was found that the dephosphorylation of adenosinetriphosphate (ATP) by a contractile protein preparation from bovine uterine muscle was inhibited by oxidation products of epinephrine. The enzymatic activity has been referred to as adenosinetriphosphatase (ATPase) activity for convenience; however, more than one enzyme may be involved.

Materials and Methods

The myometrium from four nonpregnant cows was pooled for the isolation of a contractile protein preparation. The muscle was chopped in a chilled meat grinder and 105 g of tissue were extracted with 350 ml of a solution 0.3 M in KCl, 0.15 M in K_2HPO_4 and 0.15 M in KH_2PO_4 by constant agitation with an electric stirrer for $5\frac{1}{2}$ hr. The mixture was diluted with 1.4 liters of water, filtered through cheese cloth, and the filtrate was diluted with water to a volume of 4.2 liters. This material was allowed to stand until precipitation of protein was complete. The precipitate was collected and dissolved in 2.0 M KCl; the supernatant was discarded. The protein preparation was purified by a technique which has been previously described.(2) The purification procedure was carried through four times.

ATPase assays were conducted under anaerobic conditions at 38° C in $NaHCO_3$ buffer (pH 7.3) with measurements of the rate of accumulation of inorganic phosphate. The assays were carried out in Warburg flasks gassed with a 95% N_2, 5% CO_2 mixture to produce anaerobic conditions. Inorganic phosphate was determined by the method of Fiske and SubbaRow.(3)

The concentration of the oxidation product or products of epinephrine were estimated as adrenochrome. The optical densities of reaction mixtures in one group of experiments and of partially oxidized epinephrine solutions in a second group were compared to a standard adrenochrome assay.(4) The measurements were made using the Klett-Summerson photoelectric colorimeter with No. 50 filter. The oxidation product or products were not identified further for these experiments.

*Physiology Division, Dairy Science Department, University of Illinois, Urbana.

Results

Epinephrine was incubated aerobically with the uterine preparation in the first group of assays for periods of time ranging from 1/4 to 30 min. As can be seen in Table 41, increased time of aerobic incubation resulted in progressive increases in the extent of epinephrine oxidation, and in turn, progressive inhibition of ATPase activity.

TABLE 41

Effect of oxidation products of epinephrine upon ATPase activity of a uterine muscle preparation

Oxidation period, min	Concentration of oxidation products estimated as adrenochrome, M X 10^5	μM P released per ml reaction mixture*/hr		% Inhibition
		Control	oxidized epinephrine	
1/4	0.67	0.73	0.71	2.7
1/4	0.80	0.74	0.72	2.7
3	0.87	0.74	0.69	6.8
3	0.87	0.75	0.67	10.7
10	1.07	0.74	0.63	14.9
10	1.27	0.74	0.64	13.5
21	1.66	0.73	0.53	27.4
21	1.80	0.74	0.52	29.7
30	1.86	0.69	0.39	43.5
30	2.06	0.70	0.39	44.3

*The reaction mixtures contained 37.5 μg N/ml, 0.0260 M $NaHCO_3$, 0.5 M KCl, and 0.005 M ATP.

The aerobic incubation periods were terminated by 20 min of gassing with the N_2, CO_2 mixture. After the gassing, the assay period was begun by tipping ATP in from the side arm of the Warburg flask. Estimations of the concentration of oxidation products were made at the end of the assay period. The regression of per cent inhibition of ATPase activity upon concentration of oxidation products was highly significant ($p = < 0.001$).

Autoxidation products of epinephrine, estimated as adrenochrome as described above, were also tested for an effect upon the ATPase activity of the same uterine preparation. Solutions of epinephrine were allowed to autoxidize in bicarbonate buffer to various extents before they were gassed with a 95% N_2, 5% CO_2 mixture to prevent further oxidation. These solutions

were placed in one of the side arms of double-side-arm Warburg flasks (the other side arm contained ATP). The assays were run under anaerobic conditions and were exactly comparable in other details to the first group of experiments (see footnote, Table 41). First, the autoxidized epinephrine solutions were added to the uterine preparation. The ATP was tipped in 12 min later. A 20% inhibition of ATPase activity was observed in the presence of a 3×10^{-6} M concentration of oxidation products. An inhibition could be detected even at concentrations below 10^{-6} M.

In none of the present studies was any effect observed upon ATPase activity which was attributable to epinephrine in the range of epinephrine concentrations studied (6×10^{-6} M to 6×10^{-5} M).

Discussion

Dickens and Glock[5] found that adrenochrome inhibited the ATPase activity of myosin from the skeletal muscle of the rat in concentrations of 10^{-4} M or higher. Like other quinones, adrenochrome has been found to oxidize reversibly the -SH groups of several enzymes.[6] Dickens and Glock[5] concluded that adrenochrome oxidatively inhibited the myosin preparation they studied, and Bailey and Perry[7] found that oxidative removal of the -SH groups of myosin inhibited both ATPase activity and actomyosin formation. The inhibition of ATPase activity observed in the present study may result from a similar action.

In view of the prolonged inhibition of uterine motility following epinephrine treatment *in vivo* and *in vitro*,[1] the question may be raised of a possible association of this response to the enzymatic inhibition observed in the present study. The *in vivo* conversion of epinephrine to adrenochrome is assumed under such a proposal. However, this question has not been reconciled. The possibility is favored by the work of Green and Richter[8] demonstrating enzyme systems of heart and skeletal muscle capable of readily converting epinephrine to adrenochrome *in vitro*, and Wajzer's[9] report of an apparent epinephrine-adrenochrome system in mammalian skeletal muscle. The isotope studies of Schayer and Smiley[10] however, cast doubt upon the likelihood that adrenochrome is an intermediate in the metabolism of epinephrine, although they do not rule out the possibility.

The present study suggests that oxidation products of epinephrine, if present, might be expected to have a significant physiological role.

References

1. Fitzpatrick, R. J. Uterine response to adrenaline in intact cows and sheep. J. Comp. Pathol. Therap. 67:223-238 (1957).

2. Inchiosa, M. A., Jr., J. F. Thomson, and F. J. Klipfel. Investigations upon structural elements of uterine muscle. I. Preliminary observations on a nucleic acid-protein complex from uterine muscle. Semi-annual Report of Biological and Medical Research Division, Argonne National Laboratory. ANL-5732, pp. 165-167 (1957).

3. Fiske, C. H., and Y. SubbaRow. The colorimetric determination of phosphorus. J. Biol. Chem. 66:375-400 (1925).

4. Persky, H. Chemical determination of adrenaline and noradrenaline in body fluids and tissues. In Methods of Biochemical Analysis II:66-67 (1955).

5. Dickens, F., and G. E. Glock. The mechanism of oxidative inhibition of myosin. Biochim. et Biophys. Acta 7:578-584 (1951).

6. Bacq, Z. M. The metabolism of epinephrine. Pharmacol Rev., Part II of J. Pharmacol. and Exp. Therap. 95:1-26 (1949).

7. Bailey, K., and S. V. Perry. The role of sulfhydryl groups in the interaction of myosin and actin. Biochim. et Biophys. Acta 1:506-516 (1947).

8. Green, D. E., and D. Richter. Adrenaline and adrenochrome. Biochem. J. 31:596-616 (1937).

9. Wajzer, J. Oxydation de l'adrénaline. Bull. soc. chim. biol. 28:341-345 (1946).

10. Schayer, R. W., and R. L. Smiley. The metabolism of epinephrine containing isotopic carbon. III. J. Biol. Chem. 202:425-430 (1953).

UNSATURATED FATTY ACIDS AND CHOLESTEROL METABOLISM

IV. Effect of Dietary Cholesterol on Cholesterol Levels and Cholesterol Ester Composition in Liver and Plasma of Rats

Peter D. Klein

In the previous reports in this series[1,2,3] we have considered the unsaturated fatty acids levels of the diet in relation to the levels of cholesterol present as free and ester forms in rat liver and plasma, as well as the composition of the esters found under these conditions. This report deals with the effect of dietary cholesterol on the variables previously described.

Methods

Animals and dietary conditions were identical to those of the earlier experiments except that 0.5% cholesterol was added to the diets. The methods were given in full in earlier reports.[1,2,3]

Results and Discussion

The values for the observed levels of cholesterol and cholesterol ester in liver and plasma of rats on diets containing cholesterol, as well as those found in the absence of cholesterol, are shown in Table 42. The added dietary cholesterol resulted in a significant rise in the level of esterified cholesterol (resulting in a rise of total cholesterol) in the plasma of animals fed on the FF diet.* Free cholesterol levels in the livers of all groups given cholesterol showed small rises or none at all; however the ester form rose in all cases. The lowest increase was found on the 5H diet; the highest on the 5U diet. In contrast to the relationship observed between liver ester content and dietary linoleic acid on the normal diet, no correlation could be drawn here between the content of unsaturated fatty acid in the diet and the resultant liver ester levels.

The variation in levels of liver ester points up the fact that this component reflects processes other than the esterification reactions; among these is the variation in cholesterol absorption from the gastrointestinal tract, which is, in turn, dependent upon the type and quantity of fat present in the diet. In opposition to this is the possible steatorrhea resulting from diets having a high fat content, which would result in less dietary

*The following symbols are used: FF, "fat-free diet"; 5H, 5% Crisco, 5U, 5% corn oil, 30H, 30% Crisco, 30U, 30% corn oil.

TABLE 42

Cholesterol values in liver and plasma of animals fed various levels of linoleic acid with and without 0.5% cholesterol

Diet	Plasma cholesterol, mg%			Liver Cholesterol, mg%		
	Free	Ester	Total	Free	Ester	Total
FF	8.2	20.1	28.3	152	237	389
+0.5% C	8.5	54.0	62.5	222	1036	1258
5H	10.8	27.0	37.8	158	49	207
+0.5% C	8.6	40.4	49.0	187	533	720
5U	17.3	34.0	51.3	149	101	250
+0.5% C	10.6	36.8	47.4	243	1699	1942
30H	18.2	40.0	58.2	144	109	253
+0.5% C	15.0	30.2	45.2	183	842	1025
30U	16.5	45.8	62.3	172	194	366
+0.5% C	12.5	53.2	65.7	218	1053	1271

cholesterol being presented to the liver. Since data on these factors were not obtained in the present experiment, it is perhaps sufficient to indicate their possible contribution to the observed levels of the liver ester.

Next, the unsaturated fatty acid compositions of the liver and plasma esters were determined (Table 43). In the liver esters, the total unsaturated fatty acids esterified to cholesterol were decreased by the

TABLE 43

Unsaturated fatty acid composition of cholesterol esters in liver and plasma of animals fed varying levels of linoleic acid plus 0.5% cholesterol

	Fatty acid concentration in cholesterol esters, moles/100 moles cholesterol									
	FF		5H		5U		30H		30U	
	Liver	Plasma	Liver	Plasma	Liver	Plasma	Liver	Plasma	Liver	Plasma*
Diene	1.0	3.7	3.4	8.6	6.6	15.1	3.5	7.2	24.9	51.2
Triene	0.2	1.5	1.1	1.5	0.6	0.7	1.0	1.0	1.0	4.7
Tetraene	0.0	0.4	0.1	0.5	0.1	0.1	0.3	0.2	0.3	3.2
Pentaene	0.0	0.3	0.2	0.4	0.0	0.5	0.1	0.5	0.1	0.5
Total	1.2	5.9	4.8	11.0	7.3	16.4	4.9	8.9	26.3	60.6

*Extremely small quantity of ester available for analysis; while the relative concentrations of the fatty acids are reliable, their absolute values are only approximate.

addition of cholesterol; that this was a passive process related to the concentration of these acids in the diet, is borne out by the plot of ester linoleic acid versus dietary linoleic acid (Figure 63). The upper line represents the data obtained in earlier experiments with unsupplemented diets, the lower line, the present data. With the exception of the 30H values which are definitely aberrant in this relationship, the composition of the ester appears to follow the same relationship to the diet as was previously described. However, the intercept is lower, indicating that a greater dilution of the dietary component has taken place.

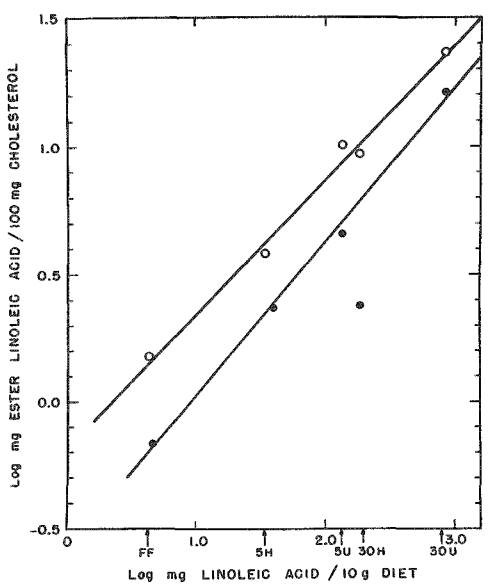

Figure 63

Liver ester linoleic acid concentration versus dietary linoleic acid concentration. Open circles, cholesterol-free diet; solid circles, 0.5% cholesterol added.

The plasma esters, however, are markedly changed, both in terms of total unsaturated fatty acid content, and in terms of the relative proportions of each acid. The total unsaturated fatty acid content of the esters dropped in all cases; for the 30H diet it was 1/10 that previously found on the corresponding diet without cholesterol. In fact, all plasma values, except those for the 30U diet, dropped after the addition of cholesterol to lower values than that of the fat-free unsupplemented diet.

Even more striking was the altered distribution of fatty acids in the plasma esters resulting from the addition of cholesterol. The change is characterized by an almost complete absence of tetraenoic acid, a component which accounted for 30-40% of the total unsaturated acids in plasma esters of animals on 30H and 30U diets, without cholesterol. Thus the animal not only seems to be unable to spare unsaturated fatty acids for plasma cholesterol esterification, but those which he uses are the less unsaturated members. This could, in part, be explained by the following observations: First, the addition of cholesterol to the diet results in almost complete abolishment of acetate incorporation into cholesterol. Second, the transformation of linoleic acid into tetraenoic (arachidonic) acid occurs by means of three or more steps, two of which involve dehydrogenation and the third the addition of a two-carbon fragment to the chain. While the precise sequence of these steps has not been established,

evidence points to the addition of acetate as the first step. Thus it is conceivable that the block in acetate incorporation into cholesterol may extend to the chain-lengthening processes required for the synthesis of tetraenoic acid.

The plasma and liver compartments of cholesterol represent two separate, though related, metabolic functions. A certain level of cholesterol must be maintained in solution in plasma, albeit this solution is mediated by a protein moiety. The system has at its disposal the ability to lengthen, shorten, saturate or desaturate the fatty acid chain and to add or subtract a dietary component which it cannot synthesize, such as the polyunsaturated fatty acids. Within these variables, the system must be poised at the optimum combination in composition. In the liver compartment, however, there is one additional facility - that of storage, though this in itself can reach limits which are harmful. Clearly, in the cholesterol feeding situation, the animal has difficulty in stemming the influx of cholesterol from the diet and stores a tremendous quantity in the liver as the ester. The accumulation of this ester draws heavily on the capability of the animal to synthesize fatty acids and/or modify dietary fat. This in turn results in the modification of the plasma cholesterol esters. It is interesting that only at the lowest dietary fat level did this added cholesterol burden result in an increase in the plasma level of cholesterol.

References

1. Klein, P. D. Unsaturated fatty acids and cholesterol metabolism I. Influence of linoleic acid on cholesterol levels in liver and blood of rats. Semiannual Report of Biological and Medical Research Division, Argonne National Laboratory. ANL-5732, pp. 180-184 (1957).

2. Klein, P. D. Unsaturated fatty acids and cholesterol metabolism II. Influence of linoleic acid in diet on the unsaturated fatty acid content of cholesterol esters in liver and plasma of rats. Semiannual Report of Biological and Medical Research Division, Argonne National Laboratory. ANL-5732, pp. 185-188 (1957).

3. Klein, P. D. Unsaturated fatty acids and cholesterol metabolism III. Distribution of unsaturated fatty acids in liver and plasma of rats fed varying levels of linoleic acid. Semiannual Report of Biological and Medical Research Division, Argonne National Laboratory. ANL-5732, pp. 189-191 (1957).

HEXURONIC DEHYDROGENASE OF AGROBACTERIUM TUMEFACIENS

James E. Zajic

A number of publications have appeared recently on the metabolism of glucuronic, galacturonic and mannuronic acids.[1-6] A hexuronic reductase has been described in Erwinia carotovora,[2] which catalyzes the conversion of glucuronic and galacturonic acids to their corresponding hexonic acids, i.e., L-gulonic and L-galactonic acids. Storey and Dutton[7] have isolated and identified uridine diphosphoglucuronic acid (UDPGa). This coenzyme-substrate complex was functional in ester glucuronide synthesis.[8,9] UDPGa is formed through the action of a specific dehydrogenase for uridine diphosphoglucose.[10-12] The latter reaction is the only known biosynthetic pathway for the synthesis of a hexuronic acid.

The following investigations pertain to a new enzymatic system for the oxidation of the hexuronic acids. This new system has been tentatively named hexuronic dehydrogenase.

Methods

The cultures used in these studies were obtained from the following sources: Agrobacterium tumefaciens, University of Wisconsin; Erwinia carotovora, University of California (Davis) and American Type Culture Collection; Aerobacter aerogenes and Escherichia coli, American Type Culture Collection. Cells were grown on a rotary type shaker in 2-liter flasks containing 2.0% glucuronic acid.[13] Adequate growth was obtained in 24 hr. Cells were harvested by centrifugation and washed in 0.02 M Tris(hydroxymethyl)-aminomethane (pH 8.0). Sonic extracts were prepared by diluting packed cells 1 to 3 with Tris buffer and subjecting to sonic disintegration for 20 min in a 10-Kc Raytheon. Cell debris was removed by centrifugation at 6000 g for 10 min. Sonic extracts were then dialyzed for 24 hr in 0.02 M Tris (pH 8.0). Following dialysis, the cytochromes, diphosphopyridine nucleotide oxidase, and other high molecular weight proteins were removed by ultracentrifugation in the Spinco centrifuge at 144,000 g for 2 hr. The supernatant from these preparations was used in all analyses. The Beckman D. U. Spectrophotometer was used to estimate the rate of reduction of diphosphopyridine nucleotide (DPN) and triphosphopyridine nucleotide (TPN).

Results

Hexuronic dehydrogenase was first observed in A. tumefaciens during a routine survey of several uronic-acid-utilizing organisms for the newly reported hexuronic reductase.(2) Cultures of E. carotovora, E. coli, A. aerogenes and R. stolonifer possessed no hexuronic dehydrogenase activity. Preliminary evidence suggesting the presence of a hexuronic dehydrogenase in A. tumefaciens was obtained during measurements of the strong DPNH-oxidase system of this organism. The rate of oxidation of reduced DPN by DPNH-oxidase could be decreased markedly upon addition of any of the hexuronic acids. This inhibition suggested the presence of a DPN-linked hexuronic dehydrogenase. To investigate this further, 90% or more of the DPNH-oxidase system was removed by ultracentrifugation in the Spinco at 144,000 g for 2 hr. Hexuronic dehydrogenase activity was then determined spectrophotometrically by following the reduction of DPN upon addition of either glucuronic, galacturonic, or mannuronic acids, or glucuronic acid lactone and mannuronic acid-γ-lactone. The rates of reduction of DPN with these substrates are shown in Fig. 64.

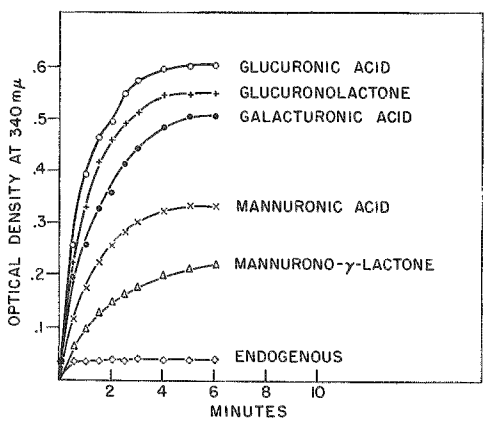

Figure 64

The rate of reduction of DPN by the hexuronic dehydrogenase of A. tumefaciens upon addition of the various hexuronic acids or their lactones. Reaction vessels contained: 4 μ moles substrate, 4 μ moles $MgCl_2$, 0.4 μ mole DPN, 50 μ moles Tris (pH 8.0) and 0.1 ml enzyme preparation.

Glucuronic acid was oxidized at a greater rate than were galacturonic and mannuronic acids. The corresponding lactones of glucuronic and mannuronic acids were not oxidized as rapidly as the parent hexuronic acid. There was no observable lag in the reduction of DPN with any of the hexuronic acids or their lactones.

TPN did not act as an electron acceptor for this dehydrogenase. No hexuronic reductase activity was observed, nor did the hexonic acids formed by the action of hexuronic reductase on the hexuronic acids act as substrates. To determine the specificity of this enzyme and the possible relation to other dehydrogenases, a variety of carbohydrates was substituted for the hexuronic acids without success. These included the parent aldoses, D-glucose, D-galactose and D-mannose; the polyhydroxy alcohols, sorbitol,

dulcitol and mannitol; and possible five-carbon decarboxylation products such as D-arabinose, D-lyxose and D-xylose. A definite but weak DPN-linked dehydrogenase for L-arabinose was present and may prove to be significant in the subsequent metabolism of glucuronic acid. DPN was not reduced when either UDP-glucose, menthol glucuronic acid or mucic acid were added as substrates.

Discussion

The occurrence of several enzymatic reactions involving the hexuronic acids have been eliminated, e.g. the hexuronic reductase reported by Starr et al.,[2] and the uridine-diphosphoglucose dehydrogenase reported by Strominger et al.[11] Decarboxylation of the hexuronic acids prior to dehydrogenation does not appear likely in A. tumefaciens. The inactivity of the enzyme on addition of several polyhydroxyalcohols would appear to eliminate any relation to the dehydrogenases specific for these compounds.[14,15]

The inability of the parent aldoses to substitute for glucuronic, galacturonic and mannuronic acids shows the high specificity of the enzyme for the carboxylic acid moiety. This specificity must extend beyond the carboxylic acid moiety, otherwise one would expect a reaction with the corresponding monocarboxylic hexonic acids and such dicarboxylic acids as mucic acid; this was not observed. Evidently the specificity includes the aldehyde portion of the hexuronic acids because when the aldehyde group is covered as in mentholglucuronic acid, no dehydrogenation occurs.

The activity of this enzyme on the less common uronic acids was not investigated. The lactones of glucuronic acid and mannuronic acids could be substituted for the non-lactonized acid. The decreased reduction of DPN with the lactonized forms may indicate delactonization prior to dehydrogenation.

The 6-carbon intermediates formed by hexuronic dehydrogenase have not been identified. Application of paper chromatography to this problem has not proven successful. Two types of conversion have been considered; the oxidation of the aldehyde group to yield a dicarboxylic acid and the formation of ketohexuronic acids. The former reactions would result in the formation of glucosaccharic, galactosaccharic (mucic) and mannosaccharic acids, and would represent the first appearance of these carbohydrates in enzymology.

References

1. Rabinowitz, J. L. Studies on the decarboxylation of radioactive glucuronolactone by *in vitro* systems. J. Am. Chem. Soc. 77:5180-5182 (1955).

2. Starr, M. P., J. DeLey, W. W. Kilgore. Catabolism of the hexuronic acids by *Erwinia carotovora*. Science 125:929 (1957).

3. Burns, J. J. and C. Evans. The synthesis of L-ascorbic acid in the rat from D-glucuronolactone and L-gulonolactone. J. Biol. Chem. 223:897-905 (1956).

4. Ashwell, G. Enzymatic degradiation of D-galacturonic and D-glucuronic acid. Federation Proc. 16:146-147 (1957).

5. Eisenberg, F. Jr. Metabolism of glucuronic acid *in vivo*. Federation Proc. 16:176-177 (1957).

6. Publitz, C., A. P. Grollman, and A L. Lehninger. Enzymatic conversion of D-glucuronate to L-ascorbate in animal tissues. Federation Proc. 16:382 (1957).

7. Storey, I. D. E. and G. J. Dutton. Uridine compounds in glucuronic acid metabolism. II. The isolation and structure of uridine-diphosphate glucuronic acid. Biochem. J. 59:279-288 (1955).

8. Dutton, G. J. Uridine-diphosphate-glucuronic acid and ester glucuronide synthesis. Biochem. J. 60:xix (1955).

9. Storey, I. D. E. and G. J. Dutton. Uridine diphosphate glucuronic acid. Proc. Inter. Congr. Biochem. 3rd Congr. Brussels 1955:162-163 (1956).

10. Strominger, J. L., H. M. Kalckar, J. Axelrod, and E. S. Maxwell. Enzymatic oxidation of uridine diphosphate glucose to uridine diphosphate glucuronic acid. J. Am. Chem. Soc. 76:6411-6412 (1954).

11. Strominger, J. L., E. S. Maxwell, J. Axelrod, and H. M. Kalckar. Enzymatic formation of uridine diphosphoglucuronic acid. J. Biol. Chem. 224:79-90 (1957).

12. Maxwell E. S., H. M. Kalckar, and J. L. Strominger. Some properties of uridine diphosphoglucose dehydrogenase. Arch. Biochem. Biophys. 65:2-10 (1956).

13. Kraght, A. J., and M. P. Starr. Pectic anzymes of Erwinia carotovora. Archives of Biochem. Biophys 42:271-277 (1953).

14. Arcus, A. C. and N. L. Edson. Polyol dehydrogenases. 2. The polyol dehydrogenases of Acetobacter suboxydans and Candida utilis. Biochem. J. 64:385-394 (1956).

15. Shaw, D. R. D. Polyol dehydrogenases. 3. Galacitol dehydrogenase and D-ıditol dehydrogenase. Biochem. J. 64:394-405 (1956).

BONE TUMOR INTEGRATED DEATH RATES

Harry Auerbach

The death rates available from Vital Statistics Offices are generally the crude death rate and the age and sex specific death rates. A specific disease crude death rate such as the male bone tumor death rate for the United States, 1950, would be recorded as 1.73 per 100,000 population. This is derived by dividing the total number of male bone tumor deaths in 1950 (1295) by the mid-year estimate of total male population (74,855,000), and means that for every 100,000 males alive during the year an average of 1.73 bone tumor deaths occurred. Age specific death rates are based on the number of deaths that occur in a specific age group of the population. In 1950 the U.S. male bone tumor death rate for age 35-44 was 0.77 per 100,000 and for age 65-74 was 8.19 per 100,000. The crude death rate is based on all deaths in the total population and because the age specific death rates increase with age, the crude death rate can increase, without any change in the age specific death rates, by an increase in the proportion of older people in the population. This may be falsely interpreted as a real increase in the incidence of bone tumors.

In studying bone tumor deaths among populations working with or subjected to environments of radium or Sr^{90}, a decision as to an increase in the number must be based on the number of tumor deaths normally expected in an unexposed population. The computation of this number is based on use of life tables for the population and on age specific bone tumor death rates for the population. Table 44 shows the calculation of bone tumor deaths to be expected in following 100,000 females from age 15 to the death of the entire group. This shows that of 100,000 fifteen-year-old females, a total of 117 would eventually die of bone tumors This can also be used to show that if 100,000 fifteen-year-old females are followed for thirty years to age 45, 5160 would die of all causes and 15 would die of bone tumors.

Table 45 shows the total deaths and bone tumor deaths to be expected in populations of 100,000 males and females observed for 30 years.

The implication of these integrated death rates is that unless large populations are observed for bone tumors, manyfold increases in bone tumor death rates due to environmental or other factors may go undetected. By constructing series of these integrated bone tumor death rates, it can be estimated that of the 170,000,000 people now alive in the United States approximately 200,000 will die of bone tumors. Similar integrated death rates can be derived for any cause of death or different populations.

TABLE 44

Bone tumor deaths in female populations*

Age group	Population at start of period	Man years at risk in period	Death rate per 100,000 man years	Bone tumor deaths in period	Cumulative bone tumor deaths
15-24	100,000	996,000	0.62	6.18	6.18
25-34	99,120	984,262	0.32	3.15	9.33
35-44	97,683	964,131	0.59	5.69	15.02
45-54	94,840	921,845	1.35	12.44	27.46
55-64	88,846	833,375	3.00	25.00	52.46
65-74	76,843	666,229	4.58	30.51	82.97
75-84	54,028	377,656	6.34	23.94	106.91
85+	21,428	104,997	9.79	10.28	117.19

*Based on U.S. life tables 1949-1951 and U.S. 1949-1951 Female Bone Tumor Death Rates.

TABLE 45

Total deaths and bone tumor deaths in populations of 100,000 followed for 30 years*

Age at beginning of observation period	Males		Females	
	Total deaths	Bone tumor deaths	Total deaths	Bone tumor deaths
15	7,921	21	5,160	15
25	16,011	27	10,365	21
35	32,907	55	21,334	44
45	58,146	96	43,032	72
55	85,084	127	75,882	89

*Based on U.S. 1949-1951 life tables and U.S. 1949-1951 Bone Tumor Death Rates.

GEOGRAPHIC STUDIES IN BONE TUMORS

II. Geographic Incidence of Bone Tumors in Illinois

Harry Auerbach

A preliminary report[1] indicated that, based on death-certificate data for the period 1949-1951, several areas in Illinois showed significant (P equal to or less than 5%) increases in bone tumor death rates. This report is based on death-certificate data for the period 1940-1950 and represents 2294 bone tumor deaths in 88,000,000 man years of experience. These data include deaths ascribed to so-called primary tumors of the jaw bone, as well as tumors of all other bones of the skeleton.

The deaths within the period were tabulated by sex for each county and all cities of 10,000 population or more. Average death rates for the period were calculated, and areas showing an increase over the average Illinois rate were tested for significance by the Poisson test. Counties having cities of 10,000 or more population were tested with and without the cities to determine whether the increase was due to an increase in the total county death rate or to an increase in the city death rate.

Table 46 lists the areas (county, city, or county less city) showing such significant (P equal to 5% or less) increases for either jaw bone or all other bones. It would appear that the majority of significant increases in jaw bone tumors occur in males whereas the majority of all other bone tumor increases occur in females. (Studies now in progress indicate that in all probability the deaths ascribed to jaw bone tumors on death certificates are not osteogenic sarcomas but carcinomas of the buccal cavity; hence they should not properly be listed as bone tumors.)

Examinations of the water supplies of these areas for natural Ra^{226} content are being made by the Radiological Physics Division, and, when these are completed, the possibility of a correlation between increased radium concentration in the water supply and increases in bone tumors will be studied. Occupational exposures to radium and other carcinogenic agents are also being studied as possible causes.

TABLE 46

Areas showing significant increases in bone tumor death rates, Illinois (1940-1950). Death rates per 100,000 population.

"Jaw bone" tumors			
Male		Female	
Illinois	(1.37)*	Illinois	(0.31)
Clay	(4.29)	Effingham	(1.82)
Jersey	(5.32)	Fayette	(2.16)
McLean	(4.64)	Kankakee less	
Bloomington city	(5.19)	Kankakee city	(1.33)
Menard	(5.80)		
Cass	(4.89)		
Richland	(5.73)		
Pope	(11.54)		
St. Clair less			
E. St. Louis city	(3.25)		
Springfield city	(3.09)		
Joliet city	(3.14)		
All other bone tumors			
Illinois	(1.91)	Illinois	(1.62)
Henry less		Clinton	(4.30)
Kewanee city	(5.49)	Elgin city	(5.01)
Menard	(7.74)	Livingston	(3.45)
Piatt	(5.40)	Macon less	
Sterling city	(11.06)	Decatur city	(3.97)
		E. Moline city	(5.60)
		Piatt	(5.40)
		Canton city	(6.48)

*The numbers in parentheses represent the death rates. The Illinois figures represent the state averages. Each area named is a county unless identified as city.

Reference

1. Auerbach, H., Geographic studies in bone tumors. Quarterly Report of Biological and Medical Research Division, Argonne National Laboratory. ANL-5332, p. 6 (1954).

MORTALITY EXPERIENCE AT ARGONNE NATIONAL LABORATORY

I. Characteristics of the Argonne National Laboratory Population

Asher J. Finkel and Harry Auerbach

This study is based on the actual work experience of 4,820 persons who were employed at Argonne National Laboratory for all or part of the period January 1951 through December 1955. The total time worked by all employees during this period was 161,182 months or 13,432 man-years. The months worked by each employee, in each year, by age group and sex, were tabulated and data were used to prepare Table 47, which presents the age and sex distribution of the man-years worked at Argonne National Laboratory during the period 1951-1955.

TABLE 47

Structure of ANL population by age and sex 1951-1955*

Age group	Male		Female	
	Total man-years	% of total	Total man-years	% of total
< 20	42.2	0.39	100.4	3.71
20-24	594.7	5.54	682.5	25.24
25-29	2090.2	19.48	577.7	21.36
30-34	2650.1	24.70	363.3	13.44
35-39	2080.6	19.39	281.8	10.42
40-44	1140.9	10.64	236.3	8.74
45-49	808.3	7.53	174.5	6.45
50-54	558.3	5.20	163.3	6.04
55-59	345.2	3.22	91.0	3.37
60-64	285.7	2.66	24.3	0.90
65-69	91.3	0.85	8.8	0.32
70-74	29.0	0.27	-	-
75-79	7.3	0.07	-	-
80+	4.1	0.04	-	-
Total	10727.9	100.0	2703.9	100.0

*Based on actual number of months worked at ANL in each age group in each year of the 5-year period.

During this period, males accounted for 79.9% of the total man-years worked, and females accounted for 20.1% of the total. In 1953, it should be noted, compulsory retirement at age 65 was established and this change affected the age structure slightly. Among males, the 15-year age span from 25 through 39 years accounted for 63.6% of man-years worked and among females a similar 15-year age span from 20 through 34 years accounted for 60.0% of man-years worked.

Table 48 gives the mean and median ages, by sex and year, of the Argonne National Laboratory population. For comparative purposes, figures for the U. S. employed population for 1953 are also given. It can be seen that at Argonne the average age for males increased 1.8 years in the 4-year period after 1951 and the female average age increased 1.7 years in the same period. In a static work population the average age should increase by one year for each year the population works. In a replacement population where new young employees enter the work population at approximately the same rate that the older categories are retired, the average age would remain unchanged. In the United States work population the average age increased by 0.45 years for males and 1.36 years for females in the period 1951-1955. It can, therefore, be concluded that the work force at Argonne National Laboratory represents a population somewhere between the static and replacement types.

TABLE 48

Mean and median age of ANL population by sex and year

	Year	Male		Female	
		Mean	Median	Mean	Median
ANL	1951	36.21	33.63	32.50	29.24
	1952	36.95	34.38	32.86	29.85
	1953	37.35	35.14	33.19	29.87
	1954	37.62	35.88	33.78	30.84
	1955	38.03	36.43	34.24	31.14
	1951-55	37.18	34.97	33.20	29.92
U. S. employed population	1951	41.09		38.06	
	1953	41.56	40.27	38.74	37.32
	1955	41.54		39.42	

Deaths among Argonne National Laboratory employees for the period 1951-1955 are being tabulated and analyzed as to age, sex, and cause. The deaths in these various categories will be compared with estimates of the expected deaths under the prevailing death rates in surrounding communities and similar industrial populations.

AN ANALYSIS OF INBREEDING IN THE EUROPEAN BISON

Herman M. Slatis

In connection with the study of inbreeding in man,[1] a survey was made of the possibility of obtaining information about inbreeding in other large mammals. It was hoped that inbreeding could be studied through the use of zoo records of mammals from wide-ranging, numerous species, such as giraffes or zebras, but inquiry indicated that such records are not available, except in a very small number of cases. However, the existence of excellent data on the European bison was pointed out.

At the census of Jan. 1, 1953, there were 181 living European bison, and individual records exist for an additional 379 specimens, which includes almost all of the animals kept in captivity within the preceding 60 years. All of the animals are at least the third generation in captivity and a few can be traced in some lines through 10 generations. The living bison trace back to a set of 17 ancestors, of which only one was born in captivity.

The coefficient of inbreeding, F, has been calculated for all of the animals on the assumption that the 17 original animals were unrelated to each other. Mortality is quite similar at all levels of inbreeding, with little or no indication of early death being correlated with inbreeding; F is not a satisfactory index for this study. An alternative index has been developed, $\ell\ell$, the likelihood of death if a given ancestor possessed a recessive lethal gene heterozygously. Application of index $\ell\ell$ to the progeny of one of the most productive bulls (chosen because he was the only animal whose ancestors had never been semidomesticated) indicates a strong correlation between early mortality and $\ell\ell$, but this correlation is very dependent upon the small group of animals with a high value of $\ell\ell$.

Reference

1. Slatis, H. M., R. H. Reis, and R. E. Hoene. Progress report: Consanguineous marriages in the Chicago region. Quarterly Report of Biological and Medical Research Division, Argonne National Laboratory. ANL-5696, pp. 120-121 (1956).